Province of British Columbia
Ministry of Energy, Mines and
Petroleum Resources
Hon. Anne Edwards, Minister

MINERAL RESOURCES DIVISION
Geological Survey Branch

GEOLOGY OF THE MIDWAY-CASSIAR AREA, NORTHERN BRITISH COLUMBIA (1040, 104P)

By JoAnne L. Nelson and John A. Bradford

This is a contribution to the Canada/British Columbia Mineral Development Agreement 1985-1990

Appendix 1 — Conodont identifications by M.J. Orchard, Geological Survey of Canada

BULLETIN 83

MINERAL RESOURCES DIVISION
Geological Survey Branch

Canadian Cataloguing in Publication Data

Nelson, JoAnne Lee, 1950-
Geology of the Midway-Cassiar area, northern British Columbia (104O, 104P)

(Bulletin, ISSN 0226-7497 ; 83)

Issued by Geological Survey Branch.
Includes bibliographical references: p.
ISBN 0-7718-9324-8

1. Geology—Cassiar Mountains (B.C. and Yukon)
2. Geology, Economic—Cassiar Mountains (B.C. and Yukon)
I. Bradford, John Allan, 1957- . II. British Columbia. Ministry of Energy, Mines and Petroleum Resources.
III. British Columbia. Geological Survey Branch. IV. Title.
V. Series: Bulletin (British Columbia. Ministry of Energy, Mines and Petroleum Resources); 83.

QE187.N44 1992 557.11'85 C93-092027-9



VICTORIA
BRITISH COLUMBIA
CANADA

January 1993

Geological fieldwork for this publication was completed during the period 1986 to 1989

TABLE OF CONTENTS

	Page
CHAPTER 1: INTRODUCTION	1
Location, Access and Topography	1
History of Exploration and Mining	1
Previous Geological Work	1
Present Study	2
Acknowledgments	2
CHAPTER 2: GEOLOGY	3
Introduction	3
Miogeoclinal Stratigraphy	3
Ingenika Group	3
Espee Formation	3
Stelkuz Formation	5
Atan Group	5
Boya Formation	5
Rosella Formation	6
Kechika Group	6
Road River Group	7
Tapioca Sandstone	7
Sandpile Group	7
McDame Group	8
Earn Group	9
Upper Mississippian to Lower Permian Chert and Argillite	11
The Sylvester Allochthon	14
General Structure	16
Division I	17
Units IMs, IMsi	17
Units IPPs	17
Division II	19
Basalt and Sedimentary Sequences	19
IIMvs and IIMs	19
IIPPvs, IIMPsi and IIb	20
IIPPsi	20
Ultramafic-Gabbro Suites; Blue Dome Fault Zone	20
Quartzrock Creek - Cassiar Body	21
Zus Mountain - Blue River Bodies	21
Foggy Mountain Body	22
Blue Dome Fault Zone	23
Table Mountain Sediments	25
Division III	26
Division III, Southern Klippen	26
Huntergroup Volcanics (IIIPPHv)	26
IIIPPs	27
IIIPls	27
IIIvs	27
IIIMt	27
Division III in the Tootsee Lake Map Area	28
IIIPi	28
South Post Ridge Volcanics	28
Whole-rock and Trace-element Petrochemistry	28
Discussion	33
Synthesis: the Sylvester Allochthon and the Slide Mountain Terrane	35
Post-accretionary Stratified Units	39
Tuya Volcanics	39
Post-accretionary Intrusive Rocks	39
Cassiar Batholith	39
Late Cretaceous Intrusions	40
Eocene Intrusions	40
CHAPTER 3: STRUCTURAL GEOLOGY AND METAMORPHISM	41
Major Structural Events	41
Thrust Faults, Folds, Associated Minor Structures	41
High-angle Faults and Fault Systems	42
Metamorphism	43
CHAPTER 4: ECONOMIC GEOLOGY	47
Syngenetic Deposits	47
Sedex Deposits	47
Deposits in Volcanic-Sedimentary Settings	47
Magmatic Chromite Deposits and other Ultramafite-hosted Occurrences	53
Mesothermal Gold (Silver) Quartz Veins	53
The Erickson-Taurus System	53
Fluid Inclusion Data	56
Derivation of Fluid Characteristics	58
Constraints on Characteristics of the Mineralizing Fluids	58
Discussion	59
Asbestos: the Cassiar and McDame Deposits	59
Mantos, Skarns, Veins and Porphyries	61
The Midway Deposit and the Midway Model	62
Mineral Occurrences in the Southeastern Blue Dome Area	64
The Marble Creek System	64
The Mount Haskin - Mount Reed System	64
Synthesis: Mineralization History and Exploration Models	64
REFERENCES	67
APPENDICES	75

FIGURES

1a. Location map of project area	1
1b. National Topographic System index of project area	2
2. Geology of the Midway-Cassiar project area, 1:100,000 scale	(in pocket)
3. Stratigraphic Column of the Cassiar Terrane	4
4. Regional distribution of Slide Mountain Terrane occurrences	15

TABLE OF CONTENTS — *Continued*

Page

5. Sylvester allochthon divisions and units ... 16
6. Cross-section of the Sylvester allochthon ... 18
   - 6a. Northwestern Blue Dome - southwestern Tootsee Lake ... 18
   - 6b. Southern Blue Dome ... 18
   - 6c. Cassiar ... 18
   - 6d. Snowy Creek ... 18
   - 6e. McDame ... 18
7. Relationships between Division III units, the Huntergroup volcanics (IIIPPHv) and Pennsylvanian-Permian sediments, IIIPPs ... 28
8. Silica-alkalies plot for Sylvester igneous rocks ... 30
9. TiO_2 vs. Zr/P_2O_5, Sylvester basalts ... 30
10. Y vs. Nb, Sylvester basalts ... 30
11. Ti-Zr-Y, Sylvester basalts ... 31
12. TiO_2 vs. K_2O, Ba, and Rb; Zr vs. K_2O, Sylvester basalts ... 31
13. $MnO-P_2O_5-TiO_2$, Sylvester basalts ... 32
14. Ti vs. Zr, Sylvester basalts ... 32
15. Ti vs. Cr, Sylvester basalts ... 32
16. Ti vs. V, Sylvester basalts ... 33
17. Nb-Zr-Y, Sylvester basalts ... 33
18. Pearce element plots ... 34
19. Sun multi-element plots ... 34
20. REE plots ... 34
21. Diagrammatic view of the evolution of the Sylvester allochthon ... 36
22. Metamorphic assemblages in the Sylvester allochthon ... 43
23. Metamorphic conditions in the Sylvester allochthon, P-T grid ... 44
24. $T-XCO_2$ grids a) below invariant point b) above invariant point ... 44
25. Lead isotopic data for Cassiar-Rancheria area ... 54
26. Temperatures of total homogenization versus melting of ice and/or clathrate for Cassiar area fluid inclusions ... 57
27. Pressure-temperature constraints for Erickson vein formation imposed by fluid inclusions and metamorphic equilibria ... 60
28. Geology around the Cassiar and McDame asbestos mines ... 61
29. Geology around the Midway deposit ... 65

PLATES

1. View of the town of Cassiar from Marble Creek ... 3
2. Espee Formation, limestone and phyllite ... 5
3. One of the skarn zones on Mount Haskin, looking north ... 6

Page

4. Kechika Group slate with limestone interbeds ... 7
5. Crossbedding in Tapioca sandstone ... 9
6. The Tapioca sandstone - McDame Group contact east of the Tootsee River ... 10
7. McDame Group limestone next to the Midway deposit ... 11
8. Well-bedded grey radiolarian chert, Unit IMs ... 17
9. Chert-quartz pebble grit, Unit IIMvs north of Snowy Creek ... 20
10. Feeder zone to Division II basalt ... 21
11. Breccia in Unit IIPPvs north of Snowy Creek ... 22
12. View of the Zus Mountain ultramafite from the west ... 23
13. The western strand of the Blue Dome fault zone east of Quartzrock Creek ... 24
14. Breccia in the Foggy Mountain gabbro body ... 25
15. Interbedded calcarenite and chert, Unit IIIPPs, near Black Friday Lake ... 27
16. Detail of Unit IIIPi. Leucotonalite intrudes tonalite ... 29
17. Thrust fault in south-central Tootsee Lake map area, looking southwest ... 41
18. The main Erickson mine in 1988 ... 55
19. The Vollaug vein, underground ... 56
20. Large type-2 inclusions in clear quartz ... 58
21. The south wall of the Cassiar mine pit in 1989, just prior to closure ... 62
22. Breccia underground at Midway ... 63

TABLES

1. Macrofossil localities ... 8
2. Conodont and radiolarian localities ... 12
3. Event-stratigraphic comparisons among the Sylvester allochthon and other terranes ... 37
4. Potassium-argon data from the Midway-Cassiar project area ... 39
5. Mines and mineral deposits and occurrences ... 48

APPENDICES

1. Descriptions of conodont collections, excerpted from the Cordilleran Conodont Data File by M.J. Orchard ... 75
2. Whole-rock and trace-element data ... 87
3. Fluid inclusion data from Cassiar area quartz veins ... 92
4. Metamorphic assemblages in the Sylvester allochthon ... 95

SUMMARY

The Midway-Cassiar project area, located in the Cassiar Mountains of far northern British Columbia, spans two distinct but inter-related terranes, the pericratonic Cassiar Terrane and the Slide Mountain Terrane, represented by Sylvester allochthon, a large, complex eugeosynclinal klippe. Cassiar Terrane exposures are of platformal to continental-slope, deep-water strata that range from late Proterozoic to Early Permian in age. These units have widespread correlatives along the ancient North American continental margin.

In the project area, the Sylvester allochthon comprises three structurally stacked divisions, each of which represents a separate late Paleozoic tectonic and depositional environment. Upper Triassic sediments are restricted to the highest structural level in Division II. It is suggested that they correlate with autochthonous Triassic strata in the Rocky Mountains and Selwyn basin. Division I, the lowest and therefore assumed to represent the facies originating closest to the late Paleozoic continental margin, is primarily a sedimentary sequence with strong similarities to the Earn Group and overlying Mississippian to Early Permian chert and argillite which occurs at the top of the Cassiar Terrane stratigraphic succession. Division II is an ophiolitic assemblage. It contains fragments of oceanic, ultramafic-gabbroic basement and stratified early Mississippian to Early Permian sequences of interbedded basalt, sediments and diabase sills. Significantly, siliciclastic units identical to Earn Group sandstones are intimately interbedded with basalt flows and tuffs in Division II.

Division III is a late Paleozoic island-arc package that resembles Yukon Tanana and Harper Ranch Terrane assemblages, rather than the Slide Mountain Terrane. It contains three suites: a pyroclastic-epiclastic sedimentary sequence with interbedded continentally derived sandstones, that is intruded by an early Mississippian pluton; a widespread Pennsylvanian-Permian island-arc edifice with fringing reefs and chert-limestone-epiclastic marginal facies; and an Early Permian intermediate pluton with a later potassium-rich volcanic suite.

Geochemical data reflect a mid-ocean-ridge signature for Division II igneous rocks and an island arc signature for Division III, in keeping with their lithologic character and associations. It is believed that Divisions I and II developed within a small, marginal ocean, which opened initially during a Devono-Mississippian rifting event that affected the entire North American continental margin, and continued to spread slowly behind the developing arc of Division III. The fusulinids in Division III resemble those in other marginal terranes from Mexico to northern Washington State, rather than those on the North American craton. The paleogeographic significance of this persistent east-west provinciality remains unclear.

The diverse geology of the Midway-Cassiar project area is reflected in its metallogeny. Deposits include Devono-Mississippian exhalites in the Earn Group and Sylvester allochthon, the Cassiar and McDame asbestos deposits in Sylvester serpentinites, the Erickson and Taurus gold deposits in mesothermal quartz veins, and silver-lead-zinc mantos, tungsten skarns and porphyry molybdenum deposits. The single-phase carbonic fluid types that generated the gold-quartz veins were introduced at 1.4 to 2.2 kilobars (140-220 MPa) total pressure and a temperature of 350 to 400°C, while the mantos resulted from two phases introduced within a temperature range of 280 to 340°C. There are strong geological ties between the Midway silver-lead-zinc manto deposit and Late Cretaceous intrusions, porphyry deposits and skarns.

CHAPTER 1: INTRODUCTION

LOCATION, ACCESS AND TOPOGRAPHY

The Midway-Cassiar project area covers approximately 3000 square kilometres in the Cassiar Mountains of northern British Columbia, between the Dease River and the Yukon border near Rancheria (Figure 1a, b). It includes the town of Cassiar, the Cassiar-Erickson mining camp and the Midway silver-lead-zinc deposit 20 kilometres southeast of Rancheria.

Cassiar is connected to the Stewart-Cassiar Highway by a short branch road. The Erickson and Taurus properties are easily accessible by road. Unimproved four-wheel-drive roads lead into other properties near Cassiar. The Stewart-Cassiar Highway joins the Alaska Highway 20 kilometres west of Watson Lake, Yukon. The Midway property is reached by a 20-kilometre dirt road that leads south from Mile 701 on the Alaska Highway. This road is subject to bridge washouts where it crosses the Rancheria River. The remainder of the area is remote. During the course of the project, a helicopter based in Watson Lake, and a pack train based near Cassiar, were used for travel within the area.

The Cassiar Mountains are moderately rugged, with peaks rising to 1600 to 2200 metres. Intervening glaciated valleys are broad and show subdued topography. Many of them contain thick blankets of till, although bedrock is extensively exposed in others, notably the lowlands around the Erickson and Taurus mines. Timberline is at 1400 metres; lowland forests range from open jackpine stands in well drained areas, to pernicious tangles of black spruce on north-facing slopes and on swampy substrates. Rock exposure above timberline is excellent.

The area has been subjected to both regional and valley glaciation. Prominent glacial features record the most recent ice retreat. At ice maximum, regional flow was from southwest to northeast. Boulders of granite from the Cassiar batholith form debris on summits and ridges throughout the map area. To the east, on the Liard plain, drumlinoid features trend northeast to east-northeast (Gabrielse, 1963).

HISTORY OF EXPLORATION AND MINING

The Cassiar area was first prospected for placer and bedrock gold in the late 19th century. Placer gold was discovered on McDame Creek in 1874, and 2.2 million grams were produced by 1895 (Diakow and Panteleyev, 1981). Hard-rock veins were not discovered until the 1930s. Free gold in quartz veins on Troutline Creek was discovered by F.F. Callison in 1934; John Vollaug, David Wing and others discovered many of the presently known veins a short time later. Small gold mining operations dominated the area until Erickson Gold Mines Limited (now Total Energold Corporation) consolidated holdings and commenced a combined operation on the Jennie and Maura veins (Erickson main mine) in 1979. The operation eventually included the Vollaug and Cusac veins as well.

The Cassiar asbestos deposit was staked in 1950 and put into production in 1953. Mining operations in the Cassiar open-pit terminated in 1989. The Cassiar mill was fed from the McDame orebody, an underground deposit 500 metres southeast of the pit, until mine closure in early 1992.

The first discoveries near the Yukon border, the Amy and Silvertip showings, were made after World War II. The Amy property is significant in that its current reserves are 73 000 tonnes grading 367 grams per tonne silver with 9 per cent combined lead-zinc. The Silvertip showing, although small, is about a kilometre from the buried Midway deposit. Midway itself was discovered by Regional Resources Ltd. in 1983, in the course of drill-testing economically insignificant exhalites in the overlying Earn Group slates.

PREVIOUS GEOLOGICAL WORK

The project area lies within the McDame (104P) and Jennings River (104O) map areas, first mapped at 1:250 000 scale by H. Gabrielse of the Geological Survey of Canada (Gabrielse 1963, 1969), although Poole's (1957) map of the Wolf Lake area in southern Yukon extends into the northern part of the Tootsee Lake area. Wolfe (1965) and Pinsent (Pinsent and Hirst, 1977) studied the Blue River ultramafite. The Cassiar-Erickson camp has been the focus of a number

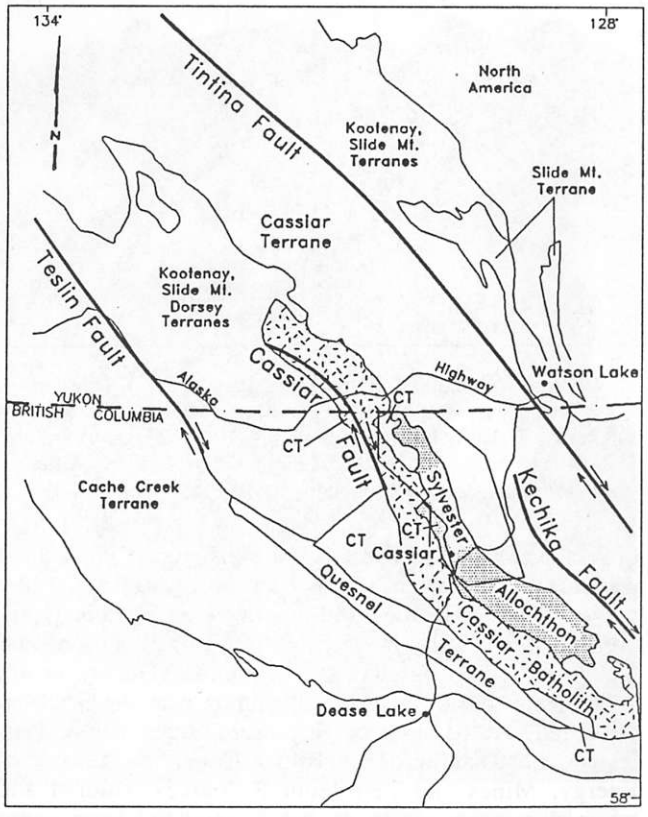


Figure 1a. Location map of project area, showing terranes and major faults. CT=Cassiar Terrane.

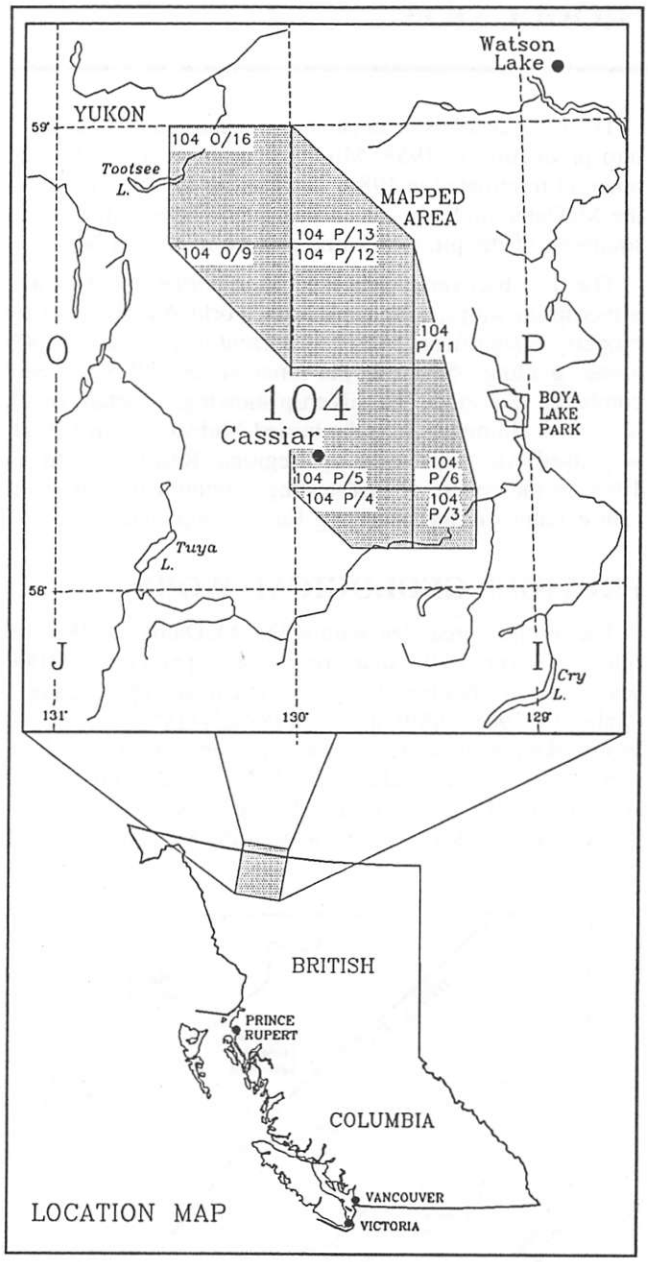


Figure 1b. National Topographic System (NTS) index of project area. 104O/16:Tootsee Lake, 104O/9:Chromite Creek, 104P/13:One Ace Mountain, 104P/12:Blue Dome, 104P/11:Dot Lake, 104P/05:Cassiar, 104P/06:Centreville, 104P/04:Needlepoint Mountain, 104P/03:McDame.

of geological studies although, until this project, no detailed geological maps of the camp have been available to the public. Theses on the gold-quartz veins include Grant (1981), Wei (1982), Hooper (1984), Dussell (1986) and Sketchley (1986). Gordey and Gabrielse (Gordey *et al.*, 1982) mapped the Sylvester allochthon near the Erickson mine and created a set of very useful subdivisions. Panteleyev and Diakow of the British Columbia Ministry of Energy, Mines and Petroleum Resources, studied and mapped mineralization of the Cassiar-Erickson camp (Diakow and Panteleyev, 1981; Panteleyev and Diakow, 1982). Their very detailed unpublished maps have provided data for our compilations. Other sources include coverage by C.J. Bloomer (1981) of Shell Minerals Canada and an informal 1:50 000 map of the Cassiar area by Ian Lyn (1983) of Brinco Limited.

The work of Tekla Harms in and near the Sylvester allochthon (Harms, 1986), although not within the immediate project area, provided a framework for our understanding of the Slide Mountain Terrane and for the thrust duplexes developed in the autochthonous strata below it.

PRESENT STUDY

This study began in 1986, as one of several regional mapping projects funded by the Canada/British Columbia Mineral Development Agreement 1985-1990. Its aim has been to produce detailed geological maps of the area between the Midway deposit and the Cassiar-Erickson camp, in order to increase understanding of the geological setting of these deposits and guide further exploration.

Geological map coverage at 1:25 000 scale now includes Tootsee Lake-104O/16 (Open File 1987-5), Blue Dome-104P/12 (Open File 1988-10), Cassiar-104P/5 and McDame NW 1/4-104P/3 (Open File 1989-9) and Needlepoint Mountain, NE 1/4-104P/4 (Open File 1989-19) (*see* Figure 1b). Nelson and Bradford are the senior authors of all of these maps, with the exception of Open File 1989-19, which was produced by Tekla Harms in cooperation with Total Energold (Erickson) geologists (Harms *et al.*, 1989). Figure 2 in pocket is a compilation and revision of the Open File maps at 1:100 000 scale, with additional mapping at 1:25 000 and 1:50 000 scales in bordering areas of the Chromite Creek (104O/9), One Ace Mountain (104P/13) and Good Hope Lake (104P/6) map areas, completed in 1989.

John Bradford's M.Sc. thesis (Bradford, 1988) involved geological mapping of the northwest quarter of 104O/16 in 1986 and a detailed study of the Midway silver-lead-zinc manto deposit.

ACKNOWLEDGMENTS

Able field assistants Kim Green, Henry Marsden, Mary MacLean and Louise Maddison contributed hard work and good ideas to the project. Discussions with Jim Hylands (Regional Resources Ltd.), Henrik Thalenhorst (Strathcona Minerals Services Ltd.), Matt Ball and Peter Fischer (Total Energold Corporation) and Roger Tyne (Cassiar Mining Corporation) improved our understanding of the ore deposits in the area. Hubert Gabrielse, Tekla Harms and Andre Panteleyev were generous in sharing their extensive knowledge. I am especially grateful for Gabe's eagle-eyed perusal and review of the manuscript. Brian Grant, John Newell, and draftsperson Martin Taylor, made many improvements to the text and maps. M.J. Orchard's conodont identifications provided an essential framework for understanding the Sylvester allochthon.

CHAPTER 2: GEOLOGY

INTRODUCTION

The Midway-Cassiar map area, shown in Figure 2, embraces two terranes: the para-autochthonous, miogeoclinal Cassiar Terrane, a sliver of the North American continental margin displaced northward at least 450 kilometres along the dextral Tintina fault; and the Slide Mountain Terrane represented by the Sylvester allochthon, a thrust-floored eugeosynclinal assemblage (Wheeler *et al.*, 1988). The Sylvester allochthon rests on top of platformal and siliciclastic strata of the Cassiar Terrane (Plate 1). It occupies an open synformal structure, the McDame synclinorium (Gabrielse, 1963). The mid-Cretaceous Cassiar batholith and younger intrusions cut both terranes. Emplacement of the Sylvester allochthon to its present position on top of the Cassiar Terrane is constrained locally to be post-Late Triassic and pre-mid-Cretaceous.

MIOGEOCLINAL STRATIGRAPHY

The Cassiar Terrane is part of the ancestral North American miogeocline. As described by Gabrielse (1963) and Harms (1986), its stratigraphy ranges in age from Late Proterozoic through early Mississippian (Figure 3). In addition, this paper places late Mississippian to Permian cherts and argillites that lie above the Devono-Mississippian Earn Group at the top of the autochthonous stratigraphic succession (Figure 3), instead of within the Sylvester allochthon as previously inferred (Nelson and Bradford, 1989).

Ingenika Group

ESPEE FORMATION (UPPER PROTEROZOIC)

Upper Proterozoic strata in the Cassiar Mountains were originally assigned by Gabrielse (1963) to the Good Hope Group, a locally defined unit. Similarities of these strata to other Upper Proterozoic sequences in the eastern Cordillera has led to usage of more widespread stratigraphic terminology. They are now included in the Ingenika Group (Mansy and Gabrielse, 1978). The Ingenika Group is divided into four formations; the upper two, the Espee and Stelkuz formations, are exposed within the map area.

The Espee Formation is the oldest exposed stratigraphic unit. It outcrops within thrust panels from Poorman Lake south to Good Hope Lake (Figure 2), where Espee-Stelkuz

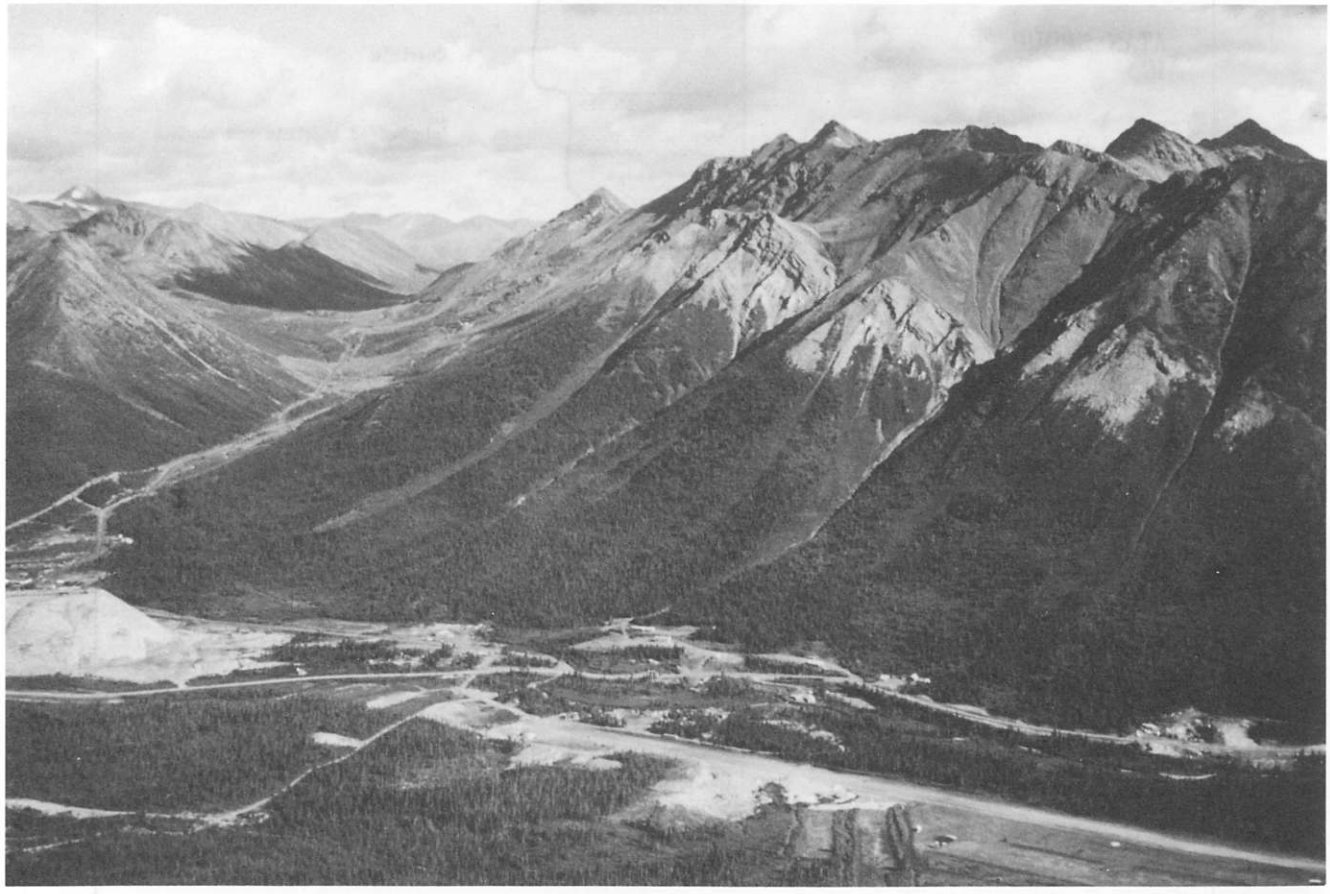


Plate 1. View of the town of Cassiar from Marble Creek. Dark-coloured basalt and interbedded black argillite, chert and sandstone of Unit IIMvs at the base of the Sylvester allochthon form the high ridges of Mount McDame, contrasting with the pale grey McDame Group limestone below. A thin recessive interval of Earn Group slate lies between them.

R

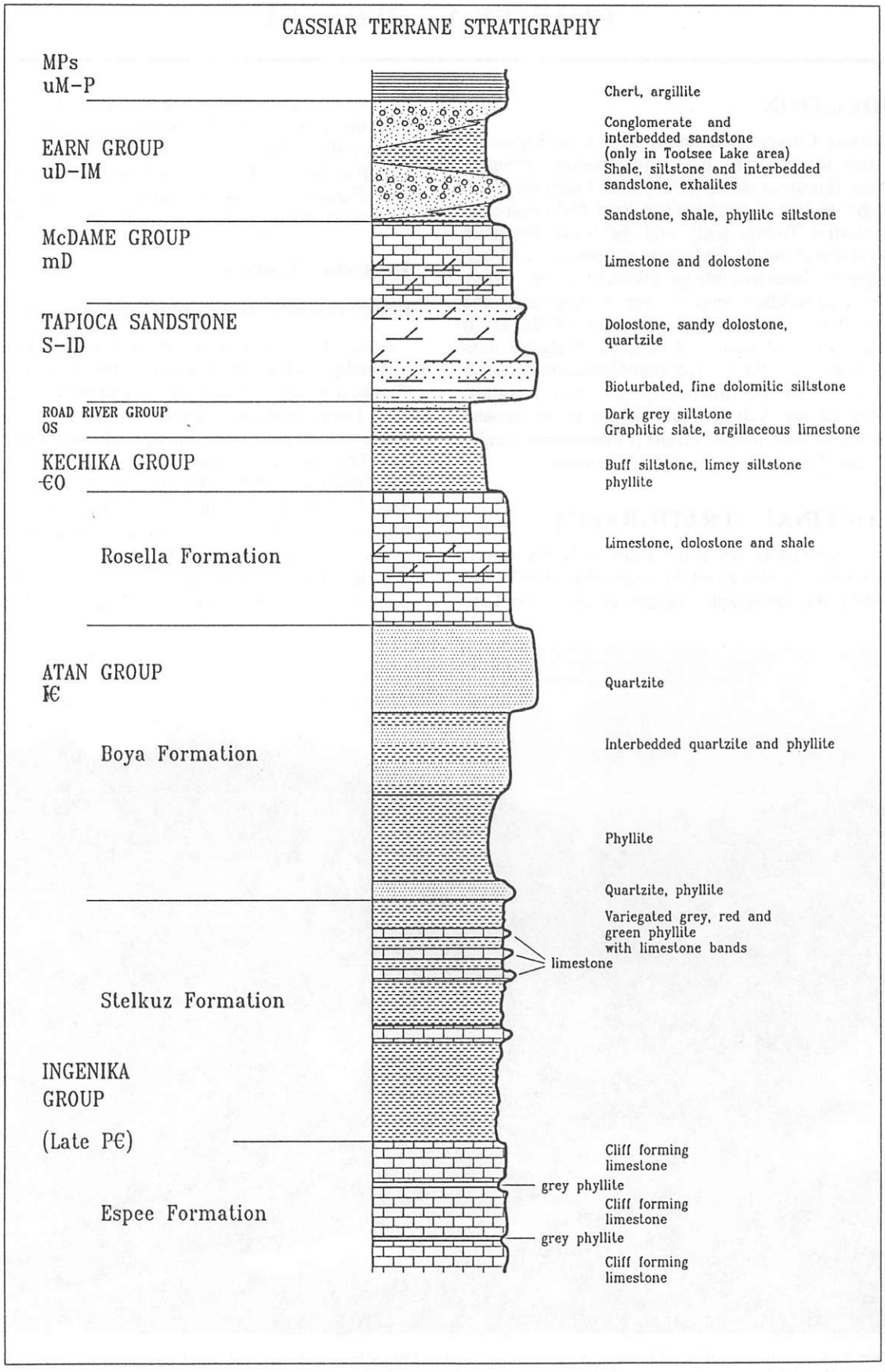


Figure 3. Stratigraphic column of the Cassiar Terrane.

sections were described by Mansy (1978). It is at least 700 metres thick, its base truncated against thrust faults (Figure 2). It consists of thick-bedded limestone and dolomite with olive-green to grey phyllitic partings, with more recessive-weathering intervals of thinner bedded carbonate and a greater percentage of phyllite (Plate 2). In the valley east of Mount Haskin, the Espee Formation outcrops as two bold limestone bands separated by a forested section corresponding to the more phyllite-rich interval.

STELKUZ FORMATION (UPPER PROTEROZOIC)

The Stelkuz Formation lies between the Espee and the Boya formations in thrust panels between Poorman and Good Hope lakes, where its thickness ranges from 400 to 700 metres (Figure 2). It also forms the base of a homoclinal, northeasterly dipping panel against the Cassiar batholith on the west side of the Cassiar map area. It shows a different character in these two areas, which are separated by the core of the McDame synclinorium. In the eastern exposures, it consists of grey, brown, and bright maroon phyllite and intervals of fairly massive limestone that range from 5 to 100 metres thick and make up approximately 25 per cent of the unit. Unlike Mansy (1978) and Fritz and Crimes (1985), we included all sandstones in the Boya Formation, thus placing the maroon phyllite marker horizon near the top of the Stelkuz Formation, about 100 metres below the lowest white quartzite that marks the base of the Boya Formation. The maroon phyllite marker – the "redbed marker" of Mansy and Gabrielse (1978) – occurs at the base of a carbonate rib. It includes green as well as maroon phyllite, and a distinctive chip-breccia, perhaps of storm origin. The Stelkuz limestones persist as bold ribs into areas of sparse outcrop, such as the lowlands south of Poorman Lake.

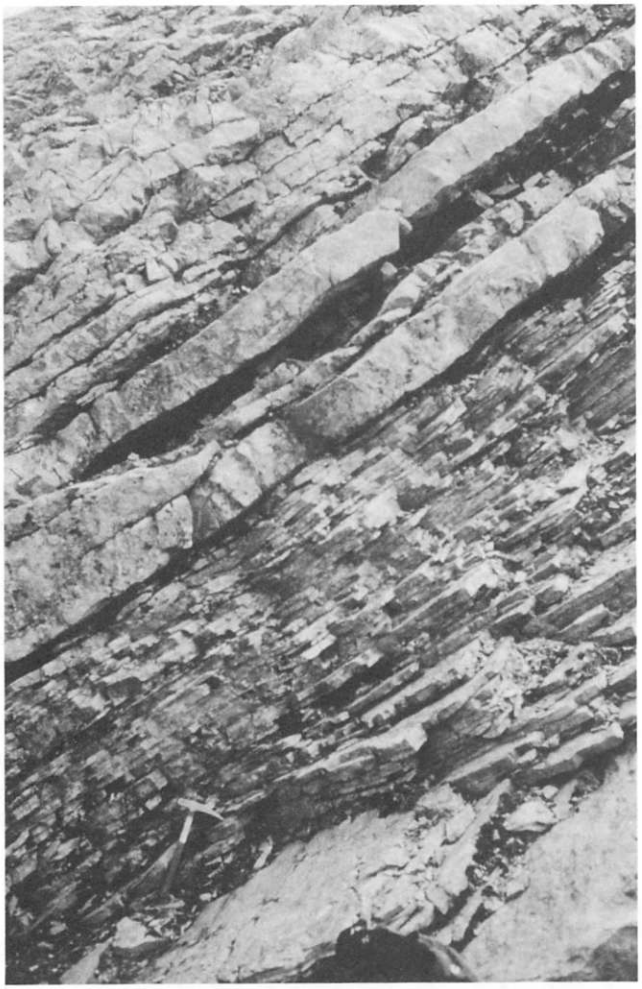


Plate 2. Espee Formation, thin-bedded limestone and recessive, olive-green phyllite.

On the west limb of the McDame synclinorium, the Stelkuz Formation is primarily phyllitic. Its exposed thickness between the granite and the overlying Boya Formation is about 1000 metres. It consists, from its base upwards, of: 200 metres of phyllite with minor quartzite, argillite and dolomitic sandstone; 350 to 400 metres of siltstone with two prominent limestone ribs 5 to 10 metres thick that continue along strike for more than 15 kilometres; and 400 metres of green to olive-brown phyllite with very minor quartzite. The contact with the overlying Lower Cambrian Boya Formation is gradational, with quartzite gradually increasing upsection. The contact is placed at the base of the lowest thick quartzite bed.

This section differs markedly from the Stelkuz sections near Good Hope Lake. A late Upper Proterozoic facies change is apparently concealed by the Sylvester allochthon. The western section strongly resembles the Stelkuz Formation described by Murphy (1988) in the north-central Wolf Lake map area in southeastern Yukon, except for the presence there of significant amounts of metasandstone. The Stelkuz-Boya contact seems to have a more transitional character in southeastern Yukon than in the Cassiar map area.

ATAN GROUP

The Atan Group of Gabrielse (1963) was formally subdivided by Fritz (1980) into a lower siliciclastic unit, the Boya Formation, and an upper carbonate unit, the Rosella Formation. Fritz (1980; Fritz and Crimes, 1985) also placed the base of the Boya Formation below the lowest thick white, resistant, quartzite bed but above 190 metres of light-coloured, recessive quartzite. We have adhered to this usage, except for some areas of the Rosella Creek drainage where resistant white quartzite is lacking and the transition from Stelkuz shale and carbonate to coarse brown sandstone is abrupt. There, the base of the Boya Formation (Figure 2) is placed below the lowest sandstone observed.

BOYA FORMATION (LOWER CAMBRIAN)

The Boya Formation is exposed on both sides of the McDame synclinorium, commonly as rubbly subcrops. Complete outcropping sections are located west of the Lamb Mountain porphyry molybdenite showing in the Cassiar map area (MINFILE 104P 003, Figure 2) and northeast of the French River (Plate 3). The formation is a siliciclastic sequence which consists predominantly of quartzite with varying percentages of interbedded slate and siltstone. Sections northeast of the French River, measured by Pope

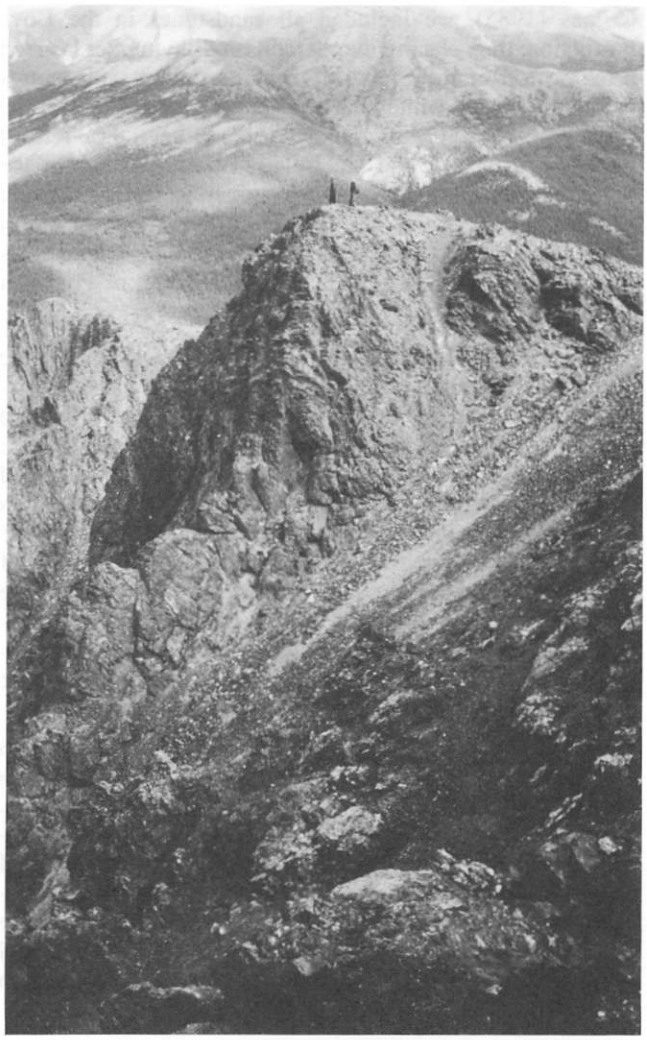


Plate 3. At one of the skarn zones on Mount Haskin, looking north. The ridge in the foreground is underlain by hornfelsed Kechika Group limy slate. The hills in the background east of the French River are underlain by thrust-imbricated Rosella and Boya Formation strata.

(1989a, b), consist of two members: a lower member of clean, well-sorted white, green and pinkish quartzite, locally micaceous and commonly crossbedded, with minor quartz-pebble conglomerate and an upper member of rhythmically interbedded, grey-weathering, thin-bedded siltstone and brown-weathering medium-bedded sandstone. The upper member is gradational into the interbedded siltstone and limestone of the lowermost Rosella Formation.

Red slate appears locally at the top of the Boya Formation in the core of the antiform northeast of the Little Blue River in the Blue Dome map area. This red slate may have been the precurser of similar slates that occur nearby within the overlying Rosella Formation. The distinction of these slates from the maroon phyllite marker is made on the basis of their association with predominantly siliciclastic and thick-bedded carbonate strata, which are unlike the banded shales and limestones of the Stelkuz Formation.

Western exposures of the Boya Formation contain less quartzite and greater percentages of dark slate; for instance, the excellent section west of Lamb Mountain, where dark grey phyllite intervals of 50 metres or more separate thinner quartzite intervals. In the southwestern corner of the Tootsee Lake map area, a thrust panel of Boya(?) Formation, in contact with the Cassiar batholith, contains a turbiditic sequence of dark grey to black slate, quartzite, crossbedded siltstone, and quartz-pebble conglomerate with minor black limestone interbeds. Boya exposures near the Tootsee River are dominated by black slate and siltstone with lesser quartzite.

In general, the Boya Formation seems to represent a shallow marine fan-top facies on the eastern limb of the McDame synclinorium, as evidenced by the crossbedded sandstones and red slates; and a deeper water, prograding fan facies on the western limb. The sites of deposition of these two facies have been telescoped by thrusting.

ROSELLA FORMATION (LOWER CAMBRIAN)

Carbonates of the Rosella Formation outcrop boldly on both limbs of the McDame synclinorium. Its Early Cambrian age was established by Gabrielse (1963) on the basis of archeocyathid and trilobite collections; Fritz (1980) gave it formal status and named it for the dramatic limestone mountains that surround Rosella Creek. Other boldly outcropping sections are seen in the Marble Creek watershed southwest of Cassiar, and in the mountains northwest of the Cassiar mine. It also forms prominent isolated hills in the eastern Blue Dome map area. The Rosella Formation consists of thin to thick-bedded limestone with recessive slatey or muddy interbeds. The limestone is in part extensively replaced by orange-weathering, coarse secondary dolomite. On the eastern limb of the synclinorium, it ranges from 200 to 700 metres thick, while in the western Cassiar map area, it ranges from 70 to 800 metres thick.

A number of measured sections near the French River, incomplete because of thrust faults, contain thicknesses up to 270 metres (Pope, 1989a, b). In them, a lower member contains interbedded siltstone and thin to medium-bedded limestone with archeocyathids and trilobite fragments. This is overlain by thin to thick-bedded limestone which locally contains abundant oolitic and intraclastic horizons.

West of Lamb Mountain, the Rosella Formation is 300 metres thick and consists, from base to top, of blue-grey pure marble, thin-bedded marble partly replaced by dolomite, dark hornfels, and a second limestone-dolomite unit. In the Marble Creek drainage, the Rosella is 800 metres thick and dominated by very thick bedded marble with large areas of dolomite and only sparse, thin, tan-weathering slate interbeds.

Pope (1989a,b) interpreted the Rosella Formation in the French River drainage as recording a lagoonal environment with archeocyathid-bearing patch reefs; the oolitic areas represent forereef environments. This implies a fluctuating shoreline.

KECHIKA GROUP (CAMBRO-ORDOVICIAN)

The Kechika Group overlies the Rosella Formation along a poorly exposed contact. Its only outcrop within the map area is in the strongly hornfelsed section west of Lamb Mountain. The age of the Kechika Group is bracketed

stratigraphically between the Lower Cambrian Rosella Formation and the overlying Ordovician-Silurian Road River Group. The Kechika Group is nearly unfossiliferous; in our study we obtained a single trilobite head and some indeterminate fossil (trilobite?) hash. The group is a thick, monotonous, distinctive unit of pale calcareous slate with sparse, thin, poddy limestone interbeds (Plate 4). The slates are golden to light olive-green and grey, and are very well cleaved. Overall structural thickness ranges from 400 to 1000 metres. The Kechika Group, because of its incompetent nature, is probably tectonically thickened.

Near the Cassiar batholith, the Kechika Group consists of thin-bedded biotite-calcsilicate hornfelses. It is distinguished from the Road River Group by its light colours and by the characteristic ribboning of thin marbles in the slates. Its base is a sharp contact with massive Rosella limestone.

Road River Group (Ordovician-Silurian)

The Road River Group is prominent on the western limb of the McDame synclinorium, and is less abundant on the eastern limb within the mapped area. It thins and probably interfingers with the Kechika Group to the east (Gabrielse, personal communication, 1991). Gabrielse (1963) recognized its characteristic black graphitic slates on both limbs of the synclinorium; and later suggested their separation from the Kechika Group and correlation with the Road River Group of the Selwyn and Kechika basins (H. Gabrielse, personal communication, 1986).

Most of the Road River Group consists of black, graphitic, commonly sooty calcareous and noncalcareous slates and lesser, black thin-bedded limestone. Its uppermost unit is in part the 'Silurian siltstone', a platy, grey calcareous siltstone that may contain *Diplograptus* fragments up to 10 centimetres long along bedding planes. Smaller, poorly preserved graptolites are common in the lower part of the Road River Group, where cleavage has not obliterated bedding surfaces. Graptolite collections from Big Creek in the Tootsee Lake map area are of Middle Ordovician (Caradoc) age (Locality 212, 213; Figure 2 and Table 1). This is in agreement with the Ordovician ages of graptolite collections from a number of 'Kechika' - (now Road River) localities in the McDame 1:250 000 map area (Gabrielse, 1963).

The Road River Group is a structurally incompetent unit and deformation within it has been strong. It is commonly imbricated with its overlying strata; a major décollement at its base resulted in independant duplexing of the Kechika Group and underlying units.

Tapioca Sandstone (Silurian - Lower Devonian)

The Tapioca sandstone is a massive-weathering, light-coloured dolomite-quartz arenite unit that abruptly overlies the dark, recessive slates of the Road River Group. It consists of two end-members: grey, buff-weathering dolomite and white to grey quartzite; and mixtures of the two, the diagnostic 'Tapioca' sandstone in which very well rounded spherical grains of clear quartz float in a dolomitic matrix. Herringbone crossbedding is locally well developed

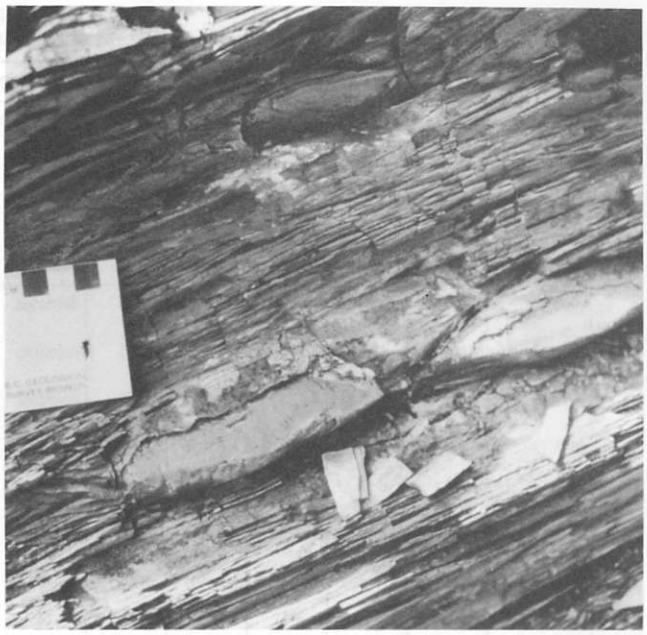


Plate 4. Kechika Group pale-coloured limy slate with boudinaged limestone interbeds.

(Plate 5). Paleocurrent directions box the compass, with preferred north-to-south and south-to-north orientations; tidal deposition is indicated. In places, the basal unit of the Tapioca sandstone is a fine sandstone with wavy, bioturbated laminations. This may indicate a transition, albeit an abrupt one, upwards from the Silurian siltstone.

The Tapioca sandstone is a partial facies equivalent of the Sandpile Group of Gabrielse (1963), which is mainly exposed east of the Kechika fault. Its age is more restricted: whereas the Sandpile Group contains carbonate strata as old as Late Ordovician, on the limbs of the McDame synclinorium the Tapioca sandstone lies above the Silurian siltstone unit, determined near Sheep Mountain to be of early or middle Silurian age (Gabrielse, 1963).

The Tapioca sandstone is also distinct from the Sandpile Group in that it does not contain fossiliferous and cherty dolomite and extensive dolomite breccia. The similarities and contrasts between the Sandpile and Tapioca sandstone can be explained as a westerly change from a reefal environment in Late Ordovician through Silurian time east of the present Kechika fault, to a deeper water, shelf-slope environment west of the fault, which evolved from a starved basin in Ordovician time to a platform by the middle Silurian.

Sandpile Group (Ordovician-Silurian)

In the eastern Blue Dome map area, carbonate strata directly overlying the Kechika Group have been assigned to the Sandpile Group. They include dolostone, dolomitic quartz arenite, dolomitic siltstone, dolostone breccia and limestone. Poorly preserved graptolites and crinoids are locally abundant. This fossiliferous character, in addition to the presence of limestone, distinguishes these strata from the Tapioca sandstone. They are located east of a probable

TABLE 1
MACROFOSSIL LOCALITIES

Map	Sample	GSC	Sheet	Easting	Northing	Unit	Lithology	Age	Species	Notes
214	86JN16-03/1	C143616	104O/16	419989	6635998	OSRR	limestone in black slate	probably Middle Ordovician-Middle Devonian	echinoderm debris; favositid? and probable colonial rugose corals; brachiopod fragments	identified by B.S. Norford
213	86JN20-13	C143615	104O/16	442601	6645681	OSRR	black limy slate	Middle Ordovician, Caradocian	*Dicranograptus* sp.	identified by B.S. Norford
212	86JN20-15	C143612	104O/16	442675	6645724	OSRR	black limy slate	Middle Ordovician, Caradocian	*Dicranograptus* sp.	identified by B.S. Norford
218	88JN28-09	C159204	104P/05	453242	6587319	SDTS	dolostone	probably Silurian or Devonian	echinoderm fragments; indeterminate tabulate corals; ?pentamerid brachiopod	identified by B.S. Norford
217	86JN20-01	C143608	104O/16	438356	6646369	SDTS	dolostone	Early Silurian to Carboniferous	possible solitary coral; *Syringopora* sp.	identified by B.S. Norford
216	86JN20-01	C143606	104O/16	438356	6646369	SDTS	dolostone	Early Silurian to Carboniferous	*Syringopora* sp.	identified by B.S. Norford
215	86JN03-12/1	C143624	104O/16	424711	6633086	SDTS	dolostone	Silurian or Devonian	echinoderm fragments; indeterminate solitary and colonial corals; rhynchonellid brachiopod	identified by B.S. Norford
219	86JB02-02/1	C143617	104O/16	423344	6648613	mDM	limestone	probably Middle Devonian	atrypid fragment showing part of spiralium	identified by A.W. Norris
220	86JB51-04/1	C143621	104O/16	421747	6646527	mDM	limestone	probably Givetian, Middle Devonian	undet. brachiopod fragments; fragmentary shell showing punctae, probably *Stringocephalus* sp.	identified by A.W. Norris
221	87KG13-3	C153832	104P/12	446077	6610363	lITrTMs	grey limestone	probably Late Triassic	serpenticone ammonoid indet., belemnoids indet.	identified by E.T. Tozer
224	88TH23-5	C159209	104P/04	461400	6561360	lITrTMs	grey limestone, argillaceous	Middle or Late Triassic	*Halobia* or *Daonella* species, indet.	identified by E.T. Tozer
222	88JN52-3	C159201	104P/12	454501	6587854	lITrTMs	grey bioclastic limestone	probably Triassic	large strongly plicated pectinid bivalve, halobiid? fragments, gastropods (indet.)	identified by E.T. Tozer
223	88TH22-7	C159208	104P/04	460780	6560685	lITrTMs	grey limestone	Middle or Late Triassic	*Halobia* or *Daonella* species indet.	identified by E.T. Tozer
203	87JN12-2	C153803	104P/12	448783	6607494	lITrTMs	grey limestone	Late Triassic	*Halobia* sp.	identified by E.T. Tozer
204	87KG13-1	C153804	104P/12	448228	6609036	lITrTMs	grey limestone	Late Triassic	*Halobia* sp.	identified by E.T. Tozer
205	87KG13-3	C153805	104P/12	446077	6610363	lITrTMs	grey limestone	Late Triassic	*Halobia* sp., ammonoid fragments	identified by E.T. Tozer
206	87KG11-5	C153806	104P/12	448391	6608908	lITrTMs	grey limestone	Late Triassic	*Halobia* sp.	identified by E.T. Tozer
202	87JN12-1	C153801	104P/12	448774	6607497	lITrTMs	grey limestone	probably Late Triassic	*Septocardia?* sp.	identified by E.T. Tozer
201	87JN14-5	C153802	104P/12	448100	6606477	lIIPPHv	limestone with pyroclastic	Early Permian	*Spirifirella* sp., productid brachiopod, bothrophyllid? coral, bryozoans, echinoderm stem	identified by E.W. Bamber
208	88LM39-4B	C159205	104P/03	479346	6558819	lIIPPHv	limestone pod in augite porphyry	Permian;? late Wolfcampian early Leonardian fusulinids	*?Schwagerina* Sp.	fusulinids — Rui Lin
209	88MM47-13	C159207	104P/03	471360	6555000	lIIPPs	limestone	Permian; early Leonardian fusulinids	productoid and ?spiriferid brachiopods, indeterminate; *Parafusulina* sp., *Schwagerina* sp.	brachiopods — E.W. Bamber; fusulinids — Rui Lin
210	88JN44-1	none	104P/03	473566	6555176	lIIPPs	limestone breccia	Late Permian, probably early Guadalupian	large fusulinids *Schwagerina* sp. and *Parafusulina* sp.; bryozoan fragments, ostracod shells	identified by W.R. Danner
207	88JN46-2	C159202	104P/03	475868	6556321	lIIPPs	limestone	probably Moscovian-Permian; early? Leonardian fusulinids	productoid and chonetid brachiopods, indeterminate; *Monodiexodina* sp., *Schwagerina* sp.	brachiopods — E.W. Bamber; fusulinids — Rui Lin
211	87JB22-7	none	104P/12	447266	6602205	lIIPIs	limestone	Probably Leonardian (Guadalupian; Ross 1969)	fragments *parafusulina;* brachiopod and pelecypod shell fragments. No giant *Parafusulina*	identified by W.R. Danner

splay of the Kechika fault (Figure 2). In general, the Kechika fault separates Sandpile-type Ordovician carbonate facies to the east from Road River black shales to the west. Gabrielse (personal communication, 1991) suggests that this is a faulted facies transition.

McDame Group (Middle Devonian)

The McDame Group comprises Middle to Upper(?) Devonian reefal-lagoonal carbonate strata that overlie the Tapioca sandstone. It is the host for the Midway manto deposit in the Tootsee Lake map area. The McDame Group consists of dolostone and somewhat lesser limestone. Sections vary in thickness, dolomite/limestone ratios, contact relationships with the underlying Tapioca sandstone, fossil content, and stratigraphic details from place to place in the mapped area.

The thickest McDame exposures are on the western side of the McDame synclinorium in the Tootsee Lake map area near the Midway deposit. Total thickness is approximately 350 metres, above an apparently transitional contact with



Plate 5. Crossbedding in Tapioca sandstone.

interbedded dolostone and quartz arenite of the Tapioca sandstone (Plate 6). The contact is drawn at the top of the uppermost quartzite bed. In the McDame Group, dark grey, laminated to massive, commonly fetid dolostone is overlain by dark grey, locally platy, partly dolomitized limestone containing abundantly fossiferous beds. Biostromal accumulation of *amphipora, stringocephalus, syringapora* and *stromatoporoids* indicates a flourishing fauna of low diversity (Plate 7). The presence of *amphipora*, algal laminae and stromatolites indicates a shallow-water subtidal to intertidal, lagoonal environment.

The McDame Group in the eastern Tootsee Lake map area, on the eastern limb of the McDame synclinorium, consists predominantly of massive to thin-bedded and laminated dolostone. Delicate colour laminations and synsedimentary, bedding-confined breccias form a minor but distinctive part of these sections. The fossiliferous limestone, which is so prominent west of the Sylvester allochthon, is missing here. It was either removed by pre-Earn Group erosion, or was never deposited. In the latter case, these exposures represent an intertidal environment, perhaps landward of the western *amphipora*-rich lagoons.

Sparse exposures in the Blue Dome map area make the McDame Group difficult to characterize: it is mostly dolostone, commonly fetid and in some cases fossiliferous. One canyon section 5 kilometres south of Alec Chief Creek contains an upper part, directly below the Earn Group, which is devoid of limestone and consists of finely laminated and massive dolostones, such as those in the eastern part of the Tootsee Lake map area, and polymictic dolostone breccias consisting of clasts up to several metres across. These spectacular breccias are poorly bedded and probably represent forereef or tidal-channel deposits. The Shawn barite prospect in the northern part of the Blue Dome map area is partly developed in polymictic dolostone breccias.

Similar breccias extend 6 kilometres along a horizon at the base of the McDame Group west of Gallic Lake. They are polymictic and clasts range from sand to boulder size in a dolostone matrix. Fragments are of dark grey to white dolostone, laminated dolostone and limestone. Clasts of immediately subadjacent Tapioca sandstone strata (quartzite and sandy dolostone) are conspicuously absent. Overlying these breccias, and everywhere in the Cassiar map area, are limestones with *amphipora* beds. Particularly fossil-rich exposures occur 6 to 9 kilometres north-northwest of Gallic Lake; they contain *Stringocephalus sp.*, bryozoa and corals as well as amphiporids.

Near the Cassiar townsite, the base of the McDame Group appears to be an unconformity where Tapioca sandstone strata are absent and McDame dolostones rest directly on black Road River slates. This unconformable relationship contrasts with the transitional contact seen in the northwestern Tootsee Lake map area. In the Cassiar pit, an outcrop described by O'Hanley (1990) shows an unconformity within the McDame Group. The entire carbonate section at this locality, well-exposed with Earn slate at its top and Road River sooty calcareous slate at its base, is less than 15 metres thick. It consists of a lower massive dolomite and an upper platy limestone. The dolomite is heavily solution-brecciated, with large irregular areas of dolomite chips floating in a matrix of white calcite. Its top surface is irregular and the platy limestone forms drapes over it.

Middle Devonian reefal carbonates correlative with the McDame Group are widespread on the North American miogeocline and continental platform, with the exception of deeper water basin-slope areas such as the Selwyn and the Kechika basins. These carbonates are important hosts not only for manto deposits such as Midway, but also for Mississippi Valley type deposits such as Robb Lake and Pine Point (Nelson and MacIntyre, 1988).

Earn Group (Upper Devonian - Lower Mississippian)

The siliciclastic Earn Group was deposited on previously uplifted and karsted strata of the McDame Group. Local relief for the top of the McDame Group is at a maximum in the western Tootsee Lake area, where it reaches 165 metres. Large karst tubes filled with coarse calcite occur near the Berg showings, and collapse breccias of black, basal Earn mudstone fragments occupy cavities at the top of the McDame on Donegal Mountain and Smoke Mountain (unofficial names of Figure 2). Karst holes on Hamlet

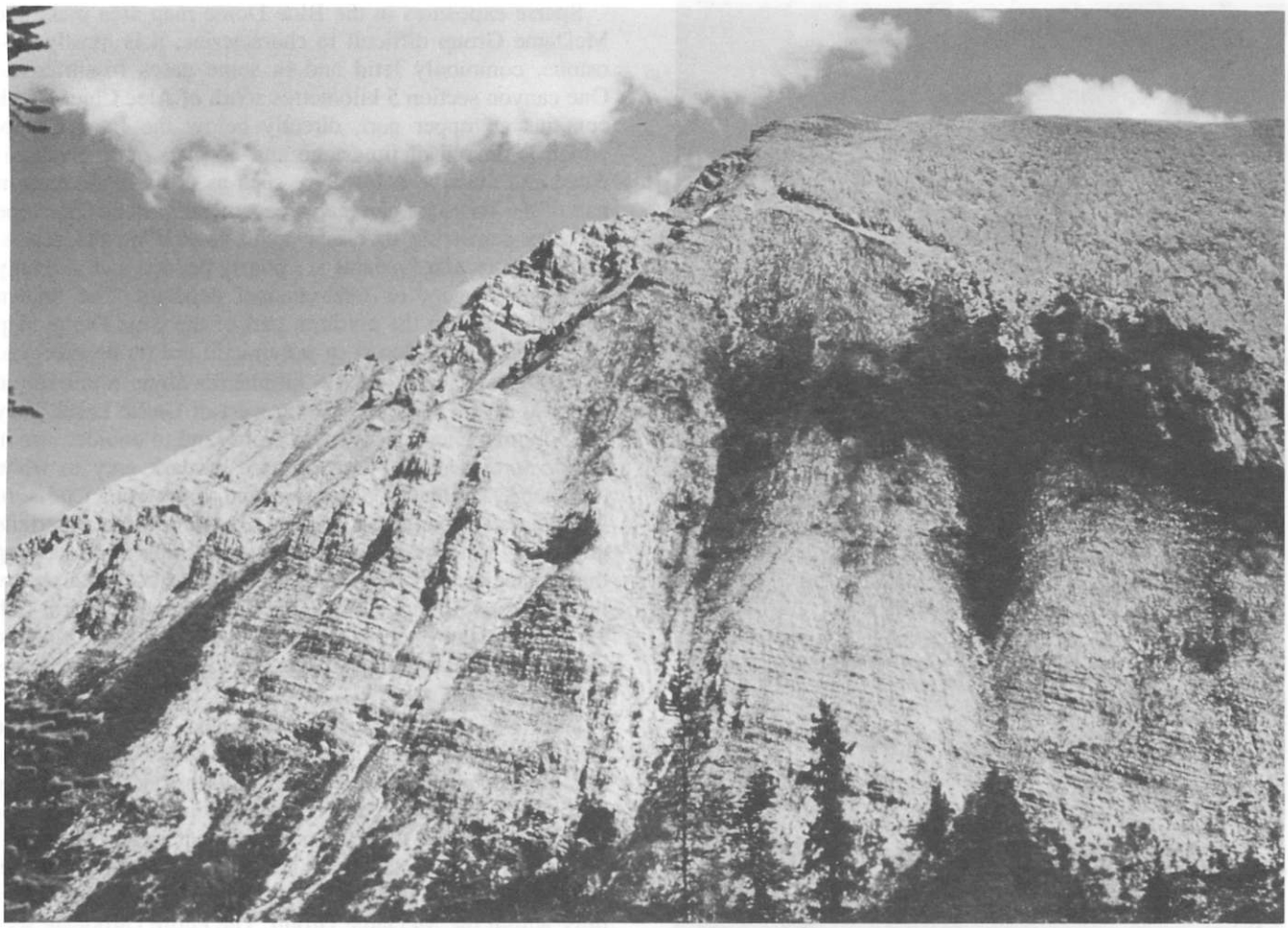


Plate 6. The Tapioca sandstone - McDame Group contact east of the Tootsee River. Here, the contact occurs across a broad zone of laminated to massive dolostone with sparse quartzite beds that decrease upwards.

Mountain are filled with pastel-coloured dolomitic sediments. These contain a Frasnian conodont fauna which is younger than the Givetian McDame Group but older than the Famennian basal Earn Group of the Cassiar Terrane. Evidence of karsting of the McDame Group diminishes southwards; in the Cassiar map area the McDame-Earn contact is essentially planar.

The Earn Group comprises two major facies in the project area. In the Tootsee Lake map area it is a thick sequence of proximal turbidite deposits interbedded with marine slates. Near the northern boundary of the Blue Dome map area, the Earn Group fines and thins dramatically to a distal, euxinic-basin facies in which very minor siliciclastic units (fine sandstones and siltstones) intertongue with black to grey slates, calcarenite and chert.

Earn Group lithologies include, in order of their abundance: black slate, chert-quartz sandstone, siltstone, grey 'gunsteel' slate, chert-quartz pebble to cobble conglomerate, thin-bedded calcarenite, chert, and baritic and silica-sulphide exhalites. Near the Midway deposit, two coarsening-upward cycles pass in ascending order from black slate into interbedded sandstone, siltstone, conglomerate and slate. Conglomerates are particularly notable in the upper coarse unit. Exhalite horizons are present in the upper of the two fine, slate-dominated units. The lower slate unit rests directly on McDame limestone and is of Famennian age. The upper fine unit is early to middle Tournaisian age (Nos. 18, 20, Table 2). The Earn Group in the Tootsee Lake map area is 650 to 1000 metres thick. By contrast, Earn sections in Blue Dome and Cassiar map areas thin from 350 metres near Alec Chief Creek in the north, to 50 to 100 metres in most of the Cassiar area. Famennian to middle Tournaisian conodont faunas in these rocks show that they represent a low-energy facies equivalent to the Tootsee Lake turbidite fan.

The siliciclastic components of the Earn Group here are identical to those in the Earn Group in the Selwyn basin (Carne and Cathro, 1982; Gordey *et al.*, 1986) and in the Kechika basin (MacIntyre, 1983; McClay and Insley, 1986). Most of the clasts are of grey to black chert and argillaceous chert, and quartz and quartzite. A few of the chert clasts contain radiolarian remains; most are recrystallized and could be either radiolarian or replacement chert. The polycrystalline quartz clasts show evidence of varying degrees of deformation prior to their incorporation in the matrix. Individual quartz grains show weak to strong undulatory extinction and may be subgrained and healed by trains of small neoblasts. Grain boundaries are strongly sutured.

These clasts are of metamorphic parentage, either directly or through recycling of older sediments. Ubiquitous trace clasts of plagioclase, muscovite, tourmaline and zircon also point to metamorphic or evolved granitic sources.

Near the Midway deposit, a few coarse conglomerates contain dolostone clasts derived from the McDame Group or Tapioca sandstone, which suggests derivation from local sources such as fault scarps. Erosion of the McDame Group prior to Earn deposition is shown by the strong relief on the contact and also by a steep syn-Earn normal fault on Donegal Mountain, which vertically offsets the base of the Earn Group by some 200 metres. This fault localizes the basal Earn breccia already described but does not penetrate a Mesozoic thrust fault.

The source of the chert and quartzite in the Earn is, here as everywhere, somewhat problematic. These clasts can be linked to miogeoclinal sources – the cherts to the Road River Group (which in the Selwyn basin contains abundant bedded radiolarian chert, *cf.* Carne, 1979) and also to replacement chert in carbonates (H. Gabrielse, personal communication, 1986); the quartz and quartzite clasts from siliciclastic units in the Ingenika Group, the Boya Formation and the Tapioca sandstone.

Most Earn siliciclastic units are virtually structureless A-E turbidites lacking current indicators. A few of the thin, fine sandstones are crossbedded; five current measurements from these indicate easterly to northeasterly transport. This is consistent with more extensive data from the Earn Group in the Selwyn and Kechika basins (Gordey *et al.*, 1986). The overall character of the Earn Group is also consistent with its other exposures, the intertonguing of coarse turbidite fans with larger areas of distal accumulation. Gordey (1988) ascribes these variations to local block-faulted uplifts, which contributed sediments to discrete fans within a broader basin. In one such uplift in the Yukon, Earn strata directly overlie Ingenika rocks with profound unconformity (Gordey, 1990). By contrast, within the Cassiar Terrane east of the Cassiar batholith, erosion represented by the sub-Earn unconformity nowhere removes even the entire McDame Group. The source region for the Cassiar Earn Group must have been uplifted miogeoclinal strata west of the batholith, or even terranes considered to be allochthonous, such as the Yukon-Tanana terrane.

UPPER MISSISSIPPIAN TO LOWER PERMIAN CHERT AND ARGILLITE

Regularly ribbon-banded radiolarian cherts with argillite partings (Unit MPs) overlie the Earn Group along most of the eastern and northern margins of the Sylvester allochthon. In the northeastern quarter of the Tootsee Lake map area such cherts are imbricated with the Earn Group (Figure 2). A similar but discontinuous chert package separates the Earn Group from the Sylvester allochthon near the Cassiar mine. Conodont and radiolarian ages obtained from this unit range from late Mississippian (No. 111, Table 2) to Permian.

Chert colours range from black through buff, red, green, olive and pink. One variation, seen in the thrust panel southwest of the Ewen barite showing, on Donegal Mountain in the Tootsee Lake map area, and 4 kilometres north of the Cassiar mine, is the 'salmon-and-green chert', a unit recognized within the Sylvester allochthon in the Cry Lake map area by Harms (1986), who assigned it a Pennsylvanian age. The salmon-and-green chert consists of regular, even, thin beds of salmon to pale green chert separated by thinner beds of green argillite.

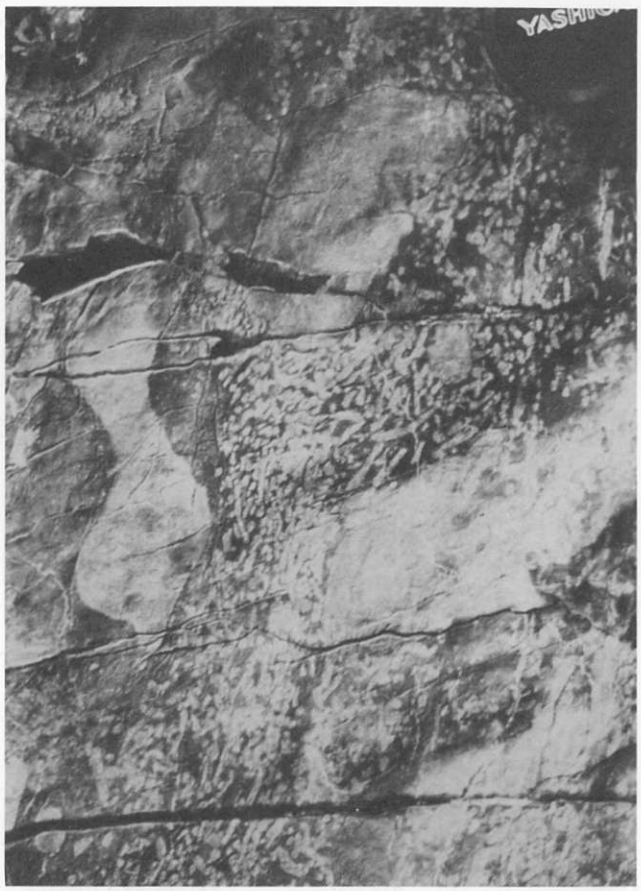


Plate 7. McDame Group limestone next to the Midway deposit, with amphipora and stromatoporoids.

A minor but characteristic component of Unit MPs is well-bedded chert-chip breccia, consisting of very angular but well-sorted chert clasts and showing graded bedding. These breccias are interbedded with chert and argillite. The angularity of the clasts suggests submarine erosion, possibly from fault scarps developed in lithified cherts. An active tectonic environment is implied. On the eastern margin of the allochthon, in the Cassiar map area, Unit MPs includes a few strongly vesicular green and maroon basalt flows with an alkalic, intraplate chemical signature (*see* details in section on whole-rock and trace-element geochemistry.)

The structural position of this Upper Paleozoic chert-argillite unit, between lower Mississippian strata of the Cassiar Terrane and obviously allochthonous units of the Sylvester allochthon, allows for two interpretations: one, that it is autochthonous and depositionally overlies the Earn Group; the other, that it is allochthonous and represents the basal thrust slice of the allochthon. Arguments for including

TABLE 2
CONODONT AND RADIOLARIAN LOCALITIES

Unit	Map No.	Sample	GSC	Sheet	Lithology	Age
mDM	8	86JN03-06	C143101	104O/16	pale dolomitic siltstone	Frasnian
DME	11	82MJO-BVH2	C087737	104O/16	baritic carbonate	Tournaisian
DME	12	82MW82003I	C102871	104O/16	limestone in black shale	Famennian-Visean
DME	21	84MJO-EWEN	C118275	104O/16	limestone under barite	early-middle Tournaisian
DME	40	87JN04-08	C153835	104P/12	black, sooty, limy slate	middle-late Famennian
DME	43	88JN06-04	C154420	104P/05	black limestone in black slate	early-middle Famennian
DME	9	86JN05-08	C143102	104O/16	limestone block	early-middle Tournaisian
DME/1AC	17	84MJO-83-341A	C118253	104O/16	limy black slate	middle Famennian
DME/1AC	19	84MJO-83-281A	C118256	104O/16	carbonate	middle Famennian
DME/2AC	18	84MJO-83-282A	C118255	104O/16	carbonate	early-middle Tournaisian
DME/2AC	20	84MJO-82-13	C118258	104O/16	carbonate	early-middle Tournaisian
MPs	106	88JB42-10	C159016	104P/03	green chert, salmon-green weathering	Bashkirian-Moscovian
MPs	111	88LM28-4	C159048	104P/05	black thin-bedded chert in salmon-green chert	late Visean - early Namurian
MPs	116	88MM24-12	C159210	104P/05	light green chert	Gzhelian-Asselian; Permian rads
MPs	130	89DSO-004	C153839	104P/05	red/white banded chert	probably Permian
MPs	61	88LM31-9CFGI	C158781	104P/05	bedded green, red chert, argillite	probably Permian
MPs	65	88JB34-14	C158770	104P/05	salmon and green chert, red argillite	probably Permian
MPs	95	87KG04-04	rad-TH	104P/12	black chert	Pennsylvanian(?)-Permian
MPs	97	87KG04-07	rad-TH	104P/12	green chert	Pennsylvanian(?)-Permian
IMs	1	86JB34-01	C143630	104O/16	dark grey limestone	late Visean - early Namurian
IMs	10	86JN22-04	C143106	104O/16	limestone, chert-replaced	late? Tournaisian
IMs	114	88LM45-2	C159014	104P/03	limestone with black argellite, chert	late Tournaisian
IMs	115	88MM12-6	C158759	104P/05	minor limestone in phyllite	?late Tournaisian
IMs	126	87JB10-3	C159217	104P/12	limestone in dark grey argillite	probably Asselian-Sakmarian
IMs	127	87JB10-4/1	C159218	104P/12	limestone in black argillite	late Visean - early Namurian
IMs	128	87KG38-10	C159221	104P/12	continuous calcarenite bed	late Visean - early Namurian
IMs	129	87KG7-1	C159223	104P/12	well-bedded calcarenite	Carboniferous?
IMs	13	84GAH-235F	C116407	104O/16	limestone	late Tournaisian
IMs	136	89KG9-2	C159229	104P/13	green chert	Carboniferous-Permian
IMs	14	84GAH-238F	C116408	104O/16	limestone, chert-replaced	Carboniferous - Early Permian
IMs	15	84MJO-SV-MT	C118251	104O/16	carbonate, Survey Mt.	late Famennian - early Namurian
IMs	16	84MJO-WJ841	C118252	104O/16	carbonate,Whitehorn Ridge	Bashkirian-Moscovian
IMs	2	86JB17-18	C143629	104O/16	black chert	early? Carboniferous
IMs	22	87JN10-01	C153811	104P/12	limestone, chert-replaced	late Tournaisian
IMs	25	87JN39-11	C153818	104P/12	grey limestone	probably late Visean - early Namurian
IMs	28	87JB08-09	C153869	104P/12	limestone lenses in argillite	?late Tournaisian
IMs	3	86JB15-01	C143625	104O/16	brown to dark grey limestone	late Tournaisian
IMs	31	87KG38-07/2	C153825	104P/12	limestone in black argillite	late Visean - early Namurian
IMs	32	87KG41-10	C153829	104P/12	black limestone	early Carboniferous
IMs	35	87HM40-04	C153889	104P/12	limestone with argillite, sandstone	late Tournaisian
IMs	4	86JB13-07	C143632	104O/16	grey limestone	late Tournaisian
IMs	41	87KG43-06	C153830	104O/09	black limestone in black argillite	Tournaisian-Visean
IMs	5	86TH02-06	C117623	104O/16	limestone, chert-replaced	Famennian-Visean
IMs	50	88MM07-01A	C154406	104P/05	turbiditic limy siltstone	late? Tournaisian
IMs	51	88MM07-01B	C154405	104P/05	turbiditic limy siltstone	early-middle Tournaisian
IMs	52	88MM07-16	C154407	104P/05	limestone	early Carboniferous
IMs	53	88MM24-17	C154446	104P/05	limestone in black argillite	Ordovician-Triassic
IMs	6	86KG21-02	C143637	104O/16	reddish weathering limestone	late Tournaisian
IMs	7	86JN22-19	C117561	104O/16	limestone, chert-replaced	late Tournaisian
IMs	96	87KG04-01	rad-TH	104P/12	chert, cherty argillite	Mississippian?
IMsi	123	88JN32-2	rad-TH	104P/05	grey chert with argillite	Mississippian
IMsi	64	88JB09-12	C158753	104P/05	limestone, chert, argillite	? Tournaisian
IMsi	67	88JB42-09	C159015	104P/03	grey chert, argillite	Devonian - early Carboniferous
IMsi	75	81GGAS-2A1	C087675	104P/03	limestone, chert, argillite	Tournaisian-Visean
IPPs	121	87KG38-8	C159220	104P/12	red and green chert	Asselian - early Artinskian
IPPs	131	87HM40-10	C159219	104P/12	green chert with red argillite	Bashkirian - early Artinskian
IPPs	132	89JN8-5	C159227	104P/13	sea-green chert 100 m above IMs	probably Bashkirian-Moscovian
IPPs	33	87HM06-01/2	C153861	104P/12	green chert, red argillite	Late Carboniferous - early Permian
IPPs	37	87HM06-03	C153862	104P/12	chert in red argillite	? Bashkirian-Moscovian
IPPs	39	87HM41-19	C153891	104P/12	grey-green, thin-bedded chert	Bashkirian-Asselian

TABLE 2
CONODONT AND RADIOLARIAN LOCALITIES — *Continued*

Unit	Map No.	Sample	GSC	Sheet	Lithology	Age
IIMvs	100	87KG23-03	rad-TH	104P/12	black chert	Mississippian
IIMvs	110	88LM1-9	C154414	104P/05	minor limestone in black argillite, chert-pebble conglomerate	Early Carboniferous
IIMvs	137	89DSO-006	C153841	104P/05	calcarenite	Famennian-Tournaisian
IIMvs	138	89DSO-007	C153842	104P/05	calcarenite	? Early Carboniferous
IIMvs	26	87JN26-01	C153871	104P/12	limestone in basalt	probably Early Carboniferous
IIMvs	30	87KG13-05	C153821	104P/12	carbonate in pillow basalt	late Tournaisian
IIMvs	44	88JN9-12	C158760	104P/05	chert-replaced limestone with basalt	probably Early Carboniferous
IIMvs	45	88JN14-08	C158752	104P/05	limestone, basalt, argillite	Early Carboniferous
IIMvs	49	88MM01-08	C154417	104P/05	limestone, cherty argillite	Tournaisian
IIMvs	58	88LM02-11	C154413	104P/05	black argillite, chert, sandstone, conglomerate	early to middle Tournaisian
IIMvs	59	88LM26-15	C158787	104P/05	limy pod in maroon, green basalt	? late Tournaisian
IIMvs	60	88LM28-13	C158785	104P/05	limestone, chert, argillite, basalt	probably Early Carboniferous
IIMvs	62	88LM43-15	C159013	104P/03	black chert, minor tuff	probably late Tournaisian
IIMvs	63	88JB06-07	C154403	104P/05	calcarenite, black chert, argillite	early-middle Tournaisian
IIMvs	68	88JB58-10	C159047	104P/05	limestone, chert-replaced	Early Carboniferous
IIMvs	73	88TH09-08	C154427	104P/04	carbonate with black argillite, chert, gabbro	late Famennian
IIMvs	83	82DY-2248	C081700	104P/04	limestone	Early Carboniferous
IIMvs	84	82DY-2249	C102619	104P/04	limestone	Early Carboniferous
IIMvs	85	CDY2819	C103507	104P/04	limestone	Tournaisian
IIMvs	86	CDY2820	C103508	104P/04	limestone	late? Tournaisian
IIMvs	87	CDY2821	C103509	104P/04	limestone	Tournaisian
IIMvs	92	84GAH-213F	C116401	104P/05	carbonate pod in greenstone/argillite	late Tournaisian
IIMvs	93	84GAH-229F	C116406	104P/05	Cassiar pit - chert	late Tournaisian
IIMvs	94	85GAH-215-R	C149998	104P/05	chert in greenstone/argillite	? Bashkirian-Moscovian
IIMPvsu	103	88JB12-3	C158754	104P/05	black chert 10 m below basalt	probably Devonian-Permian
IIMPvsu	117	88MM36-5	C158795	104P/05	dark grey, green chert in phyllite, above basalt	probably Gzhelian - early Artinskian
IIMPvsu	118	88MM36-7	C158765	104P/05	buff-weathering green chert, minor basalt	probably Permian, poss. Triassic
IIMPvsu	120	88JB21-13	rad-TH	104P/05	grey chert cut by gabbro	late Pennsylvanian - Early Permian
IIMPvsu	122	88LM30-12	rad-TH	104P/05	grey green chert with basalt	late Mississippian - Early Pennsylvanian
IIMPvsu	124	88JN35-9	rad-TH	104P/05	well-bedded black chert in basalt	Early(?) Permian
IIMPvsu	46	88JN20-06	C154447	104P/05	basalt, limy sediments interbedded	Givetian-Tournaisian
IIPPvs	101	86KG25-01	rad-TH	104O/16	red chert in basalt	Early-Late Permian boundary
IIPPvs	102	86KG20-04	rad-TH	104O/16	black chert with diabase	late Mississippian - early Pennsylvanian
IIPPvs	107	88JB48-4	C159029	104P/03	green chert with basalt	Permian
IIPPvs	108	88JB50-11	C159028	104P/03	green chert	Permian
IIPPvs	109	88JN4-10	C154408	104P/05	red chert with diabase sill	probably Permian
IIPPvs	113	88LM42-12	C159011	104P/03	green chert in basalt with jasper	Permian
IIPPvs	125	88JN38-8	rad-TH	104P/05	thin bedded grey chert, rhodonite	late Pennsylvanian - Early Permian
IIPPvs	133	88JN9-7	C159231	104P/05	red chert with gabbro breccia	Ordovician-Triassic
IIPPvs	134	88JN12-4A	C159234	104P/05	red chert	Silurian-Triassic
IIPPvs	135	89JN13-4	C159236	104P/05	black/green chert 50 m from rhodonite	Ordovician-Triassic
IIPPvs	27	87JB09-08	C153834	104P/12	green tuff, chert	Gzhelian - early Artinskian
IIPPvs	89	83MJO-P83-62F	C103665	104P/05	grey bedded chert, argillite	Late? Carboniferous
IIPPvs	90	83MJO-P83-63F	C103666	104P/05	light grey-green chert	Late Carboniferous
IIPPvs	98	87KG08-05/2	rad-TH	104P/12	white chert with diabase	late Pennsylvanian-Wolfcampian
IIPPvs	99	87KG08-06/2	rad-TH	104P/12	red chert with diabase	Permian
IIPPsi	104	88JB40-08	C158796	104P/03	thin-bedded black chert	Permian
IIPPsi	105	88JB41-19	C159018	104P/03	green chert, block in serpentinite	Permian
IIPPsi	112	88LM35-7	C158797	104P/03	black chert with argillite, diabase	probably Gzhelian-Artinskian
IIPPsi	66	88JB41-17	C159017	104P/03	silicified limestone; chert, basalt clasts	probably Bashkirian-Moscovian
IIPPsi	76	81GGAS-5B1	C087682	104P/03	chert	Artinskian
IIs	38	87HM20-01/3	C153883	104P/12	grey-green chert block	Permian

TABLE 2
CONODONT AND RADIOLARIAN LOCALITIES — *Continued*

Unit	Map No.	Sample	GSC	Sheet	Lithology	Age
IIFMum	119	88JN53-1	C159203	104O/16	carbonate-matrix of breccia	Late? Permian
IITrTMS	23	87JN12-1/1	C153812	104P/12	limestone	late Ladinian - early Carnian
IITrTMS	55	88LM02-01	C154416	104P/05	calcareous siltstone	middle? Norian
IITrTMs	56	88LM02-02	C154415	104P/05	calcareous siltstone	late? Norian
IITrTMs	57	88LM02-07	C154411	104P/05	grey limestone, tiny crinoids	early Norian
IITrTMs	74	88TH11-01	C154429	104P/04	black limestone, brown-weathering	early Norian
IITrTMs	88	CDY2581	C103518	104P/04	grey limestone, Plaza pit	late middle Norian
IITrTMs	91	84GA-SYL1	C116151	104P/12	grey fossiliferous limestone	early? Carnian
IIIPPHv	24	87JN19-1	C153815	104P/12	limestone in andesite	Asselian - early Artinskian
IIIPPHv	42	88JN45-2	rad-TH	104P/03	jade-green chert in volcanics	Pennsylvanian-Permian
IIIPPHv	69	88TH01-08	C154422	104P/04	limestone lens in augite porphyry	probably Late Carboniferous
IIIPPHv	70	88TH01-09	C154423	104P/04	limestone pod in augite porphyry	Bashkirian
IIIPPHv	71	88TH02-04/1	C154424	104P/04	limestone lens in augite porphyry	Bashkirian
IIIPPHv	72	88TH03-04/2	C154426	104P/04	carbonate with basalt, argillite, rhyolite	Late? Permian
IIIPPHv	81	81GGAS-15E1	C087676	104P/04	limestone pod in augite porphyry	late Namurian-Bashkirian
IIIPPs	29	87JB19-07	C153879	104P/12	limestone turbidite	early Artinskian
IIIPPs	34	87HM17-04	C153881	104P/12	limestone with crinoids, corals	Late Carboniferous - Early Permian
IIIPPs	36	87HM17-01	C153880	104P/12	calcarenite with chert	early Artinskian
IIIPPs	47	88JN44-02	C159036	104P/03	calcilutite, rare chert	Bashkirian-Asselian
IIIPPs	48	88JN44-09	C159035	104P/03	limestone with green tuff	Bashkirian-Asselian
IIIPPs	54	88MM47-01	C159007	104P/03	limestone	? Artinskian
IIIPPs	77	81GGAS-8B2	C087678	104P/03	massive limestone	Late? Permian
IIIPPs	78	81GGAS-13A-1	C087679	104P/03	limestone	Artinskian-Guadalupian
IIIPPs	79	81GGAS-13-A2	C087680	104P/03	limestone; red and green chert	late Artinskian-Guadalupian
IIIPPs	80	81GGAS-13-A3	C101995	104P/03	limestone; red and green chert	Permian
IIIPPs	82	81GGAS-18D1	C087677	104P/03	limestone; red and green chert	late Namurian-Moscovian

Notes: *rad-TH: radiolarians identified by T. A. Harms; personal communication.*

the chert-argillite unit within the allochthon include its oceanic character and similarity to Unit IPPs in Division I; the lack of equivalent non-carbonate, non-siliciclastic packages in other parts of the ancestral North American margin; the angular discordance of its basal contact in places, due to cascading folds within the chert; and its absence within the thrust-imbricated stack of Tapioca sandstone - McDame - Earn slivers near the Cassiar mine. On the other hand, the chert-argillite unit is younger than the Earn Group, an apparently normal stratigraphic relationship that makes even a thrust fault between them difficult to prove, much less an allochthonous contact. A possible analogue of Unit MPs occurs in the Pelly Mountains, where 100 metres of thin-bedded chert lie between mid-Mississippian Earn-like sediments and siltstones and limestones of Triassic age (Tempelman-Kluit *et al.*, 1976). The structural disturbance along the basal contact of Unit MPs is comparable to that observed at the contact between the Kechika Group and the underlying Rosella Formation. Certainly detachment occurred, but motion could have been a few kilometres rather than the hundreds necessary to emplace an allochthonous terrane onto the Cassiar Terrane from the west. The chert-argillite unit is imbricated with the Earn Group in the northeastern Tootsee Lake map area and in the northern part of the Blue Dome map area. Its structural relationships with the Sylvester allochthon are less intimate. On the eastern and northern sides of the allochthon, it is overlain on an older-over-younger thrust fault by late Tournaisian siliciclastic sediments of Unit IMs, whereas on the western side of the allochthon it is overlain by late Tournaisian basalts and siliciclastic sediments of Unit IIMvs. Thus its top is a profound thrust fault above which imbrication of radically different facies has occurred, while its base is a thrust 'flat' that may have accommodated minor or major motion. In this discussion and on Figure 2, the chert-argillite Unit MPs is considered to represent the highest stratigraphic unit in the Cassiar Terrane.

THE SYLVESTER ALLOCHTHON

The Sylvester allochthon is a klippe of eugeosynclinal rocks that structurally overlies the miogeoclinal strata of the Cassiar Terrane. It occupies the core of the McDame synclinorium, measuring 150 kilometres along the northwesterly structural trend and 15 to 30 kilometres wide. On the crest of Mount McDame, above the Cassiar townsite, the dark green basalt flows and interbedded black argillites of the basal Sylvester offer a profound visual contrast to the pale grey McDame limestone below, (Plate 1). The allochthon has been assigned to the Slide Mountain Terrane (Monger and Berg, 1984) and is one of a number of scraps and klippen of that terrane that festoon the ancient North American margin (Figure 4). Like the rest of the Slide Mountain Terrane, it is of mainly late Paleozoic age. Fossil and radiometric ages obtained during this study range from late Tournaisian (early Mississippian) through Guadalupian (Late Permian) with the exception of one highly distinctive Late Triassic sedimentary package.

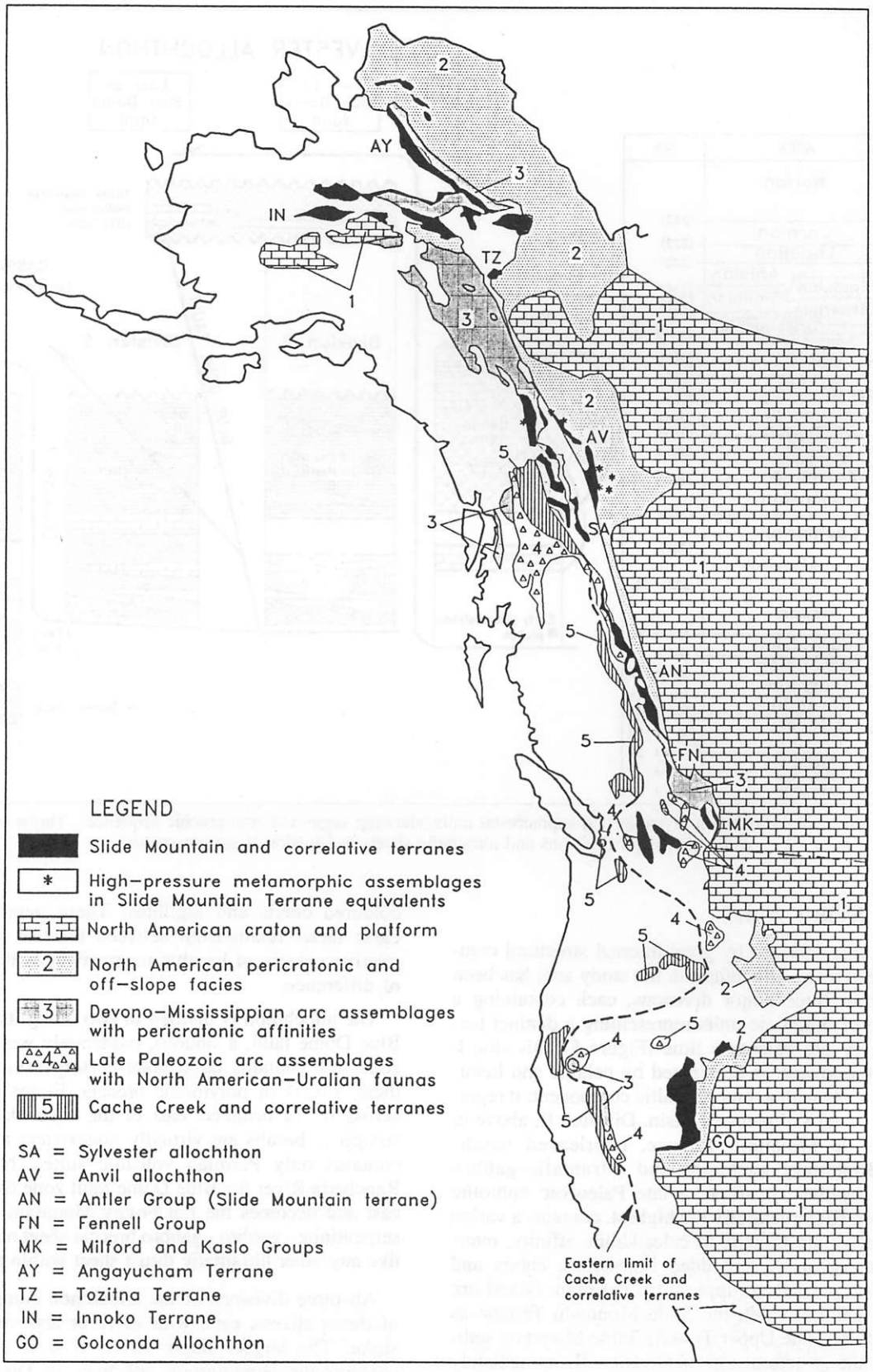


Figure 4. Regional distribution of Slide Mountain Terrane occurrences. This figure shows the regional consistency in the tectonic setting of the Slide Mountain Terrane. All Slide Mountain Terrane outliers lie structurally above or west of North American cratonic or pericratonic units, which include some Devono-Mississippian arc elements. Other late Paleozoic (Devonian-Permian) arcs with Early Permian McCloud-type, North American-Uralian faunas, lie above or west of the Slide Mountain outliers. Except for Stikinia, these in turn all lie east of the strongly allochthononous Cache Creek Terrane and its correlatives.

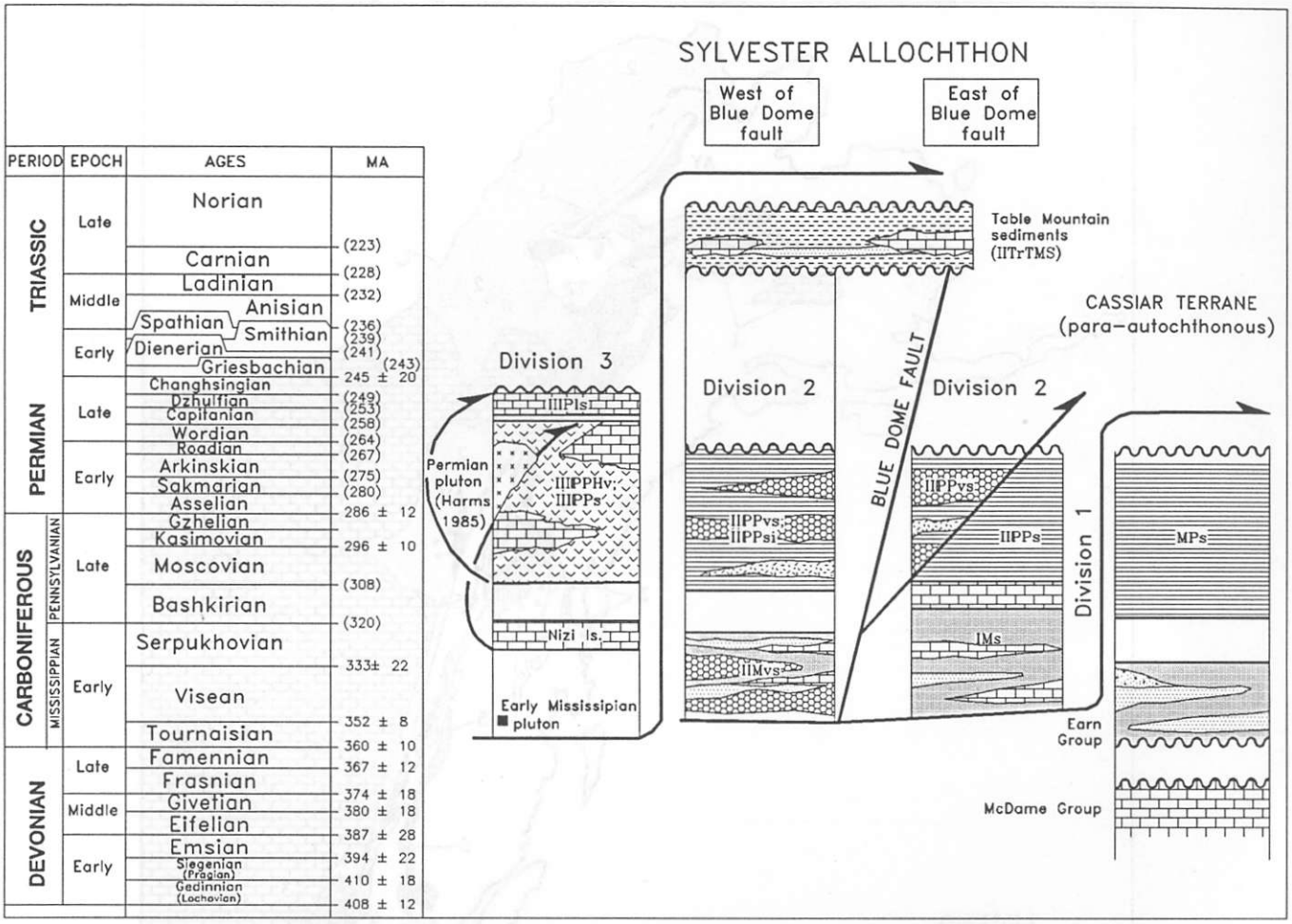


Figure 5. Sylvester allochthon divisions and supracrustal units, showing suggested stratigraphic sequences. Thrust imbricates within the major divisions and ultramafic sheets in Division II are not shown.

General Structure

Although characterized by great internal structural complexity, the Sylvester allochthon in the study area has been subdivided into three major divisions, each containing a distinct suite of lithologic units representing a distinct tectonic setting in late Paleozoic time (Figure 5). Division I, structurally the lowest, is dominated by pelagic and hemipelagic sediments with a minor basaltic component: it represents a deep-water sedimentary basin. Division II, above it, is classic Slide Mountain Terrane, interleaved basalt-diabase-sedimentary packages and ultramafic-gabbro slivers that together constitute a late Paleozoic ophiolite suite. Division III, structurally the highest, contains a varied volcanic suite of arc-tholeite to calcalkaline affinity, intermediate plutons, and interbedded limestones, cherts and tuffs. It is a pre-Mississippian to Permian island-arc assemblage, unique within the Slide Mountain Terrane as currently defined. The Upper Triassic Table Mountain sediments lie at the structural top of Division II, immediately below the basal thrust of Division III.

Sedimentary packages can be correlated between Divisions I and II, notably siliciclastic sequences of Mississippian age and late Pennsylvanian to Early Permian varicoloured cherts and argillites. These parallels suggest a close facies relationship between the two divisions, with relative volume of basaltic magmatism as their chief point of difference.

The allochthon is divided in two along its length by the Blue Dome fault, a sinuous, moderately west-dipping fault zone that contains large pods of serpentinite and, within them, slivers of polymictic breccia. Facies changes occur across it; for instance, east of the Blue Dome fault Mississippian basalts are virtually nonexistent and Division II contains only Permian volcanic suites. Near the Little Rancheria River the Blue Dome fault zone turns over to the east and becomes the flat Foggy Mountain thrust sheet, a serpentinite - gabbro - gabbro breccia sheet morphologically like any other ultramafic thrust sheet within the allochthon.

All three divisions of the allochthon comprise packages of thrust slivers, each with more or less continuity along strike. The largest single sliver, if it is a single sliver, contains the Huntergroup volcanics of Division III. This tectonostratigraphic unit outcrops near Black Friday Lake in the southwestern Blue Dome map area and in the Huntergroup massif near the Erickson mine, 35 kilometres to the south. Other slivers may be less than a kilometre across.

Individual slivers repeat map units, for example the interleaved basalt and serpentinite-gabbro slivers in the Tootsee Lake map area on Gum and Foggy mountains.

Division I

Division I is the lowest structural division of the allochthon east of the Blue Dome fault. It is made up of two sedimentary units, a lower one of Mississippian age (IMs, IMsi) and an upper Pennsylvanian to Early Permian sequence (IPPs). The two units are structurally repeated in some areas, for example in the northwest corner of the Blue Dome map area (Figure 6a). The base of Division I, and also the base of the allochthon, is an older-over-younger, bedding-parallel thrust fault on which early Mississippian sediments of Unit IMs lie structurally above autochthonous Pennsylvanian-Permian cherts of Unit MPs. Both units of Division I have close parallels in the underlying autochthonous strata: Unit IMs mirrors the Earn Group, albeit younger by part of a faunal stage; while the cherts of Unit IPPs are very similar in age and lithology to those of Unit MPs.

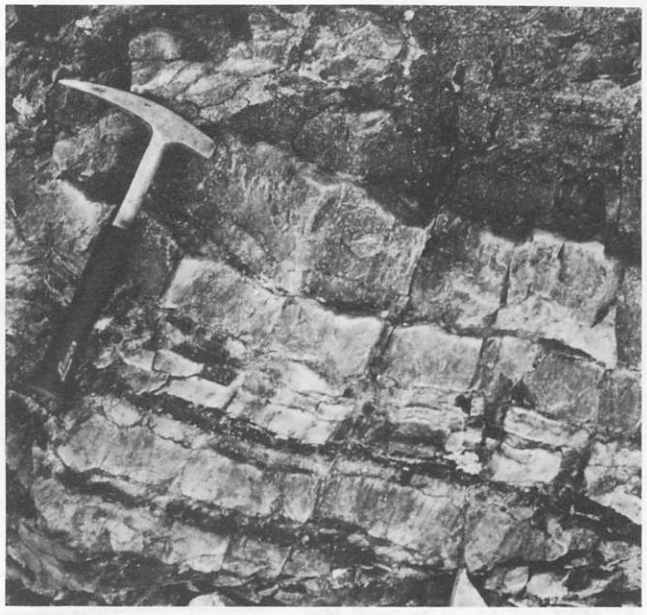


Plate 8. Well-bedded grey radiolarian chert, Unit IMs.

Units IMs and IMsi

For the most part, Mississippian suites in Division I are easily distinguished from Permo-Pennsylvanian suites, and conodont and radiolarian ages concur with field determinations. However, both units contain widespread grey, black and dull green argillite and chert; and where no conodonts were recovered, local correlations are uncertain.

Unit IMs/IMsi consists of black argillite, black, grey and dull green chert (Plate 8) and argillite, bedded grey calcarenite variably replaced by black nodular chert, thicker grey calcarenite without chert replacement, sandstone, siltstone, diorite and diabase sills, and bedded quartz-pyrite-barite exhalites. The most specific conodont ages from the chert-replaced limestones are late Tournaisian (early Mississippian); ages from the thicker, unreplaced limestone are Visean to early Namurian (late Mississippian). The late Mississippian limestone only occurs on Shambling Mountain in the Tootsee Lake map area and in the northwest corner of the Blue Dome map area (Localities 25, 31, 127, 128, Table 2). Three Pennsylvanian to Permian conodont ages from limestones in this unit (Localities 14, 16 and 126) are unexplained. One of them, No. 14, is Carboniferous to Early Permian (Appendix 1). The location of No. 16 on Whitehorn Mountain is very imprecise. Number 126 is a limestone interbedded with typical graphitic argillites of Unit IMs along the northern edge of the Blue Dome map area. Eight other collections nearby are of Mississippian age.

Large volumes of black argillite with lesser interbedded siliciclastics, carbonate and chert and scattered exhalites are the characteristic lithologies of this unit. The siliciclastics are chert-quartz sandstones and siltstones. Petrographically, they consist of chert, cherty argillite, recrystallized chert, chert with radiolarian ghosts; single grain and polycrystalline quartz with pronounced strain textures indicative of a metamorphic source terrain; and a trace-mineral suite that includes muscovite, tourmaline and zircon. They are identical in every lithologic detail to Earn sandstones. Their major difference is that they are slightly younger and part of a package that is separated from the Cassiar Terrane by a major older-over-younger thrust fault. They are of late Tournaisian age, while the youngest Earn within the study area is early to middle Tournaisian (Table 2). So close are they to Earn lithologies that on a map of the Blue Dome area (Nelson *et al.*, 1988b), a siliciclastic-rich package within the Sylvester allochthon north of Alec Chief Creek, which hosts the Chief West exhalite showings, was assigned to the Earn Group.

Unit IPPs

In general, Unit IPPs contrasts strongly with the Mississippian sediments. It consists of dull to bright green, red, pink, maroon, grey, black and tan interlayered, well-bedded radiolarian chert and argillite. In areas where Unit IMs is dominated by chert and argillite and IPPs cherts and argillites are drab, the contact cannot be accurately drawn without detailed conodont or radiolarian data. Conodont ages from this unit are Bashkirian (early Pennsylvanian) through Early Permian. It should be noted that the brightly coloured bedded cherts, the reds, maroons and greens, in this unit as well as in MPs and IIPPvs invariably contain Pennsylvanian-Permian faunas. No brightly coloured cherts of Mississippian age were found. This generalization may hold true more widely in the Sylvester allochthon and Slide Mountain Terrane: Harms (1986) and Struik and Orchard (1985) report several Pennsylvanian to Permian microfossil ages from red cherts.

In general, Division I represents a structurally disrupted and tectonically thickened sedimentary succession in which lower Mississippian black argillite, siliciclastics, carbonates and cherts are overlain by upper Mississippian limestone and then by Pennsylvanian-Permian varicoloured cherts and argillites. The close affinity between Unit IMs/IMsi and the autochthonous Earn Group strongly suggests that Division I

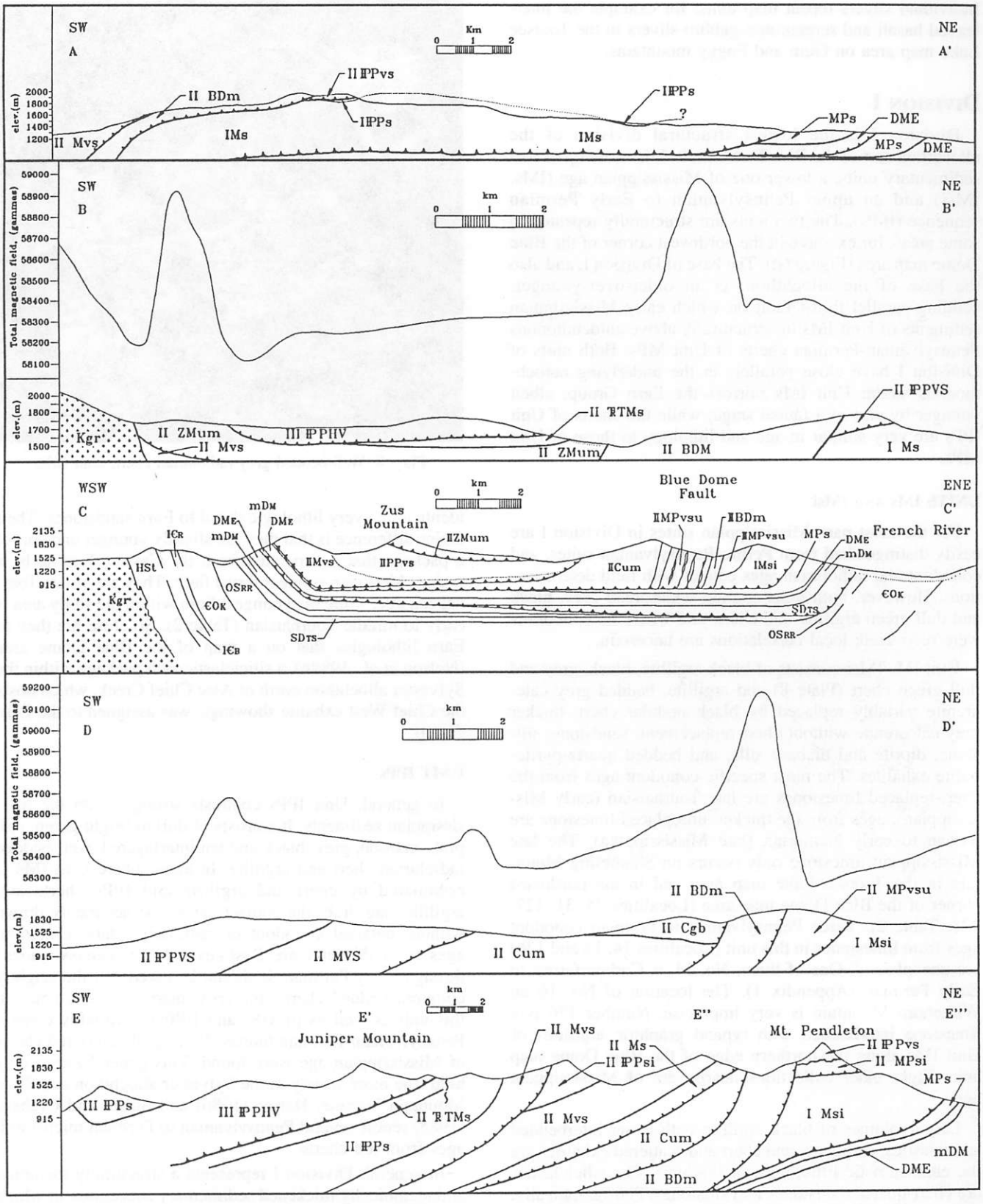


Figure 6. Cross-sections of the Sylvester allochthon (*see* Figure 2 for locations)

a. Northwestern Blue Dome - southwestern Tootsee Lake
b. Southern Blue Dome
c. Cassiar
d. Snowy Creek
e. McDame

developed close to the ancient North American margin and that this part at least of the Sylvester allochthon represents telescoping of facies, not obduction of unrelated oceanic material.

Division II

Division II structurally overlies Division I. East of the Blue Dome fault, diabases or basalts of Unit IIPPvs define its base. In the Tootsee Lake map area, its basal unit is either basalt and diabase of Unit IIPPvs or IIMPsi, serpentinite, or serpentinite and gabbro of the Foggy Mountain ultramafite. Southwest of the Blue Dome fault, along the western margin of the allochthon, its basal unit is either Unit IIMvs or the Cassiar ultramafite, which directly overlie strata of the Cassiar Terrane.

Division II is an ophiolite suite that includes late Paleozoic basalt-diabase-sedimentary sequences and ultramafic and gabbro bodies. With the exception of the Triassic Table Mountain sediments, which form its structural top and are probably an overlap sequence, conodont and radiolarian data indicate that the rocks in it are of early Mississippian to Early Permian age, exactly contemporaneous with those in Division I.

BASALT AND SEDIMENTARY SEQUENCES

Sequences of interbedded basalt flows and breccias, pelagic, hemipelagic and siliciclastic sediments, and intercalated diabase-gabbro-diorite sills (Plate 10) make up the bulk of Division II. Subdivision of these into units has been guided by the character and age of the sedimentary rocks. Basalts and their intrusive equivalents are identical in the various packages, both in terms of field characteristics and even in major and trace-element geochemistry.

Although strong structural disruption has affected the volcanic-sedimentary sequences, stratigraphic successions can still be recognized. North of Snowy Creek in the Cassiar map area, Unit IIMvs passes upwards into Unit IIPPvs through a gradational zone dominated by basalt and diabase sills, shown in section in Figure 6d. Chert becomes dominant over argillite upward. About 150 metres above the highest sandy bed, the chert becomes brightly coloured and interbedded with maroon argillite. Small rhodonite pods occur interbedded with black, grey and pale green chert near the base of Unit IIPPvs. These are described in more detail in Chapter 4.

In several thrust panels south of Mount Pendleton in the McDame map area, Mississippian black argillite and basalt of Unit IIMvs/IIMs is overlain by Early Permian black chert and argillite of Unit IIPPsi; this repeated succession is inferred to be stratigraphic (Figure 6e). These two instances demonstrate that stratigraphic sequences can be found within the Sylvester allochthon, which span its entire late Paleozoic age range.

Sediments within the Mississippian packages correlate closely with those in Unit IMs/IMsi in Division I; whereas the varicoloured upper Pennsylvanian to Lower Permian chert and argillite in Unit IIPPvs correlate with those in Unit IPPs. These parallels suggest that Divisions I and II are remnants of two adjoining pieces of crust, with their supracrustal portions representing nonvolcanic and volcanic facies respectively (Figure 5).

Units IIMvs and IIMs

Unit IIMvs is widespread west of the Blue Dome fault and apparently absent east of it. Particularly good exposures are at the western base of the allochthon on Mount McDame near the Cassiar mine, south of Troutline Creek, and south of Mount Pendleton in the McDame map area. In the McDame map area, packages of interbedded sediments are large enough to form mappable units; they are designated Unit IIMs. Their interbedding with basalts distinguishes them from the purely sedimentary Unit IMs.

The sediments within Units IIMvs and IIMs include black argillite, black to dull green chert, waterlain tuff, grey calcarenite variably replaced by nodular black chert, chert-quartz sandstone, siltstone, chert-pebble conglomerate and rare massive sulphide bodies (Lang Creek and a small showing in the east wall of the Cassiar pit) that may be exhalites. The most specific conodont ages from the chert-replaced limestone are uniformly late Tournaisian (early Mississippian with one late Famennian exception (Locality 73, Table 2)), identical to the age of similar limestones in Units IMs and IMsi. Two limestone pods within basalt are also early Mississippian. Unlike Unit IMs, which contains a few Visean faunas, no late Mississippian ages have been obtained from Unit IIMvs.

The siliciclastic sediments are chert-quartz clastics, identical in field aspects and petrographic details to those in the Earn Group and in Units IMs and IMsi. They are interbedded with the basalts that give this unit its ophiolitic affinity. Near Mount McDame, chert-quartz sandstone with detrital muscovite, tourmaline and zircon is interbedded with chlorite-rich tuff on thin-section as well as outcrop scale. On the ridge east of Quartzrock Creek and north of Snowy Creek, clasts of basalt occur within sandstone. It is noteworthy that the coarsest siliciclastic sediments found in the allochthon are chert and quartz-pebble conglomerates on Mount McDame and north of Snowy Creek (Plate 9); and the overall coarsest sequence is a panel 500 metres thick on the northeast shoulder of Juniper Mountain that contains 80 per cent sandstone and grit. Both of these localities are west of the Blue Dome fault, in the western part of the allochthon, most distal to the Cassiar Terrane. These coarse sediments may imply western sources or, alternatively, considerable lateral movement on the Blue Dome fault.

Basalt flows, pillowed flows, pillow breccias and tuffs are an important component of Unit IIMvs. They tend to drab colours with olive-green and brown weathering surfaces, although jasperoid patches and areas of bright green epidote occur on Sphinx Mountain in the northern Cassiar map area. Flows are commonly variolitic. Pillow forms are more abundant in Mississippian than in Pennsylvanian-Permian basalts.

A bedded polymictic breccia, in contact with black argillite, occurs in Unit IIMvs north of Snowy Creek in the Cassiar map area. It contains clasts of basalt, greenstone, tonalite and granophyre.

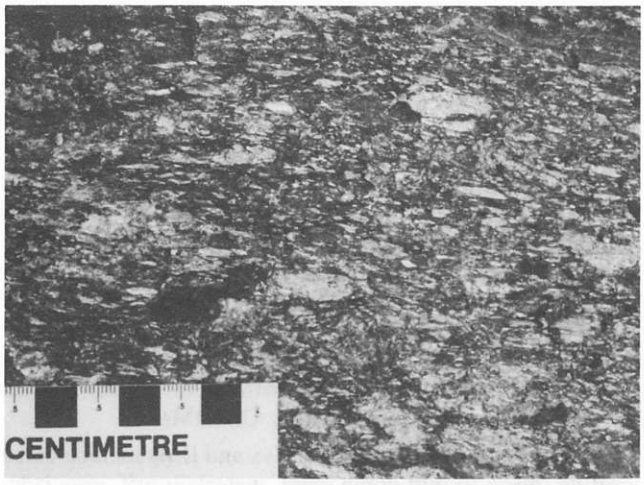


Plate 9. Chert-quartz pebble grit, Unit IIMvs north of Snowy Creek.

Units IIPPvs, IIMPsi and IIb

Unit IIPPvs is widespread on both sides of the Blue Dome fault. In addition to interbedded basalt, basalt breccia, and sediments with diabase sills, it includes extensive exposures of monotonous basalt and diabase; these are designated Unit IIb. Locally east of the Blue Dome fault, the base of Unit IIPPvs is a sill complex within sediments that range upwards from black argillite, calcarenite and quartz-chert sandstone, like those in Unit IMs, to brightly coloured cherts affiliated with Unit IPPs. This sediment-sill complex is included in Unit IIMPsi. Its contact with Unit IIPPvs is the base of the lowest massive basalt flow.

The sediments in Unit IIPPvs include maroon, red, bright to dull green, grey, black and tan chert and argillite, and waterlain tuff. Chert-chip breccias like those in Units IPPs and IPPsv are present locally. Radiolarian ages from the cherts range from late Mississippian - early Pennsylvanian (Locality 102) to Permian. Thus these sediments correlate both in character and age with Unit IPPs.

Basalts within Unit IIPPvs exhibit a variety of textures and colours. One characteristic basalt, which occurs widely northeast of the Blue Dome fault in the Blue Dome map area, is drab green and holocrystalline to somewhat glassy. It is seamed with clinozoisite-filled fractures, creating a crackle-breccia texture. In more brecciated form, the fractures have developed into a matrix between clasts derived from different parts of flows, for instance more or less variolitic or of slightly different grain sizes. Another characteristic, indeed diagnostic, basalt type is strongly coloured maroon and green basalt, best exposed north of Snowy Creek and on Mount Pendleton in the McDame map area. Drab-coloured variolitic basalts are also abundant in this unit; they are indistiguishable from basalts of Unit IIMvs. Reddish brown hornblende is present in a few thin sections from this unit. It occurs either in fractured areas that may represent early hydrothermal conduits, or distributed in the matrix as a primary magmatic phase.

Polymictic depositional breccias are part of Unit IIPPvs east of Quartzrock Creek in the Cassiar map area and on Blackfox Mountain in the McDame map area. The breccia east of Quartzrock Creek is a single massive unit 700 metres in strike length and 100 metres thick. At its northern margin it interfingers with red and green tuffaceous argillite and chert. The breccia includes clasts of gabbro and leucogabbro as well as local basalt and red chert. The bedded cherts along its base are plastically deformed and mixed with breccia (Plate 11).

These breccias attest to seafloor basement exposure, probably along fault scarps, during the accumulation of the Permian volcanic-sedimentary sequence. The breccias east of Quartzrock Creek outcrop less than 5 kilometres from the polymictic breccia in the underlying Mississippian stratigraphy, indicating a long-lived local fault.

Unit IIPPsi

Unit IIPPsi is restricted to the McDame map area, where it depositionally(?) overlies Unit IIMvs. It consists of very well bedded, uniformly dark grey to black, rarely pink, chert and argillite, intruded by widely spaced but continuous diorite and diabase sills. The intrusive rocks do not exceed 10 per cent of the section, and extrusive equivalents, basalts and tuffs, were seen only in a single exposure. Unusual for mafic bodies in Division II, some of the sills contain primary hornblende. Pennsylvanian and Permian conodont ages have been obtained from this unit (Localities 66, 76, 104, 105, 112).

This package, although partly equivalent in age to Unit IIPPvs, contrasts strongly with it in the colour of the cherts and the lack of extrusive rocks. The two units are structurally juxtaposed on Blackfox Mountain. This relationship is evidence for the telescoping of oceanic facies. The original distance between their loci of deposition is not known; it may or may not have been significant.

ULTRAMAFIC-GABBRO SUITES; BLUE DOME FAULT ZONE

Slivers of serpentinized ultramafic rocks are present at several levels within Division II. Scattered, small, discontinuous serpentinite slivers (Unit IIs) enclose blocks of basalt, sediments, gabbro, rodingite, amphibolite, greenstone and breccia. There are three major bodies: the Quartzrock Creek - Cassiar body in the Cassiar map area, the Blue River - Zus Mountain body and the Foggy Mountain body. All of these are composite slivers that include both ultramafic and large gabbroic bodies. Of the three, only the Blue River - Zus Mountain body contains intact oceanic upper mantle and ultramafic cumulate material. The others are serpentinite mélanges that enclose blocks of a variety of lithologies. The only blocks of significant size are mafic intrusions such as the Foggy Mountain and Quartzrock Creek gabbros.

The Blue Dome fault zone is included within this discussion because it has been mapped as part of the Foggy Mountain body to the north; throughout its length it is in part defined by the presence of serpentine-matrix mélange.



Plate 10. Typical feeder zone to Division II basalt, an irregular sill-dike in bedded chert.

Quartzrock Creek - Cassiar Body (Units IICum, IICgb)

This unit includes two separate exposures, an irregular shaped sliver, measuring roughly 10 by 10 kilometres, that outcrops extensively in the mountains east of Quartzrock Creek in the Cassiar map area, and the small ultramafic sliver that hosts the Cassiar and McDame asbestos orebodies. Although their continuity cannot be proven, the structural position of these two bodies is equivalent: they both lie immediately below a single panel of Unit IIMvs on the upturned limbs of the McDame synclinorium. Therefore they are treated together, and separately from the Zus Mountain - Blue River bodies, which lie above the inferred stratigraphic sequence of Units IIMvs and IIPPvs. At the Cassiar mine, the Cassiar ultramafic body lies at the base of the allochthon. However, to the east, the Quartzrock Creek body lies above Unit IIMPvsu. This geometry can be explained by depicting Division II on the west side of the Blue Dome fault as a stack of easterly-verging horses, as is implied in the cross-section in Figure 2.

The ultramafic portion of the Quartzrock Creek and Cassiar bodies, Unit IICum, is serpentinite-matrix mélange, composed mostly of scaly serpentinite, which contains blocks of a variety of mafic and ultramafic lithologies. Most notable and characteristic are ultramafic and mafic cumulates, layered clinopyroxenite and dunite, and layered clinopyroxenite and gabbro. Harzburgite tectonites are also present, as well as amphibolite, basalt and remnants of fine-grained, unfoliated, partly rodingitized gabbro dikes which, judging by their tabular form, may be original intrusions into now-serpentinized ultramafites.

The Quartzrock Creek gabbro is a single bulbous body that rests structurally above the ultramafite. It is coarse grained, generally unfoliated and layered in part. Comparatively leucocratic and even quartz-bearing phases are intercalated with normal gabbro. Large poikilitic, late-magmatic hornblendes overprint the clinopyroxene-plagioclase fabric in a few areas. It has yielded an Early Permian zircon age (Gabrielse *et al.*, in preparation).

The structural position of the Quartzrock Creek - Cassiar ultramafite and gabbro body, below the supracrustal panel encompassing a sequence from Mississippian to Permian volcanics and sediments, is not inverted, although the presence of Permian gabbro directly below Unit IIMvs requires some translation. The breccias within both Units IIMvs and IIPPvs in this area, which contain gabbro and serpentinite clasts, point at exposed ultramafic basement during their deposition. Thus the structural succession from ultramafite to gabbro to Units IIMvs and IIPPvs may represent a fairly intact section of oceanic uppermost mantle and crust. This sort of abbreviated oceanic section, in which supracrustal sediments and basalts directly overlie mantle peridotites, forms a significant part of the present Atlantic ocean floor, particularly in areas of long-lived slow spreading (Lagabrielle and Cannat, 1990), or where low-angle detachment faulting has exposed oceanic basement (Boillot *et al.*, 1987; Lemoine *et al.*, 1987).

Zus Mountain - Blue River Bodies (Units IIZMum and IIZMgb)

The Zus Mountain body is exposed on Zus and Sphinx mountains in the Cassiar map area. The Blue River ultramafite outcrops in the Chromite Creek watershed and near Black Friday Lake in the southwest corner of the Blue Dome map area. They occupy the same structural level in the allochthon, resting above the supracrustal panel composed of Units IIMvs and IIPPvs (Figure 6b, c and Plate 12). They are separated by the valley of the Blue River, which is incised deeply into the underlying panel. Although they are two distinct klippen, they are interpreted as the erosional remnants of a single continuous thrust sheet. Certainly the Blue River and Zus Mountain ultramafites share a common character: they both consist mostly of harzburgite tectonite and intact, relatively fresh, dunite (-wehrlite-clinopyroxenite-chromitite) cumulate.

The Blue River ultramafite was originally mapped by Wolfe (1965); its petrography and metamorphic history were the subject of a detailed study by Pinsent and Hirst (1977). It includes both harzburgite tectonite, and a single, albeit partly dismembered body composed of dunite with sparse clinopyroxenite-rich layers and chromite laminae. The base and top of the body consist of serpentinite; serpentinite is particularly thick at the base and contains mélange blocks of a variety of lithologies, including a large amphibolite-metagabbro sliver from which an unreliable K-Ar whole-rock age of 251+80 Ma has been obtained (GSC 64-1, corrected to revised decay constants).

Fabrics in the Blue River body attest to strong early deformation. This is especially true of the harzburgite tectonites, which are protomylonites in which orthopyroxene paleoblasts form trains of augen in a matrix of recrystallized olivine. The cumulates are also deformed: chromite laminae are folded in some cases, and the original olivines are recrystallized to finer grain sizes and subsequently polygonalized in an annealing event. Near the Cassiar batholith, these textures are overprinted by contact metamorphic

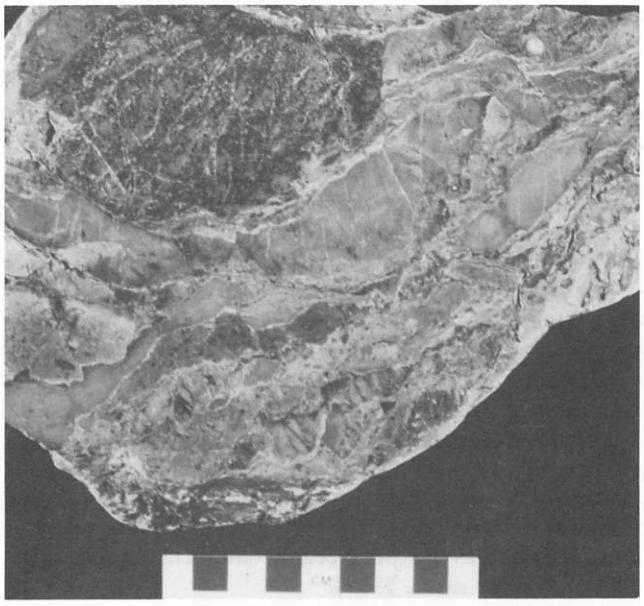


Plate 11. Breccia in Unit IIPPvs north of Snowy Creek. The microgabbro clast has undergone greenschist facies metamorphism. This sample, from the base of the debris flow, shows soft-sediment deformation of the underlying chert.

effects. Pinsent and Hirst (1977) outlined prograde isograds for olivine, talc, tremolite and enstatite.

The Zus Mountain body consists of a lower ultramafic klippe, structurally overlain by a bulbous gabbro body that has yielded a Permian zircon date (Gabrielse *et al.*, in preparation). The Zus Mountain ultramafite, above a base of serpentinite-matrix mélange, comprises harzburgite tectonite intimately intruded by dunite with clinopyroxene-rich layers and sparse chromite laminae. It appears to represent the transitional zone between mantle and the base of subcrustal magma chambers. Very well developed augen and flaser textures characterize the harzburgite tectonites. The cumulates also show early, high-temperature olivine fabrics. Both harzburgites and dunites are crosscut by fairly fine grained, unfoliated, rodingitized gabbro dikes with euhedral garnet and idocrase as secondary phases.

The Zus Mountain gabbro body is generally uniform, unfoliated and unlayered, although the low cliff exposures along its northern edge show consistent layering to trondjhemite. Clinopyroxenes are mantled by late-magmatic hornblende, and pegmatititic hornblende-plagioclase segregations occur in places. Tonalitic phases are rare. The original relationship between the gabbro and the structurally underlying ultramafite is obscure. The present contact between them is across scaly serpentinite. In a model magma chamber (Nicholas *et al.*, 1980), a harzburgitic floor, which may be riddled with dunite magma pockets, is succeeded upwards by major dunite and then peridotite cumulates, with gabbro and then tonalite forming the top of the sequence. In this case, gabbro (-trondjhemite-tonalite) cumulates rest directly on harzburgite with dunite pockets: the middle section of the hypothetical cumulate body is absent.

The Blue River ultramafite locally forms the top of Division II directly below Units IIIPls and IIIPPHvs; farther north this structural level is occupied by the Table Mountain sediments. The Zus Mountain body occupies the centre of the McDame synclinorium in the Cassiar map area (Plate 12), and thus the highest exposed levels in the allochthon there. Farther south, on the southern shoulder of Mount McDame and on Table Mountain on the Total Energold property, discontinuous scraps of serpentinite, talc schist and listwanite directly underlie the Table Mountain sediments. These small ultramafic bodies, which are considered to be controls of high-grade gold ore shoots in the quartz veins, occupy the same structural level as the Zus Mountain - Blue River thrust sheet, and probably are its attentuated edge.

Foggy Mountain Body (Units IIFMum, IIFMgb)

The Foggy Mountain body outcrops on Foggy Mountain, Rocky Top Ridge and the intervening hills. In it, slices of coarse-grained gabbro, polymictic gabbro-breccia and gabbro with sheeted dikes are interleaved with serpentinite. The gabbro is coarse grained to nearly pegmatitic, and amphibolitic to mylonitic in discrete zones. The foliation in these zones is cut at high angles by contacts with serpentinite. In the gabbros, original clinopyroxenes are heavily mantled by green actinolitic hornblende, which also forms lepidoblastic trains in the more highly strained zones. Coarse-grained, subhedral epidote and euhedral to clumped sphene accompany the amphibole. Although the plagioclases are now albitized and strongly saussuritized due to a later prehnite-pumpellyite overprint (*see* Chapter 3), the overall granoblastic textures of these rocks suggest that they experienced epidote-amphibolite facies metamorphism.

Fine-grained unfoliated basalt dikes, which have only undergone texturally nondestructive prehnite-pumpellyite metamorphism, crosscut the foliated amphibolite. In one sliver on the east flank of Foggy Mountain, dikes constitute up to 90 per cent of outcrop, with gabbro as narrow, discontinuous screens. This is the only instance of sheeted diking observed in the allochthon. Polymictic breccias outcrop in broad areas on the southern slope of Foggy Mountain and on Rocky Top Ridge. In these breccias, angular clasts of gabbro, basalt, diabase, serpentinite and greenschist are surrounded by a matrix of rock dust and clinozoisite. These breccias are direct counterparts of those within the Blue Dome fault zone; their significance is discussed in that section.

The Foggy Mountain gabbro crystallized and was metamorphosed in epidote-amphibolite facies and plastically deformed along discrete zones prior to the intrusion of the dikes. Both the gabbro and the dikes are strongly brecciated. Clasts of gabbro identical to the Foggy Mountain body, and indeed clasts of gabbro-basalt breccia in clinozoisite matrix, are incorporated in a limy matrix depositional breccia on nearby Gum Mountain, which occurs as a sliver within serpentinite mélange (Plate 14). In addition to gabbro, this breccia contains clasts of basalt, red and green chert, amphibolite, greenschist and chloritized serpentinite. The limestone matrix on Gum Mountain contains Permian conodonts (Locality 119). It is thus likely that the high-grade metamor-



Plate 12. View of the Zus Mountain ultramafite from the west. The recessive-weathering ultramafite overlies more rugged basalt and sediments of Unit IIMvs along a gently dipping contact in the centre of the McDame synclinorium.

phism and deformation experienced by the Foggy Mountain gabbro body occurred as part of its very early history, probably within a spreading-ridge setting (*cf.* Mevel *et al.*, 1978). Subsequently it was intruded by dikes, uplifted and exposed on submarine scarps during deposition of the Early Permian supracrustal units. The crystallization age of the gabbro is not known; it contains no felsic differentiates suitable for zircon separation and an attempt to date the hornblende by K-Ar techniques failed due to very low potassium content.

Blue Dome Fault Zone (Units IIBDm and IIMPvsu)

The Blue Dome fault extends from the western edge of the Sylvester allochthon near Toozaza Creek, across Blue Dome and southwards along the eastern side of the allochthon at least as far south as the Dease River (Figure 2). H. Gabrielse (personal communication, 1989) traces it nearly to the southern end of the allochthon, although Harms (1986) does not recognize a major, through-going fault south of the Dease River.

The Blue Dome fault zone is marked by discontinuous pods of serpentinite-matrix mélange (Unit IIBDm; Plate 13). Scaly serpentinite encloses blocks and slivers of gabbro, intact ultramafite, basalt, and most characteristic, polymictic breccias including gabbro and ultramafite as well as basalt clasts. In places the fault zone anastomoses and splays diverge into surrounding basalts. Areas containing numerous such splays were assigned to Unit IIMPvsu to emphasize their structural style and content of serpentinite mélange slivers; they are considered to be part of the Blue Dome fault zone (Plate 13). Mapping of the fault zone in areas of scanty bedrock exposure, such as the southern part of the Blue Dome map area, was aided by 1:25 000-scale magnetic maps kindly provided by Brinco (now Western Canadian Mining Corporation). The fault zone has a very strong linear signature on these maps. Generally the anomaly peak occurs west of the surface exposure of the fault, indicating a moderate westward dip (Figure 6b, c).

Unit IIMPvsu forms a single large, pod-shaped body along the western side of the fault from the central Cassiar map area to Blue Dome. It is considered part of the Blue Dome fault zone. It superficially resembles the other supracrustal units, except for its strongly slivered structural style and the presence in it of numerous shear zones that contain slips of serpentinite. It cannot be structurally equivalent to Units IIMvs and IIPPvs, because they occur structurally higher than the Cassiar ultramafic sheet, whereas



Plate 13. The western strand of the Blue Dome fault zone east of Quartzrock Creek. The Quartzrock Creek ultramafite to the west, and Unit IIMPvsu to the east, are juxtaposed across a moderately southwest-dipping serpentinite body.

Unit IIMPvsu lies structurally below it (Figure 2). In cross-section (Figure 6c) Unit IIMPvsu is shown as a steep wedge enclosed within strands of the Blue Dome fault. Several conodont and radiolarian ages (Localities 46, 103, 110, 117, 118, 120, 122, 124) range from the Devono-Mississippian boundary to Permian. It seems to represent a much thinner stratigraphic sequence than that of Units IIMvs and IIPPvs, with many more structural repetitions.

The cross-sections, Figure 6, show the nature of the Blue Dome fault. Throughout most of its length, the fault trends northwesterly and dips moderately to steeply southwest (Plate 13), except in the Tootsee Lake map area where it turns over to the east and becomes a flat thrust, the Foggy Mountain thrust: there it is identical in morphology to the other ultramafic sheets in the allochthon. Farther south, however, it commonly truncates gentler Sylvester thrust faults, for example in the saddle south of Mount Pendleton in the McDame map area.

Sense-of-motion indicators, mostly quartz slickenfibres and slickensides on serpentinite, show gentle plunges and dextral latest movement. On the other hand, the preferred distribution of serpentinite bodies along southwest-concave bends in the fault trace in the Cassiar map area might be interpreted as a series of pull-aparts developed during sinistral faulting. The eastward-recumbent Foggy Mountain sheet shows that easterly directed shortening also played an important role in the movement history of the Blue Dome fault.

The Blue Dome fault is a major structural break within the Sylvester allochthon. It juxtaposes different facies, for instance a Mississippian sequence with a minor igneous component (Units IMs, IMsi) to the east against a volcanic-sedimentary Mississippian sequence to the west (Unit IIMvs). The fault does not penetrate below the basal thrust of the allochthon; its projection into the underlying Cassiar Terrane shows no displacements either to the south (H. Gabrielse, personal communication, 1989) or to the northwest in the Little Rancheria River drainage (Figure 2).

Slivers of breccia occur within serpentinite both in the Blue Dome fault zone and in Unit IIMPvsu beside it. These breccias vary from shattered gabbro and serpentinite through monolithic to polymictic, incorporating a wide variety of clasts. The latter are either matrix or clast supported; the matrix consists of angular, sand to dust-sized rock particles and secondary cement such as clinozoisite. The clasts are basalt, coarse gabbro, greenschist, serpentinite, grains of chromite, chert, diabase and felsic volcanic rocks including andesite and dacite. In one thin section, basalt clasts contain

xenoliths of chloritized serpentinite and chromite. This relationship shows close timing between breccia formation and basaltic volcanism. Some of the polymictic breccias contain sandstone interbeds with graded bedding. In the northeastern corner of the Chromite Creek map area, fine-grained breccias and sandstones are interbedded with siliceous argillite that contains poorly preserved radiolaria and sponge spicules. In thin section, the sand grains are angular and of the same lithologies as those in the coarser breccias. Shattered serpentinite in a calcareous ooze matrix, ophicalcite, is also present. Soft-sediment deformation textures show slumping of the sediments, together with their enclosed ultramafic detritus.

No conodont ages were obtained from the inter-breccia argillites or the ophicalcites in the Blue Dome fault zone. However, the Permian breccia within the Foggy Mountain serpentinite mélange (Plate 14) may be correlative with them.

Barany and Karson (1989) describe very immature sedimentary breccias from the Clipperton fracture zone, an oceanic transform fault near the East Pacific Rise. Photographs taken from the Alvin manned submersible show that these breccias formed as slump deposits, accumulating at the base of steep slopes and fault scarps within the fracture zone. Ophicalcites and seafloor serpentinites have also been dredged from oceanic fracture zones (Saleeby, 1984, Bonatti *et al.*, 1974). By analogy, the breccias of the Blue Dome fault zone may represent seafloor exposure of deep crustal and upper mantle rocks through tectonic uplifts. The Blue Dome fault zone is a good candidate for an early transform fault within the Sylvester marginal sea, particularly given the Permian age of one of the breccias in the Foggy Mountain body, an extension of the Blue Dome serpentinite mélange. Like other early transform faults described in the literature (Saleeby, 1984, Karson and Dewey, 1978), it also accommodated later motion. There is evidence that this later motion had two senses: dextral and convergent.

The Blue Dome fault had a significant phase of motion that postdated some or most of the shortening of the Sylvester allochthon, as is shown by its truncation of gently dipping thrust faults in Division II to the west and between Divisions I and II to the east. A small outlier of Triassic Table Mountain limestone containing a Carnian conodont fauna (Location 91) overlies gabbro breccia and serpentinite of a strand of the Blue Dome fault near the southern edge of the Blue Dome map area. If its base is depositional, or nearly so, then motion on the Blue Dome fault was pre-Late Triassic. At its northern end the Blue Dome fault zone becomes the Foggy Mountain sheet, the footwall to Division III. If Division III thrust emplacement on Division II was post-Late Triassic everywhere, then the evolution of the Blue Dome fault from a steep fault to a flat thrust sheet entrained beneath Division III was also post-Late Triassic. In any event, truncation of the Blue Dome fault by the basal Sylvester thrust implies that all motion on it must have ceased before the allochthon was emplaced onto the Cassiar Terrane.

The Blue Dome fault zone records a long and complex history of movement. Its inferred inception was as a late Paleozoic transform fault. Later, dextral strain was partitioned into it during assembly of the allochthon. At its northern extent, a later(?) phase of compression created an easterly overturn of the zone. After encounter with the North American margin, movement on it ceased. It was then transported eastward as a dead structure, together with the rest of the allochthon.

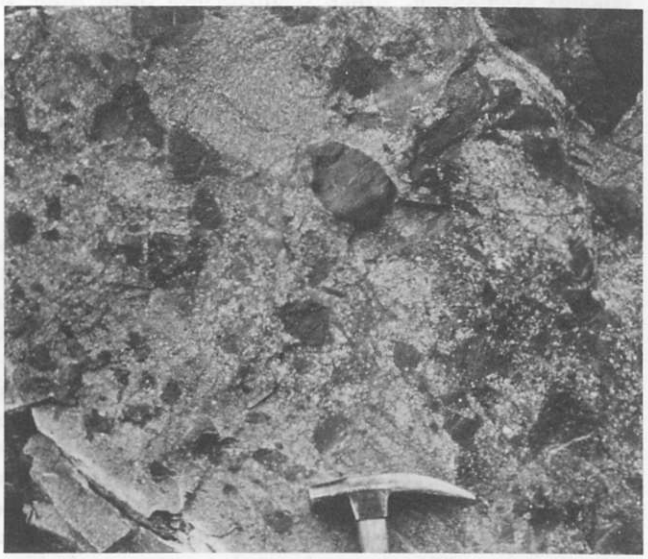


Plate 14. Breccia in the Foggy Mountain gabbro body. The clasts are of basalt, diabase and coarse-grained gabbro. The carbonate matrix has yielded Late? Permian conodonts (No. 119).

TABLE MOUNTAIN SEDIMENTS (UNIT IITrTMS)

This unit takes its name from Table Mountain, the low, flat hill south of McDame Lake in the Needlepoint Mountain map area, on which the major veins of the Erickson system, the Vollaug, Cusac and Jennie veins, are located. It also outcrops on the southeast shoulder of Mount McDame and in the lowland southwest of Wing's Canyon. In these exposures, the Table Mountain sediments are a distinctive package of glossy black to dark grey slate, calcareous siltstone, micaceous quartz sandstone, and, near the Cusac veins, flaggy, medium grey *Halobia*-bearing limestone. Farther north, in the southwestern Blue Dome map area, the Table Mountain sediments consist entirely of limestone, which contains *Halobia*, ammonites, belemnites, and a single reported ichthyosaur vertebra (Gabrielse, 1963 and personal communication).

The siliciclastic sediments in this unit are easily distinguished from those of early Mississippian age. They contain primarily quartz as clasts, with very little chert. Laminated and in some cases crossbedded siltstones predominate, as opposed to structureless or graded sandstone, greywacke and grit. Coarse detrital muscovite is visible on bedding surfaces, and muscovite, tourmaline and zircon are observed in thin section. The well-cleaved, lustrous slates contrast with cherty argillites in the Mississippian sequences. Finally, the Table Mountain sediments lack any

igneous component, which distinguishes them from all other units in Division II.

The presence of *Halobia* establishes a Late Triassic age for the Table Mountain sediments. A number of conodont determinations are also now available, from both the Blue Dome and Cassiar-Erickson areas (Localities 23, 55, 56, 57, 74, 88, 91). They range from Ladinian or early Carnian to Norian.

The Table Mountain sediments are in the footwall of a major thrust fault, with a hangingwall of Pennsylvanian and Permian rocks of Division III. The nature and significance of their basal contact is less certain. They overlie basalts and sediments of Mississippian to Permian age and also ultramafic slivers. The contact is everywhere sheared; in the McDame map area it seems to form the flat roof of a duplex that involves more steeply dipping Division II panels below (Figure 6e). However, the superposition of Late Triassic sediments above a variety of late Paleozoic lithotectonic units is suggestive less of a thrust fault than of a remobilized unconformity, although basal conglomerates are lacking. The clean, mature character of the Table Mountain sediments, and their total lack of volcanic detritus, indicates that a profound change in basin paleogeography took place between mid-Permian and Late Triassic time.

The Table Mountain sediments are close analogues of autochthonous Triassic units in the Selwyn basin (Gordey *et al.*, 1981), northern Cassiar Terrane (Gordey, 1981) and Kechika basin (Gabrielse, 1980), and 'suspect' units such as the 'Black Phyllite Unit' in the Quesnel trough (Struik, 1986, 1988) and the Slocan Group of southeastern British Columbia (Klepacki and Wheeler, 1985), interpreted to unconformably overlie the Crooked amphibolite and the Kaslo Group, respectively (Rees and Ferri, 1983; Rees, 1987; Klepacki and Wheeler, 1985), which probably belong to the Slide Mountain Terrane. Basal conglomerates occur between the Slocan and Kaslo Groups (Klepacki and Wheeler, 1985) and at the base of the Slocan Group where it overlies the Chapperon Group, a possible Slide Mountain remnant near the Salmon River (Read and Okulitch, 1977). Black slates and quartz siltstones near Manson Creek, previously included in the Slide Mountain Terrane (Ferri and Melville, 1988), have recently yielded Late Triassic conodont faunas (Ferri and Melville, in preparation).

Division III

Division III occupies the highest exposed structural level in the Sylvester allochthon, comprising four isolated klippen. Two are in the Huntergroup massif - Juniper Mountain area in the Needlepoint Mountain - McDame map areas, one is near Black Friday Lake in the Blue Dome map area, and one is in the centre of the Sylvester allochthon in the Tootsee Lake map area (Figures 2, 6b, 6e). Differences between the Black Friday Lake and Huntergroup massif exposures can be explained by facies changes in an overall consistent package; therefore they are treated together and common unit names are used. Division III in the Tootsee Lake map area has a somewhat different character and is considered separately. In spite of their differences, all Division III sequences contain island-arc volcanic suites, ranging from basic through intermediate to felsic in composition and containing abundant pyroclastic material and intermediate plutons. The nature of the igneous suites in Division III serves to distinguish it from Division II. In addition, Pennsylvanian and Permian shallow-water, commonly fossiliferous limestones occur within it, in marked contrast to the deep-water sediments of Divisions I and II.

DIVISION III, SOUTHERN KLIPPEN

In both the Huntergroup massif - Juniper Mountain and Blue Dome exposures, two facies are present: a volcanic suite with interbedded limestones, termed the Huntergroup volcanics (Unit IIIPPHv), and a ribbon chert - limestone turbidite - limestone - epiclastic facies (Unit IIIPPs). South of Juniper Mountain, a fault separates the Huntergroup volcanic rocks from a mixed sedimentary and pyroclastic package of unknown age (Unit IIIvs) that is intruded by an early Mississippian coarse-grained tonalite (Unit IIIMt). The lowest unit of Division III in the Blue Dome map area is an Upper Permian fusulinid limestone (Unit IIIPs) that may be a facies equivalent of some of the youngest limestones in Unit IIIPs.

Huntergroup Volcanics (Unit IIIPPHv)

The Huntergroup volcanics in their type area, the headwaters of Huntergroup Creek, comprise coarse augite porphyry flows and breccias with hornblende and plagioclase as less common phenocrysts, pods of limestone, and polymictic pyroclastic to epiclastic breccias, lapilli tuffs and volcanic sandstones. Farther east, Juniper Mountain is underlain in part by pillowed augite porphyry flows and polymictic lapilli tuffs. The lapilli tuffs include clasts of dacite, which does not appear locally as flows.

The stratigraphic top of the Huntergroup volcanics is well exposed on the ridge south of Juniper Mountain. The contact varies from abrupt to transitional over as much as 50 metres. To the east, augite porphyry pyroclastic breccias are interbedded with fossiliferous volcanic sandstones and impure limestones, which pass upwards into Unit IIIPPs. Farther west, a mountain-sized carbonate buildup of nearly pure limestone overlies augite porphyry. Within 10 centimetres of the contact, augite porphyry clasts occur in the limestone.

In the southwestern corner of the Blue Dome map area, Division III augite and plagioclase porphyry flows and pyroclastic units form the highest structural unit in the Sylvester allochthon, resting above limestone of Unit IIIPIs, Triassic Table Mountain sediments, or directly on Division II (Figure 2). They are correlated with the Huntergroup volcanics on the basis of their similar lithologic character and age. The similar chemistry of the volcanic rocks is further evidence for the affinity of these two packages (see Chapter 2).

Conodont ages from small limestone pods near the structural base of the Huntergroup volcanics in the Huntergroup massif, including our samples and those collected by Gordey *et al.* (1982), are early to middle Pennsylvanian (Table 2). A small limestone pod on the ridge south of Juniper Mountain, interbedded with lapilli tuff, contains a Permian fauna of fusulinids and bryozoa (No. 208). The

Huntergroup volcanics near Black Friday Lake contain poddy, highly fossiliferous synvolcanic limestones. In them, angular, pillow-like and wispy volcanic clasts are caught up in a mixed limy tuffaceous matrix that includes macrofossils. Single macrofossils also occur in volcanic sandstones. These features suggest the informal name of 'Pompeii facies'. The Pompeii units contain a diverse Early Permian macrofauna of *spiriferella,* horn corals, crinoids, fusulinids and bryozoa (No. 201).

Unit IIIPPs

Unit IIIPPs is exposed in a syncline on the ridge south of Juniper Mountain in the McDame map area, and overlying the Huntergroup volcanics in the southwestern Blue Dome map area near Black Friday Lake. In the McDame map area, it includes spectacular limestone-matrix epiclastic breccias, epiclastic breccias and tuffaceous sandstones, red and green chert, limy epiclastic sandstones and pure, commonly fossiliferous limestone. The volcanic clasts in the breccias are red and green and range from basalt to quartz-eye rhyolite porphyry. Quartzite clasts consisting of very well rounded grains, reminiscent of the Tapioca sandstone, are a minor but paleogeographically very important constituent. The macrofossil fauna includes horn corals, brachiopods, crinoids, bryozoa and *parafusulina*. Near Black Friday Lake, interbedded sea-green cherts and bedded limy turbidites (Plate 15), showing graded bedding and containing volcanic debris as well as shelly fragments including a few horn corals and crinoids, overlie the augite porphyries of the Huntergroup volcanics. Augite porphyry dikes cut the cherts and limestones, indicating continued igneous activity.

The oldest conodont age from this unit, obtained by Gordey *et al.* (1982) from limestone interbedded with red and green chert on the ridge south of Juniper Mountain, is middle Pennsylvanian (No. 82, Table 2). Fusulinids identified by Danner (personal communication, 1989) from limestones on the same ridge and in apparently the same stratigraphic position [one (No. 210, Table 1) is from a silty limestone directly overlying augite porphyry at the top of Unit IIIPPvs], are of Middle to Late Permian age (No. 209-211). In the Blue Dome map area, a number of Early Permian conodont ages have been obtained from the limy turbidites that overlie the Huntergroup volcanics (Table 2). These conflicting ages, and indeed the Permian ages from the underlying Huntergroup volcanics, suggest that the contact between the two is strongly diachronous, and that the Unit IIIPPs sediments are a distal facies of the Huntergroup volcanics, perhaps fringing carbonate buildups developed on the flanks of volcanic edifices (Figure 7).

Unit IIIPls

Pure, white limestone occurs as a discontinuous sliver at the base of Division III north of Chromite Creek in the Blue Dome map area. It contains abundant fusulinids, including a giant form that reaches several centimetres in length. Ross (1969) identified this as a new species, *Parafusulina macdamensis*, which has affinities with *Parafusulina* species in Texas, Washington and the State of Sonora, Mexico. He assigned it an early Guadalupian age. An identical age is reported for a fusulinid collection from Unit IIIPPs south of Juniper Mountain (No. 210).

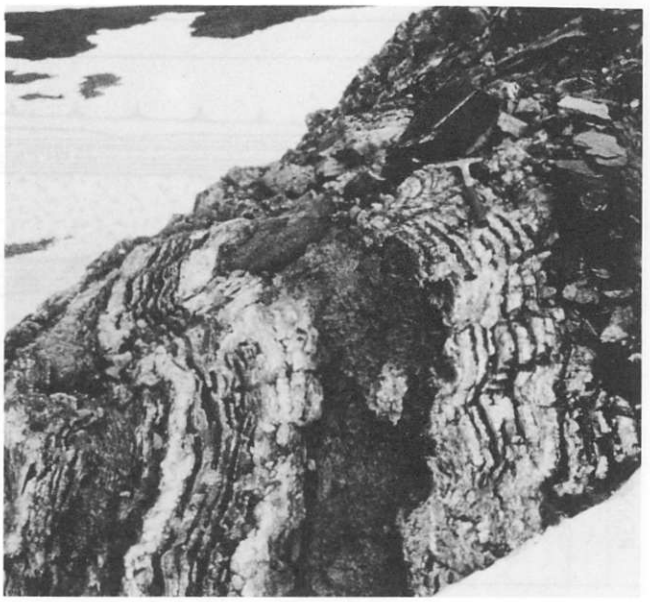


Plate 15. Interbedded calcarenite with graded bedding and lithic debris (limestone turbidite) and chert, Unit IIIPPs, near Black Friday Lake.

Unit IIIvs

Unit IIIvs is exposed on the ridge south of Juniper Mountain, south of an east-northeast-striking fault which separates it from the Huntergroup volcanic/IIIPPs sequence described above. Unit IIIvs shows a combination of small-scale interbedding and later structural slivering of different lithologies, giving it a heterogeneous character that defies subdivision at regional mapping scale. It consists of interbedded thin-bedded green tuff and lapilli tuff, limestone pods and laminated dirty calcarenite beds, quartz arenite, subarkosic sandstone, grit and grey slate, maroon and green slate, and small diorite bodies.

Petrographic examination of the sandstones shows that they consist of protoclastic quartz and minor, equally deformed, plagioclase; the trace mineral suite includes muscovite, tourmaline and zircon. The sandstones range from quartz arenite to matrix-supported greywacke with abundant sericite.

All of the conodont samples from this unit were barren. It is intruded by the early Mississippian tonalite body, Unit IIIMt, and therefore is early Mississippian or older.

Unit IIIMt

A lens-shaped tonalite body intrudes Unit IIIvs. The contact between the two is clearly intrusive; hornfelsing is observed in the field and in thin section, and large xenoliths of thin-bedded lithologies identical to those in Unit IIIvs are included in the tonalite.

The tonalite is a homogeneous, coarse-grained intrusion consisting of plagioclase, quartz, about 10 per cent potassium feldspar, and chloritized mafic minerals. It is not

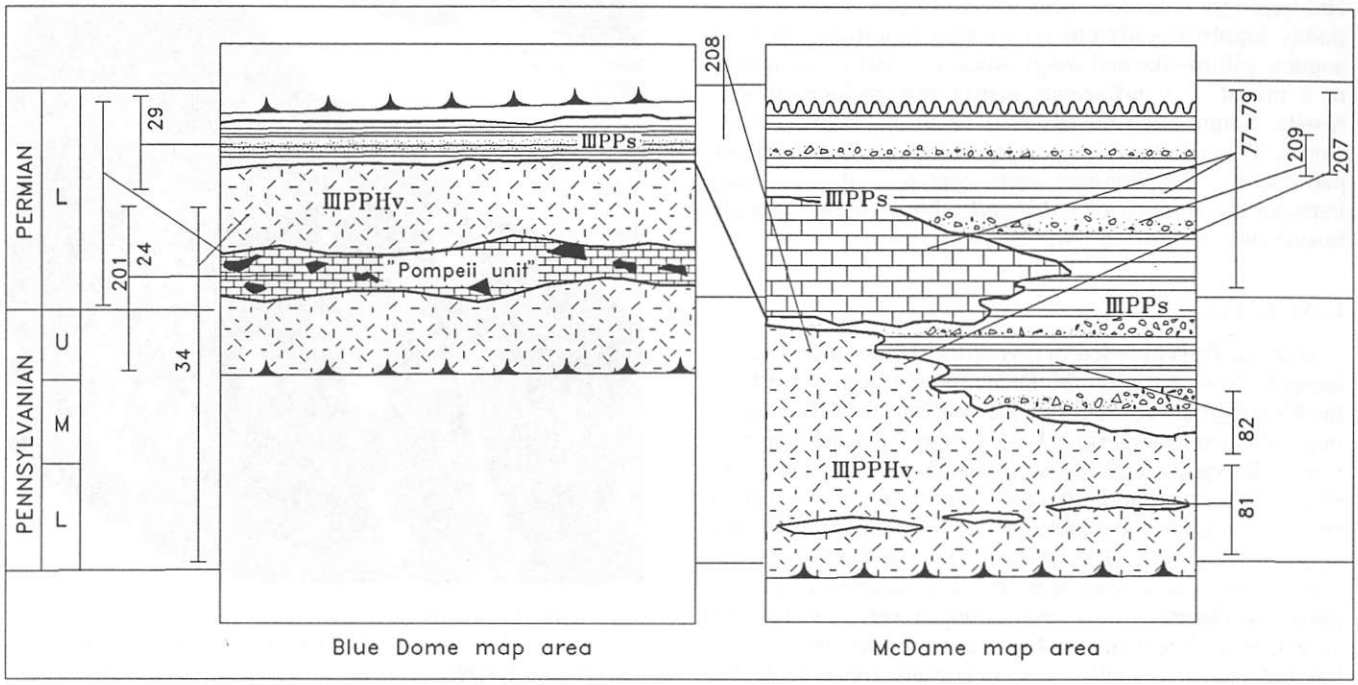


Figure 7. Relationships between Division III units, the Huntergroup volcanics (IIIPPHv) and Pennsylvanian-Permian sediments (IIIPPs) in two klippen near Black Friday Lake in the southwestern Blue Dome map area and around Juniper Mountain in the McDame map area. In both, the sediments depositionally overlie the Huntergroup volcanics. Microfossil ages (bars; numbers correspond to Tables 1 and 2) show considerable overlap, suggesting facies changes telescoped by thrust faults.

foliated, although in places it is strongly fractured and sheared, particularly adjacent to the fault that places it against the Huntergroup volcanics to the north.

An early Mississippian zircon age with strong Precambian inheritance has been obtained from this body (Gabrielse *et al.*, in preparation).

DIVISION III IN THE TOOTSEE LAKE MAP AREA

North of Toozaza Creek, a Division III klippe rests on top of the Foggy Mountain ultramafic mélange. It consists of two units, a zoned pluton (Unit IIIPi), and an undated volcanic-epiclastic-subvolcanic suite, the South Post Ridge volcanics. A dike similar in lithology and chemistry to the South Post Ridge volcanics intrudes the pluton, establishing a tentative age relationship between the two major units.

Unit IIIPi

This pluton is exposed on a low mountain east of Gum Mountain. It is zoned from hornblende gabbro to granodiorite. Interphase boundaries are either transitional, or sharp with more felsic phases diking the older, more mafic ones (Plate 16). Along its southern margin the pluton intrudes fine-grained white quartzite, probably contact-metamorphosed chert. All phases of the pluton are equigranular to slightly inequigranular, fairly coarse grained and unfoliated. In the hornblende gabbro, magmatic hornblendes contain ragged cores of clinopyroxene. The hornblende is partly replaced by actinolite, indicating subsolidus uralitic recrystallization. The most felsic phases are granodiorites consisting of small quartz and plagioclase phenocrysts in a slightly finer grained matrix of potassium feldspar, quartz and plagioclase.

A concordant late Early Permian uranium-lead age was obtained from zircons extracted from a granodioritic phase of this body (Gabrielse *et al.*, in preparation).

South Post Ridge Volcanics (Unit IIISPv)

The South Post Ridge volcanics are exposed on South Post Ridge (informal name on Figure 2) in the southern part of the Tootsee Lake map area, and on small hills to the north. They are a mixed subvolcanic-volcanic-volcaniclastic-epiclastic suite that ranges from porphyritic intrusions through flows, lapilli tuffs and breccias to volcanic sandstones with graded bedding. Compared to the Huntergroup volcanics, the South Post Ridge volcanics are much richer in potassium feldspar, although quartz is rare. They are alkalic in composition, ranging from clinopyroxene-bearing trachyandesites to latites and trachytes. The more felsic lithologies are uncommon and generally are seen as clasts in breccias and lapilli tuffs.

This unit is undated, however, trachyandesite dikes identical to it in lithology and chemical composition cut the southeastern corner of the pluton of Unit IIIPi.

Whole-Rock and Trace-Element Petrochemistry

Petrochemical analyses for major and minor elements were obtained for 52 samples of extrusive and intrusive igneous rocks representing the major units of Divisions II and III. The suite was analysed for major oxides, including

FeO, and the stable trace elements zirconium, chromium, vanadium, yttrium, scandium and niobium. Most samples were also analysed for the large-ion lithophile elements rubidium, strontium and barium; and a selected few for thorium, uranium and rare-earth elements. The results are presented in Appendix 2. All of these rocks have undergone prehnite-pumpellyite to actinolite facies metamorphism, as shown by loss on ignition values ranging from 1.36 to 8.40 per cent with an average of 3.47 per cent. Although unweathered and massive material was selected in sampling, in thin section most of the rocks are seen to contain veinlets of chlorite and/or prehnite-calcite. All plagioclases are albitized, and heavy concentrations of clay, sericite and saussurite are common. Gains and losses of mobile elements are therefore to be expected. For this reason ratios of the immobile elements were emphasized in petrochemical classification; on the other hand, classifications on the alkali-silica plot in Figure 8 agree with field and thin section nomenclature. On this plot, Division II analyses, except for the lower crustal samples, cluster exclusively within the basalt field, whereas Division III shows a strongly varied petrologic character, ranging from subalkaline to alkaline and from basalt to dacite. The Huntergroup volcanics are all subalkaline, with silica contents ranging from 49.25 to 64.17 per cent. Three samples from the zoned pluton, Unit IIIPi, show a nearly linear, subalkaline differentiation trend. The trachyandesites of Unit IIISPv on South Post Ridge plot in the alkaline field. They contain significant amounts of primary potassium feldspar coexisting with clinopyroxene and hornblende. All but one, however, are quartz normative. They are low in niobium, phosphorus and titanium and high in zirconium and yttrium, as shown in Figures 9 and 10. These are typical characteristics of shoshonites in contrast with other alkalic suites (N.W.D. Massey, personal communication, 1990). The only truly alkalic sample, shown on Figures 9 and 10, is of a rare amygdaloidal basalt flow (Sample 37635) interbedded with red and green cherts of autochthonous Unit MPs. It also plots within the range of alkalic, intraplate basalts on the Ti-V diagram (Figure 16), and at the edge of the within-plate field in terms of Ti-Zr-Y (Figure 11).

The more mobile major and trace elements have been enriched, and less commonly depleted, due to alteration. These effects are shown by a few examples. Figure 12 shows three of the more geochemically mobile elements, potassium, rubidium and barium, plotted against stable titanium and zirconium for the basalts. The wide scatter in these plots is good evidence that potassium and the large-ion lithophile elements were redistributed after recrystallization. In extreme cases barium, for instance, is enriched nearly 700 times its abundance in average oceanic basalts. By contrast, the plots involving two or more of the stable high field-strength elements (small ionic radii and high charges) show either tight clusters or clear linear trends. Mullen's (1983) MnO-P_2O_5-TiO_2 diagram (Figure 13), used to discriminate mid-ocean-ridge basalt (MORB) from island-arc tholeiites (IAT) and from calcalkaline basalts (CAB), shows that Division II basalts form a linear spread across all three fields, pointing towards the MnO apex. This is probably due to addition of manganese from hydrothermal fluids; manganese coatings on fractures are common.

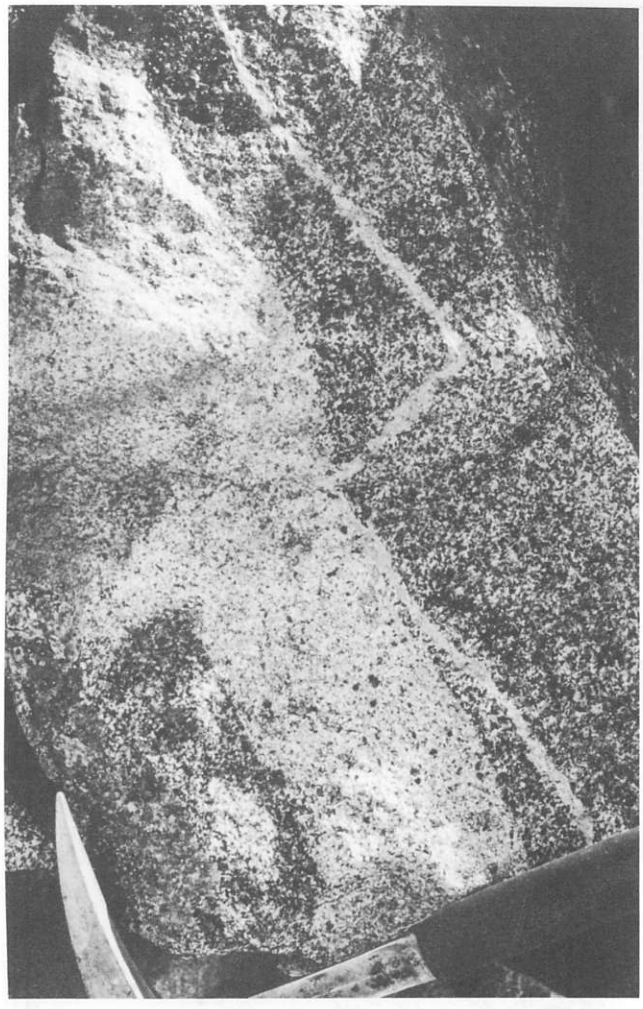


Plate 16. Detail of Unit IIIPi. Leucotonalite intrudes tonalite.

Therefore any plots involving mobile elements must be regarded with suspicion. This caveat includes major-element plots such as AFM diagrams as well as spidergrams that use large-ion lithophile elements as part of their characterization. Discriminant plots that use the more immobile elements are emphasized in the following discussion.

Geologically, a fundamental distinction has been drawn between the igneous rocks of Division II and Division III. Division III shows an island-arc character, whereas Division II is oceanic. One important possible environment for Division II, not discussed so far, is that of intraplate magmatism: ocean islands. The stratigraphic context of the Division II basalts, particularly their ubiquitous interbedding with pelagic and hemipelagic sediments, and their feeder complexes, which are not dikes but sills within older sedimentary sequences, are compatible with intraplate magmatism. Aggarwal *et al.* (1984) suggested that the Fennell Group basalts in the southern Slide Mountain Terrane were ocean islands, on the basis of their aluminum and titanium-rich clinopyroxenes and amphiboles and radiogenic lead compositions. This conclusion is at odds with the data of Schiarizza and Preto (1987) and Hall-Beyer (1976).

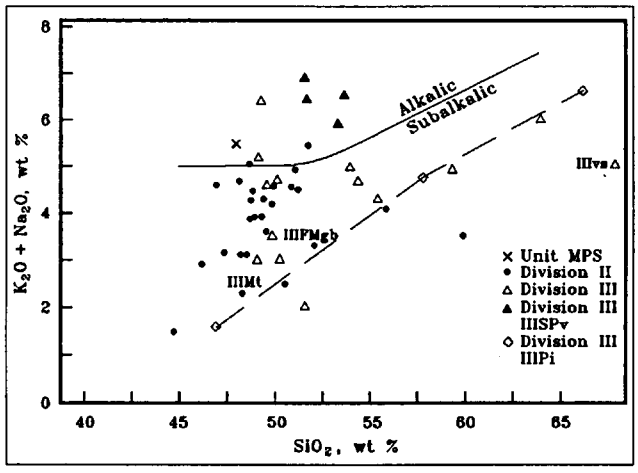


Figure 8. Silica-alkalies plot for Sylvester igneous rocks. All suites are generally subalkalic, except for the South Post Ridge volcanics, Unit IIISPv, which show shoshonitic affinities.

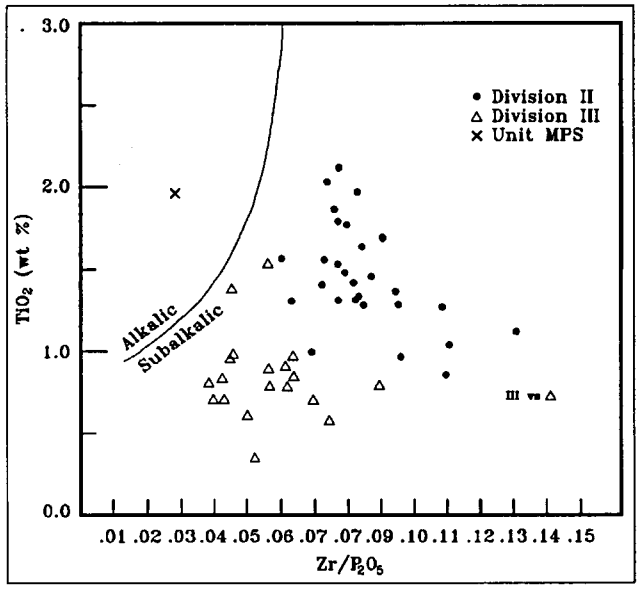


Figure 9. TiO_2 vs. Zr/P_2O_5, Sylvester basalts. Except for one sample from Unit MPs, all analyses fall in the subalkalic field, with a clear separation between Divisions II and III. (after Floyd and Winchester (1975); Winchester and Floyd (1976)).

One of the most useful discriminants for evaluating the within-plate option is the Ti-Zr-Y diagram of Pearce and Cann (1973). The source analyses for this, as well as all diagrams discussed subsequently, are true basalts and diabases with silica contents from 45 per cent to 52 per cent and MgO+CaO between 12 per cent and 20 per cent. Only samples that fall within at least one of these limits (and near the other) are plotted. This requirement eliminates most Division III analyses as too silica rich. Figure 11 is a Ti-Zr-Y plot of all Sylvester basalts. None of them occupy the within-plate field: this effectively eliminates ocean islands as a possible paleoenvironment for Division II.

Figure 11 shows some overlap between Division II and III basalts. Two-element diagrams in which titanium is plotted against zirconium, chromium or vanadium (Figures 14, 15, and 16) demonstrate a clear contrast between the two suites. These diagrams were devised to aid in the discrimination of ocean-floor from island-arc basalts (Shervais, 1982; Garcia, 1978). With few exceptions, Division II analyses clearly occupy the ocean-floor fields while Division III basalts are of island-arc affinity. In the titanium versus chromium plot, both show linear trends. The Division II trend shows a strong negative correlation between titanium and chromium, indicating chromite fractionation. The Division III trend is at a lower titanium value and nearly parallels the chromium axis; it represents the fractionation of magnetite. Magnetite fractionation is shown even more clearly on the Ti-V plot, where Division III values form a steep trend parallel to that calculated by Shervais (1982) for 10 per cent removal of magnetite. The Ti-Zr plot (Figure 14) not only discriminates between Division II mid-ocean ridge basalts and Division III basalts; it also shows that the latter include both island-arc tholeiites and calcalkaline basalts. This evidence, coming from high field-strength elements, is more reliable than discriminants that utilize alkalies, such as the AFM diagram, or CaO, such as normative plagioclase versus alumina.

Subclassification of Division II magmatic types is shown on Figure 17, the Nb-Zr-Y diagram of Meschede (1986), which contains a field for enriched-MORBs as opposed to normal N-MORBs, which are derived by melting of previously depleted upper mantle (Saunders *et al.*, 1980). E-MORBs may be derived from deep-mantle plumes that tap undepleted mantle. On this diagram, Division II basalts of both Mississippian and Pennsylvanian-Permian age range from the field of N-MORBs into the E-MORB field.

Discriminants based on high field-strength elements show a clear separation between the two basalt populations of Divisions I and II. Two significant exceptions to this rule are present. Sample 37627 is of a fine-grained gabbro-

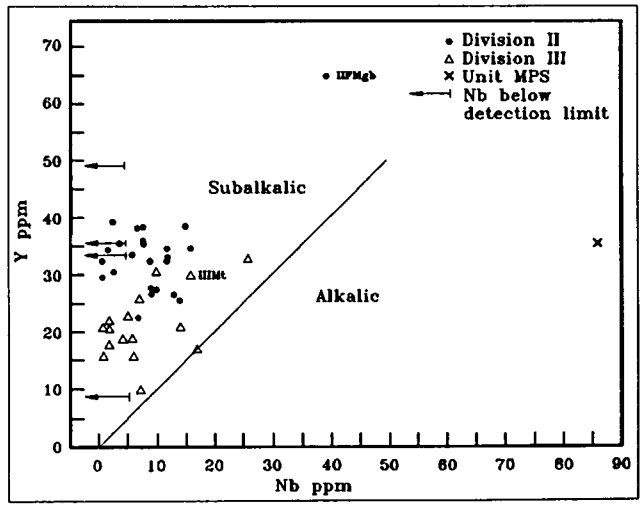


Figure 10. Y vs Nb, Sylvester basalts. All analyses fall in the subalkalic field, except Unit MPs. The Foggy Mountain gabbro sample is coarse grained and probably a cumulate. (after Garcia (1978)).

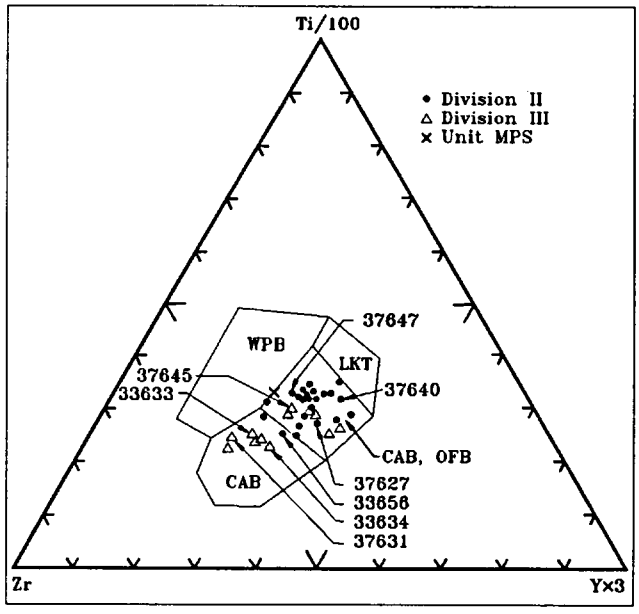


Figure 11. Ti-Zr-Y, Sylvester basalts. WPB=Within-plate basalt, LKT=Low-potassium tholeiite, CAB=Calcalkaline basalt, OFB=Ocean-floor basalt. (after Pearce and Cann (1973)).

diorite sill within Unit IIPPsi south of Mount Pendleton. It contains primary hornblende, a rarity in Division II. Gordey *et al.* (1982) also noted the presence of hornblende in the sills of this unit. Sample 37627 plots within the Division III island-arc trend on the Ti-Cr and Ti-V diagrams; its low titanium and zirconium contents place it in the area of overlapping oceanic and island-arc tholeiite fields on the Ti-Zr diagram. It may thus represent a tectonic environment that is transitional between island-arc and ocean basin. In general, the broad distribution of Division II basalts on the Ti-V diagram is more compatible with Shervais' (1982) data for marginal basins, as opposed to the midoceanic environment *sensu strictu*. In Division III, Sample 37631 from the Huntergroup volcanics plots well within the MORB fields on Ti-Cr and Ti-V diagrams. It is petrographically unexceptional except for abundant plagioclase phenocrysts.

In order to more fully characterize the Division II and III volcanic suites, four basalts from each and two andesites from Division III were analysed for thorium, uranium and rare-earth elements. They are plotted on diagrams after Pearce (1982), normalized against a MORB composition (Figure 18), on diagrams after Sun *et al.* (1979), normalized against a slightly different MORB composition (Figure 19), and the rare-earth elements are plotted on Figure 20, normalized against average chondrite. The rare-earth element diagram shows the clearest contrast between Division II and Division III samples. All of the Division II samples, even 37627 with depleted high field-strength elements, suggest an arc component, but show the slight depletion to slight enrichment in light rare earths that are typical of ocean-floor basalts. In contrast, all Division III samples show strong enrichment in light rare earths, characteristic of island arcs.

Although their rare-earth behavior emphasizes the integrity within and distinction between the two suites, com-

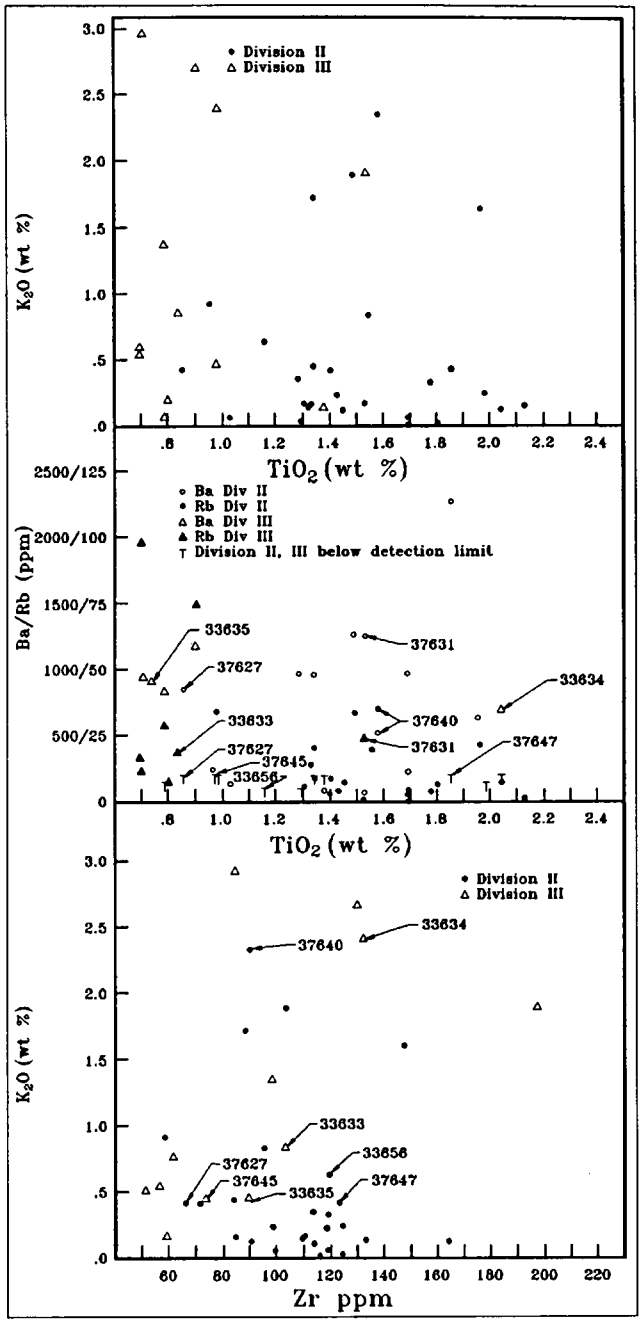


Figure 12. TiO_2 vs K_2O, Ba, and Rb; Zr vs. K_2O, Sylvester basalts. Numbered samples are those specifically discussed in the text.

parison of the patterns on the Pearce and Sun diagrams (Figures 18 and 19), which integrate high field-strength and rare-earth elements, tends to show the character of individual samples. The left-hand sides of both diagrams, with their erratic strong enrichment of the large-ion lithophile elements in both suites, are of dubious diagnostic value. Therefore attention is focused on elements to the right of thorium on the Pearce diagram and to the right of potassium on the Sun diagram. Of the four Division II basalts, two of them, 37640 and 37647, show fairly flat, typical MORB patterns on the Pearce diagram. Sample 37647 is chrome depleted,

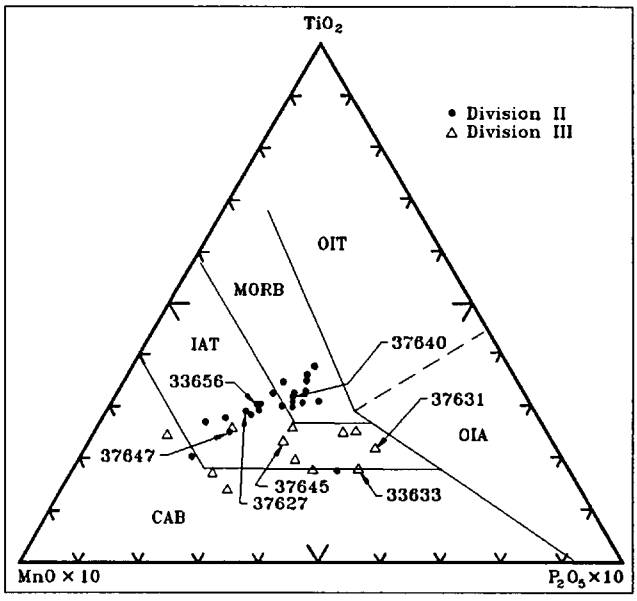


Figure 13. MnO-P_2O_5-TiO_2, Sylvester basalts. CAB=Calcalkaline basalt, IAT=Island-arc tholeiite, MORB=Mid-ocean ridge basalt, OIT=Ocean-island tholeiite. Numbered samples discussed in text. (after Mullen (1983)).

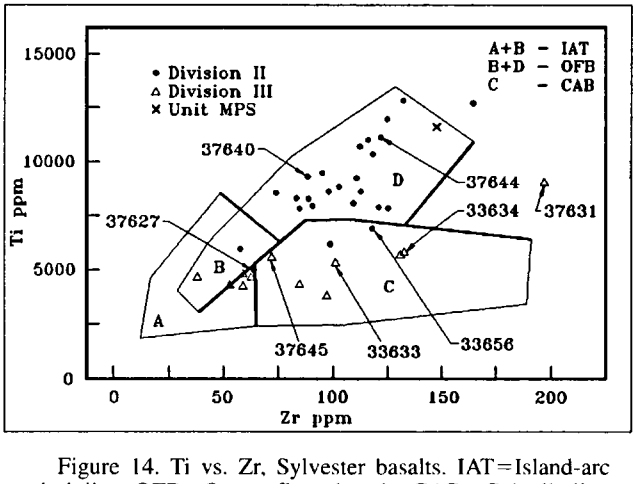


Figure 14. Ti vs. Zr, Sylvester basalts. IAT=Island-arc tholeiite, OFB=Ocean-floor basalt, CAB=Calcalkaline basalt. Numbered samples discussed in text. (after Pearce and Cann (1973)).

probably due to chromite fractionation; it plots at the chromium-poor end of the Division II trend on the Ti-Cr diagram (Figure 15). Sample 37640, with its enriched cesium and niobium, could have some transitional-MORB character. This is also indicated on the Nb-Zr-Y diagram, Figure 17. Sample 37631, the hornblende-bearing sill, is depleted in all of the high field-strength elements as well as phosphorus and cerium. It compares most closely with island-arc tholeiites (Pearce, 1982), except that it does not show a negative niobium anomaly. Sample 33656 is erratically depleted in some high field-strength elements, which may indicate a slight island-arc influence.

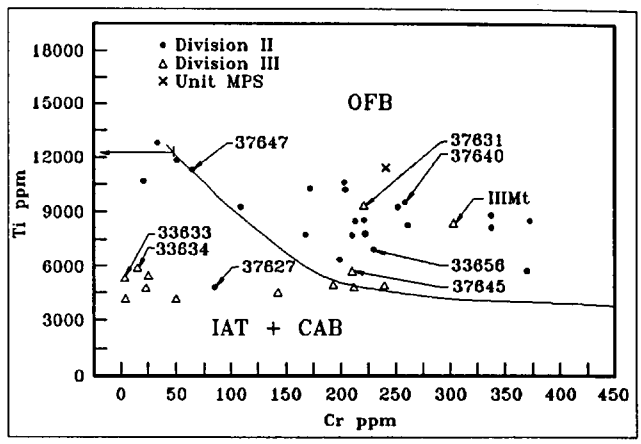


Figure 15. Ti vs. Cr, Sylvester basalts. OFB=Ocean-floor basalt, IAT=Island-arc tholeiite, CAB=Calcalkaline basalt. Numbered samples discussed in text. The Mississippian tonalite sample is coarse grained and probably cumulate. (after Garcia (1978)).

On the Sun diagram (Figure 19), all of the Division II samples show fairly flat patterns to the right of potassium; these indicate their close affinity to typical tholeiites. Erratic strontium values may be due to remobilization. Sample 37627 is depleted uniformly in all elements. Samples 37640 and 37647 show slight enrichments in lanthanum, cesium, zirconium and titanium – evidence for a transitional character. Although sample 37640 plots as a transitional MORB on the Pearce and rare-earth element diagrams, and also on Figure 17 because of its relatively high niobium, sample 37647 is less enriched in light rare earths and contains little niobium.

Division III basalts and andesites are generally depleted in high field-strength elements on the Pearce diagram, except for sample 37631. This sample is also progressively enriched in zirconium, phosphorus, cesium and niobium, a pattern more indicative of transitional MORBs than island-arc tholeiites (Pearce, 1982). The others have arc or transitional-arc signatures; 33633, 33634 and 33635 show troughs at niobium, a clear arc fingerprint. The behaviour of Division III samples on the Sun diagram (Figure 19) is strongly influenced by their light rare-earth enrichment. The strong negative niobium anomalies are of questionable significance, as they are bracketed by the mobile elements potassium and uranium.

Taken as a whole, the trace-element geochemistry of Sylvester igneous rocks shows a clear distinction between Division II and III and the single alkalic, within-plate basalt sampled in Division I. Trace-element geochemistry also demonstrates that Division II contains both normal and enriched mid-ocean ridge basalts, suggesting that plume activity may have influenced patterns of rifting. The existence of a few samples, transitional in their character between arc and oceanic basalts hints at ties between the two divisions, for instance, arc and back-arc marginal basin. A marginal basin tectonic environment for Division II is favoured by the wide scatter on the Ti-V plot (Figure 16).

These results agree with interpretations in the field. The association of Division II igneous rocks with, in some cases,

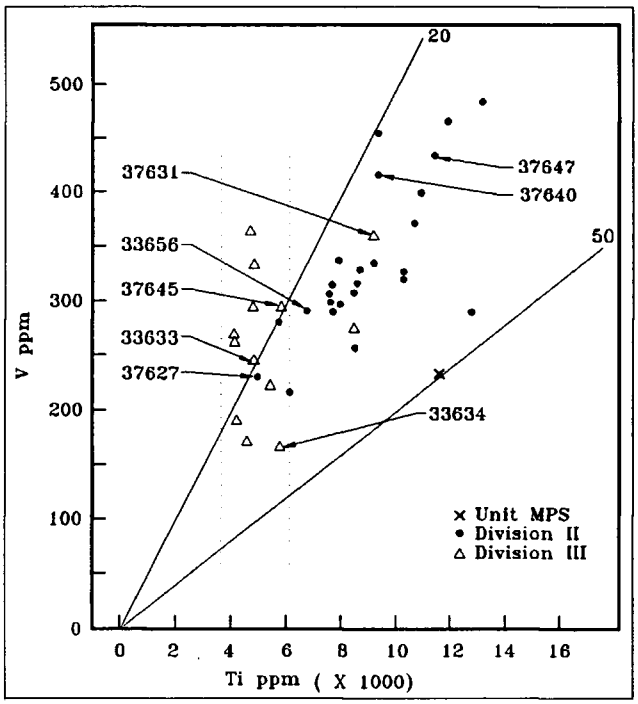


Figure 16. Ti vs. V, Sylvester basalts. The ocean-floor field spans ratios from 20 to 50 at higher absolute titanium values. The vertical trend outlined by the fine dots is typical of island arc suites. (after Shervais (1982)).

much more voluminous sediments is not evidence for intraplate magmatism, but rather for a marginal basin environment with high sedimentation rates. The lack of olivine phenocrysts in Division II basalts is also compatible with such a tectonic environment, in contrast to a true mid-ocean ridge setting where olivine-phyric flows are prevalent (Saunders *et al.*, 1980). The presence of rare hornblende in the basalts of Unit IIPPvs, and typical hornblende in the Unit IIPPsi sills, indicates hydrous melts and perhaps the influence of island-arc magmatic sources.

Discussion

The Sylvester allochthon in the report area consists of three structurally stacked facies packages. If their present stacking order reflects their original disposition with respect to the margin of ancestral North America, then the allochthon represents, from east to west, a late Paleozoic sediment-dominated marginal basin, an adjacent but volcanic-dominated marginal basin floored by contemporaneous oceanic lower crust and upper mantle, and an island arc built on a basement of continental crust, or at least continental margin sediments. This inferred model is shown in Figure 21. The Blue Dome fault zone defines a major facies break within the marginal basin, juxtaposing Mississippian sediments to the east against Mississippian basalts and sediments to the west.

The overturn of the Blue Dome fault zone into the Foggy Mountain serpentinite mélange offers an important insight into the mechanism of assembly of the allochthon in general. Each ultramafic sheet within it, the Quartzrock Creek - Cassiar and the Zus Mountain - Blue River bodies, could have originated in such a transform fault or pull-apart zone. Examples of similar bodies exposed within modern rift and transform settings include the Zabargad ultramafite in the Red Sea (Bonatti *et al.*, 1981) and ultramafites in the Owen fracture zone in the Indian Ocean (Bonatti and Hamlyn, 1978). During subsequent crustal transpression, these zones would be favourable loci for transcurrent motion and also serve as thrust ramps. The resulting pattern would be that of different crustal segments stacked vertically, marked by now-flat ultramafic-gabbro sheets. The eventual emplacement of the Sylvester allochthon led to the decapitation of these sheets from their roots; except for the Blue Dome fault, their steep sections are now eroded off.

Cartoon restoration (Figure 21) emphasizes east-west shortening rather than the effects of lateral translation. The actual magnitudes of pre-emplacement transcurrent motions between parts of the allochthon, or between the allochthon and the Cassiar Terrane, are not known. The principal tie between Divisions I and II and ancestral North America is the correspondence between the black clastic equivalents and the autochthonous Earn Group of the Cassiar Terrane, Kechika basin and Selwyn basin. However, similar Devono-Mississippian siliciclastic sequences occur as far south as the Barriere area in British Columbia (Schiarizza and Preto, 1987). Turner *et al.* (1989) point out correspondences between the Earn Group of the Selwyn basin and the Slaven chert of the Roberts Mountain allochthon in Nevada. The Mississippian Bragdon Formation of the eastern Klamath Mountains and the Picayune Valley Formation in the Sierra Nevada also contain Earn-like siliciclastic sediments (Miller and Cui, 1989; Harwood *et al.*,1991). Sedimentary exhalites and evidence of growth faulting in the Slaven chert suggest a mildly extensional Late Devonian tectonic regime, like

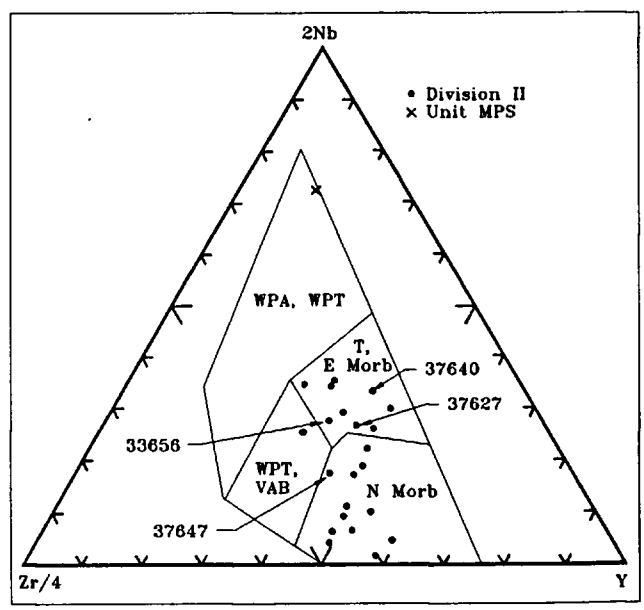
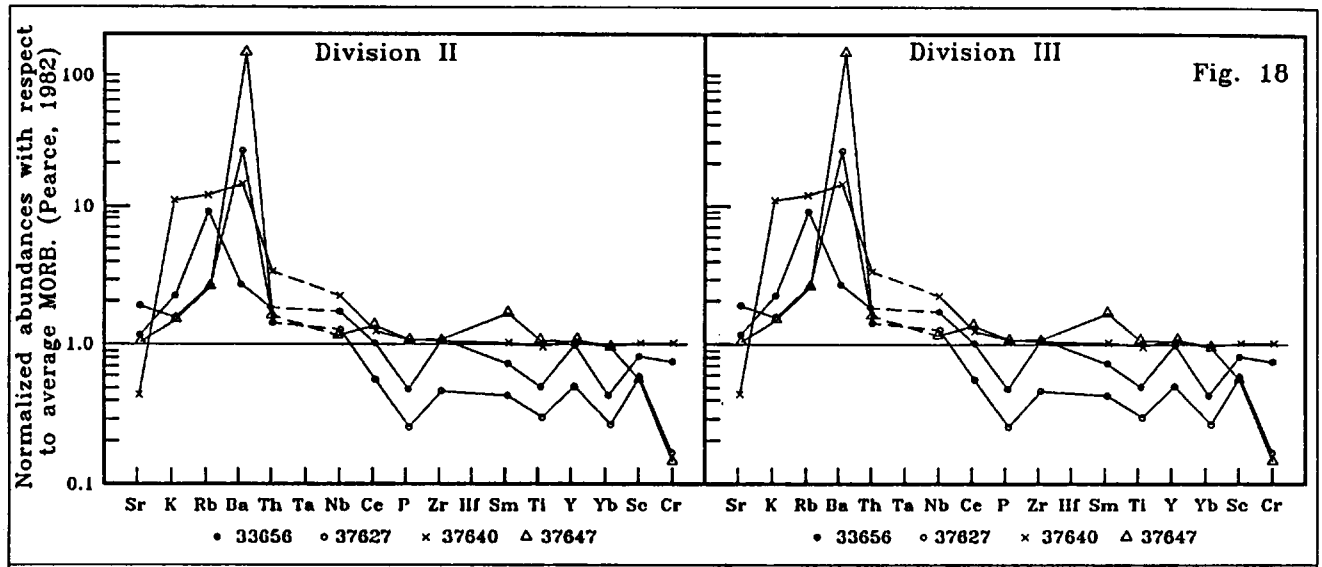
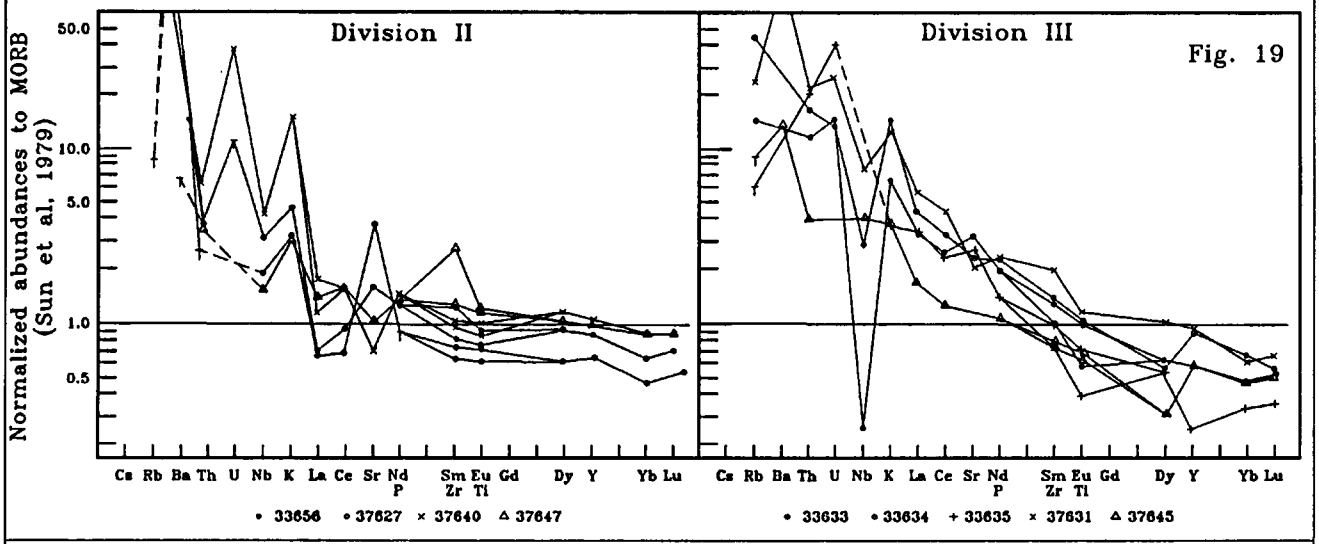
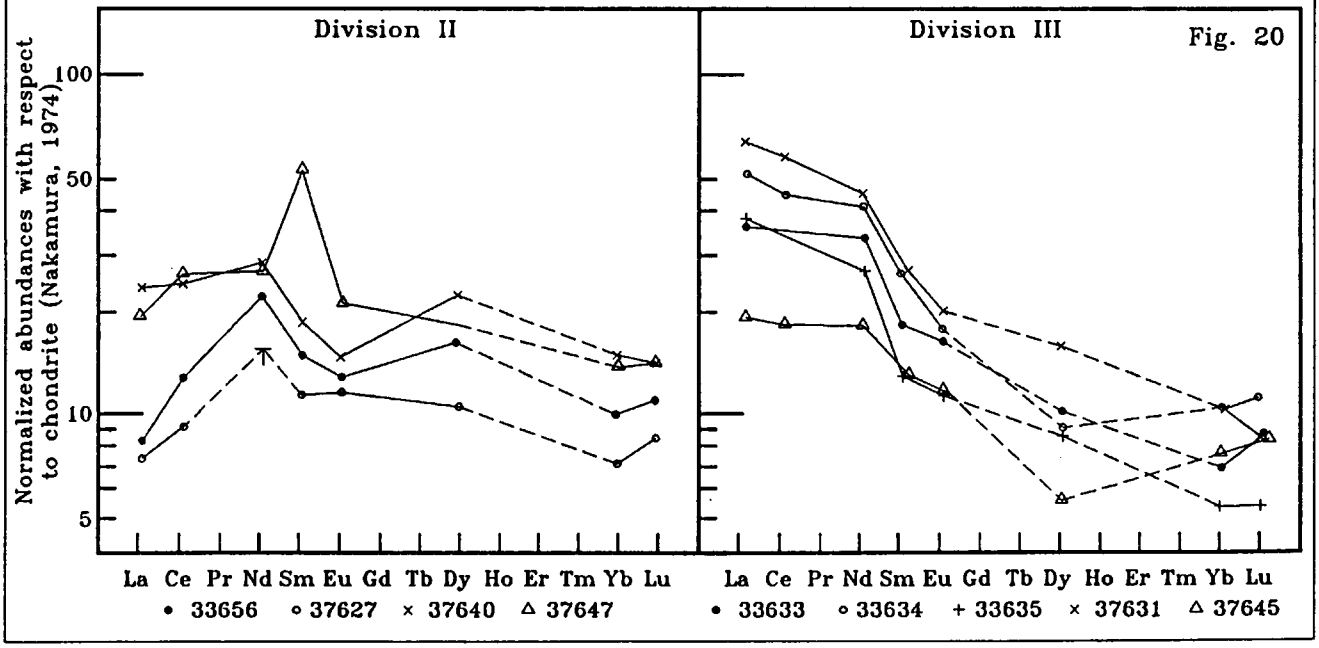


Figure 17. Nb-Zr-Y plot, Sylvester basalts. WPA=Within-plate alkalic, WPT=Within-plate tholeiite, VAB=Volcanic-arc basalt, T-transitional, E-enriched, N-normal MORB. (after Meschede (1986)).


Division II
Division III
Fig. 18
Normalized abundances with respect to average MORB. (Pearce, 1982)
100
10
1.0
0.1
Sr K Rb Ba Th Ta Nb Ce P Zr Hf Sm Ti Y Yb Sc Cr
• 33656 ∘ 37627 × 37640 △ 37647


Division II
Division III
Fig. 19
Normalized abundances to MORB (Sun et al, 1979)
50.0
10.0
5.0
1.0
0.5
Cs Rb Ba Th U Nb K La Ce Sr Nd P Sm Zr Eu Ti Gd Dy Y Yb Lu
• 33656 ∘ 37627 × 37640 △ 37647
• 33633 ∘ 33634 + 33635 × 37631 △ 37645


Division II
Division III
Fig. 20
Normalized abundances with respect to chondrite (Nakamura, 1974)
100
50
10
5
La Ce Pr Nd Sm Eu Gd Tb Dy Ho Er Tm Yb Lu
• 33656 ∘ 37627 × 37640 △ 37647
• 33633 ∘ 33634 + 33635 × 37631 △ 37645

that inferred in the northern Cordillera. Therefore, in terms of sedimentological ties, the Sylvester allochthon could be placed as a marginal basin and island arc outboard of North America, anywhere from Alaska to Nevada.

Further study of the macrofaunal assemblages of Division III is needed in order to clarify their paleogeographic affinities. The brachiopods of collection number 201 from limestone in the Huntergroup volcanics belong to the Uralian - North American faunal province (E.W. Bamber, personal communication, 1987); and preliminary examination of fusulinids from Unit IIIPPs (Nos. 207 and 210) suggests that they are of North American affinity, similar to suites in the Golconda allochthon and the Permian limestones near Kettle Falls, Washington, rather than 'Cordilleran' like those accompanying McCloud-type coralline faunas in, for instance, the Harper Ranch Group and the Chilliwack Group (W. Danner, personal communication, 1989). The *Parafusulina macdamensis* of Unit IIIPIs has an autochthonous parallel in the Word Formation of West Texas (Ross, 1969). It also resembles *Parafusulina antinomensis* in the Caborca Terrane of northwestern Mexico (Ross, 1969), a terrane that is probably an Ordovician to Permian North American offshelf facies (Campa and Coney, 1983; J. Stuart, personal communication, 1989). These similarities may indicate that in late Paleozoic time Division III belonged to a more southerly North American faunal province.

Whatever the translational history of the Sylvester allochthon, it bears no evidence of westward subduction. Division II was a late Paleozoic marginal basin developed between the continent and the island arc of Division III. Division II contains no elements indicative of a subduction zone: accretionary prism, sedimentary mélange, extremely shuffled stratigraphy, or high pressure - low temperature metamorphic suites. Eastward subduction beneath Division III is the most likely case, and is shown in Figure 21. A reasonable position for the late Paleozoic subduction zone is within the Cache Creek Terrane, which is recognized at least as far south as the western Sierran foothills (Miller, 1987).

Synthesis: the Sylvester Allochthon and the Slide Mountain Terrane

The Slide Mountain Terrane is a key element in the reconstruction of the suspect terranes vis-a-vis ancestral North America in late Paleozoic time, because it is broadly oceanic in character and yet typically lies in direct structural or even stratigraphic contact with continental-margin sequences. This detailed study of the Sylvester allochthon has implications for the nature of the Slide Mountain Terrane in general and for its relationships to adjacent terranes – North America, the Yukon-Tanana and Harper Ranch terranes. Divisions I and II of the Sylvester allochthon are representative of the Slide Mountain Terrane which also includes, from north to south (Figure 4 and Table 3): the Angayucham Terrane (Roeder and Mull, 1978; Jones *et al.*, 1988), the Anvil allochthon proper (Tempelman-Kluit, 1979a; Mortensen and Jilson, 1985) as well as scraps of 'Anvil' type within the Yukon-Tanana Terrane west of the Tintina fault (Hansen, 1987, 1988, 1989); the Slide Mountain Terrane in the Manson Creek - Quesnel area (Struik, 1988; Ferri and Melville, 1988, 1989, 1990); the Crooked amphibolite (Struik, 1988); the Fennell Group (Schiarizza and Preto, 1987); the Milford and Kaslo groups (Klepacki, 1983; Klepacki and Wheeler, 1985); the Chapperon Group, the Kobau Group and parts of the Anarchist Group in the Okanagan area (Little, 1960; Read and Okulitch, 1977); and the Golconda allochthon of Nevada (Miller *et al.*, 1984). Of these, the Milford Group shows demonstrable depositional ties to a North American pericratonic unit, the Broadview Formation (Klepacki and Wheeler, 1985), and siliciclastic detritus in the Golconda allochthon is strongly suggestive of continental provenance (Miller *et al.*, 1984).

Division III of the Sylvester allochthon is representative of the Harper Ranch subterrane of Quesnellia (Wheeler *et al.*, 1988) and also the Yukon-Tanana Terrane. The Pennsylvanian-Permian Huntergroup volcanics and their associated limestones resemble parts of the Harper Ranch subterrane (Smith, 1979; Monger, 1977), whereas the early Mississippian tonalite with its strong Precambrian inheritance is like orthogneisses in the Yukon-Tanana Terrane (Mortensen and Jilson, 1985). The tonalite and the rocks that it intrudes may have equivalents south of the Dease River, Gabrielse and Harms (1989). These relationships within the Sylvester allochthon show rocks of Harper Ranch affinity faulted against Yukon-Tanana-type rocks; but both together in a klippe that rests above Slide Mountain rocks. Moreover, suggestions of early ties between Divisions II and III, arcgeochemical signatures in Division II, siliciclastic sediments in it that require a "continental" source, and the identification of Division II as a back-arc marginal basin, all tend to model Divisions II and III as two linked paleogeographic elements. Similar ties have been proposed by Miller *et al.* (1984) and Miller (1987) for the Golconda allochthon (basinal) and Eastern Klamath (arc) terranes.

These relationships suggest that the late Paleozoic Slide Mountain - Harper Ranch Terrane as a whole was a series of island arcs and marginal basins connected to each other and to North America, with loci of arc and rift magmatism shifting through time so that locally the two distinct tectonic environments were in depositional contact. This model probably also applies in the southern Okanagan, where older geological relationships are obscured by intrusion, high-grade metamorphism and extensional faulting. There, both basinal elements of Slide Mountain affinity and arc elements of Harper Ranch affinity occur in scattered exposures. Basinal elements include the Chapperon Group and Knob Hill Formation. Arc elements include the Mount Roberts Formation (Little, 1960; Roback and Walker, 1989), *Schwagerina*-bearing (W. Danner personal communication, 1989) 'Pompeii' limestone interbedded with

Facing Page:

Figure 18. Pearce element plots, selected Sylvester samples.
Figure 19. Sun multielement plots, selected Sylvester samples.
Figure 20. REE plots, selected Sylvester samples.

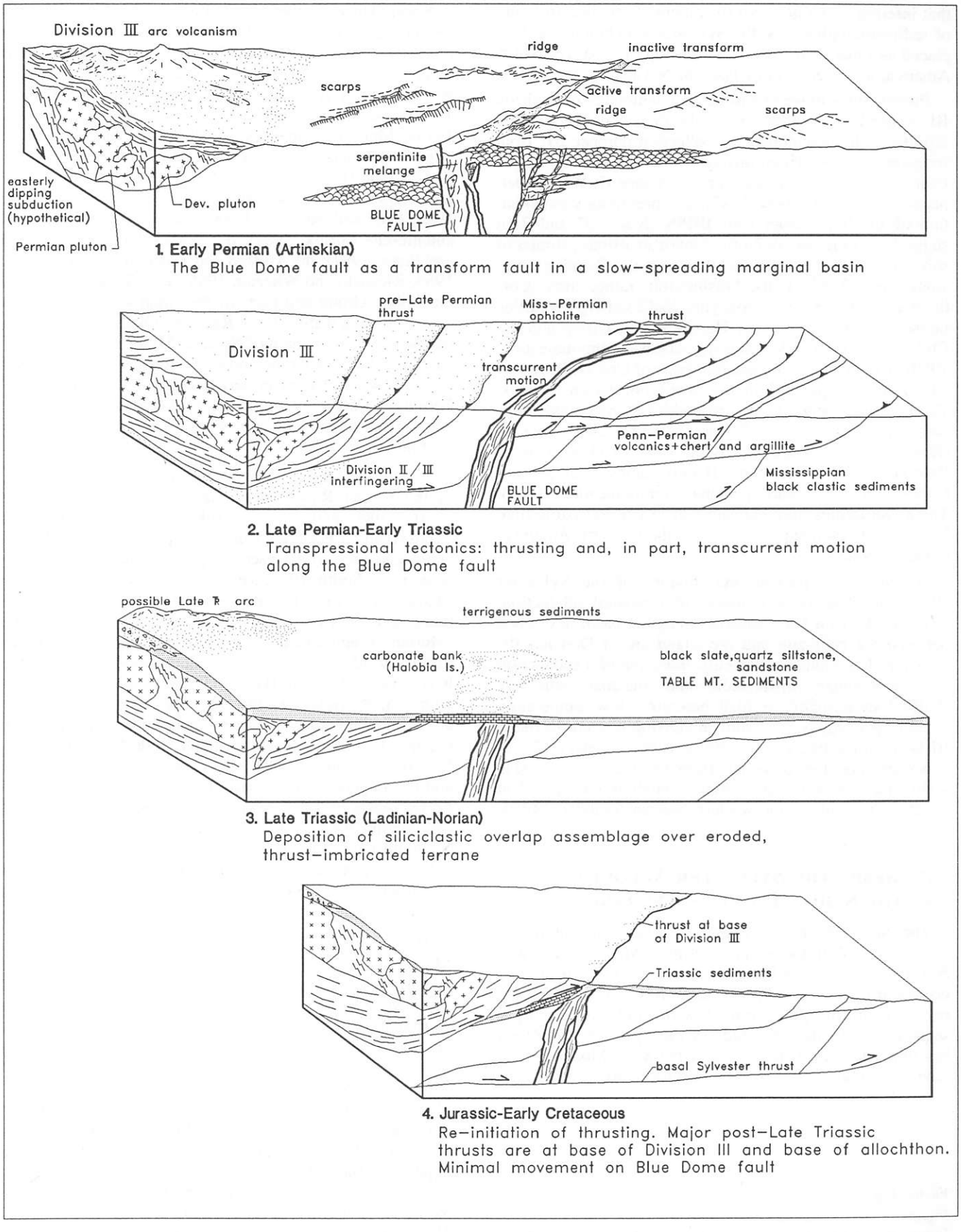


Figure 21. Diagrammatic view of the evolution of the Sylvester allochthon.

TABLE 3
EVENT-STRATIGRAPHIC COMPARISONS AMONG THE SYLVESTER ALLOCHTHON AND OTHER TERRANES

Shared Elements	Cache Creek	Yukon-Tanana	Quesnellia		Sylvester Allochthon		Pericratonic Terranes	Ancestral North America
			Harper Ranch	Slide Mountain	Division III	Division I, II		
Upper Triassic siliciclastic/ carbonate sediments		* siliciclastics/ synorogenic conglomerate[1] east of Tintina fault		*Slate Creek fm. Manson Creek[6] * Black phyllite		Table Mountain sediments	* N. Cassiar Terrane[19,20,21]	* Rocky Mtns.[25] * Kechika[26] * Selwyn basin[27]
Permo-Triassic deformation		* pre-Upper Triassic (Faro locality)[1] * Teslin suture zone[3]		*S.E. B.C.[11,12]				
Pennsylvanian-Permian arc facies, parafusilina limestone		* Permian plutons[4] * parafusilina limestone[5]	* Harper Ranch Group[13] * Lay Range[14] * S.E. B.C./ N.E. Washington[15,16]		IIIPPHV, IIIPPs			
Pennsylvanian-Permian oceanic rocks with interbedded chert; or chert without volcanics	*greenstone/ chert; but fossil assemblages are distinct from other terranes[5]			* Germansen[6,7] * Antler Fm.[17] * Upper Fennell Gp.[18] * Kaslo Gp.[11]		IIPPvs, IPPs	* radiolarian chert, Cassiar Terrane (MPs); also in N. Cassiar terrane[21]	
Devono-Mississippian siliciclastics and plutons		* siliciclastics[4] * plutons[2,4]		* qz-chert ss, rhyolite: – Germansen[6,7] * qz-chert ss, rhyolite, Lower Fennell Gp.[18] * siliciclastics, Milford Gp.[11]	IIIMt IIIvs	IMs, IMsi IIMvs	* siliciclastics: – Earn Group[28] – Black Stuart Gp.[21] * plutons[22,23] * felsic to intermediate volcanic rocks[18,24]	* Earn Group[28]

References:

[1] Tempelman-Kluit (1979b)
[2] Mortenson and Jilson (1985)
[3] Hansen (1989)
[4] Mortensen (in press)
[5] Wheeler *et al.* (1988)
[6] Ferri and Melville (in preparation)
[7] Ferri and Melville (1990)
[8] Bloodgood (1987)
[9] Bloodgood (1988)
[10] Struik (1988)
[11] Klepacki and Wheeler (1985)
[12] Read and Okulitch (1977)
[13] Smith (1979)
[14] Monger (1973)
[15] Roback and Walker (1989)
[16] Dutro and Gilmour (1989)
[17] Struik and Orchard (1985)
[18] Schiarizza and Preto (1987)
[19] Tempelman-Kluit *et al.* (1976)
[20] Abbott (1977)
[21] Gordey (1981)
[22] Okulitch (1985)
[23] Mortenson *et al.* (1987)
[24] Mortenson (1982)
[25] Gibson (1975)
[26] Gabrielse (1980)
[27] Gordey *et al.* (1981)
[28] Gordey *et al.* (1986)

volcanic sandstone on July Creek near the Phoenix mine, and the limestones near Kettle Falls.

The Anvil allochthon, as originally defined by Tempelman-Kluit (1972) and modified by Gordey (1983), comprises an ophiolitic suite in the Anvil Range comprised of green and red impure chert, amygdaloidal pyroxene-porphyry basalt, pyroclastics and Late Permian tuffaceous, fusulinid-bearing limestone. In the Sylvester allochthon, this package would correlate most closely with the Hunter-group volcanics and Unit IIIPPs of Division III, rather than with the typically oceanic Slide Mountain Terrane near Quesnel (Struik and Orchard, 1985) or in Division II. Tempelman-Kluit (1979a) extended the Anvil allochthon to include packages of serpentinite, amphibolite and basalt that occupy a particular structural level within the Yukon-Tanana Terrane. Subsequent mapping has located Anvil-type lithologic packages at a number of structural levels in the Yukon-Tanana Terrane (*cf.* Mortensen and Jilson, 1985: Hansen, 1987, 1989). The limited definition serpentinite-amphibolite-basalt strips the Slide Mountain Terrane of its distinctive character: such packages could equally belong to the Cache Creek Terrane. In the Sylvester allochthon, extensive siliciclastics, similar to those in the Yukon-Tanana Terrane (Mortensen, in press), are interbedded with basalts of Anvil affiliation. The purpose of this observation is to introduce a cautionary note and to emphasize the importance of detailed mapping in the unravelling of these complex tectonic entities.

The Anvil allochthon differs significantly from the Slide Mountain Terrane farther south. The easternmost exposures of ophiolites in the Campbell Range belt (Mortensen and Jilson, 1985), are in klippen above cataclasites of the Finlayson Lake fault zone and, locally, above autochthonous North American rocks. Permian blueschists and eclogites occur within the Finlayson Lake fault zone (Erdmer, 1987; Erdmer and Armstrong, 1988) which is evidence of a late Paleozoic plate boundary on the North American margin. The Anvil allochthons were derived from an ocean west of this boundary, the late Paleozoic Anvil ocean of Tempelman-Kluit (1979a). If all of the Slide Mountain Terrane remnants represent parts of a single ocean, then this ocean seems to increase in width and significance from south to north. Its southernmost exposures in the Goat Range show depositional contacts

with autochthonous strata of the Lardeau Group (Klepacki and Wheeler, 1985). The Fennell Group (Schiarrizza and Preto, 1987), the Slide Mountain Terrane near Manson Creek (Ferri and Melville, in preparation) and the Sylvester allochthon are in tectonic contact with autochthonous strata, but all show ample evidence of early ties to North America and no evidence for an intervening plate margin. By contrast, the Anvil allochthon was separated from North America by a Permian plate boundary. Still farther north, in the Brooks Range of Alaska, the Angayucham Terrane, a proposed Slide Mountain correlative (Harms, 1986; Figure 4 this pnblication), contains Mississippian through Early Jurassic radiolarian cherts (Jones *et al.*, 1988), thoroughly unlike the Triassic siliciclastic overlap sequence of the Slide Mountain Terrane. The ophiolitic Angayucham Terrane rests on deformed and metamorphosed North American marginal rocks, including blueschists. Patton and Box (1989) model this zone as southward Jura-Cretaceous subduction of the continental margin. In a large sense, perceived differences in the nature and history of the oceanic terranes in contact with North America may be in part a function of the latitude at which one looks.

The initial telescoping of the marginal basin of Divisions I and II occurred after mid-Permian time. This is the age of the youngest sediments in the base of Division II, which were thrust over Division I. This thrust fault was subsequently truncated along the Blue Dome fault, which shows evidence of transcurrent movement. The younger limit of this deformational event may be Late Triassic: the Table Mountain sediments overlap flat thrusts in Division II and, at one locality, the Blue Dome fault.

The Middle(?) to Upper Triassic Table Mountain sediments represent a renewed pulse of siliciclastic sedimentation that followed telescoping of oceanic rocks of Division II in Permo-Triassic time. They have widespread parallels, both on the North American margin and at the base of the Quesnel Terrane (Table 3). Their siliciclastic facies, black slate, quartz sandstone and siltstone, is lithologically identical to "synorogenic" sediments in the Yukon-Tanana Terrane (Tempelman-Kluit, 1979b), the 'Black Phyllite Unit' of the Quesnel trough (Bloodgood, 1987; Struik, 1986,1988), to the Triassic black slate in the Slide Mountain Terrane near Manson Creek (F. Ferri, personal communication, 1989; and senior author's observations) and to parts of the Slocan Group (Klepacki and Wheeler, 1985; D. Klepacki, personal communication, 1989 and senior author's observations near Kaslo). The limestone facies of the Table Mountain sediments resembles the southern Slocan Group and limestones that rest unconformably on the Old Tom - Shoemaker Group near Keremeos.

Permo-Triassic unconformities are well documented at the base of the Quesnel Terrane in the Goat Range (Klepacki and Wheeler, 1985), near the Salmon River (Read and Okulitch, 1977) and in the Middle to Upper Triassic Brooklyn conglomerate in the Greenwood - Grand Forks area, which contains clasts of Permian diorite and Carboniferous or Permian limestone (Fyles, 1990). Arguments for interpreting the base of the Table Mountain sediments as a sheared unconformity were outlined above. The siliciclastic character of the overlapping sediments, as well as their correlation with similar autochthonous sediments, suggests that the Permo-Triassic telescoping led to at least a partial amalgamation with the North American continent.

A second post-Late Triassic, Jurassic to Early Cretaceous imbrication emplaced Division III above the Table Mountain sediments and Division II. How much eastward travel of Divisions I and II was accomplished in Permo-Triassic as opposed to Jurassic time, remains a question.

The Sylvester allochthon and other segments of the Slide Mountain Terrane farther south tell an important story with respect to tectonics of the North American margin in Devonian through early Mesozoic time. A major extensional episode affected the western part of ancestral North America in latest Devonian to early Mississippian time, as originally suggested by Tempelman-Kluit (1979a). The autochthonous Earn Group was deposited in rift basins in the Selwyn and Kechika basins and Cassiar Terrane (Gordey *et al.*, 1986); its siliciclastic sediments were derived from miogeoclinal horsts and its exhalites were associated with growth faults (Gordey, 1988; Turner and Rhodes, 1990). Turner *et al.* (1989) point to similar depositional-tectonic environments in the Roberts Mountain allochthon, although there extension was interrupted by a compressional event, the Antler orogeny, in earliest Mississippian (Kinderhookian) time. Local basalt and felsic, partly alkalic volcanism accompanied this event (Mortensen, 1982; Turner and Abbott, 1990; Schiarizza and Preto, 1987).

The age of the oldest sedimentary units in the Sylvester allochthon in the report area is late Tournaisian (Osagean). The oldest ages recorded in the Slide Mountain Terrane, from the Fennell and Milford groups, are also early Mississippian (Table 3). These correspond to the youngest Earn ages; and suggest that widespread, diffuse extension in the Late Devonian stepped westward and focused in the early Mississippian to create marginal basins. Mississippian basalt magmatism, well established in the Sylvester allochthon by conodont dates from interbedded sediments, may also have taken place in the correlative terranes. The creation of these marginal basins implies the presence farther west of detached continental slivers. In the case of the Sylvester allochthon, one such sliver may form the basement of Division III.

Rifting, basalt volcanism, and creation and submarine exposure of new ophiolite basement continued in Division II of the Sylvester allochthon up to the mid-Permian, together with arc volcanism and shallow-water sedimentation in Division III. The conceptual cross-section of continent edge - marginal sea - island arc of Figure 21 could, slightly modified, fit Rees' (1987) hypothetical cross-section in the Quesnel area, Klepacki's (1983) cross-section for the southern Okanagan, and Miller's (1987) for California and Nevada.

In summary, shown in Table 3, study of marginal terranes such as the Sylvester allochthon reveals a remarkable degree of integration between the geological evolution of North America and the inner suspect terranes (*e.g.*, Devono-Mississippian rifting; Late Triassic siliciclastic sedimentation), and also a remarkable degree of along-strike synchroneity of events in the suspect terranes (the transition from Devono-Mississippian siliciclastic sedimentation to

TABLE 4
POTASSIUM-ARGON AGE DATA FROM THE MIDWAY-CASSIAR PROJECT AREA

Sample Number	Location	UTM coordinates	Material	Date (Ma)
86JN30-11[1]	Gum Mountain	428523E 6640115N	sericite from altered quartz-biotite porphyry dike	67.1±2.3
86JB23-02[1]	Brinco Hill	426066E 6642094N	sericite from altered clastic sediments	65.4±2.3
86KG28-07[1]	Lucky prospect	418618E 6651791N	muscovite from envelope around quartz-galena vein	105±4
86JB26-12[1]	Amy prospect	416642E 6643819N	muscovite from griesen-altered, tourmaline-bearing granite	97.3±3.4
SYA85-91[2]	Midway DDH B82-1 (284.2 m)	425500E 6642500N	whole-rock, sericite-altered clastic sediments	74.7±2
DY3077[3]	stock at bend of Tootsee R.	419500E 6644300N	biotite from granite	106±4
DY3090[3]	Silverknife prospect	423750E 6645500N	biotite hornfels	98.9±3.5
78-AP-60a[4]	Cassiar Moly prospect	450508E 6563363N	muscovite from mineralized greisen	73.7±2.6
78AP-43[4]	Cassiar Moly prospect	450508E 6563363N	biotite from porphyry dike	73.6±2.5
78AP-127[4]	Storie Moly prospect	450564E 6567694N	muscovite from mineralized vein	71.4±2.5
78AP-126[4]	Storie Moly prospect	450564E 6567694N	biotite from porphyry dike	72.5±2.5
78AP-158[4]	Lamb Mtn. prospect	449250E 6583500N	biotite from porphyritic stock	73.9±2.5
88JN10-8[5]	Snowy Creek	465859E 6572750N	whole-rock, biotite-rich lamprophyre dike in earbonate-altered zone	63.7±2.2 K=5.01±0.07 n=2 $^{40}Ar_{rad}/^{40}Ar_{tot}$=.927 $^{40}Ar_{rad}$=12.617×10^{-6} cc/gm
83-146[6]	Erickson mine	461750E 6564500N	sericite from Alison vein	122±4
83-188[6]	Erickson mine	461750E 6564250N	sericite from Jennie vein	127±4
83-250[6]	Erickson mine	461750E 6564250N	sericite from Caitlin vein	112±4
83-216[6]	Taurus mine	460800E 6570650N	sericite from quartz vein	137±5
80AP-160[6]	Snowy Creek	462800E 6569850N	sericite from quartz vein	131±5
89-JN[5] 6-2	Cassiar pit	452800E 6577700N	Cr-phlogopite from dike (?)	94.5±3.3

[1] Bradford and Godwin (1988).
[2] W.D. Sinclair, written communication 1986. Analysis by Geological Survey of Canada Geochronology Section, Ottawa.
[3] K. Dawson, written communication, 1987. Analysis by The University of British Columbia Geochronology Laboratory.
[4] Pantaleyev (1980).
[5] this publication; analysis at The University of British Columbia Geochronology Laboratory.
[6] Sketchley *et al.* (1986).

Pennsylvanian-Permian cherts; and Permo-Triassic deformation). These parallels support the idea that these terranes are allochthonous but not utterly exotic. They suggest that the development of the Cordillera inboard of the Cache Creek Terrane is best understood as an interrelated whole.

POST-ACCRETIONARY STRATIFIED UNITS

Tuya Volcanics

Outliers of young basalts are preserved along some valleys in the Tootsee Lake and Blue Dome areas. None were seen in the Cassiar map area. These basalts are very fresh and generally olivine bearing. Columnar jointing is common. The most spectacular Tuya outcrop is a table-shaped ridge surrounded by columnar cliffs south of the Little Rancheria River in the northeastern corner of the Chromite Creek map area. This flow was dated at 4.3 ± 0.3 Ma (whole-rock K-Ar; M.L. Bevier, personal communication, 1991). The close correspondence of the Tuya flows with present-day topography suggests that they are all of Quaternary age. Potassium-argon whole-rock ages on correlative basalts outside the report area range from 230 000 to 700 000 years (D.Westerveld, personal communication to H. Gabrielse).

POST-ACCRETIONARY INTRUSIVE ROCKS

Cassiar Batholith

The Cassiar batholith is a northwest-elongate body, measuring roughly 350 by 20 to 25 kilometres (Gabrielse, 1963, 1969). It follows the Cassiar fault, a Cretaceous dextral-transcurrent fault (Gabrielse, 1985), and is deformed and displaced by it (Murphy, 1988). It is not composite, but shows gradational variations in composition between true granite and granodiorite. It is coarse grained and massive to strongly foliated, particularly along its western margin, which is bounded by the main strand of the Cassiar fault. Along subsidiary strands of the fault, one of which passes through the southeastern corner of the Tootsee Lake map area, protomylonites to ultramylonites are developed within the batholith.

Typical Cassiar granites consist of 55 per cent plagioclase, 15 per cent quartz, 10 per cent microcline, 10 per cent biotite and 10 per cent hornblende. Muscovite is present in many exposures and the microcline may form coarse, pink megacrysts. Granodiorites are somewhat more hornblende rich and lack potassium feldspar megacrysts and muscovite. Pegmatites and aplites are rare; they may be part of younger plutonic suites.

Outside the map area, the Cassiar batholith has been previously dated by K-Ar methods as 110 to 100 Ma (GSC 60-28; 67-12; 89-3, 4, 5, 6). In the present study, one age of 97.3±3.4 Ma was obtained from a tourmaline-muscovite greisen sample near the Amy silver-lead-zinc showing west of the Tootsee River, and one at 105±4 Ma from sericite envelopes of veins at the Lucky showing in the northwestern corner of the Tootsee Lake map area (Table 4).

Contacts of the batholith are sharp and show little chilling. They are either very steep, or dip moderately to the east.

Late Cretaceous Intrusions

A series of small, very felsic intrusions lies along and near the eastern margin of the Cassiar batholith. They include quartz porphyry dikes near the Midway deposit and two small intrusions in the Cassiar map area, the Contact and Lamb Mountain stocks. Panteleyev (1980) also considers a large area of granite, the Cassiar stock, west of the Cassiar townsite to belong to this 70-Ma suite, although the available radiometric ages are from small, discrete intrusive phases, and much of the main body displays a coarse-grained microcline-megacrystic texture indistinguishable from the Cassiar batholith itself. This problem could be resolved by further radiometric dating.

Muscovites in quartz-sericite alteration zones associated with the Midway dikes contain anomalously large amounts of fluorine, up to 2.19 per cent (D. Sinclair, personal communication, 1986; data recorded in Bradford, 1988). This fluorine-rich character, together with the relatively young age of these granites with respect to the Cassiar batholith, led Sinclair (1986) to postulate that they belong to the anorogenic granite suite, with affinities to topaz rhyolites. Fluorine-rich granite of Eocene age occurs at the Blue Light tungsten showing west of the report area (Gabrielse, 1969).

Eocene Intrusions

The Mount Haskin and Mount Reed stocks east of Hot Lake are the only Eocene plutons recognized in the map area (*see* Christopher *et al.*, 1972). The Mount Haskin stock is a composite body dominated by leucogranite. It also contains granodioritic phases, and garnetiferous alaskite near its eastern border. Tourmaline coats fractures in the alaskite.

CHAPTER 3: STRUCTURAL GEOLOGY AND METAMORPHISM

MAJOR STRUCTURAL EVENTS

The fundamental structural framework of the map area is the result of two regional tectonic events: early Mesozoic crustal shortening, expressed as thin-skinned duplex-style thrusting, and late Mesozoic to early Cenozoic block faulting related to an overall transtensional regime. The crustal shortening event involved Triassic sediments in the Sylvester allochthon, although pre-Triassic telescoping occurred in the allochthon and possibly in the miogeocline as well. The mid-Cretaceous Cassiar batholith crosscuts the thrust faults and is not deformed by them; most likely the batholith formed by melting of crust thickened during the shortening event. The batholith is, in turn, cut by the Cassiar fault, one of the major dextral faults in the area. The Tootsee River fault zone, a major complex of normal faults in the Tootsee Lake map area, has localized both Late Cretaceous and Eocene intrusive bodies with their associated mineral deposits (*see* Chapter 4), and may have been active during the intrusive and metallogenetic events.

THRUST FAULTS, FOLDS AND ASSOCIATED MINOR STRUCTURES

Both the miogeoclinal sequence and the Sylvester allochthon responded to compression mainly by thrusting rather than regional-scale folding. The structural style of the area resembles the Rocky Mountains (Figure 2, Plates 3, 17). Thrust systems consist of long, stratigraphically controlled flats and short frontal ramps. In the miogeocline, flats follow the incompetent Kechika and Road River groups and the Earn Group. These units also form the roofs and floors of duplexes. The duplex style of deformation is most clearly shown in the Cassiar map area, where horses composed of Road River - Tapioca - McDame - Earn strata are stacked below the Sylvester allochthon on the west limb of the McDame synclinorium, and horses composed of Ingenika - Boya - Rosella - Kechika strata are structurally stacked on the east limb of the synclinorium east of the French River (Figure 2, in pocket). The three divisions of the Sylvester allochthon are also independent thrust duplexes.



Plate 17. Thrust fault in south-central Tootsee Lake map area, looking southwest. Tapioca sandstone overlies graptolitic Road River Group slate in the hangingwall; Earn Group overlies McDame Group karsted limestone along a highly irregular contact in the footwall. The steeply dipping cleavage indicates northeasterly vergence, as do hangingwall stratigraphic cutoffs (Figure 2, in pocket).

Individual horses are bounded in part by lateral ramps. Most of these are gradual, for instance along the Blue River north of Cassiar. Immediately south of Cassiar, however, a single unrepeated Road River - Tapioca - McDame - Earn panel passes into four horses over a distance of less than 2 kilometres. Exposed frontal ramps are rare. O'Hanley (1990) has identified a northeasterly verging frontal ramp in McDame and Tapioca strata south of the Cassiar mine. One very clear frontal ramp in the southern Tootsee Lake map area (Figure 2, Plate 17), also cuts up-section to the northeast. On the other hand, a thrust fault that places Road River on Earn strata in the valley 10 kilometres north of Cassiar mine (Figure 2) appears to cut up-section to the west in its hangingwall, possibly indicating westerly vergence. This fault geometry is complicated by the steep bedding dips in Tapioca sandstone in the hangingwall, which project directly into the Road River slates. This may be due to rotation during later extensional faulting, in which case the original sense of vergence may be obscured.

Thrust faults within Lower Cambrian strata near the French River are more deeply eroded to the south, where they repeat Stelkuz, Boya and Espee panels. Major open folds in the lowest thrust sheets (Figure 2) probably indicate draping over yet lower horses.

The Sylvester allochthon occupies the core of an open, northwest-trending synclinorium, the Sylvester synclinorium (Gabrielse, 1963). This feature is flat-bottomed as a barge, with steeply inclined unit contacts only at its sides (Figures 2, 6). Its eastern limb is parallel to the thrust flats on the western side of the sub-Kechika duplex. This major anticlinal stack may not only have created the steep upturn that is the eastern limb of the Sylvester synclinorium, it may also have blocked further eastward transport of the allochthon. The regional dip of the western limb of the Sylvester synclinorium ranges from very gentle in the Tootsee Lake map area to moderately steep in the southern Blue Dome, Cassiar and Needlepoint Mountain map areas. The steepening may be due to one or all of the following: doming above and around the Cassiar batholith, stacking of supra-Kechika horses, and a prebatholithic structural culmination.

The earliest cleavage, seen in pelitic rocks of both the miogeocline and the Sylvester allochthon, is parallel to bedding. It is very well developed, giving glossy partings to slates. As already noted, no tight major folds are present, so the cleavage cannot be the result of regional isoclinal folding. Because the cleavage is developed only in incompetent strata, it may be axial planar to abundant overturned minor isoclines. Due to the homogeneous character of the slatey units, fold hinges are usually difficult to distinguish. The ribbon cherts of Unit MPs and the incompetent thin-bedded slates and siltstones of the Kechika Group locally show cascading recumbent folds.

The F_1 cleavage is cut by steeper, northwest-trending cleavages, which dip variously to the northeast and southwest. In a given area, one or both dips are seen. They are axial planar, in some cases, to tight mesoscopic folds. Steep, northwest-trending fracture cleavages are developed in more competent units such as McDame Group and Tapioca sandstone. These cleavages are geometrically consistent with the structures involved in 'snakes head' frontal ramps in northeast or southwest-vergent thrusting (McClay, 1986). They are all considered to be a single generation, F_2.

The youngest cleavages are northeast-trending fractures; the youngest minor folds are small kinks with northeast-trending fold axes. These F_3 minor structures are particularly noticeable within the Tootsee River fault zone.

HIGH-ANGLE FAULTS AND FAULT SYSTEMS

The Midway-Cassiar project area lies in a zone of prominent and large-scale Cretaceous-Tertiary transcurrent faults. The Tintina fault with 450 kilometres or more post-mid-Cretaceous dextral offset (Gabrielse, 1985) lies 70 kilometres northeast of the map area (Figure 1a). The Kechika and Cassiar faults lie immediately to the northeast and southwest of it. A number of late high-angle faults and fault systems within the area may have formed as subsidiary strands and accommodation zones to these regional faults.

High-angle faults are most prominent in the Midway area (Tootsee River fault system), in the eastern part of the Blue Dome map area, and near Cassiar (the Marble Creek fault). The Tootsee River fault system is a northerly trending array of steep faults with a variety of strike orientations. Some faults are listric and show pronounced block rotations, for instance the southeast-dipping McDame panel west of the Tootsee River. This fault system continues north of the Yukon border, where it joins a strand or offset of the Kechika fault (Figure 1a and Lowey and Lowey, 1986). The listric nature of some of the Tootsee River faults and the general northerly trend of the system suggest a stress regime of east-west extension. The Kechika fault loses significance and may even terminate in the southern Yukon (Lowey and Lowey, 1986), but the Cassiar fault continues as a strong structure to the north. The Tootsee River fault system may be the result of transfer of movement from the Kechika fault to the Cassiar fault. This left-stepping displacement would lead to extension within the intervening block.

The northwesterly striking high-angle faults that dominate the structural grain of the eastern Blue Dome map area southwards into the Spring Creek - Rosella Creek watershed may be strands of the Kechika fault.

The Marble Creek fault is a northerly striking, west-side-up high-angle fault that extends from the Marble Creek drainage into the valley of Lang Creek, where it disappears under till. South of Cassiar, this fault juxtaposes Rosella marble and Road River black slate. Two other lesser, north-trending faults occur in the Cassiar and Needlepoint Mountain map areas. One of them, the Erickson Creek fault, has been important in the mining history of the Erickson deposits as it offsets the veins. The other trends southerly from a shoulder of Mount McDame, where it juxtaposes Triassic Table Mountain sediments and the basalts that underlie them. This group of faults may represent a minor extensional zone like the Tootsee River system; however dextral movement has been documented on some of them (Boronowski, 1988; Ey, 1986). Most of the gold-quartz veins of the Erickson camp occupy fractures and faults

which were affected by minor movement. The Sky vein is an exception. It lies within a west-trending high-angle fault that offsets the base of the Table Mountain sediments.

METAMORPHISM

Many metamorphic events have affected some or all of the rocks in the report area. The earliest events are the development of amphibolite and greenschist facies in slivers of oceanic basement rocks in the Sylvester allochthon. Incorporation of amphibolite clasts in breccias of Units IIPPvs and IIBDm, in which the breccia matrix contains only prehnite-pumpellyite assemblages, indicates that high-grade metamorphism occurred in the oceanic lower crust during late Paleozoic time. Prehnite-pumpellyite metamorphism is widespread in the allochthon. It reflects a combination of seafloor metamorphism and regional thermal effects during and after emplacement. Regional metamorphism of Cassiar Terrane strata was at very low grade. Fine-grained white mica is the only regional metamorphic mineral, even in the Espee Formation at the deepest stratigraphic level exposed.

The Cassiar batholith and the later plutons all have contact aureoles. Tremolite occurs in dolostone and andalusite and cordierite in metapelites within a kilometre of the contact. Ultramafic bodies contain regenerated olivine plus talc, tremolite and enstatite (Gabrielse, 1963; Wolfe, 1965; Pinsent and Hirst, 1977). The Cassiar batholith, late Cretaceous Lamb Mountain stock and Eocene Mount Haskin pluton have associated skarn occurrences, which are discussed in Chapter 4.

Mafic lithologies in the Sylvester allochthon provide an excellent opportunity for studying its metamorphic history. Amphibolite-facies metamorphism is restricted to the gabbros of Division II. In them, magmatic augite is rimmed by actinolitic hornblende, which also forms lepidoblastic, oriented aggregates. These rocks grade into amphibolites and even mylonites. Amphibolite clasts are incorporated in the polymictic breccias deposited within the Blue Dome fault zone and in Unit IIPPvs. Amphibolite forms blocks surrounded by scaly serpentinite. These features all suggest that the amphibolite metamorphism is primary, and affected the gabbros just after they crystallized but before they were exposed on the sea floor. Diabases metamorphosed to greenschist facies are also present as clasts in the breccias, showing perhaps geothermal gradients during initial cooling.

Seafloor, as opposed to later metamorphism is difficult to prove in the Sylvester allochthon, as the same subgreenschist assemblages probably typify both. One indicator of early metamorphism may be the intense alteration of some Huntergroup augite porphyries, in which plagioclases are completely replaced by coarse-grained epidote. On the other hand, conodont alteration indices in both the Sylvester allochthon and in the underlying autochthonous Earn Group are similar (Appendix 1), both averaging C.A.I. = 5, and there is widespread metamorphic sericite in the Earn Group. This suggests that the thermal peak postdated emplacement of the allochthon.

All of the units in the Sylvester allochton have undergone regional low-grade metamorphism. Assemblages range from prehnite-pumpellyite to actinolite-chlorite-epidote-albite (lowest greenschist). Textures of the mafic rocks are generally isotropic. Some tuffs show a weak to moderate fabric but in all cases metamorphic minerals overgrow the foliation, showing that the thermal peak succeeded deformation.

Prehnite-pumpellyite metamorphism is developed in all lithotectonic units of the allochthon. It overprints the early amphibolite-facies assemblages in the Division II gabbros.

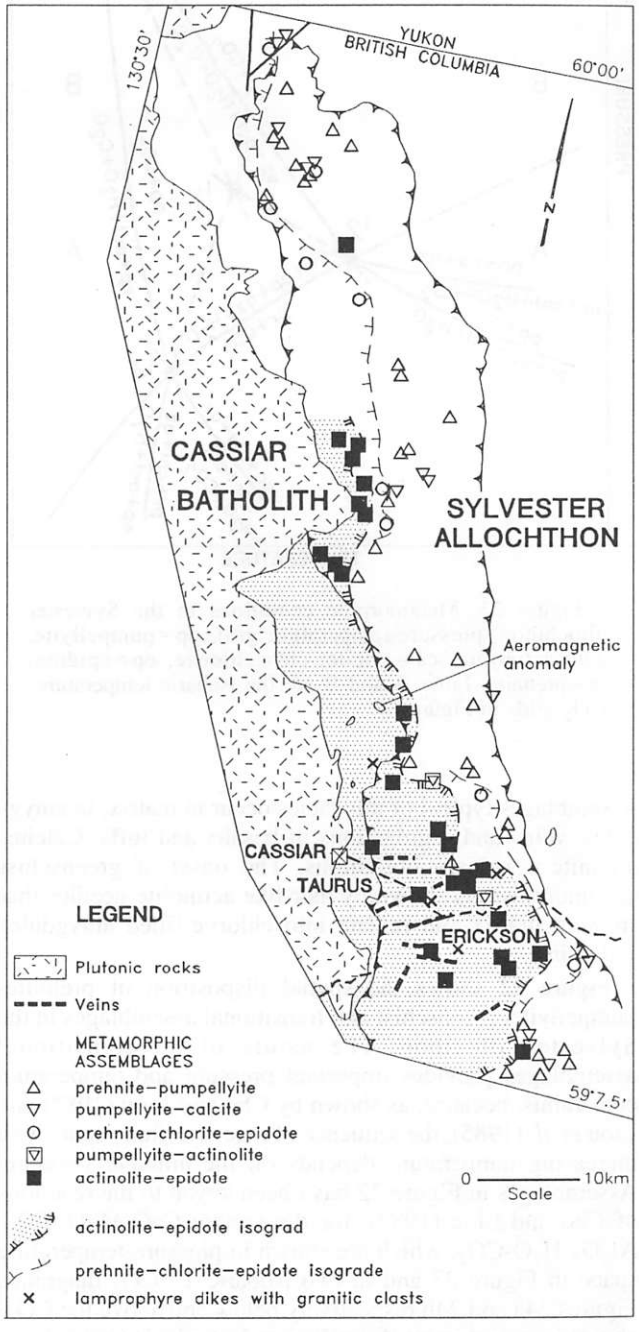


Figure 22. Metamorphic assemblages in the Sylvester allochthon. Lamprophyre dikes with granitic clasts, all within the actinolite-epidote zone, suggest buried intrusions. The gold-quartz veins of the Erickson-Taurus camp occur within the broadest part of the actinolite-epidote zone.

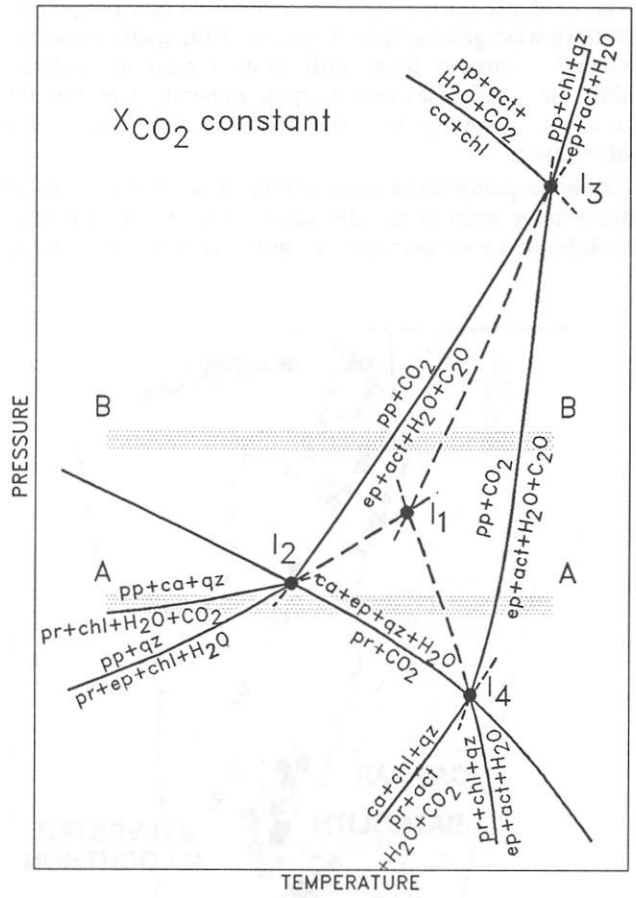


Figure 23. Metamorphic conditions in the Sylvester allochthon, pressure-temperature grid. pp=pumpellyite, act=actinolite, ca=calcite, chl=chlorite, ep=epidote, pr=prehnite. Lines A and B are the isobaric temperature-CO_2 grids in Figure 24.

Assemblages typical of this facies occur in matrix, in amygdules, veins and segregations in basalts and tuffs. Calcite-prehnite veins are ubiquitous. The onset of greenschist metamorphism is shown by hair-like actinolite needles that crosscut matrix and radiate into chlorite-filled amygdules and veins.

Figure 22 shows the spatial disposition of prehnite-pumpellyite, greenschist and transitional assemblages in the Sylvester allocthon. The nature of the transitional assemblages provides important pressure and temperature constraints, because, as shown by Cho and Liou (1987) and Liou *et al.* (1985), the sequence of reactions that occurs with increasing temperature depends on the ambient pressure. Assemblages in Figure 22 have been keyed to the reactions of Cho and Liou (1987), for the system CaO-MgO-SiO_2-Al_2O_3-H_2O-CO_2, which are shown in pressure-temperature space in Figure 23 and in two isobaric T-$^{X}CO_2$ diagrams, Figures 24a and 24b respectively below and above the CO_2-absent invariant point (I_1 on Figure 23), which establishes a useful bathograd. The ubiquity of calcite in these rocks indicates that $^{f}CO_2$ must be taken into account. As outlined by Cho and Liou, increasing $^{f}CO_2$ enlarges the triangle I_2-I_3-I_4 around the calcite-free, CO_2-free invariant point I_1.

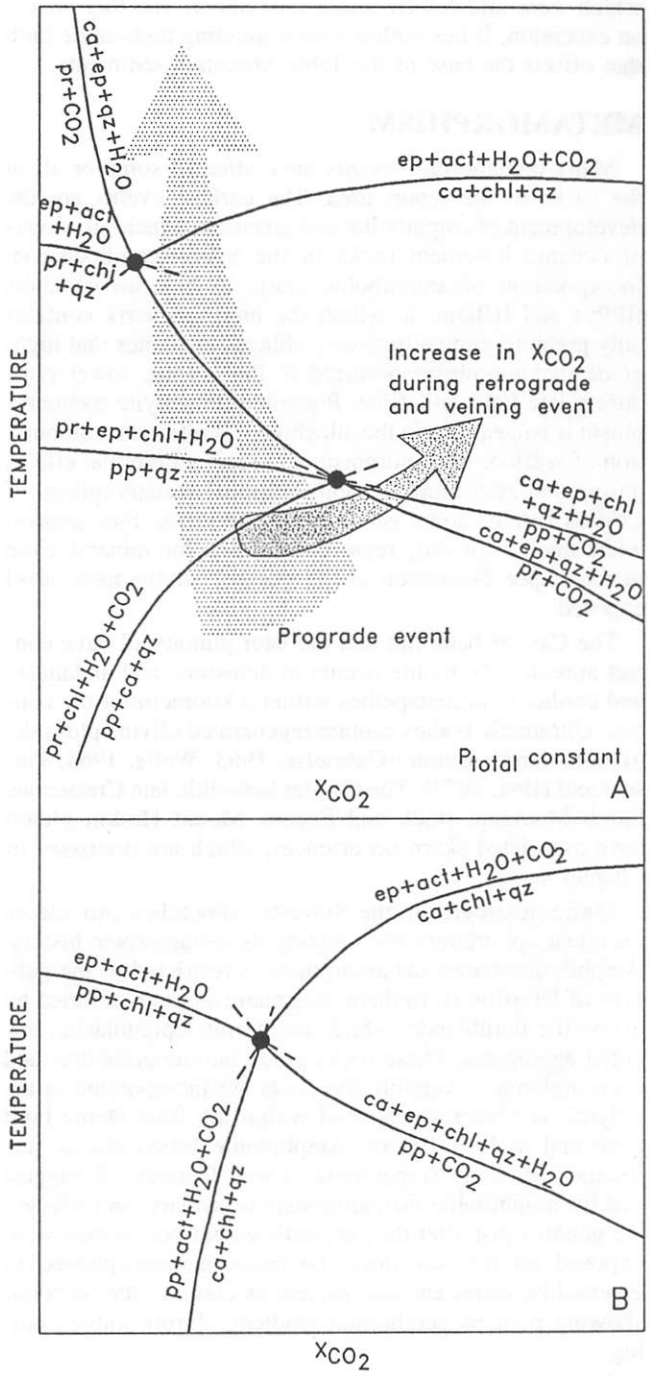


Figure 24. T-XCO_2 grids A) below invariant point B) above invariant point I_1. Mineral abbreviations as in previous figure.

Calcite-bearing assemblages can be used as indicators of total pressure: for instance the assemblages prehnite + chlorite + CO_2, and prehnite + CO_2, cannot exist above the pressure of the invariant point; the observed assemblages prehnite-chlorite-calcite and prehnite-calcite are assumed to have been formed in the presence of carbon dioxide.

Appendix 4 presents the metamorphic assemblages observed in thin sections of Sylvester volcanic rocks.

Quartz is present in nearly all of them. Groups 7 and 9 in Appendix 4 are greenschist facies; the remainder are prehnite-pumpellyite to transitional facies. Of the transitional assemblages, ten are the low-pressure assemblage prehnite-chlorite-epidote, and two are the high-pressure assemblage pumpellyite-actinolite. Of these, only in 88JN19-8 do the two phases appear to be in equilibrium. In 81AP9, pumpellyite is restricted to the eores of plagioclases, while actinolite occurs with chlorite and epidote in the matrix. In the prehnite-pumpellyite facies, assemblages on both sides of the reactions

$$\text{prehnite} + CO_2 = \text{calcite} + \text{epidote} + \text{quartz}$$

and

$$\text{pumpellyite} + \text{calcite} = \text{prehnite} + \text{chlorite}$$

are common. These variations may reflect changes in $^fCO_2$, rather than temperature effects. In any event, they suggest total pressure at or below invariant I_1. Most of the transitional assemblages plot on Figure 24a, below 2.2 kilobars (220 MPa), while a few plot on Figure 24b. Also shown on Figure 24a is a retrograde path reconstructed from the prehnite-pumpellyite assemblages that are overprinted on greenschist-facies rocks near veins of the Erickson-Taurus system. These are discussed in greater detail in Chapter 4. Here it is sufficient to note that, like the prograde assemblages, they suggest pressures near and generally less than invariant point I_1. The coexistence of low-pressure and high-pressure transitional assemblages suggests that the lithostatic pressure during metamorphism was close enough to invariant point I_1, or 2.2 kilobars, so that compositional variations such as the iron-magnesium ratio and $^fO_2$ could shift the equilibria across that point.

This pressure implies the effect of about 7 kilometres of structural burial during the regional metamorphic event, above currently exposed Sylvester rocks. The nature of this additional load is a topic for interesting speculation. Was it a much greater thickness of Division III than is anywhere preserved? Was it another radically different late Paleozoic package? Was it an early Mesozoic Quesnel package?

Metamorphic textures suggest that the metamorphic peak was postkinematic. It postdated the penetrative deformation of the allochthon which, as was argued above, accompanied its emplacement as thrust sheets. The spatial disposition of the actinolite isograd suggests that it is a contact metamorphic effect. In the Blue Dome area and probably farther north as well, it follows the edge of the Cassiar batholith. In the Cassiar area, the isograd sweeps easterly around an area of small and cryptic intrusions near the Lamb Mountain stock, and continues in a broader arc to include the area around the Erickson and Taurus mines (Nelson, 1990). The isograd is steep; it cuts across the boundary between Division II and Division III. It behaves, not like a regional-metamorphic isograd, but like part of a contact aureole. Granitic clasts have been observed in lamprophyre dikes 4 kilometres southeast of the Lamb Mountain stock and at three locations within the Erickson gold camp. This theme is developed further in discussions of the tetrahedrite-bearing quartz veins near Lamb Mountain, and of the Erickson veins.

Prehnite-pumpellyite metamorphism of the Sylvester allochthon is probably the result of a combination of seafloor metamorphism, metamorphism during its assembly and emplacement, and later thermal metamorphism. The thermal peak reached in these rocks, which generated a broad zone of lowest greenschist assemblages, was a postemplacement contact metamorphic event or events. Maximum temperatures ranged across the prehnite-pumpellyite/greenschist boundary, perhaps 350 to 450°C; pressure was slightly more than 200 megapascals (2 kilobars).

CHAPTER 4: ECONOMIC GEOLOGY

The Midway-Cassiar project area contains a wide spectrum of mineralization types and mineral commodities. This is due to its complex geology: the tectonic juxtaposition of oceanic and miogeoclinal terranes, and a history that includes late Paleozoic rifting and multiple Cretaceous-Tertiary faulting and magmatic events. This chapter describes the mineral deposits in the context of mineralizing episodes and favourable hostrocks. It integrates the various types of deposits into systems, inter-related in time and space. Individual deposits are identified by their MINFILE numbers on Figure 2; brief descriptions can be found in Table 5.

Seven mineralizing episodes produced the mineral deposits of the Midway-Cassiar area (Table 5):

- Devono-Mississippian extensional tectonics generated the exhalite deposits of the Earn Group and also exhalites within Units IMsi and IIMvs of the Sylvester allochthon.
- Rhodonite interbedded with grey to pale green cherts near the base of Unit IIPPvs north of Quartzrock Creek, and with black, grey and green cherts of less certain age elsewhere, is probably exhalative in origin (Nelson *et al.*, 1990a).
- Permian layered ultramafites in the allochthon, the Zus Mountain - Blue River and Cassiar bodies, host syngenetic chromite and traces of platinum.
- An early mid-Cretaceous thermal event, probably related to a cryptic intrusive body, gave rise to the Erickson gold-quartz veins about 130 million years ago. These veins are hosted by basalts of the Sylvester allochthon and are most productive near the base of the Triassic Table Mountain sediments, which is marked by a series of listwanitized ultramafic slivers. This same thermal event may have given rise to the crystallization of asbestos fibres in extension veins in the Cassiar and McDame mines, which structurally relate to the folding of the western limb of the McDame synclinorium (O'Hanley, 1990).
- The mid-Cretaceous Cassiar batholith generated skarns such as the Nancy and silver-lead-zinc veins and replacement bodies such as the Lucky and the Amy.
- The 70-Ma intrusive event, although it produced only a minor volume of granite, generated proximal molybdenum-copper skarns and porphyries, and distal silver-lead-zinc replacemem bodies, most notably the Midway deposit.
- The Eocene Mount Haskin and Mount Reed stocks also have associated porphyry mineralization, skarns and silver-lead-zinc veins.

SYNGENETIC DEPOSITS

SEDEX DEPOSITS

The discovery and development of major stratiform, sedimentary exhalative or 'sedex' (Carne and Cathro, 1982) deposits in the Earn Group in the Selwyn and Kechika basins led to intensive exploration of the Earn Group in the Cassiar Terrane, primarily during the period 1978 to 1982. A number of sedex deposits were identified including those around the Midway deposit, the Perry and Ewen barite deposits in northeastern Tootsee Lake map area, the Chief showings in strata previously considered to be Earn Group (Nelson *et al.*, 1988a) but now assigned to Unit IMsi of the Sylvester allochthon, the Blue showings in southwestern Blue Dome map area, and the Diablo and Jan in the Cassiar map area. In the course of the present project additional sedex occurrences were located, including the ET in the northwestern corner of the Cassiar map area and an unnamed silica-barite occurrence in Unit IMs of the Sylvester allochthon in the northwestern corner of the Blue Dome map area (Nelson *et al.*, 1988a). They add to the continuity of this type of mineralization within the Earn Group, and point to its existence in the Sylvester allochthon.

These exhalative deposits consist either of bedded fine-grained pyritic quartz and lesser barite with scattered concentrations of sphalerite and rare galena, or of bedded or nodular barite with lesser fine-grained, intergrown quartz. They occur in slates in the finer grained parts of the siliciclastic sequences. In the Midway area, the main sedex showings occur within Unit 2AC, the upper fine-grained interval within the Earn Group (Bradford, 1988). They are of early Tournaisian age, as are the Ewen and Perry barite deposits (Orchard and Irwin, 1987). Late Tournaisian conodonts were collected from Unit IMs 4 kilometres from the main Chief showing (No. 35 Table 2). The Cassiar Terrane and Sylvester allochthon deposits correspond in age to the youngest sedex occurrences of the Selwyn basin (Dawson and Orchard, 1982).

DEPOSITS IN VOLCANIC-SEDIMENTARY SETTINGS

The Lang Creek showing (MINFILE 104P 008), in the Lang Creek valley 10 kilometres south of Cassiar (Figure 2), is a pyrite-chalcopyite lens that occurs parallel with bedding in Unit IIMvs of the Sylvester allochthon. Late Tournaisian conodonts collected nearby (Nos. 85-87, Table 2 and Figure 2) suggest that, if syngenetic, it is the same age as the Sylvester sedex deposits such as the Chief. In mineralogy and lithologic setting, it is a Besshi-type deposit like the Chu Chua copper deposit in the Fennell Group (Schiarizza and Preto, 1987). Its lead isotopic composition is highly anomalous and inconclusive (Figure 25). In terms of $^{207}Pb/^{204}Pb$ to $^{206}Pb/^{204}Pb$ it plots with the Erickson camp mesothermal veins, but its $^{208}Pb/^{204}Pb$ signature places it well off any known growth curve. Because only traces of galena are present in the Lang Creek showing, the lead may have been contaminated by other sulphides.

Scattered rhodonite pods and beds occur associated with grey, bedded chert in Units IIMvs and IIPPvs of the Sylvester allochthon. In thin section, the rhodonite is intergrown with rhodochrosite, siderite, cherty quartz and, in some cases, stilpnomelane and adularia. One rhodonite locality in

TABLE 5
MINES, MINERAL DEPOSITS AND OCCURRENCES IN THE MIDWAY-CASSIAR PROJECT AREA
BY DEPOSIT CLASSIFICATION

Deposit Type	Names(s)	MINFILE Number	Economic Minerals	Description
Sediment-hosted exhalite	Jan	104P 117	barite, chalcopyrite	Fine-grained, pale grey bedded barite and irregular nodular to lensoidal white barite occur in a sequence of siliceous exhalite with disseminated pyrite and chalcopyrite in black rusty slates and porcellanites of the Earn Group. This is the southernmost in a series of Earn exhalites that includes the ET and the Blue showings.
	ET	104P 116	barite	Thin-bedded grey barite occurs within fine-grained siliciclastics and porcellanite of the Devono-Mississippian Earn Group.
	Blue	104P 104	barite, galena, sphalerite	Bedded quartz-pyrite-barite exhalites from .5 to 11.0 m thick are exposed at four locations along a 7-km strike length. All localities contain minor galena with only local yellow sphalerite and low silver values (A.R. 10751).
	Midway-Discovery and Upper zones	104O 038	sphalerite, pyrite	Bedded siliceous pyritic exhalites; in some cases with minor barite, sphalerite, galena (in veinlets from manto below?); in fine-grained Earn Group clastics
	Ewen barite, Perry barite	104O 050	barite	Pure to siliceous bedded barite exhalite in fine-grained Earn clastics. Perry barite is more or less on strike with Ewen barite and forms a synclinal keel cut off by a gently dipping thrust/ décollement.
	Shawn barite Captain Lake	104P 049	barite, chalcopyrite	Coarse, stratiform barite beds up to 1 m thick; associated veins and replacements within McDame Group dolomite breccia and siltstone. Barite contains minor chalcopyrite. $BaSO_4$ from 52.1 to 90.1 weight per cent (A.R. 10334).
	Chief Southwest	104P 103	barite, chalcopyrite, pyrrhotite	Bedded quartz-pyrite-barite exhalites interbedded with argillites and clastics of Unit IMs of the Sylvester allochthon. Large boulder of quartz stockwork with chalcopyrite and locally massive pyrrhotite-pyrite.
Volcanogenic massive sulphides	Lang Creek	104P 008	chalcopyrite, sphalerite, chalcocite, pyrite, pyrrhotite,	A gently dipping conformable massive sulphide lens up to 2 m thick occurs in cherty argillite, interbedded with greenstone, of Unit IIMvs of the Sylvester allochthon. About 27 000 t have been outlined grading 1.52% Cu and 0.9% Zn (A.R. 7912).
	Cassiar pit	104P 114	chalcopyrite, sphalerite	On east wall of Cassiar Asbestos pit, a small (1 m) lens of finely layered massive chalcopyrite-sphalerite-pyrite is hosted in fine tuffs with interbedded argillite.
Alteration within Division III intermediate volcanics	Mare	104P 105	chalcopyrite, pyrite	Numerous small zones of quartz-carbonate-clay-pyrite-chaleopyrite alteration. Extensive sampling by Falconbridge Ltd. yielded only two anomalous samples: 222.13 g/t Ag, no gold, and 4.6 g/t Ag, 2.38 g/t Au (A.R. 11335). The age of mineralization is unknown.
Mesothermal Au (-Ag) quartz veins	Erickson mine (Jennie, Maura veins)	104P 029	gold, tetrahedrite	Steeply dipping multiphase quartz veins in sheared, basalts contain free gold and gold disseminated within pyrite and tetrahedrite. Total production from Erickson, Vollaug and Cusac since production began in 1978 has been 490 000 t grading 15.6 g/t Au and 11.3 g/t Ag (Boronowski, 1988).
	Vollaug	104P 019	gold, tetrahedrite	An easterly striking ribbon quartz vein dips 30° along the contact between footwall listwanites and overlying Triassic sediments. A width of 2.7 m is exposed. About 107 000 t grading 10.5 g/t Au have been produced (Boronowski, 1988).
	Cusac (Eileen, Katherine veins)	104P 070	gold, tetrahedrite	A quartz vein trending 060°-070/60°N has been mined along a strike length of 300 m. Mineralization occurs along listwanite bodies bounding the upper contact of basalt-sediment sequences. Gold grades average 30 g/t (MINFILE).
	Sky	104P 078	gold, tetrahedrite	A quartz vein 4 m wide lies along an east-trending fault that dips 75° north. Listwanite occurs along the hangingwall between the vein and Triassic sediments. Erratic gold assays up to 36 g/t have been reported (MINFILE).

TABLE 5
MINES, MINERAL DEPOSITS AND OCCURRENCES IN THE MIDWAY-CASSIAR PROJECT AREA
BY DEPOSIT CLASSIFICATION — *Continued*

Deposit Type	Names(s)	MINFILE Number	Economic Minerals	Description
	Pete	104P 025	gold, tetrahedrite	East to northeast-trending quartz veins up to 1.8 m wide contain tetrahedrite and minor gold.
	Hunter	104P 034	gold, tetrahedrite	A wide north-trending shear zone contains northeasterly trending quartz veins up to 1 m wide. Erratic gold values up to 6.9 g/t have been reported (MINFILE).
	Rocky Ridge Gold Hill Nora	104P 016 104P 017 104P 018	gold, tetrahedrite	A zone with quartz veins trending either 040° to 055° or 070° can be traced for 2.5 km. Erratic gold assays up to 35 g/t over 0.6 m have been reported (MINFILE).
	Taurus mine	104P 012	gold, tetrahedrite, arsenopyrite	East-trending, moderately to steeply dipping auriferous quartz veins are hosted in massive and pillow basalts. Veins have large carbonate-sericite-clay-pyrite alteration haloes and pyrite-tetrahedrite selvages. An easterly trending lamprophyre dike with granitic xenoliths occurs in the mine area. Production (1988): 3990 t milled, production suspended in March 1988. Reserves (June 1987): 42 600 t, 6.38 g/t; 13 600 t, 8.23 g/t Au (Taurus Resources).
	Hopefull Mack	104P 011 104P 010	gold, tetrahedrite	East-trending vertical to steeply south-dipping quartz veins in massive and pillow basalts occur in an extensive quartz-carbonate alteration zone. I.P. surveys, trenching and diamond drilling indicate significant potential for open pittable reserves (Taurus Resources).
	Wings Canyon (Red Rock)	104P 015	gold, tetrahedrite	An extensive zone of en echelon quartz veins and carbonate alteration trending 070/60S occurs in massive basalt. A selected sample of oxidized material contained 5.14 g/t Au (MINFILE).
	Rich, Snow Creek	104P 046	gold, tetrahedrite	Quartz veins to about 80 cm in width with quartz-carbonate alteration haloes cut massive basalt. Veins trend 045°.
	Berubé (Bozo)	104P 076	gold, tetrahedrite	En echelon 045-trending quartz veins with quartz-carbonate alteration cut massive and pillow basalt near a contact with underlying chert/argillite.
	Snowy Creek	104P 014	gold, tetrahedrite	Intensely faulted and quartz-carbonate-altered basalt is cut by northeast-trending quartz veins and stringers.
	Klondike fraction	104P 013	gold, tetrahedrite	A quartz knot 2 m wide occurs at the contact between strongly folded chert/argillite and overlying basalt or diabase. A sample across 1 m contained 5.47 g/t Au (MINFILE).
	Al (Dekalb)	104P 041	gold	Swarms of quartz veins cut very pyritic altered basalt/ metasediments next to the Blue Dome fault zone.
	Reo (including Blueberry Hill)	104P 009	gold	Quartz veins to 5 m wide occur in a northeast-trending zone 180 m wide in basalt. Both 090 and 045-trending veins are present. A grab sample of graphitic quartz contained 1.02 g/t Au and 52 g/t Ag.
	Elan	104P 075	tetrahedrite	An easterly trending quartz vein with locally abundant tetrahedrite extends about 4 km in massive basalt. The vein is 1 to 3 m wide, with a strong quartz-carbonate alteration halo.
	Lyla, Boomerang	104P 112	tetrahedrite	Tetrahedrite-bearing quartz veins are hosted in basalts immediately below Table Mountain sediments on the ridge north of the Elan vein.
	Ram	104P 042	tetrahedrite	An intensely fractured zone in argillite and chert contains tetrahedrite-bearing quartz veins.
	Cap	104P 041	pyrite, pyrrhotite	A prominent gossan occupies a canyon in a westerly tributary of Toozaza Creek. In the canyon, metasediments of Unit IIMvs of the Sylvester allochthon are bleached and altered and cut by numerous granite dikes. Two kilometres to the northeast, listwanite lenses occur along a fault in metadiabase. The highest assay reported from this property is 0.754 g/t Au over 1 metre (A.R. 11494).

TABLE 5
MINES, MINERAL DEPOSITS AND OCCURRENCES IN THE MIDWAY-CASSIAR PROJECT AREA
BY DEPOSIT CLASSIFICATION — *Continued*

Deposit Type	Names(s)	MINFILE Number	Economic Minerals	Description
Polymetallic veins	Joe Reed	104P 021	galena, sphalerite, pyrite, arsenopyrite	A steeply west-dipping quartz vein averaging about 1.5 m wide occurs along a fault that cuts Rosella carbonates and Boya siliciclastics. Inferred ore in 1956 was 40 000 t of 219.43 g/t Ag, 5.5% Pb and 4.1% Zn (MINFILE)
	Second North Fork	104P 065	sphalerite, galena, pyrite	On the north side of the Stewart-Cassiar Highway, near McDame Creek, a quartz vein/vein breccia 3 m wide cuts sheared McDame Group carbonates. Sphalerite-pyrite replacements are exposed in a trench.
	Diablo	104P 115	tetrahedrite, chalcopyrite	Quartz stockwork zones in black slate and porcellanite, blebs and disseminated pyrite-tetrahedrite-chalcopyrite (Earn Group).
	Goldbreak	104P 096	chalcopyrite	Irregular quartz veins up to 25 cm wide in Tapioca sandstone quartzite host disseminated chalcopyrite-pyrite. Twelve samples averaged 5.8 g/t Ag, 0.33% Cu, 0.02% Pb and 0.02% Zn. (MINFILE).
	Ax	104P 106	galena, chalcopyrite, barite, chalcocite, sphalerite	Silicified zone 10 to 15 m wide with 30-cm to 1-m-wide mineralized zone exposed along 300 m. Contains massive to disseminated galena, coarse white with chalcopyrite-barite-chalcocite and late brecciated quartz with iron oxides and galena blebs. Grab samples assayed 248, 2 and 40 g/t silver. Hosted in Lower Cambrian Rosella carbonates
	Ella Rose	104P 097	chalcopyrite, covellite, sphalerite, galena	A 20-m zone of silicification in dark grey brecciated dolomite. Quartz is fine grained and vuggy with limonite and malachite. Chalcopyrite, covellite, brown sphalerite and galena occur in boulders in a sloughed creek bank 20 m north of the outcrop. A grab sample from the showing assayed 24 ppm Ag, less than 20 ppb Au. Host is Rosella Fm.
	Captain Lake, Pip	104P 060	chalcopyrite, chalcocite	Silicified zone with locally intense stockwork containing chalcopyrite and chalcocite occurs along strongly brecciated fanlt contact between Kechika Group calcareous shale and Rosella Formation carbonates. The zone is up to 40 m wide and exposed along 125 m. Best reported assays are 1.36% Cu over 25 m (A.R. 6087). An old trench exposes similar mineralization 600 m on strike to the northwest.
	Cyathid Mtn.	104P 098	chalcopyrite	A strong quartz stockwork in Rosella carbonates with very minor chalcopyrite is exposed over 70 by 15 m. Grades into limonitc calcite breccia zone 1.5 km along strike to the northeast.
	Chief East	104P 102	pyrite, chalcopyrite	A northwest-trending gossanous zone (0.5 by 3.5 km) of strong quartz-sericite-pyrite alteration that hosts numerous quartz veins with pyrite and chalcopyrite. Hosted in chert-argillite of Unit IMs of the Sylvester allochthon.
	Reggie	104P 099	galena, pyrite	En echelon tension gashes in a narrow zone up to 0.7 m wide with disseminated galena and pyrite.
	Tootsee Star	104O 039	galena, sphalerite, pyrite	Quartz veinlets in narrow shear zone in Sylvester allochthon argillites and cherts. A grab sample assayed 35.3 g/t Ag. Probably related to the Midway manto deposit.
	Luck, Lucky	104O 033	galena, sphalerite, pyrite, tetrahedrite	A group of massive sulphide veins hosted by K-spar megacrystic and medium-grained granite of the Cassiar batholith. Muscovite from a vein selvage on the Lucky claims gives a K-Ar date of 105±4 Ma (Table 3).
	Ran, Reb, Hat claims	104O 037	pyrite, molybdenite, argentite, galena	Extensive sericite alteration zone in Cassiar batholith; fine-grained granite, rhyolite dikes. Mineralization in quartz veins: Au to 0.7 g/t (A.R. 9128), Ag to 3800 g/t on Ran claims (Nelson and Bradford 1987a,b).
	Gunnar Berg	104O 032	galena, molybdenite, scheelite	Quartz breccia zone in Tapioca sandstone quartzite adjacent to altered, quartz-veined Cassiar batholith contact zone. Mineralization is minor.

TABLE 5
MINES, MINERAL DEPOSITS AND OCCURRENCES IN THE MIDWAY-CASSIAR PROJECT AREA
BY DEPOSIT CLASSIFICATION — *Continued*

Deposit Type	Names(s)	MINFILE Number	Economic Minerals	Description
Replacement bodies in carbonate	Midway Lower zones – Discovery and Silver Creek deposits	104O 038	galena, sphalerite, arsenopyrite, pyrite, pyrrhotite, marcasite, chalcopyrite, freibergite pyrargyrite, geocronite, stannite, cassiterite	Irregular replacement silver-bearing massive sulphide bodies located at or near the top of the McDame Group. The Silver Creek deposit consists of two high-grade core zones, Silver Creek North and Silver Creek South. Sulphide textures indicate several phases of brecciation, replacement and open-space drusy growth. Pyrrhotite and chalcopyrite in the southern part of the deposit zone to abundant lead sulphosalts in the northern part. The Discovery deposit occurs about 300 m east of the Silver Creek deposit. Massive and brecciated sulphides and sulphide-matrix breccias occur in several discrete zones. Total drill-indicated tonnage in January 1991 is 1.19 Mt of 410 g/t Ag, 7% Pb, 9.6% Zn.
	Silvertip	104O 003	galena, sphalerite, tetrahedrite, stannite, pyrite	Lead-zinc-silver replacement bodies in McDame limestone. Surface exposures strongly oxidized. Presence of tin indicates magmatic hydrothermal source and probable relationship to Midway manto deposit.
	Berg	104O 032	galena, sphalerite, hydrozincite, cerussite, pyrite	Strongly oxidized mineralization, mostly chunks of Fe-Mn gossan, occurs where a thin screen of Earn porcellanite which overlies McDame limestone, probably at the top of a thrust sliver with McDame carbonates also in the hangingwall.
	Silverknife	104O 048	galena, sphalerite pyrargyrite, tetrahedrite, pyrite	Sulphide replacement zones, generally concordant, in marble at gradational Atan-Kechika contact. Hornfelsing is pervasive although the source is not exposed. No surface showings. Strike length reported 137 m, true width 4.6 m. weighted average assay values to 511 g/t Ag, 3.7 g/t Au, 12.25% Pb, 4.8% Zn.
	Contact	104P 004	galena, sphalerite, chalcopyrite, tetrahedrite, molybdenite, dyscrasite, pyrargyrite, bismuthinite	Galena-sphalerite pods have replaced a marble bed within a screen of Hadrynian Stelkuz Formation hornfels. Garnet-diopside(-scapolite?) skarn is developed in marble near the showing. 25 t milled (1956) produced 10 451 g Ag, 25 kg Cu and 1947 kg Pb.
	D Zone including Lower, Middle and Upper zones and Granite Creek	104P 044 104P 080 104P 088	galena, sphalerite	Magnetite-galena-sphalerite pods occur in Rosella Formation marble and dolomite. In the Middle D Zone, 90 000 t grading 3.3% Pb, 6.3% Zn, and 70 g/t Ag have been outlined. A 7.6 m intersection in the Upper D Zone ran 4.73% Pb, 4.74% Zn, 240 g/t Ag, and 0.069 g/t Au. Tin values up to 0.12% have been obtained.
	Magno (Marble Creek, Silver Queen)	104P 006	galena, sphalerite	Irregular galena-sphalerite-magnetite-pyrrhotite pods occur along an easterly trending fracture system about 1 km long west of the north-trending Marble Creek fault. Drill-indicated reserves for the West, Middle West and East zones total 426 417 t grading 5.92% Pb, 4.15% Zn, 192 g/t Ag.
	Pant	104P 082	galena, arsenopyrite, pyrrhotite, pyrite, sphalerite, cassiterite	Replacement pods occur in Rosella carbonates next to a fault that juxtaposes them against graphitic phyllites of the Road River Group. Assay results from drilling include 0.6 m of 49 g/t Ag, 0.74% Zn, 0.22% Pb, 0.1% Sn, 0.08% Cu; and 0.4 m of 296.2 g/t Ag, 2.28% Ph.
	Mt. Haskin NW (A Zone)	104P 059	sphalerite, galena	Two pyrrhotite-sphalerite-galena-chalcopyrite lenses occur in skarn in the Rosella Formation
	Dalziel	none	sphalerite	A massive pyrrhotite-diopside(?)-sphalerite lens occurs in Rosella Formation marble.
	Amy	104O 004	sphalerite, galena, pyrite, arsenopyrite, freibergite	Concordant lead-zinc-silver replacement zones in limy Kechika Group sediments adjacent to Cassiar batholith The Kechika rocks are cut by several muscovitic, greisenized late-stage dikes of the Cassiar batholith. Muscovite from one of these dikes gives a K-Ar date of 97.3±3.4 Ma (*see* Table 3).

TABLE 5
MINES, MINERAL DEPOSITS AND OCCURRENCES IN THE MIDWAY-CASSIAR PROJECT AREA
BY DEPOSIT CLASSIFICATION — *Continued*

Deposit Type	Names(s)	MINFILE Number	Economic Minerals	Description
Skarn	McDame Belle	104P 022	galena, sphalerite, chalcopyrite scheelite, pyrite, pyrrhotite	Several mineralized skarn zones occur along McDame Creek in faulted Rosella carbonates. Mineralization is in massive pods along bedding and as disseminations in footwall garnet-diopside skarn zones.
	Mt. Reed	104P 043	molybdenite, scheelite, magnetite, sphalerite, pyrite, arsenopyrite, chalcopyrite, galena	Lower Cambrian Rosella carbonates and Boya siliciclastics are intruded by the Eocene (49.6±1.9 ma) Mt. Reed stock. Zoned skarns are developed around the stock; skarn minerals include magnetite, garnet, diopside, fluorite, phlogopite and chondrodite.
	Dead Goat (Balsam)	104P 079	scheelite, chalcopyrite, sphalerite	Massive pyrrhotite with sphalerite, chalcopyrite, scheelite and fluorite occurs as lenses in layered garnet-diopside containing tremolite/actinolite, hosted by Stelkuz metasediments. Drill-indicated reserves include 100 900 t grading 0.49% WO_3 and 27 600 t grading 0.39% WO_3 and 0.16% Cu.
	Kuhn	104P 071	scheelite, molybdenite, chalcopyrite, sphalerite	Rosella Formation zebra dolomite and marble is replaced by garnet-diopside skarn with pods and veins of massive magnetite and massive pyrrhotite containing disseminated scheelite, chalcopyrite and molybdenite. Drill-indicated and inferred reserves for the Kuhn North zone include 409 300 t grading 0.48% WO_3 and 0.134% MoS_2 and an additional 78 700 t grading 0.50% WO_3.
	Lamb Mtn.	104P 003	molybdenite, scheelite, chalcopyrite	Rosella Formation marbles are replaced by magnetite-garnet-diopside and retrograde actinolite skarn adjacent to the Lamb Mountain stock. Disseminated scheelite occurs in magnetite skarn and pyrrhotite lenses, with abundant molybdenite rosettes in actinolite skarn. Massive pyrrhotite-chalcopyrite pods occur farther from the stock.
	Mt. Haskin	104P 020	sphalerite, galena, chalcopyrite, pyrrhotite, arsenopyrite	Late high-angle faults cut a series of Kechika-Rosella-Boya thrust imbricates near the contact of the Eocene Mt. Haskin stock. Massive pyrrhotite and fluorite-rich skarn occurs along a fault that juxtaposes Rosella marble and Kechika hornfelses and along the Rosella-Boya contact nearby. One drill intersection assayed 67.2 g/t Ag, 9.0% Zn and 4.5% Pb over 3.6 m (A.R. 048).
	Nancy	104O 013	molybdenite, galena, sphalerite, scheelite	Molybdenite plus minor pyrite, galena and sphalerite in quartz veins cutting coarse-grained granite; scheelite skarns in adjacent Kechika Group rocks.
Porphyry molybdenum - copper stockworks	Cassiar Moly	104P 035	molybdenite, chalcopyrite, pyrite	Hosted within the eastern Cassiar batholith, associated younger phases, including pink megacrystic, porphyritic and fine-grained granites. Molybdenite occurs as small rosettes and flakes in the fine-grained phases and in fractures and joints in the porphyries. K-Ar mineral ages from fresh, crosscutting porphyrytic granite and greisen are 73.6±2.5 and 73.7±2.6 Ma respectively (Pantaleyev, 1980).
	Storie Moly	104P 069	molybdenite, pyrite	Hosted by megacrystic granite of the Cassiar batholith and younger, crosscutting, sheet-like, finer grained porphyritic and equigranular phases. Mineralization concentrates along intrusive contacts. In addition to sulphides, fluorite, muscovite and minor beryl occur in fractures. Deposit dimensions are approximately 1000 by 500 by 100 m; inferred ore in 1985 was 42 Mt grading 0.137% MoS_2 (MINFILE). Two K-Ar mineral dates from a dike and a mineralized vein are 72.5±2.5 and 71.4±2.5 Ma respectively (Pantaleyev, 1980).
	Blue Dome	104P 054	molybdenite	A small pod less than 1 m long with 5% MoS_2 was reported by Wolfe (1965) within the Cassiar batholith near the Ice Lake chromite showings.
	Anvil	104P 101	molybdenite	A quartz vein 0.5-m wide with less than 1% molybdenite is exposed along a 100-m strike length adjacent to a biotite granodiorite dike cutting the Blue River ultramafite.

TABLE 5
MINES, MINERAL DEPOSITS AND OCCURRENCES IN THE MIDWAY-CASSIAR PROJECT AREA
BY DEPOSIT CLASSIFICATION — *Continued*

Deposit Type	Names(s)	MINFILE Number	Economic Minerals	Description
Ultramafite-hosted Asbestos	Cassiar mine	104P 005	asbestos, jade	A crescent-shaped, moderately east-dipping and south-plunging stockwork of cross-fibre asbestos veins is developed in serpentinites of the Cassiar ultramafic sheet, near the basal thrust of the Sylvester allochthon. The Cassiar open pit was in production from 1952 to 1989.
	McDame mine	104P 084	asbestos	A stockwork of long-fibre asbestos veins is developed in serpentinite of the Cassiar ultramafic sheet, near the base of the Sylvester allochthon. In 1990, drill-indicated reserves were 16 Mt at 5.6% mill yield.
Ultramafite-hosted chromite, nickel	Ice Lake Wolfe	104O 018 104P 055	chromite	Disseminated to semimassive chromite as pods in peridotites at two locations in the Blue River ultramafite. Largest pod is exposed over 15 cm by 15 m.
	Anvil Chromite Anvil Nickel	104P 100	chromite, pentlandite, pyrrhotite	Semimassive to massive chromite occurs over 3 m by 50 cm in talc-bearing metaperidotite within the Blue River ultramafite. Semimassive net-textured sulphides occur nearby along the margin of coarse-grained, foliated gabbro.
	Nickel Creek Blue River Nickel Heazlewood	104P 001	heazlewoodite	Heazlewoodite was identified by x-ray diffraction in partially serpentinized dunite. Assays to 0.21% Ni (Wolfe, 1965).
	Zus	104P 002	asbestos	Widely scattered cross-fibre asbestos veinlets occur in serpentinized ultramafic cumulates of the Zus Mountain ultramafic sheet.
	Moon	104P 036	asbestos	Chrysotile veins up to 0.6 cm wide cut serpentinite of the Cassiar ultramafic sheet.

the headwaters of Snowy Creek (MINFILE 104P 120) is of significant size. There, some of the finely banded rhodonite contains crystals of chalcopyrite and sphalerite. The textures and associated mineralogy of the Cassiar rhodonites suggest that they are hydrothermal to exhalative in origin (Nelson *et al.*, 1990a).

Magmatic Chromite Deposits and Other Ultramafite-hosted Occurrences

Cumulate dunite bodies form a major part of the Zus Mountain - Blue River ultramafite, and are also present within the Cassiar ultramafic body. The dunites typically contain streaks, laminae and disseminated grains of chromite, although observed chromite concentrations are not great. Assays of chromite-rich dunites returned only traces of platinum-group metals. One copper-stained gabbro from the Zus Mountain body contains 48 ppb platinum and 180 ppb palladium (Nelson *et al.*, 1990b). A few placer grains of platinum-iron alloy occur in the Rosella - Spring Creek watershed, east of the Sylvester allochthon (Nelson *et al.*, 1990b). The nickel sulphide heazlewoodite, identified by x-ray diffraction analysis, was reported by Wolfe (1965), from Nickel Creek.

MESOTHERMAL GOLD (SILVER) QUARTZ VEINS

The Erickson-Taurus System

Placer gold derived from mesothermal veins in the valleys of McDame and Snowy creeks first attracted prospectors and miners to the Cassiar Mountains in the late 1800s. Discovery of the first veins in the 1930s began a history of small to medium-scale hardrock mining that continues to the present day. At the time of writing, ownership of the camp is divided between two companies, Total Energold Corporation, which owns the Erickson mine (Plate 18) and property, and Taurus Resources Inc. Taurus controls the Taurus and Hopeful veins; the rest, except for the Ram vein, belong to Total Energold.

The Erickson-Taurus camp has been the subject of a number of studies. Diakow and Panteleyev (1981) and Panteleyev and Diakow (1982) produced the first camp-scale maps of the vein systems. Sketchley (1986; Sketchley and Sinclair, 1987) studied the alteration assemblages around the veins, which consist of two types: carbonate, and carbon. A third type of alteration, listwanite, was studied by Dussell (1986). Sketchley *et al.* (1986) reported K-Ar ages from sericites in the veins. These dates average 120 Ma, slightly older than the oldest cooling age of the Cassiar batholith, 110 Ma. Nesbitt *et al.* (1985), on the basis of oxygen and hydrogen isotopes from the Erickson veins, hypothesized that deep-circulating meteoric water dominated the ore-forming fluids.

The veins of the Erickson-Taurus system, as pointed out by Diakow and Panteleyev (1981), occur either as steep northeast to east-northeast-trending pods in the upper part of Units IIMvs and IIb, or occupy the base of the Table Mountain sediments (Figure 2). The slivers of serpentinite that separate the Table Mountain sediments and the volcanic-sedimentary packages are at the same structural level as the Zus Mountain - Blue River ultramafic sheet, and are considered part of it.

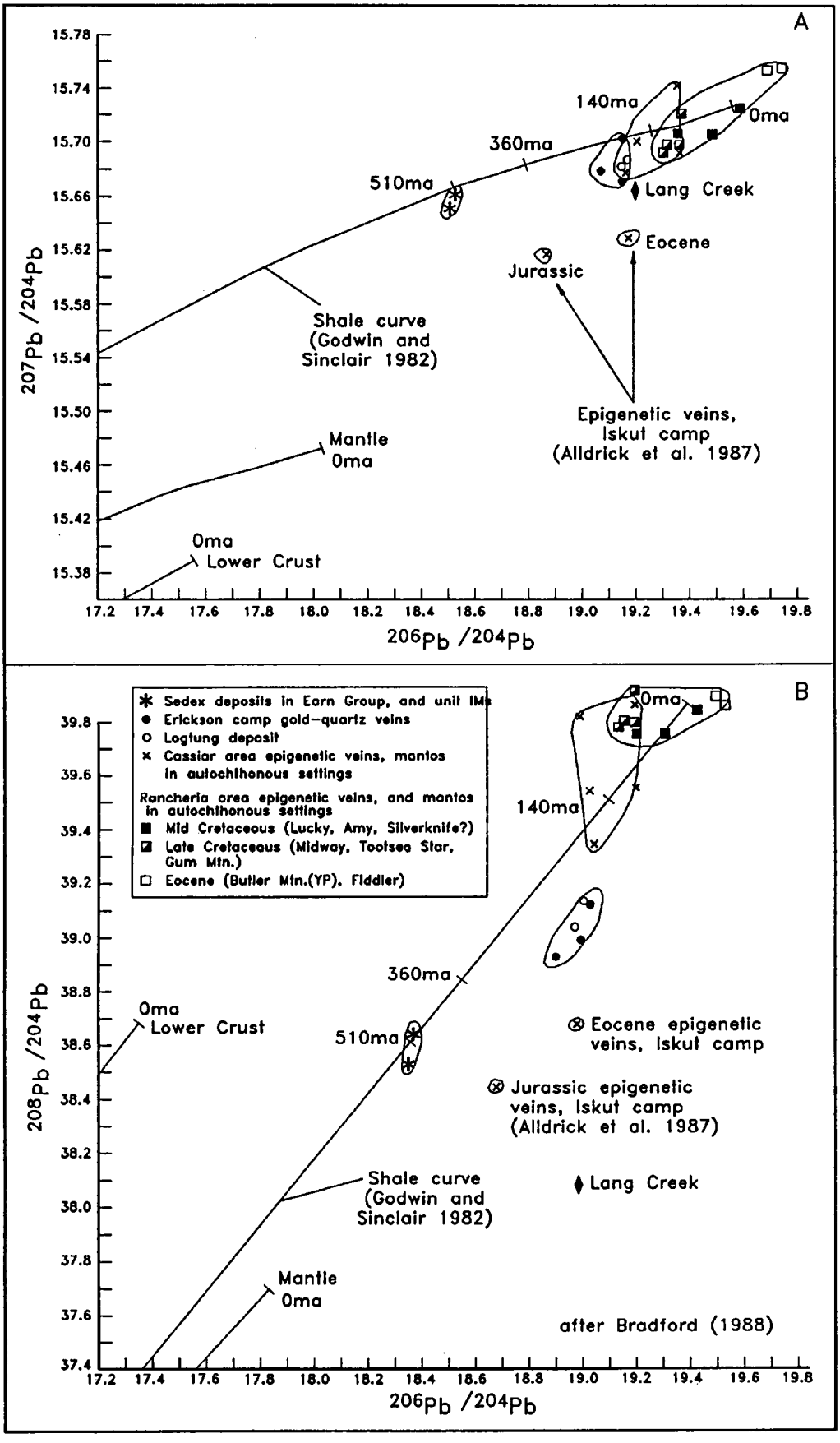


Figure 25. Lead isotopic data for Cassiar-Rancheria area.

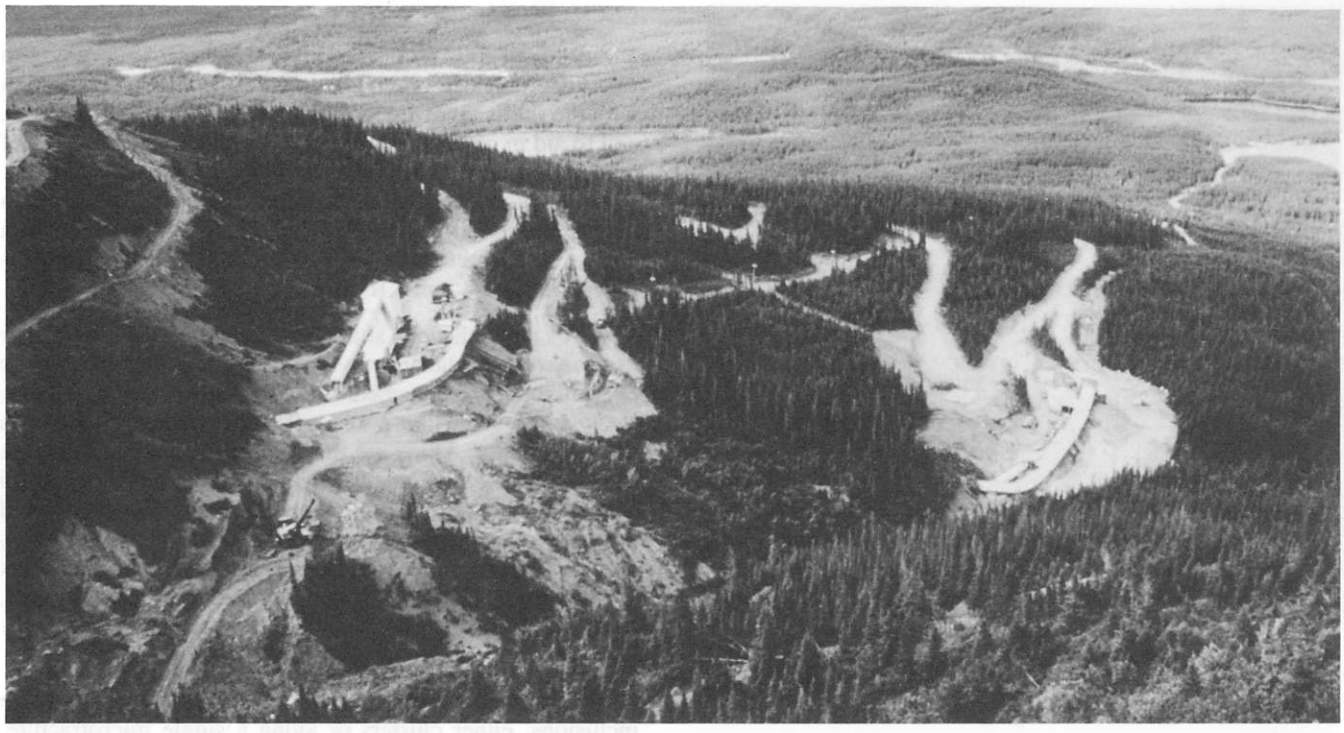


Plate 18. The main Erickson mine in 1988.

The veins are typically mesothermal in character. Their textures, mineralogy, fluid-inclusion populations (*see* below) and associated alteration are identical to mesothermal veins in other volcanic terranes, such as Bralorne (Leitch and Godwin, 1988) and the Mother Lode district of California (Bohlke and Kistler, 1986). They consist of white to clear bull quartz with subordinate iron-magnesium carbonate and calcite, and traces of sericite. Sooty carbon folia are a locally important constituent, particularly in veins along the base of the Table Mountain sediments such as the Vollaug vein. The Vollaug vein shows spectacular ribboning, with carbon laminae marking the ribbons (Plate 19). Orange-weathering iron-magnesium carbonate alteration haloes surround veins and fractures. Alteration assemblages include ankerite, siderite, kaolinite, dolomite, pyrite, carbon, titanium oxide, arsenopyrite and sericite (Sketchley, 1986). At the Taurus mine and the Hopeful vein, the alteration assemblage includes large pyrite crystals and arsenopyrite grains. Significant gold values are associated with this type of alteration (Gunning, 1988; Nelson *et al.*, 1988a).

Serpentinite pods along the base of the Table Mountain sediments are commonly converted to coarse-grained listwanite in the vicinity of the veins. The largest pod is at the Pete showing west of the Huntergroup massif. A second large listwanite pod is exposed in the valley of Snowy Creek 2 kilometres north of the Cassiar branch highway. This pod is exceptional in that it occurs at a much lower structural level in the allochthon than the base of the Table Mountain sediments, which cap the southern end of McDame Mountain 700 metres above Snowy Creek. It may be a small window that exposes the top of the Cassiar ultramafic sheet (Nelson *et al.*, 1989).

In underground exposures, lamprophyre dikes crosscut the veins and alteration zones; however some of them are themselves altered to clay and/or carbonate. A K-Ar age of 110 Ma was reported by Panteleyev (personal communication to Sketchley, 1986), slightly younger than the veins. A lamprophyre dike from the main Erickson mine returned a biotite K-Ar age of 77.6 $\pm$ 2.7 Ma in this study (Table 4). Lamprophyre dikes in the vicinity of the Taurus veins (P.B. Read, unpublished report for Taurus Resources Ltd.) and also on the eastern side of Table Mountain (Sketchley, 1986) contain accidental clasts of granite. Two clast-rich lamprophyre dikes were mapped in this study (Figure 23). One, on the ridge north of Berubé's vein, contains granite clasts. A K-Ar whole-rock date from this dike is 63.7 $\pm$ 2.2 Ma (Table 4). This age coincides with the Late Cretaceous magmatic episode. It provides a minimum time constraint on the age of the enclosed granites. A second lamprophyre dike, more remote from the Erickson-Taurus vein system, contains clasts of Tapioca sandstone, McDame and Road River lithologies, but not granite. This evidence for subsurface granites concentrated in the area of gold mineralization, combined with the broad postkinematic lower greenschist zone over the Erickson-Taurus system, suggests that a large granite body was cooling under the vein system at approximately the same time as the veins were filled. This body could have driven the hydrothermal cell that carried the ore-forming fluids.

Most of the mineralized veins contain free gold in association with pyrite, chalcopyrite, sphalerite, galena, arsenopyrite and tetrahedrite. Gold:silver ratios are slightly greater than 1. In polished section, gold occurs in microfractures that crosscut sulphides, or as coatings on sulphides. These

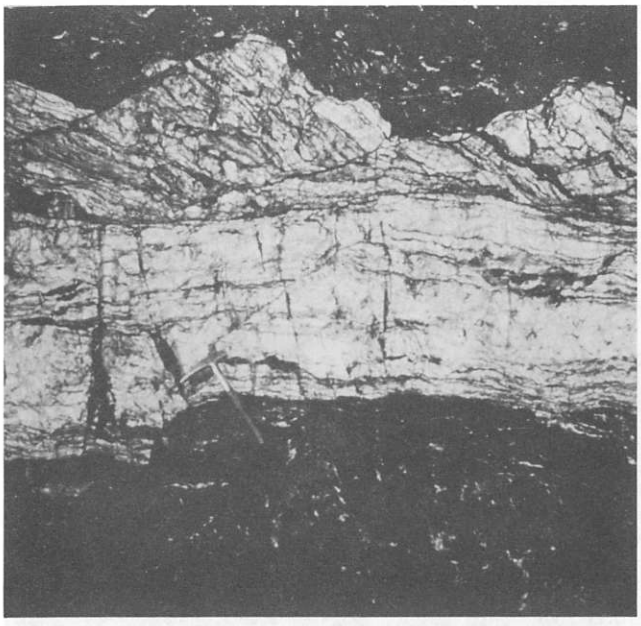


Plate 19. The Vollaug vein, underground. Black carbon-rich partings give the vein a ribboned texture. Note the extensional duplex in the hangingwall.

textures suggest that it crystallized fairly late in the paragenesis. Tourmaline is reported from the Taurus veins (Grant, 1981). Some of the veins at the northern and eastern limits of the system, the Elan, Boomerang and Ram veins, contain little gold but abundant large grains of argentiferous tetrahedrite. This example of mineralogical zoning may be indicative of systematic camp-scale variations in hydrothermal fluids; a doctoral thesis by M. Ball (in preparation) addresses this issue and also the sequence of veining events in the Erickson-Taurus system.

A few lead isotopic analyses are available from the Erickson veins (Bradford, 1988). These are plotted on Figure 25. Also shown are values for other Cretaceous deposits in the Cassiar platform, and for the somewhat older Jurassic veins of the Iskut camp. Although Erickson veins contain relatively primitive lead compositions and lie significantly below the shale curve, they approximate lead in galenas from the Logtung deposit, which occur in veins in metamorphosed miogeoclinal rocks. They show a far greater upper-crustal (cratonal?) component than the Iskut veins, which are underlain by island-arc crust probably no older than Devonian (Alldrick *et al.*, 1987). The Erickson lead isotope data, particularly for urogenic versus thorogenic isotopes (Figure 25), reflects mixing of relatively primitive lead from the allochthon with lead from subjacent miogeoclinal sources: in the Cassiar area the allochthon is probably no more than 1.5 kilometres thick, and ore-forming fluids must have originated far deeper within the Cassiar Terrane. The mesothermal character of the Erickson veins – bull quartz, high gold:silver ratios, carbonate alteration and listwanites – is not peculiar to fluids derived from oceanic source terrain. At Erickson, these features are controlled by oceanic lithologies at the site of deposition, not at the source.

FLUID INCLUSION DATA

A study of fluid inclusions in the Erickson-Taurus system was undertaken in order to compare the fluid composition with the fluids involved in other mesothermal gold deposits, and to aid in constraining the temperatures and pressures of gold deposition. A variety of vein types were sampled: gold-bearing veins, tetrahedrite-bearing veins of the Elan type, milky, barren quartz, and clear, euhedral, barren quartz. Measurements were done on a USGS heating-cooling stage obtained from Fluid Inc.

All of the inclusions studied are secondaries. They occur as clusters and planar arrays in milky and also later, clear quartz which forms euhedral overgrowths into vugs. Relatively clear, inclusion-poor zones also surround sulphides and gold grains. These are the result of 'cushioning' by the more malleable minerals during subsequent deformation, so that later microfracturing events were less severe around their margins (T.J. Reynolds, personal communication, 1989). Except in the late quartz overgrowths, all inclusions are small (less than 5 microns) with round, negative-crystal, or regular outlines. The late, clear quartz also contains very large (up to 20 microns) irregular inclusions (Plate 20).

Measurements were taken of groups of five to twelve inclusions, either clusters or along a single microfracture. Inconsistent groups in terms of homogenization temperature were rejected, as a means of guarding against data from necked inclusions. Most groups studied were consistent within 40°C. Measurements were taken of:

- T_m* final melting temperature of the carbonic phase
- T_e first melting (eutectic) of the aqueous phase
- T_{mi} final melting of ice in the aqueous phase
- T_{mc} final melting of clathrate (hydrated CO_2 compound)
- T_{hc} homogenization of the carbonic phase
- T_h total homogenization.

The data are presented graphically in Figure 27; the complete data are in Appendix 3.

In terms of compositions, T_{hc} and T_h, only two main populations are present (Figure 26, Appendix 3). Type 1 inclusions occur only within the milky quartz and the clear areas around sulphides, including gold-bearing, tetrahedrite-bearing and barren varieties. They contain H_2O, CO_2, traces of CH_4, and salts. Type 1 inclusions are either two or three-phase at room temperature. They contain 5 to 40 per cent vapour phase at room temperature (visual estimates), and in all but a few isolated cases they homogenize to liquid. Type 2 inclusions are H_2O-salt solutions. They are most prominent in the clear quartz (Plate 20). This population consists of the large irregular inclusions as well as swarms of small ones on microfractures. Type 2 inclusions also occupy late microfractures within the cloudy quartz. Total homogenization temperatures (T_h) for the Type 1 inclusions ranges from 200 to 350°C; T_h for Type 2 inclusions, 140 to 209°C, slightly overlaps Type 1. Where crosscutting relationships are seen, Type 2 inclusions post-date Type 1. In general, the presence of Type 1 and Type 2 inclusions in the cloudy, ore-bearing quartz, and only Type 2 in the clear overgrowths, suggests that the Type 1 H_2O-CO_2 inclusions

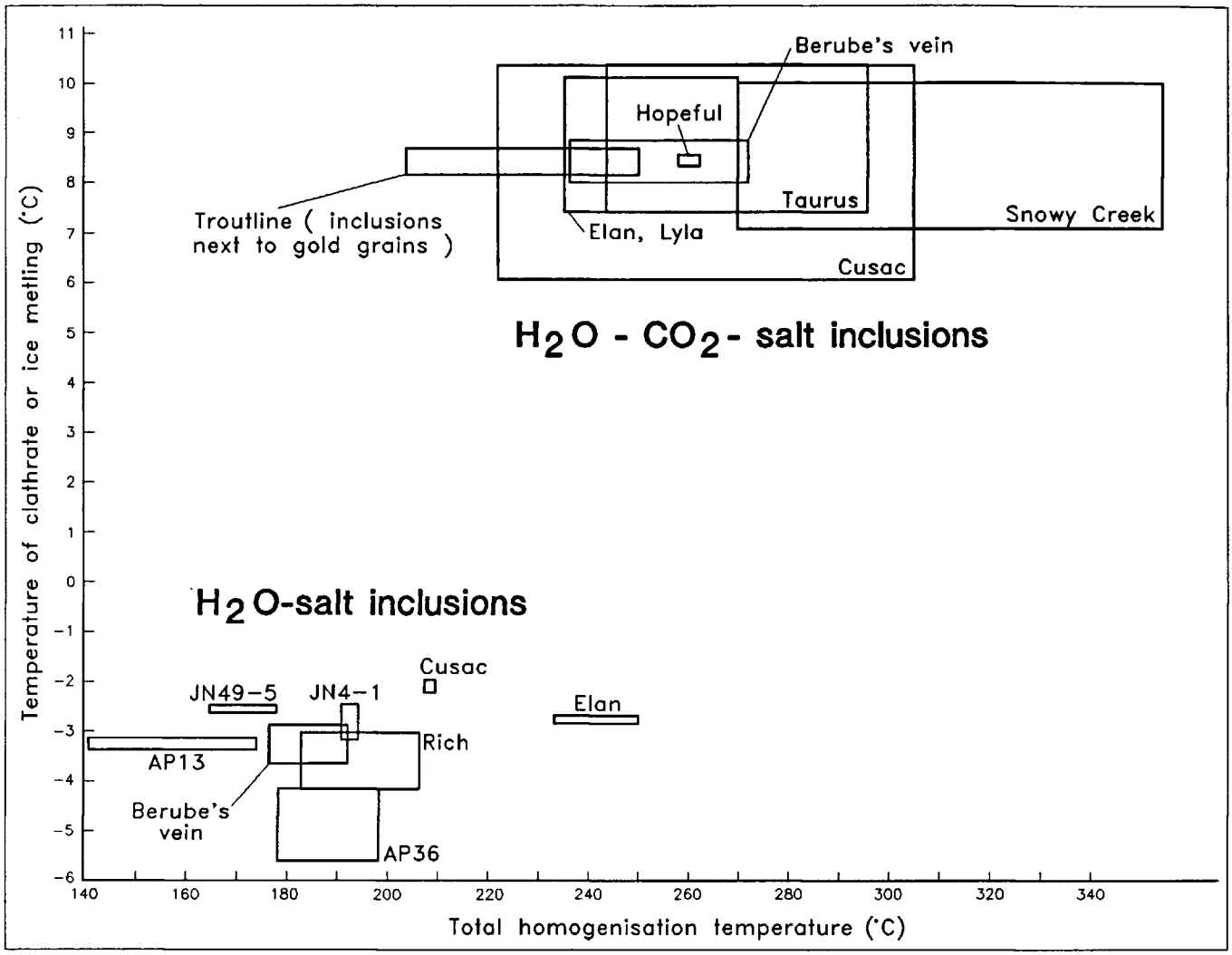


Figure 26. Temperatures of total homogenization versus melting of ice and/or clathrate for Cassiar area fluid inclusions. Complete data in Appendix 3.

sample ore fluids, wheras the H_2O-salt inclusions are of local waters that entered the system during or after it cooled to ambient rock temperatures. The highly irregular shapes of some of the large Type 2 inclusions suggest that they formed at temperatures less than 250°C (T.J. Reynolds, personal communication, 1989).

The lack of two distinct coexisting populations of carbonic inclusions, vapour-poor and vapour-rich, with identical ranges of total homogenization temperatures, demonstrates that fluids were entrapped in the one-phase field, above the solvus. The phenomenon of fluid unmixing, reported for some other mesothermal systems and invoked as a mechanism for gold deposition (Botrell *et al.*, 1988; Goldfarb *et al.*, 1988), did not occur here.

The wide range of total homogenization temperatures (T_h) for Type 1 inclusions shown in this study was also noted by Dussell (1986), although his data were from isolated inclusions and did not eliminate the effect of necking. This study of consistent groups of inclusions shows that the variation is real and characteristic of the system. It should be emphasized that the entire range in T_h can be observed in single chips. Type 1 inclusions also show considerable variation in T_{hc}, which ranges from −2.5 to +29.5°C. No systematic variations in Type 1 inclusion populations between individual veins or between classes of veins were observed in our study, although detailed work with different phases within veins may illuminate subtle patterns. Although many of the Type 1 inclusions are near sulphides, only one set in a sample from the Taurus mine (81AP21) co-occupies a microfracture with gold. These inclusions show some of the lowest total homogenization temperatures of any Type 1 group, 200 to 220°C.

The variation of carbonic phase and total homogenization temperatures in Type 1 inclusions indicates that they cooled along a set of isochores below the CO_2-H_2O solvus. This variability in the vein-forming fluids may have been the result of temperature differences at a single pressure, pressure differences at a single temperature, different fluid batches with varying $^{X}CO_2$ and salt, or simultaneous variations in pressure, temperature and fluid composition.

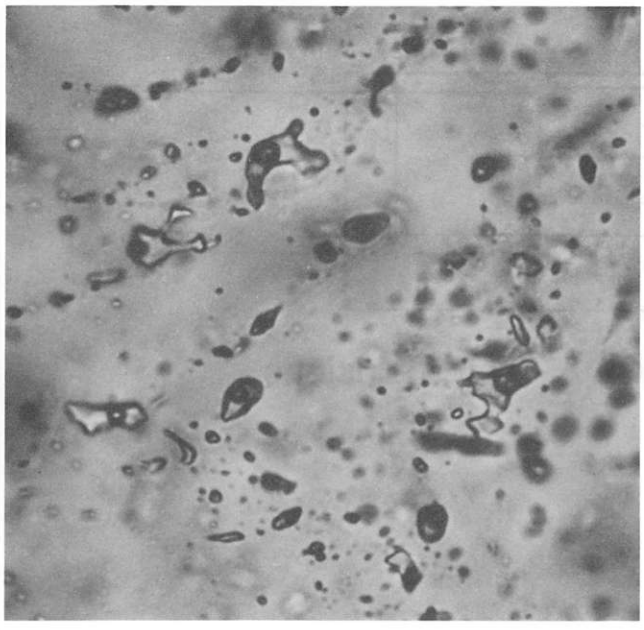


Plate 20. Large type-2 inclusions in clear quartz. Field of view 310 micrometres.

Derivation of Fluid Characteristics

Type 1 CO_2–bearing Inclusions: Freezing Data

Melting temperatures for the carbonic phase (T_m*) range from −56.9 to −58.4°C, with a mean of −57.4°C (estimated). All CO_2 melting temperatures indicate the presence of minor amounts of CH_4, (mole fraction CH_4 of the carbonic component = 0.05; estimated from Figure 8.23, Roedder, 1985). Other volatile components may also be involved.

Observed eutectic melting temperatures (T_e) range from −20 to −43°C, with temperatures of −24, −28 and −32°C occurring most often. These temperatures are based on ice recrystallization textures and/or bubble movement during warming, and in most cases the relevant observation is obscure and somewhat subjective. Eutectic temperatures of approximately −22°C (Snowy Creek and unnamed veins north of Berubé's) suggest that solutions were dominated by monovalent cations Na+ and K+ (T_e NaCl – KCl = −22.9°C), while lower T_e measurements imply the presence of a divalent cation, probably Mg^{2+} (T_e NaCl – $MgCl_2$ = −35°C; Table 4.1 in Crawford, 1981).

Ice and clathrate melting temperatures are seldom observed in the same inclusion. Only clathrate melting is useful in determining salinities in inclusions with carbonic phases. Clathrate melting temperatures range from +7.2 to 10.3°C, indicating minimum salinities of up to 6 weight per cent NaCl equivalent. These are minimum salinities because the presence of methane and other volatiles offsets the effect of salts on clathrate melting temperatures. The range in T_{mc} therefore reflects variability in both salinity and volatile content.

Type 1 CO_2-bearing Inclusions: Heating Data

Homogenization of the carbonic phases, where observed, is almost invariably to the liquid phase, and spans a temperature range from −2.5 to +29.5°C. This corresponds to a range in density of the carbonic component of 0.70 to 0.94 gram per cubic centimetre (visually estimated from Figure 1.1, Hollister, 1981). The vast majority of these occur in the 13 to 27°C range (= 0.76 to 0.86 gram per cubic centimetre). A reasonable value for mean density of the carbonic component is about 0.80 gram per cubic centimetre.

Schwartz (1989) provides a series of convenient diagrams for the determination of the H_2O/CO_2 ratio, the volume per cent of the CO_2 phase, and the pressure at total homogenization for mixed H_2O-CO_2-NaCl inclusions, given T_h and CO_2 density calculated from T_{hc}. For typical Erickson inclusions with a total homogenization temperature of 250 to 300°C, with densities of the carbonic phase in the 0.76 to 0.86 gram per cubic centimetre range, and with 6 per cent dissolved salt, the derived pressure at homogenization is 1400 to 1800 bars, the derived $^{X}CO_2$ is 0.08 to 0.14, and the calculated CO_2 content is 10 to 30 volume per cent (Schwartz, 1989, Figures 2 and 4). The last value agrees with the spread of visual CO_2 volume estimates.

Type 2 Aqueous Inclusions: Freezing Data

Most final ice-melting temperatures (T_{mi}) for aqueous inclusions range from −2.7° to −4.8°C, corresponding to salinities of about 4.5 to 7.6 weight per cent NaCl equivalent (method of Potter *et al.*, 1977). This range is roughly equivalent to that of the Type 1 inclusions.

Type 2 Aqueous Inclusions: Heating Data

Homogenization temperatures for aqueous inclusions range from about 140 to 200°C, with a few higher temperatures. Most of these inclusions homogenize between 175 and 195°C, with a mean (estimated) of 180°C. This corresponds to a density of 0.87 gram per cubic centimetre, disregarding salinity (Figure 4.1, Crawford, 1981). A somewhat higher density is predicted for a slightly saline solution. Trapping temperatures are essentially unconstrained, provided that the timing of microfracturing episodes relative to the earlier CO_2-bearing system is unknown. Textural considerations, that is the irregular shapes of most (but not all) of these inclusions, suggest that trapping temperatures were below about 250°C (*cf.* Bodnar *et al.*, 1985). For an inclusion with T_h = 180°C and 5 per cent NaCl equivalent, a trapping temperature of 250°C corresponds to a trapping pressure of about 100 megapascals (1000 bars) (visually estimated using Figures 4.1 and 4.12 in Crawford, 1981). This is somewhat less than the minimum pressure estimate for the CO_2-bearing fluids, indicating that some of the aqueous fluids may reflect a much later event, postdating a significant erosional interval.

Constraints on Characteristics of the Mineralizing Fluids

The Type 1 inclusions are samples of the fluids that deposited the milky bull quartz veins of the Erickson-Taurus system, together with their sulphides and the free gold. The

pressure-temperature range of their homogenization data is depicted by the 'box' in pressure-temperature space in Figure 27. It corresponds with the calculated isoplethic unmixing curve for a 6 weight per cent NaCl and $^{X}CO_2 = 0.1$ (Gehrig *et al.*, 1979), also shown on Figure 27. The Erickson-Taurus fluids were trapped in the one phase field above the solvus. Super-solvus isochores are sketched on Figure 27. Their slopes are derived from Brown and Lamb (1986), who present super-solvus isochores for various H_2O-CO_2-NaCl mixtures. Their isochores are undefined near the solvus, which is the region of interest here. However approximate slopes can be estimated from their diagrams, using the carbonic phase densities calculated from Schwartz (1989). The isochores on Figure 27 were derived in this way.

The isochores, of course, only define pressure-temperature relationships, not specific values. Additional pressure and temperature constraints are provided by observed metamorphic assemblages. As discussed in Chapter 3, the prehnite-pumpellyite/greenschist transition in the Sylvester allochthon took place at at less than about 250 megapascals (2.5 kilobars), near the CO_2-free invariant point . This provides an estimated maximum total pressure, line (a) on Figure 27. The Erickson-Taurus veins are associated with a strong retrograde event, in which, farthest from the veins, low-CO_2 prehnite-pumpellyite assemblages occur in veinlets that crosscut actinolite-bearing rocks. Proximal, high-CO_2 assemblages (chlorite+calcite±epidote) pass inwards to iron-magnesium carbonate alteration haloes abutting the veins. This sequence probably reflects increase of $^{X}CO_2$ inwards at constant or nearly constant temperature, as shown by the path on Figure 27. Lamprophyre dikes, some of which are Early Cretaceous, are also affected by strong prehnite-pumpellyite metamorphism. These relationships suggest that the veins were emplaced in a regime of declining temperatures and invasion of carbon dioxide bearing fluids following the contact-metamorphic peak.

The presence of pumpellyite and/or prehnite, developed at the expense of earlier actinolite in the outer envelopes of the veins, suggests that they formed at temperatures below the reactions:

pumpellyite + chlorite + H_2O = clinozoisite + tremolite + H_2O,

and

prehnite + chlorite + quartz = clinozoisite + tremolite + H_2O

(Liou *et al.*, 1985), shown as lines (b) and (c) on Figure 27. Finally, talc is stable in ultramafic rocks next to the veins. Line (d) shows the low-temperature limit of its stability, defined by the reaction serpentine + quartz = talc + H_2O calculated by Johannes (1969). These four constraints mark out a fairly small region in pressure-temperature space, which is shaded on Figure 27. It lies between 180 and 250 megapascals (1.8 and 2.5 kilobars) and 350 to 400°C. The presence of iron in the system would shift this region to lower pressures and temperatures. The region is intersected by the isochores corresponding to the highest observed homogenization temperatures. Perhaps these represent the earliest and hottest vein-forming fluids, with which talc was in equilibrium. Later H_2O-CO_2 fluid batches, including those associated with native gold, were introduced at, and also unmixed, at lower temperatures. The effect of fluid overpressures is not taken into account in this model, however, it is unlikely they would exceed a few thousand kilopascals.

In conclusion, the fluids that created the Erickson-Taurus veins were essentially H_2O-CO_2 solutions with about 5 to 6 per cent dissolved salt. Probable minor components include CH_4, and salts with bivalent cations such as $CaCl_2$ and $MgCl_2$. Ambient pressures were at about 200 megapascals (2 kilobars) and temperatures 350 to 400°C. The vein-forming fluids may have been slightly hotter than the surrounding rocks. They were introduced as a single fluid with $^{X}CO_2 = 0.1$; no evidence of immiscibility was found. The calculated temperatures and pressures for the Erickson-Taurus vein fluids are comparable to those of the California Mother Lode (Weir and Kerrick, 1987), but are somewhat lower than estimates for Archean deposits (Brown and Lamb, 1986) which formed under conditions of greenschist metamorphism.

Discussion

The presence of a cryptic contact aureole centred on the Erickson-Taurus vein system, and the presence of granitic clasts in postmineral dikes, suggests that a subjacent intrusion provided the heat that drove the ore-forming fluids. This plutonic-cupola model for the veins accounts for the important difference between their structural setting and that of classic mesothermal vein systems such as the Sigma mine, the California Mother Lode, Bralorne, and Giant Yellowknife, which occur in major, probably crustal-scale fault zones, where deep circulation of fluids is a likely event (Sibson *et al.*, 1988; McHaig, 1988; Allison and Kerrich, 1981). The Erickson-Taurus veins occupy a set of east-northeasterly trending fractures without significant offsets; even the northerly faults in the area, such as the Erickson Creek and Marble Creek faults, show only moderate throws. A subjacent intrusion under the Erickson-Taurus system would account for the existence of a strong hydrothermal cell without the control of steep, deeply penetrating fault zones. Further, the north-south array of east-northeasterly controlling fractures can be explained as the reactivation of dominant earlier joints (Gabrielse, 1963) as a result of doming over the axis of the intrusion. Extensional duplex structures in the Vollaug vein, near the southern edge of the system, show an appropriate sense of top-to-the-south motion. Finally, the presence of a cryptic intrusive body explains why the Erickson-Taurus gold-quartz vein system has no apparent parallels elsewhere in the Sylvester allochthon.

ASBESTOS: THE CASSIAR AND McDAME DEPOSITS

The Cassiar and McDame asbestos mines are stockworks of chrysotile fibre veins developed in serpentinite within a thin western salient of the Cassiar ultramafic body (Figure 2, Plate 21). The Cassiar deposit was the first major orebody discovered in the area (Smitheringale, 1957; Plumb, 1989). It has remained the most economically sig-

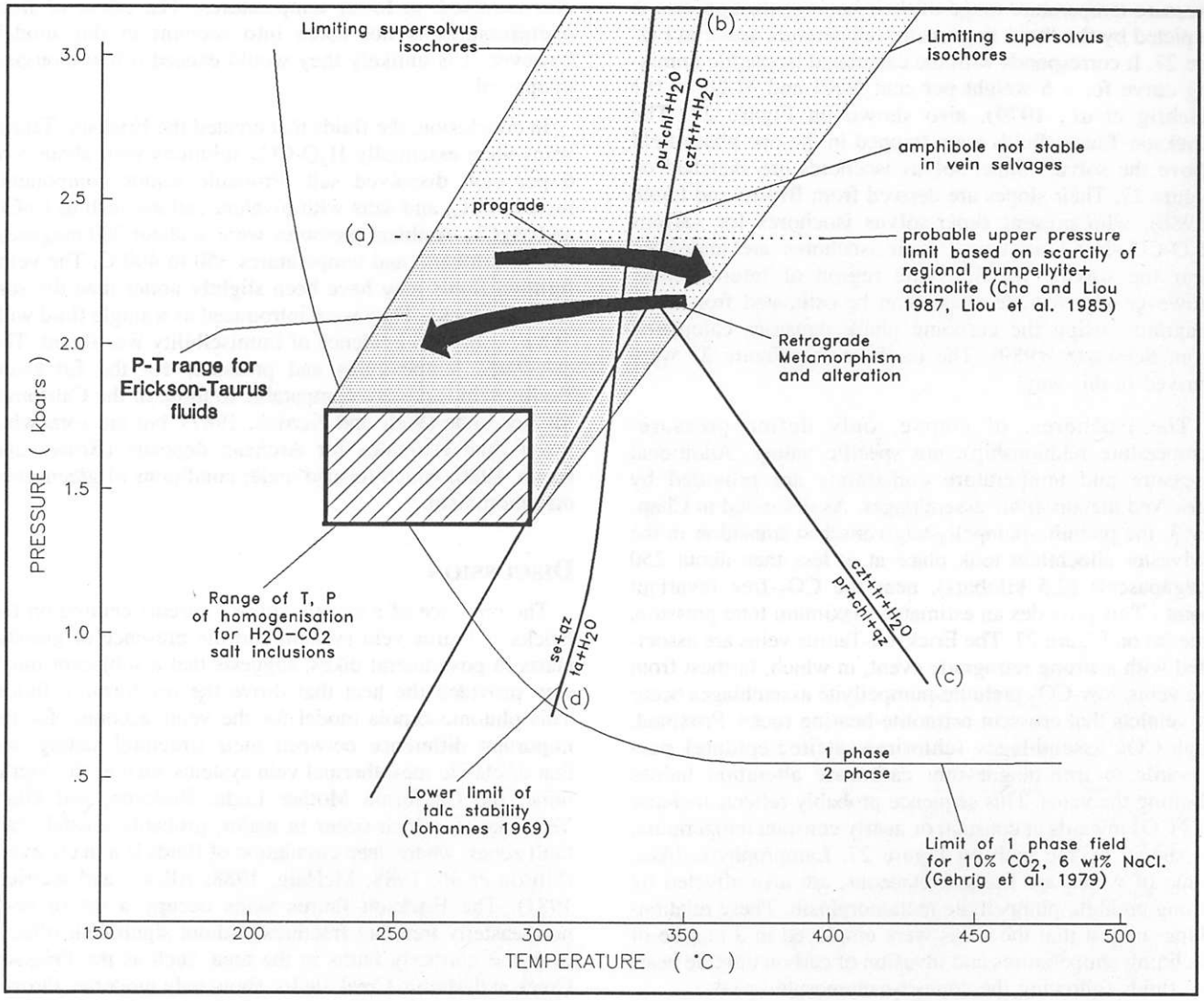


Figure 27. Pressure-temperature constraints for Erickson vein formation imposed by fluid inclusions and metamorphic equilibria.

nificant and longest lived producing mine, with 37 million tonnes of 7.23 per cent asbestos fibre produced from the pit (Plate 21) over the mine life 1953 to 1990. The underground McDame orebody, located downdip to the south of the Cassiar deposit, was discovered in the early 1980s (Burgoyne, 1986). It closed in early 1992 after less than a year of production. Resources at the end of 1990 were 18.9 million tonnes 5.6 per cent fibre.

The geology of the mine area is complex. The Cassiar orebody and its enclosing serpentinite lie at the base of the Sylvester allochthon. The North American section below it is thrust imbricated, but individual units – the Tapioca sandstone, McDame Group and Earn Group – are unusually thin or even absent. This seems to be the result of several unconformities together with later faulting (Nelson, 1989; Nelson and Bradford, 1989; O'Hanley, 1990). In the mine area the Cassiar ultramafic body lies structurally above bedded black and salmon-and-green chert (Unit MPs), and structurally below well-bedded argillite, tuff, basalt, greywacke and calcarenite of Unit IIMvs. This is the only occurrence of serpentinite at the base of the allochthon in the map area. Farther south, a sliver of serpentinite lies within Unit IIMvs, separating two thrust imbricates (O'Hanley, 1990; Figures 2, 28).

Structure within and near the Cassiar pit was the subject of detailed studies by O'Hanley (1988, 1990). He has shown that two phases of deformation affected the mine area. The first was east-side-down motion on low-angle faults. When eastward tilting of the west limb of the McDame synclinorium is restored, this event is the eastward emplacement of the Sylvester allochthon. A thrust ramp in McDame dolomite and Tapioca sandstone south of the pit climbs upsection to the east, indicating easterly vergence. The second event, associated with the asbestos-bearing veins, involved top-to-the-west motion and simultaneous dextral strike slip. It was probably related to the formation of the western limb of the McDame synclinorium.

The Road River Group within and near the Cassiar pit contains unique metapyroclastic lithologies not observed elsewhere in the map area. Lapilli tuff consisting of clasts

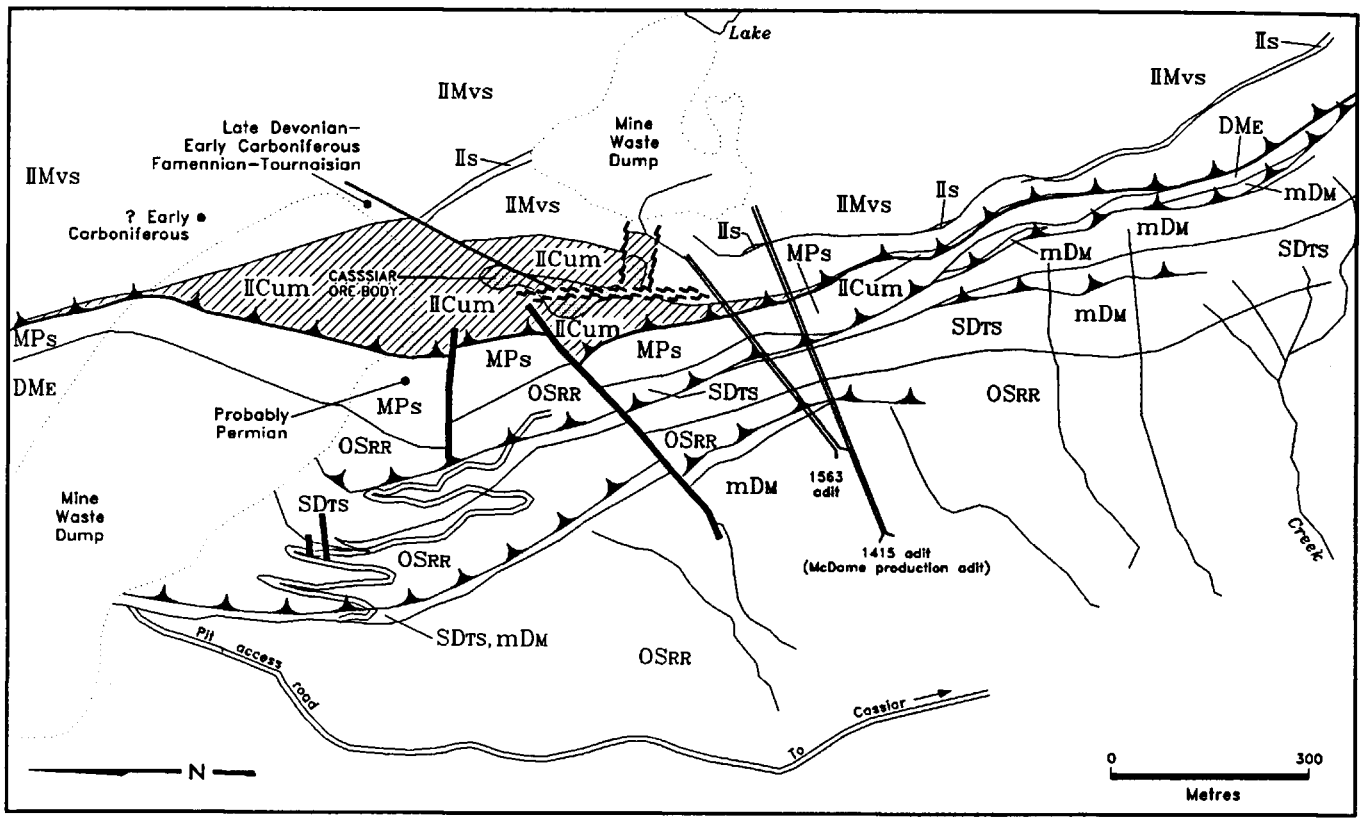


Figure 28. Geology around the Cassiar and McDame asbestos mines. Compiled from O'Hanley (1990). Dots are conodont sample localities. Geologic units as on Figure 2.

and matrix of red-brown metamorphic biotite and calcite is exposed under a ledge at the second switchback on the mine road. The biotite plates are poorly oriented, and likely crystallized during contact metamorphism by the Cassiar batholith. Within the pit, wispy, pale grey fine-grained pyroclastic horizons with bright green specks occur within sooty black Road River Group slates. The bright green mineral is a chromium-rich phlogopite (D. O'Hanley, personal communication, 1989). It shows strongly preferred orientation parallel to the regional foliation.

A K-Ar age of 94.5±3.3 Ma was obtained from a mica separate (roughly 50% Cr-phlogopite) from a sample of one of these pyroclastic lenses on the southwest wall of the Cassiar pit (Table 4). This corresponds to the youngest ages assigned to the Cassiar batholith (Chapter 2). It marks the latest time that rocks of the Cassiar pit experienced temperatures in excess of 280 to 350°C. (Harrison and McDougall, 1980, 1982), depending on the exact nature of the micas. This mid-Cretaceous quenching may help provide a time constraint on the development of chrysotile asbestos at the Cassiar mine. O'Hanley *et al.* (1989), using $^{18}O/^{16}O$ water-serpentine fractionation geothermometry, determined that the ore-zone chrysotile developed at 300±36°C. Rodingites that formed at the same time as the chrysotile asbestos contain aqueous fluid inclusions with 4 to 10 weight per cent dissolved salt (O'Hanley *et al.*, in preparation). Their average homogenization temperature is 276±29°C. Projection along the appropriate isochores to 300°C leads to pressure estimates of less than 80 megapascals (800 bars) and possibly 25 megapascals (250 bars) (O'Hanley *et al.*, in preparation). Combining these estimates with the K-Ar mica age and O'Hanley's (1988, 1990) geological constraints leads to a model of Cassiar asbestos formation that postdated emplacement of the allochthon but predated cooling of the Cassiar batholith. Estimated pressures during Early Cretaceous formation of the nearby Erickson gold-quartz veins are much higher, in excess of a 100 megapascals (1 kilobar). Considerable erosion must have taken place after deposition of the gold veins and before the formation of chrysotile asbestos at the Cassiar mine. Most reasonably, the mica closure age corresponds to the age of asbestos formation and both were related to thermal effects of the Cassiar batholith. The recrystallization of serpentine to asbestos and the related formation of rodingites resulted from circulation of fluids in the outermost part of the contact aureole.

MANTOS, SKARNS, VEINS AND PORPHYRIES

All three intrusive episodes in the area, the 100 Ma Cassiar batholith, and the 70 Ma and 50 Ma events, can be linked to porphyry molybdenum (copper) mineralization, precious metal veins and stockworks in granite, tungsten (molybdenum) skarns, and silver-lead-zinc mantos and veins in miogeoclinal carbonates. Previous studies have focused on single deposits or groups of similar deposits. Panteleyev (1980) described the Cassiar and Storie por-

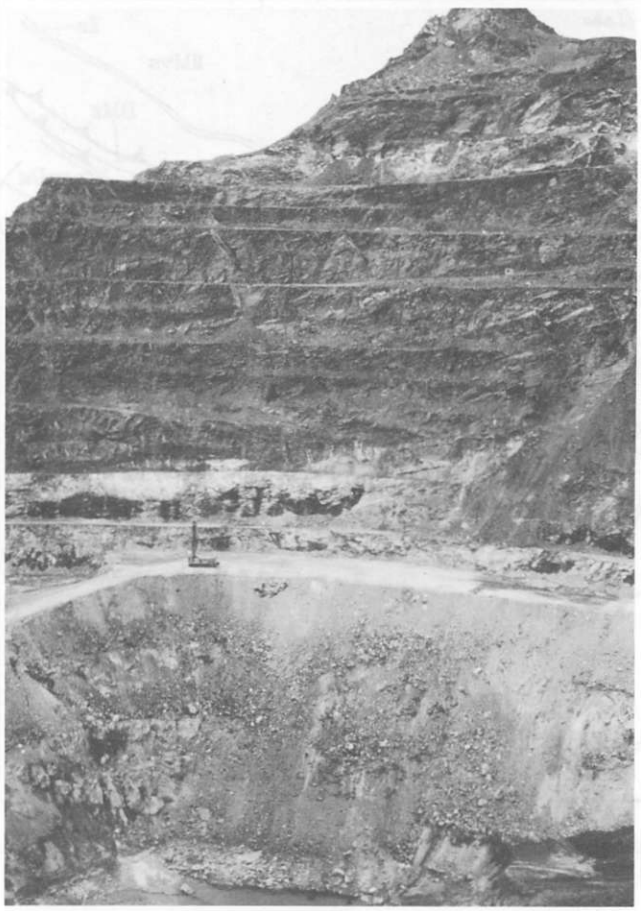


Plate 21. The south wall of the Cassiar mine pit in 1989, just prior to closure.

phyry molybdenum deposits and, through K-Ar dating, first showed the existence of a 70-Ma intrusive suite on the eastern side of the Cassiar batholith. Cooke and Godwin (1984) published a detailed study of the Contact skarn deposit. Gower *et al.* (1985) described the Mount Haskin skarn deposits

This study aims at demonstrating links between the different types of epigenetic deposits. Much of the new evidence relating carbonate-hosted silver-lead-zinc deposits in the project area to granite emplacement comes from detailed work on the Midway deposit by the junior author, which forms part of his M.Sc. thesis (Bradford and Godwin, 1988; Bradford, 1988). In addition to the Midway deposit, carbonate-hosted silver-lead-zinc deposits form all or part of four other mineral deposit suites in the project area: the mid-Cretaceous Amy-Silverknife system, the Ax and Ella Rose showings in the southeastern Blue Dome map area, the 70-Ma Marble Creek system and the Eocene Mount Haskin - Mount Reed system. All of these are worthy targets for manto exploration. Favourable carbonate hosts are: the McDame Group (Midway); the Kechika Group (Amy); the Rosella Formation, which hosts all the others so far known; and also carbonates within the Stelkuz Formation, which hosts the Contact and Dead Goat skarns and could easily contain silver-lead-zinc bodies.

The Midway Deposit and Midway Model

Midway is a blind deposit discovered in 1980 by deep drilling of sedimentary exhalite targets. It consists of two separate sets of sulphide bodies, the Silver Creek and Discovery deposits, located at and near the top of the McDame Group. They are made up of numerous worm-shaped sulphide-rich shoots measuring metres to tens of metres across. Total estimated reserves are currently 1.2 million tonnes grading 410 grams per tonne silver and 12 per cent combined lead-zinc. The mineralogy of the Midway deposit is complex. Phases include pyrite, chalcopyrite, pyrrhotite, marcasite, sphalerite, galena, arsenopyrite, freibergite, pyrargyrite, stannite, frankeite, acanthite, boulangerite and geocronite with quartz, barite, and late gypsum (Archambault, 1985; Bradford, 1988).

The Midway deposit is classified as a silver-lead-zinc manto deposit rather than a Mississippi Valley type, based on the following characteristics:

- Its mineralogy includes sulphosalts, sulphides that are more common at high temperatures (pyrrhotite and arsenopyrite), and tin-bearing minerals such as stannite and geocronite. Calcsilicates with pyrrhotite occur in the deeper parts of the deposit near Brinco Hill (Bradford, 1988).
- Mineralization proceeded by both replacement and open space filling.
- Large areas of quartz-sericite alteration in the superjacent Earn Group and Sylvester allochthon, and minor rhyolite dikes, suggest the presence of a cryptic intrusion. Both the dikes and the alteration have K-Ar ages of about 70 Ma.
- Fluid inclusion data indicate that ore-forming fluids were H_2O-CO_2-salt solutions with temperatures in the range from 280 to 340°C, in part showing immiscible behaviour (Bradford, 1988).
- Lead isotope signatures from Midway galenas show a very young, Cretaceous to Tertiary model age, which is consistent with the K-Ar data (Figure 25; Bradford, 1988).

A predominance of replacement as opposed to open-space-filling textures is one feature that separates mantos from Mississippi Valley deposits. At Midway, ore textures show that both mechanisms were operative. Evidence for replacement includes sulphides along stylolites and ghosts of limestone textures in silicified zones adjacent to ore. On the other hand, a variety of breccia types both in the orebodies (Plate 22) and in the surrounding area show the existence of open spaces at times ranging from Late Devonian to the time of mineralization. The earliest event was karsting, which occurred in the hiatus between McDame and Earn deposition. Local differential topography on the top of the McDame group reaches several hundred metres, particularly in the area between Smoke Mountain and Hamlet Mountain south of the Midway deposit. Cavities in the top of the McDame Group on Hamlet Mountain are filled with pastel-coloured dolomitic siltstones. Conodonts from these are of Frasnian age (No. 8, Table 2), intermediate between the Givetian McDame Group and the oldest, Fam-

ennian, Earn Group. Large karst tubes filled with coarse calcite occur northwest of Midway near the Berg showing. In Midway core, Bradford (1988) describes lag sediments in karst cavities in the upper McDame Group.

Further solution brecciation postdated deposition of the Earn Group. On Donegal Mountain, chips of black basal Earn shale have collapsed into a cavity at the top of the McDame Group, next to a steep growth fault that is cut off by a Mesozoic thrust fault. These shale fragments lack the ubiquitous crenulations that developed during Mesozoic tectonism; therefore the breccia formed early, perhaps during the nondepositional interval that succeeded the Earn. Similar breccias are seen on Smoke Mountain.

A third important brecciation event accompanied mineralization at Midway. Breccias containing fragments of crenulated Earn black slates and fragments of sulphides are also a common feature. Their matrix is either fragmental, or consists of crystalline quartz, calcite or sulphides. Formation of these breccias must have been due to solution of McDame carbonates by ore-forming solutions, causing collapse of basal Earn and previously formed sulphides. Thus early karsting and further solution brecciation at the McDame-Earn contact provided ground preparation for mineralization, while brecciation coeval with the introduction of the ore-forming fluids enlarged the available room for sulphide deposition.

Quartz-sericite alteration zones extend east-southeast of the Midway deposit across Brinco Hill and into the valley west of Gum Mountain (Nelson and Bradford 1987b; Figure 29). Altered quartz-eye porphyry dikes occur within the zone, together with flinty, purple, pyrrhotite-bearing hornfels exposed in a small area. Sericite ages from the dikes and the alteration zones are 65.4±2.3 Ma and 67.1±2.3 Ma (Table 4). W.D. Sinclair (personal communication, 1987) has obtained a 74.7±2 Ma whole-rock age from a thoroughly altered dike, and 78.7±2.5 Ma from a hornfels on the Hot claims on the British Columbia - Yukon border 25 kilometres northeast of Midway. The Hot claims cover a large, intense contact aureole in which the only exposed intrusive bodies are a few rhyolite dikes. (Nelson and Bradford, 1987a). These radiometric ages suggest a widespread but unobtrusive Late Cretaceous plutonic suite as the main causative agent for Midway-type mineralization.

Aeromagnetic surveys of the Midway area show a strong negative anomaly below Brinco Hill, 3 kilometres east of the deposit. This is interpreted as a buried intrusion (J.J. Hylands, personal communication, 1986). It illustrates the use of aeromagnetic techniques in locating possible cryptic intrusive centres, which are a critical component of the Midway model. As discussed previously the Midway alteration shows a strong enrichment in fluorine and affiliation with the topaz rhyolite suite (Sinclair, 1986). Fluorine lithogeochemical and stream-water anomalies could be used as tracers for this type of system.

Controls on sulphide deposition at Midway included not only ground preparation at the top of the McDame Group and hydrothermal fluid circulation driven by a Late Cretaceous felsic intrusion, but local structural controls as well. The Midway deposit is located within the Tootsee River

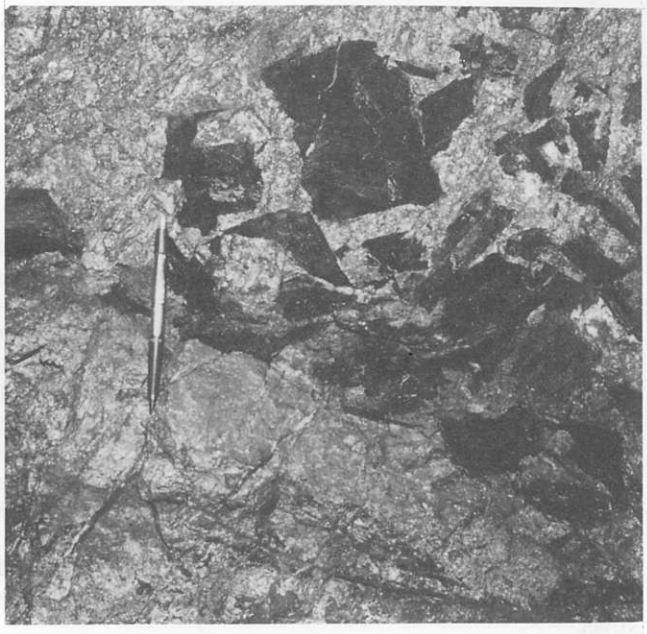


Plate 22. Breccia underground at Midway. The clasts are of black basal Earn Group slate; the matrix is sulphide.

fault system which, as discussed earlier, is a complex of high-angle extensional faults. These faults probably played an important role in channelling magma and also in creating solution pathways. It is noteworthy that three other significant silver-lead-zinc manto deposits of varying ages are located within this fault system – the mid-Cretaceous Amy and Silverknife deposits, and 5 kilometres north of the Yukon border, the Eocene Butler Mountain deposit. Butler Mountain, described by Abbott (1984), shows interesting parallels to and differences from the Midway deposit. It is hosted by the Rosella Formation. Associated quartz porphyry dikes have 50-Ma K-Ar ages (Abbott, 1986) and contain fluorite and topaz in vugs (W.D. Sinclair, personal communication, 1986). Orebodies are primarily breccias, containing clasts of limestone, sulphides and dike material: as at Midway, brecciation was an important ore control. The mineralogy of Butler Mountain is simpler than that of Midway, consisting of pyrite, chalcopyrite, and minor galena and sphalerite. Despite this, Butler Mountain is sufficiently similar to the Midway deposit to encourage exploration for mantos in Lower Cambrian, as well as in Devonian carbonates, and to focus attention on small felsic intrusions of any age.

In summary, the Midway model requires the following components:

- A suitable carbonate host, the top of the McDame Group in the Midway deposit with its impermeable cap of Earn slates, but other carbonates such as the Rosella Formation should be considered as well.
- A felsic intrusion, probably at a level below that of the manto occurrence and therefore poorly exposed, if at all. Indirect evidence for it might include dikes, alteration, hornfelsing and a negative magnetic anomaly.
- High-angle, post-orogenic faults, which controlled emplacement of the stock.

These criteria are useful in exploration for manto deposits in the project area, and in the Cassiar Terrane as a whole. In the course of the project, four additional areas with manto potential have been identified.

Mineral Occurrences in the Southeastern Blue Dome Area

Poorly exposed strata of the Rosella and Boya formations and the Kechika Group in the southeastern corner of the Blue Dome map area are cut by through-going, northwest-striking faults, one of which, the Rosella Creek fault, has a demonstrable 2-kilometre dextral offset farther south in the Rosella Creek watershed (Figure 2). Two occurrences of silver mineralization are located on or near the fault, the Ax and the Ella Rose (Nelson *et al.*, 1988a). The Ella Rose was discoverered in 1987. It is a Rosella-hosted silicified breccia located on the Rosella Creek fault trace. It contains pyrite and minor amounts of galena, sphalerite and tetrahedrite. The Ax is a vein set; galena pods within wide silicified zones in Rosella limestone carry up to 248 grams per tonne silver.

These two showings are associated with two major elements of the Midway model: platformal carbonate hosts and major faults. No evidence was seen of cryptic intrusions in their vicinity; perhaps they represent higher levels in such a system.

The Marble Creek System

Occurrences in the Marble Creek watershed and north to Lamb Mountain illustrate all three aspects of the Midway model, and also the coexistence of different mineralization types within a single coherent system. In this area, a miogeoclinal sequence including Stelkuz, Rosella and McDame carbonates, is intruded by a suite of 70-Ma plutons (Table 4). The most northerly of these is the Lamb Mountain stock. Four kilometres northeast of Lamb Mountain, a strong negative magnetic anomaly, traces of dike material and hornfelsing provide evidence for a cryptic intrusion.

A structurally repeated Tapioca-McDame-Earn section is exposed on the mountain immediately north of the negative magnetic anomaly. Coarse tetrahedrite occurs in quartz veins in the Earn Group (Dfablo showing, MINFILE 104P 115). The subjacent, poorly exposed McDame Group in this area is a favourable target for manto mineralization.

Granites in the Marble Creek system contain porphyry molybdenum mineralization, notably the Storie Moly and Cassiar Moly prospects, and also traces of molybdenite within the Lamb Mountain stock. Tungsten-molybdenum skarns, the Kuhn, Contact, Dead Goat and Lamb Mountain prospects, occur at granite-limestone contacts and also along limestone-siliciclastic contacts near the granites. These skarns contain tremolite, garnet, diopside, epidote, biotite and scapolite; some contain massive sulphide lenses (Cooke and Godwin, 1984).

A number of silver-lead-zinc replacement lenses occur within Rosella carbonates in the Marble Creek watershed. They lie on two east-west trends, the "D" and the Magno, that abut against the Marble Creek fault, a northerly striking, west-side-up normal fault. Farther south, this fault hosts the Pant tin showing (MINFILE 104P 082, Figure 2). Movement on the Marble Creek fault closely followed granite emplacement. Subsidiary faults that terminate against it offset the margin of the granite; on the other hand, skarn development, coarse tremolite sprays, as well as tin-sulphide mineralization are localized along it.

The Mount Haskin - Mount Reed System

Mounts Haskin and Reed are underlain by thrust-imbricated Boya, Rosella and Kechika strata (Figure 2). These structures are cut by later high-angle fault swarms that centre on the north-trending Rosella Creek fault. Two small granite intrusions are exposed at surface, one on the western flank of Mount Haskin and one on the southern slope of Mount Reed, although the intensity of contact metamorphism, particularly on Mount Haskin, suggests the presence of a larger intrusive body at depth. Within this mineralized system, porphyry molybdenum-copper mineralization is developed in the granites, and skarns occur at their contacts against carbonates and also at Rosella-Boya and Rosella-Kechika contacts (Gower *et al.*, 1985). On the summit plateau of Mount Haskin, the best-developed massive sulphide skarn, a banded 'wrigglite' pod containing pyrrhotite and fluorite, occurs at a Rosella-Boya contact where it intersects a high-angle fault; Kechika hornfelses are exposed to the northeast. Silver-lead-zinc lenses (Joe Reed vein) occur in the Rosella Formation up to 3 kilometres from the nearest exposed intrusion. Parallels with the Marble Creek system include the presence of a through-going transcurrent fault, presence of small, high-level intrusions, and the same porphyry-skarn-vein spectrum of mineralization. The role of the Rosella Creek fault is also noteworthy, in that it is also associated with the Ax and Ella Rose deposits farther north.

SYNTHESIS: MINERALIZATION HISTORY AND EXPLORATION MODELS

Two tectonic regimes brought about most of the patterns of mineralization evident in the Midway-Cassiar area. Devono-Mississippian extension gave rise to sedimentary exhalative deposits in the Earn Group and Division I of the Sylvester allochthon, and Besshi-type deposits in Division II. These deposits are host-specific and distributed throughout the Cassiar Terrane and the allochthon; indeed parallels are found along the entire margin of ancestral North America in Canada, from MacMillan Pass in Yukon to the Chu Chua deposit in southern British Columbia. A further area of sedimentary exhalite potential is the ill-defined Dorsey Terrane west of the Cassiar batholith, which contains large tracts of Mississippian siliciclastic sediments (Gabrielse, 1969).

The second key tectonic regime was the multi-episodic granitic emplacement that postdated early Mesozoic compression. Intrusive events *circa* 120, 100, 70 and 50 Ma all had associated metallogenetic processes. In terms of the most significant precious metal deposits in the Cassiar Terrane and Sylvester allochton, the associated granites are more likely to be cryptic than exposed: Midway and

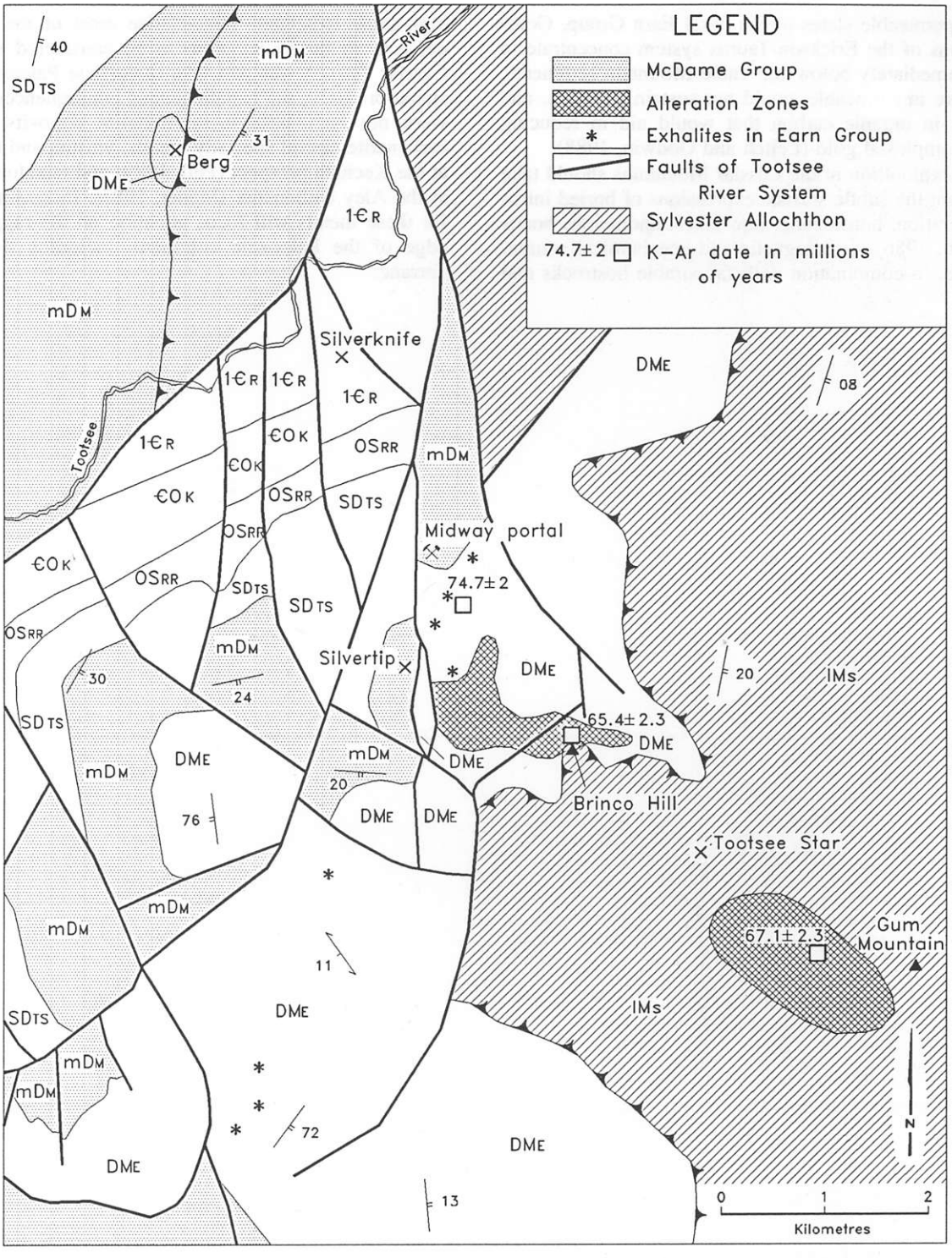


Figure 29. Geology around the Midway deposit. After Nelson and Bradford (1987b) and Bradford (1988). Geologic units as on Figure 2.

Erickson, like the Ketza River and Mount Hundere mantos in Yukon (Abbott, 1977, 1986), are characterized by buried granites.

An additional ore control was provided by high-angle faults, many of them related to the major dextral-transcurrent faults that dominated stress patterns in Late Cretaceous to Eocene time (Abbott, 1986). The third control was the chemical and physical characteristics of the mainly stratified, or at least structurally pseudostratified, hostrocks. The autochthonous Paleozoic carbonates, most notably the Lower Cambrian Rosella Formation and Middle Devonian McDame Group, contain most of the silver-lead-zinc deposits. Permeability contrasts are also important. The Midway deposit occurs at the top of the McDame Group,

below impermeable slates of the basal Earn Group. Gold-quartz veins of the Erickson-Taurus system concentrate in basalts immediately below the Table Mountain sediments, which were impermeable, could not sustain fractures, and were rich in organic carbon that would aid in reducing sulphite-complexed gold (Leitch and Godwin, 1988).

Metals exploration in the Cassiar Mountains should take into account the subtle surface expressions of buried intrusions: alteration, hornfelsing, rare dikes, anomalous horsts (*cf.* Abbott, 1986), aeromagnetic and geochemical anomalies. These, in combination with favourable hostrocks and high-angle structures, characterize most of the important deposits so far found. Also to be considered is that the Cassiar Terrane was part of a major late Paleozoic extensional province, the metallogenetic consequences of which were not only base metal exhalite deposits, but also carbonatite-hosted specialty metals; yttrium and rare earths at the Kechika prospect (Pell, 1989) and tantalum-niobium at the Aley carbonatite (Mäder, 1987). Increasing demand for these metals will focus attention on the ragged, rifted edge of the Paleozoic continent, including the Cassiar Terrane.

REFERENCES

Abbott, J.G. (1977): Structure and Stratigraphy of the Mt. Hundere Area, Southeastern Yukon; unpublished M.Sc. thesis, *Queen's University*, 111 pages.

Abbott, J.G. (1984): Silver-bearing Veins and Replacement Deposits of the Rancheria District; *in* Yukon Geology and Exploration 1983, *Department of Indian and Northern Development*, pages 34-44.

Abbott, J.G. (1986): Epigenetic Mineral Deposits of the Ketza-Seagull District, Yukon; *in* Yukon Geology, Volume 1, Exploration and Geological Sciences Division, Yukon, *Indian and Northern Affairs Canada*, pages 56-66.

Aggarwal, P.K., Fujii, T. and Nesbitt, B.E. (1984): Magmatic Composition and Tectonic Setting of Altered Volcanic Rocks of the Fennell Formation, British Columbia; *Canadian Journal of Earth Sciences*, Volume 21, pages 743-752.

Alldrick, D.J., Gabites, J.E. and Godwin, C.I. (1987): Lead Isotope Data from the Stewart Mining Camp; *in* Geological Fieldwork 1986, *B.C. Ministry of Energy, Mines and Petroleum Resources*, Paper 1987-1, pages 93-102.

Allison, I. and Kerrich, R. (1981): History of Deformation and Fluid Transport in Shear Zones at Yellowknife; *in* Proceedings of the Gold Workshop, Yellowknife, N.W.T., December 1979, pages 202-231.

Archambault, M. (1985): Geology and Mineralogy of the Silver Creek Deposit, Midway Property, North-central British Columbia; unpublished M.Sc. thesis, *The University of British Columbia*, 95 pages.

Barany, I. and Karson, J.A. (1989): Basaltic Breccias from the Clipperton Fracture Zone (East Pacific): Sedimentation and Tectonics in a Fast-slipping Oceanic Transform; *Geological Society of America Bulletin*, Volume 101, pages 204-220.

Bloodgood, M.A. (1987): Geology of the Triassic Black Phyllite in the Eureka Peak Area, Central British Columbia; *in* Geological Fieldwork 1986, *B.C. Ministry of Energy, Mines and Petroleum Resources*, Paper 1987-1, pages 135-142.

Bloodgood, M.A. (1988): Geology of the Quesnel Terrane in the Spanish Lake Area, Central British Columbia (93A/11); *in* Geological Fieldwork 1987, *B.C. Ministry of Energy, Mines and Petroleum Resources*, Paper 1988-1, pages 139-145.

Bloomer, C.J. (1981): Cassiar Project-3191P: Geology, Drilling and Geochemistry, Bev, Red, Lang and Peggy Claims, NTS 104P; *B.C. Ministry of Energy, Mines and Petroleum Resources*, Assessment Report 9548.

Bodnar, R.J., Reynolds, T.J. and Kuehn, C.A. (1985): Fluid-inclusion Systematics in Epithermal Systems; *in* Geology and Geochemistry of Epithermal Systems, Berger, B.R. and Bethke, P.M., Editors, *Reviews in Economic Geology*, 2.

Bohlke, J.K. and Kistler, R.W. (1986): Rb-Sr, K-Ar, and Stable Isotope Evidence for the Ages and Sources of Fluid Components of Gold-bearing Quartz Veins in the Northern Sierra Nevada Foothills Metamorphic Belt, California; *Economic Geology*, Volume 81, pages 296-322.

Boillot, G., Recq, M., Winterer, E.L., Meyer, A.W., Applegate, J., Baltuck, M., Bergen, J.A., Comas, M.C., Davies, T.A., Dunham, K., Evans, C.A., Girardeau, J., Goldberg, G., Haggerty, J., Jansa, L.F., Johnson, J.A., Kasahara, J., Loreau, J.P., Luna-Sierra, E., Moullade, M., Ogg, J., Sarti, M., Thurow, J. and Williamson, M. (1987): Tectonic Denudation of the Upper Mantle along Passive Margins: A Model Based on Drilling Results (ODP Leg 103, Western Galicia Margin, Spain); *Tectonophysics*, Volume 132, pages 335-342.

Bonatti, E. and Hamlyn, P. (1978): Mantle Uplifted Block in the Western Indian Ocean; *Science*, Volume 201, pages 249-251.

Bonatti, E., Emiliani, C., Ferrara, G., Honnorez, J. and Rydell, H. (1974): Ultramafic Carbonate Breccias from the Equatorial Mid-Atlantic Ridge; *Marine Geology*, Volume 16, pages 83-102.

Bonatti, E., Hamlyn, P. and Ottonello, G. (1981): Upper Mantle Beneath a Young Oceanic Rift: Peridotites from the Island of Zabargad; *Geology*, Volume 9, pages 474-479.

Bottrell, S.H., Shepherd, T.J., Yardley, B.W. and Dubessy, J. (1988): A Fluid Inclusion Model for the Genesis of the Ores of the Dolgellau Gold Belt, North Wales; *Journal of the Geological Society*, London, Volume 145, pages 139-145.

Boronowski, A. (1988): Erickson Gold Camp, Cassiar, B.C.; *in* Geology and Metallogeny of Northwestern British Columbia, *Smithers Exploration Group-G.A.C. Cordilleran Section*, Extended Abstracts, pages A10-A21.

Bradford, J.A. (1988): Geology and Genesis of the Midway Silver-Lead-Zinc Deposit, North-central British Columbia; unpublished M.Sc. thesis, *The University of British Columbia*, 280 pages.

Bradford, J.A. and Godwin, C.I. (1988): Midway Silver-Lead-Zinc Manto Deposit, Northern British Columbia; *in* Geological Fieldwork 1987, *B.C. Ministry of Energy, Mines and Petroleum Resources*, Paper 1988-1, pages 353-362.

Brown, P.E. and Lamb, W.M. (1986): Mixing of H_2O-CO_2 in Fluid Inclusions: Geobarometry and Archean Gold Deposits; *Geochimica and Cosmochimica Acta*, Volume 50, pages 847-852.

Burgoyne, A.A. (1986): Geology and Exploration, McDame Asbestos Deposit, Cassiar, B.C.; *Canadian Institute of Mining and Metallurgy*, Bulletin, Volume 7, pages 1-7.

Campa, M.F. and Coney, P.J. (1983): Tectono-stratigraphic Terranes and Mineral Resource Distributions in Mexico; *Canadian Journal of Earth Sciences*, Volume 20, pages 1040-1051.

Carne, R.C. (1979): Geological Setting and Stratiform Lead-Zinc-Barite Mineralization, Tom Claims, MacMillan Pass, Yukon Territory; *Indian and Northern Affairs Canada*, Report 1979-4, 30 pages.

Carne, R.C. and Cathro, R.J. (1982): Sedimentary Exhalitive (Sedex) Zinc-Lead-Silver Deposits, Northern Canadian Cordillera; *Canadian Institute of Mining and Metallurgy*, Bulletin, Volume 75, pages 66-79.

Cho, M. and Liou, J.G. (1987): Prehnite-Pumpellyite to Greenschist Transition in the Karmutsen Metabasites, Vancouver Island, B.C.; *Journal of Petrology*, Volume 28, Part 3, pages 417-443.

Christopher, P.A., White, W.H. and Harakal, J.E. (1972): Age of Molybdenum and Tungsten Mineralization in Northern British Columbia; *Canadian Journal of Earth Sciences*, Volume 9, pages 1727-1734.

Cooke, B.J. and Godwin, C.I. (1984): Geology, Mineral Equilibria, and Isotopic Studies of the McDame Tungsten Skarn Prospect, North-central British Columbia; *Economic Geology*, Volume 79, pages 826-847.

Crawford, M.L. (1981): Phase Equilibria in Aqueous Fluid Inclusions; *in* Short Course in Fluid Inclusions: Applications to Petrology, Hollister, L.S. and Crawford, M.L., Editors, *Mineralogical Association of Canada*, Calgary, pages 75-97.

Dawson, K.M. and Orchard, M.J. (1982): Regional Metallogeny of the Northern Cordillera: Biostratigraphy, Correlation and Metallogenetic Significance of Bedded Barite Occurrences in Eastern Yukon and Western District of MacKenzie; *in* Current Research, Part C, *Geological Survey of Canada*, Paper 82-1C, pages 31-38.

Diakow, L.J. and Pantaleyev, A. (1981): Cassiar Gold Deposits, McDame Map Area (104P/4, 5); *in* Geological Fieldwork 1980, *B.C. Ministry of Energy, Mines and Petroleum Resources,* Paper 1981-1, pages 55-62.

Dussell, E. (1986): Listwanites and their Relationship to Gold Mineralization at Erickson Mine, British Columbia, Canada; unpublished M.Sc. thesis, *Western Washington University*, 90 pages.

Dutro, J.T. and Gilmour, E.H. (1989): Paleozoic and Lower Triassic Biostratigraphy of Northeastern Washington; *in* Geologic Guidebook for Washington and Adjacent Areas, Joseph, N.L., Editor, *Washington Division of Geology and Earth Resources*, Information Circular 86, pages 23-44.

Erdmer, P. (1987): Blueschist and Eclogite in Mylonitic Allochthons, Ross River and Watson Lake Areas, Southeastern Yukon; *Canadian Journal of Earth Sciences*, Volume 24, pages 1439-1449.

Erdmer, P. and Armstrong, R.L. (1988): Permo-Triassic Isotopic Dates for Blueschist, Ross River Area, Yukon, *in* Yukon Geology, Volume 2; Exploration and Geological Sciences Division, Yukon, *Indian and Northern Affairs Canada*, pages 33-36.

Ey, F. (1986): Structural Analysis of the Cusac Decline, Erickson Gold Mine, British Columbia; unpublished report submitted by Minatco Ltd. to *Erickson Gold Mining Corporation.*

Ferri, F. and Melville, D.M. (1988): Manson Creek Mapping Project; *in* Geological Fieldwork 1987, *B.C. Ministry of Energy, Mines and Petroleum Resources,* Paper 1988-1, pages 169-180.

Ferri, F. and Melville, D.M. (1989): Geology of the Germansen Landing Area, British Columbia; *in* Geological Fieldwork 1988, *B.C. Ministry of Energy, Mines and Petroleum Resources,* Paper 1989-1, pages 209-220.

Ferri, F. and Melville, D.M. (1990): Geology Between Nina Lake and Osilinka River, North-central British Columbia (93N/15, North Half and 94C/2, South Half); *in* Geological Fieldwork 1989, *B.C. Ministry of Energy, Mines and Petroleum Resources,* Paper 1990-1, pages 101-114.

Ferri, F. and Melville, D.M. (in preparation): Geology of the Germanson Landing - Manson Creek Area, British Columbia; *B.C. Ministry of Energy, Mines and Petroleum Resources,* Bulletin.

Floyd, P.A. and Winchester, J.A. (1975): Magma Type and Tectonic Setting Discrimination Using Immobile Elements; *Earth and Planetary Science Letters*, Volume 27, pages 211-218.

Fritz, W.H. (1980): Two New Formations in the Lower Cambrian Atan Group, Cassiar Mountains, North-central British Columbia; *in* Current Research, Part B, *Geological Survey of Canada*, Paper 80-1B, pages 217-225.

Fritz, W.H. and Crimes, T.P. (1985): Lithology, Trace Fossils and Correlation of Precambrian-Cambrian Boumdary Beds, Cassiar Mountains, North-central British Columbia; *Geological Survey of Canada*, Paper 83-13.

Fyles, J.T. (1990): Geology of the Greewood - Grand Forks Area, British Columbia; *B.C. Ministry of Energy, Mines and Petroleum Resources,* Open File 1990-25.

Gabrielse, H. (1963): McDame Map Area, Cassiar District, British Columbia; *Geological Survey of Canada*, Memoir 319, 138 pages.

Gabrielse, H. (1969): Geology of the Jennings River Map Area, British Columbia; *Geological Survey of Canada*, Paper 68-55, 37 pages.

Gabrielse, H. (1980): Operation Finlay; *in* Current Research, Part A, *Geological Survey of Canada*, Paper 80-1A, page 348.

Gabrielse, H. (1985). Major Dextral Transcurrent Displacements Along the Northern Rocky Mountain Trench and Related Lineaments in North-central British Columbia; *Geological Society of America*, Bulletin, Volume 96, pages 1-14.

Gabrielse, H. and Harms, T.A. (1989). Permian and Devonian Plutonic Rocks in the Sylvester Allochthon, Cry Lake and McDame Map Areas, Northern British Columbia; *in* Current Research, Part E, *Geological Survey of Canada*, Paper 89-1E, pages 1-4.

Gabrielse, H., Harms, T.A., Mortensen, J.K., Nelson, J.L. and Parrish, R. (in preparation): Late Paleozoic Plutons in the Sylvester Allochthon, North-central British Columbia; *in* Age Determinations and Geologic Studies, *Geological Survey of Canada.*

Garcia, M.O. (1978): Criteria for the Identification of Ancient Volcanic Arcs; *Earth-Science Reviews*, Volume 14, pages 147-195.

Gehrig, M., Lentz, H. and Franck, E.U. (1979): Thermodynamic Properties of Water - Carbon Dioxide - Sodium Chloride Mixtures at High Temperatures and Pressures; *in* High-Pressure Science and Technology, Volume 1: Physical Properties and Material Synthesis, Timmerhaus, K.D. and Barber, M.S., Editors, *Plenum Press.*

Gibson, D.W. (1975): Triassic Rocks of the Rocky Mountain Foothills and Front Ranges of Northeastern B.C. and West-central Alberta; *Geological Survey of Canada*, Bulletin 247, 61 pages.

Goldfarb, R.J., Leach, D.L., Pickthorn, W.J. and Paterson, C.J. (1988): Origin of Lode-gold Deposits of the Juneau Belt, Southeastern Alaska; *Geology*, Volume 16, pages 440-443.

Gordey, S.P. (1981): Stratigraphy, Structure and Tectonic Evolution of Southern Pelly Mountains in the Indigo Lake Area, Yukon Territory; *Geological Survey of Canada*, Bulletin 318, 44 pages.

Gordey, S.P. (1983): Thrust Faults in the Anvil Range and a New Look at the Anvil Range Group, South-central Yukon; *in* Current Research, Part A, *Geological Survey of Canada*, Paper 1983-1A, pages 225-227.

Gordey, S.P. (1988): Devono-Mississippian Clastic Sedimentation and Tectonism in the Canadian Cordilleran Miogeocline; *in* Devonian of the World, McMillan, N.J., Embry, A.F. and Glass, D.J., Editors, *Proceedings of the Second International Symposium on the Devonian System*, Calgary, Canada, Volume II, pages 1-14.

Gordey, S.P. (1990): Geology and Mineral Potential, Tiny Island Lake Map Area, Yukon; *in* Current Research Part E; *Geological Survey of Canada*, Paper 1990-1E, pages 23-30.

Gordey, S.P. and Irwin, S.E.B. (1987): Geology of Sheldon Lake (105J) and Tay River (105K) Map Areas, Yukon Territory; *Geological Survey of Canada*, Map 19-1987.

Gordey, S.P., Wood, D. and Anderson, R.G. (1981): Stratigraphic Framework of Southeastern Selwyn Basin, Nahanni Map Area, Yukon Territory and District of MacKenzie, *in* Current Research, Part A, *Geological Survey of Canada*, Paper 81-1A, pages 395-398.

Gordey, S.P., Abbott, J.G., Tempelman-Kluit, D.J. and Gabrielse, H. (1986): "Antler" Clastics in the Canadian Cordillera; *Geology*, Volume 15, pages 103-107.

Gordey, S.P., Gabrielse, H. and Orchard, M.J. (1982): Stratigraphy and Structure of Sylvester Allochthon, Southwest McDame Map Area, Northern British Columbia; *in* Current Research, Part B, *Geological Survey of Canada*, Paper 82-1B, pages 101-106.

Gower, S.J., Clark, A.H. and Hodgson, C.J. (1985): Tungsten-Molybdenum Skarn and Stockwork Mineralization, Mount Reed - Mount Haskin District, Northern British Columbia, Canada; *Canadian Journal of Earth Sciences*, Volume 22, pages 728-747.

Grant, D.R. (1981): A Study of the Sulfide Mineralogy and Geology of the McDame Gold Camp, Cassiar, B.C.; unpublished B.Sc. thesis, *The University of British Columbia*, 77 pages.

Gunning, M.H. (1988): Gold Distribution in the Taurus Mine Quartz Veins; *in* Exploration in British Columbia 1987, Part B, *B.C. Ministry of Energy, Mines and Petroleum Resources*, pages B95-B105.

Hall-Beyer, B. (1976): Geochemistry of Some Ocean-floor Basalts for British Columbia; unpublished M.Sc. thesis, *University of Alberta*, Edmonton, 105 pages.

Hansen, V.L. (1987): Structural, Metamorphic and Geochronologic Evolution of the Teslin Suture Zone, Yukon: Evidence for Mesozoic Oblique Convergence Outboard of the Northern Canadian Cordillera; unpublished Ph.D. thesis, *University of California*, Los Angeles, 221 pages.

Hansen, V.L. (1988): A Model for Terrane Accretion: Yukon-Tanana and Slide Mountain Terranes, Northwest North America; *Tectonics*, Volume 7, pages 1167-1177.

Hansen, V.L. (1989): Structural and Kinematic Evolution of the Teslin Suture Zone, Yukon: Record of an Ancient Transpressional Margin; *Journal of Structural Geology*, Volume 11, pages 717-733.

Harms, T.A. (1985): Pre-emplacement Thrust Faulting in the Sylvester Allochthon, Northeast Cry Lake Map Area, British Columbia; *in* Current Research, Part A, *Geological Survey of Canada*, Paper 1985-1, pages 301-304.

Harms, T.A. (1986): Structural and Tectonic Analysis of the Sylvester Allochthon, SW McDame Map Area, Northern British Columbia: Implications for Paleogeography and Accretion; unpublished Ph.D. thesis, *University of Arizona*.

Harms, T.A., Ball, M., Fischer, P. and Nelson, J. (1989): Geology of the Needlepoint Mountain Map Area, NTS 104P/4 (NE1/4); *B.C. Ministry of Energy, Mines and Petroleum Resources*, Open File 1989-19, 1 sheet.

Harrison, T.M. and McDougall, I. (1980): Investigations of an Intrusive Contact, Northwest Nelson, New Zealand – II. Diffusion of Radiogenic and Excess ^{40}Ar in Hornblende Revealed by $^{40}Ar/^{39}Ar$ Age Spectrum Analysis; *Geochemica Cosmochemica Acta*, Volume 44, pages 2005-2020.

Harrison, T.M. and McDougall, I. (1982): The Thermal Significance of Potassium Feldspar K-Ar Ages Inferred from $^{40}Ar/^{39}Ar$ Age Spectrum Results; *Geochemica Cosmochimica Acta*, Volume 46, pages 1811-1820.

Harwood, D.S., Yount, J.C. and Seiders, V.M. (1991): Upper Devonian and Lower Mississippian Island-arc and Back-arc Deposits in the Northern Sierra Nevada, California; *in* Paleozoic Paleogeography of the Western United States, Cooper, J.D. and Stevens, C.H., Editors, *Society of Economic Paleontologists and Mineralogists*, Pacific Section, Volume 67, pages 717-733.

Hollister, L.S. (1981): Information Intrinsically Available from Fluid Inclusions; *in* Short Course in Fluid Inclusions: Applications to Petrology, Hollister, L.S. and Crawford, M.L., Editors, *Mineralogical Association of Canada*, Calgary, May 1981. pages 1-9.

Hooper, D. (1984): A Study of the Gold-Quartz Veins at Erickson Gold Camp, Cassiar, North-central British Columbia, unpublished B.Sc. thesis, *The University of British Columbia*, 96 pages.

Johannes, W. (1969): An Experimental Investigation of the System $MgO-SiO_2-H_2O-CO_2$; *American Journal of Science*, Volume 267, pages 1083-1104.

Jones, D.L., Coney, P.J., Harms, T.A. and Dillon, J.T. (1988): Interpretive Geologic Map and Supporting Radiolarian Data from the Angayucham Terrane, Coldfoot Area, Southern Brooks Range, Alaska; *United States Geological Survey*, Miscellaneous Field Studies Map, MF-1993.

Karson, J. and Dewey, J. (1978): Coastal Complex, Western Newfoundland: An Early Ordovician Oceanic Fracture Zone; *Geological Society of America*, Bulletin, Volume 89, pages 1037-1049.

Klepacki, D.W. (1983): Stratigraphic and Structural Relations of the Milford, Kaslo and Slocan Groups, Roseberry Quadrangle, Lardeau Map Area, British Columbia; *in* Current Research, Part A, *Geological Survey of Canada*, Paper 1983-1A, pages 229-233.

Klepacki, D.W. and Wheeler, J.O. (1985): Stratigraphic and Structural Relations of the Milford, Kaslo and Slocan Groups, Lardeau and Nelson Map Areas, British Columbia; *in* Current Researeh, Part A, *Geological Survey of Canada*, Paper 85-1A, pages 277-286.

Lagabrielle, Y. and Cannat, M., (1990): Alpine Jurassic Ophiolites Resemble the Modern Central Atlantic Basement; *Geology*, Volume 18, pages 319-322.

Leiteh, C.H.B. and Godwin, C.I. (1988): Isotopic Ages, Wallrock Chemistry and Fluid Inclusion Data from the Bralorne Gold Vein Deposit (92J/15W); *in* Geological Fieldwork 1987, *B.C. Ministry of Energy, Mines and Petroleum Resources*, Paper 1988-1, pages 301-324.

Lemoine, M., Tricart, P. and Boillot, G. (1987): Ultramafic and Gabbroic Ocean Floor of the Ligurian Tethys: In Search of a Genetic Model; *Geology*, Volume 15, pages 622-625.

Liou, J.G., Maruyama, S. and Cho, M. (1985): Phase Equilibria and Mineral Parageneses of Metabasites in Low-grade Metamorphism, *Mineralogical Magazine*, Volume 49, pages 321-333.

Little, H.W. (1960): Nelson Map Area, West Half, British Columbia; *Geological Survey of Canada*, Memoir 308.

Lowey, G.W. and Lowey, J.F. (1986): Geology of Spencer Creek (105B/1) and Daughney Lake (105B/2) Map Areas, Rancheria District, Southeast Yukon; *Indian and Northern Affairs Canada*, Yukon Region, Open File 1986-1.

Lyn, I. (1983): Cassiar Pit Geology; unpublished 1:6000 scale map; *Brinco Mining Ltd.*

Mäder, U.K. (1987): The Aley Carbonatite Complex, Northern Rocky Mountains, British Columbia; *in* Geological Fieldwork 1986, *B.C. Ministry of Energy, Mines and Petroleum Resources*, Paper 1987-1, pages 283-288.

Mansy, J.L. (1978): Stratigraphy and Structure of Proterozoic Rocks Near Good Hope Lake, McDame Map-Area, British Columbia; *in* Current Research, Part A, *Geological Survey of Canada*, Paper 78-1A, pages 5-6.

Mansy, J.L and Gabrielse, H. (1978): Stratigraphy, Terminology and Correlation of Upper Proterozoic Rocks in Omineca and Cassiar Mountains, North-central British Columbia, *Geological Survey of Canada*, Paper 77-19.

McClay, K.L. (1986): Mapping Geological Structures: Short Course Number 2; *Geological Association of Canada*, Cordilleran Section, 194 pages.

McClay, K.L. and Insley, M.W. (1986): Structure and Mineralization of the Driftpile Creek Area, Northeastern British Columbia; *in* Geological Fieldwork 1985, *B.C. Ministry of Energy, Mines and Petroleum Resources*, Paper 1986-1, pages 343-350.

McHaig, A.M. (1988): Deep Fluid Circulation in Fault Zones; *Geology*, Volume 16, pages 867-870.

MacIntyre, D.G. (1983): Geology and Stratiform Barite-Sulphide Deposits of the Gataga District, Northeast British Columbia; *Mineralogical Association of Canada*, Short Course in Sediment-hosted Stratiform Lead-Zinc Deposits, Victoria, May 1983, pages 85-116.

Meschede, M. (1986): A Method of Discriminating Between Different Types of Mid-ocean Ridge Basalts and Continental Tholeiites With the Nb-Zr-Y Diagram; *Chemical Geology*, Volume 56, pages 207-218.

Mevel, C., Caby, R. and Kienast, J-R. (1978): Amphibolite Facies Conditions in the Oceanic Crust: Example of Amphibolitized Flaser Gabbro and Amphibolites from the Chenaillet Ophiolite Massif (Hautes Alps, France); *Earth and Planetary Science Letters*, Volume 39, pages 98-108.

Miller, M.M. (1987): Dispersed Remnants of a Northeast Pacific Fringing Arc: Upper Paleozoic Terranes of Permian McCloud Affinity, Western U.S.; *Tectonics*, Volume 6, pages 803-830.

Miller, M.M. and Cui, B. (1989): Submarine-fan Characteristics and Dual Sediment Provenance, Lower Carboniferous Bragdon Formation, Eastern Klamath Terrane, California; *Canadian Journal of Earth Sciences*, Volume 26, pages 927-940.

Miller, E.L., Holdsworth, B.K., Whiteford, W.B. and Rodgers, D. (1984): Stratigraphy and Structure of the Shoonover Sequence, Northeastern Nevada: Implications for Paleozoic Plate-margin Tectonics; *Geological Society of America*, Bulletin, Volume 95, pages 1063-1076.

Monger, J.W.H. (1973): Upper Paleozoic Rocks of the Western Canadian Cordillera; *Geological Survey of Canada*, Paper 73-1A, pages 27-28.

Monger, J.W.H. (1977): Upper Paleozoic Rocks of the Western Canadian Cordillera and their Bearing on Cordilleran Evolution; *Canadian Journal of Earth Sciences*, Volume 14, pages 1832-1859.

Monger, J.W.H. and Berg, H.C. (1984): Lithotectonic Terrane Map of Western Canada and Southeastern Alaska; *in* Lithotectonic Terrane Maps of the North American Cordillera, Silberling, N.J. and Jones, D.L., Editors, *United States Geological Survey*, Open File Report 84-523, pages B1-B31.

Mortensen, J.K. (1982): Geologic Setting and Tectonic Significance of Mississippian Felsic Metavolcanic Rocks in the Pelly Mountains, Southeastern Yukon Territory; *Canadian Journal of Earth Sciences*, Volume 19, pages 8-22.

Mortensen, J.K. (in press): Pre-mid-Mesozoic Tectonic Evolution of the Yukon-Tanana Terrane, Yukon and Alaska; *Tectonics*.

Mortensen, J.K. and Jilson, G.A. (1985): Evolution of the Yukon-Tanana Terrane: Evidence from Southeastern Yukon Territory; *Geology*, Volume 13, pages 806-810.

Mortensen, J.K., Montgomery, J.R. and Fillipone, J. (1987): U-Pb Zircon, Monazite, and Sphene Ages for Granitic Orthogneiss of the Barkerville Terrane, East-central British Columbia; *Canadian Journal of Earth Sciences*, Volume 24, pages 1261-1266.

Mullen, E.D. (1983): $MnO_2/TiO_2/P_2O_5$: A Minor Element Discriminant for Basaltic Rocks of Oceanic Environments and its Implications for Petrogenesis; *Earth and Planetary Science Letters*, Volume 62, pages 53-62.

Murphy, D.C. (1988): Geology of the Gravel Creek (105B/10) and Irvine Lake (105B/11) Map Area, Southeastern Ynkon; *Indian and Northern Affairs Canada*, Yukon Region, Open File 1988-1, 61 pages.

Nakamura, N. (1974): Determination of REE, Ba, Mg, Na and K in Carbonaceous and Ordinary Chondrites; *Geochimica and Cosmochimica Acta*, Volume 38, pages 757-775.

Nelson, J.L. (1989): The McDame Asbestos Orebody: Development Progress and New Geological Interpretations; *in* Exploration in British Columbia 1988, Part B, *B.C. Ministry of Energy, Mines and Petroleum Resources*, pages B173-B176.

Nelson, J.L. (1990): The Blue Dome Fault: The Evolution of a Transform Structure into a Thrust Fault in the Sylvester Allochthon, Cassiar Mountains, British Columbia; *in* Geological Fieldwork 1989, *B.C. Ministry of Energy, Mines and Petroleum Resources*, Paper 1990-1, pages 217-222.

Nelson, J. and Bradford, J. (1987a): Geology of the Area Around the Midway Deposit, Northern British Columbia (104O/16); *in* Geological Fieldwork 1986, *B.C. Ministry of Energy, Mines and Petroleum Resources*, Paper 1987-1, pages 181-192

Nelson, J.L. and Bradford, J.A. (1987b): Geology of the Midway Area, Northern British Columbia (104O/16); *B.C. Ministry of Energy, Mines and Petroleum Resources*, Open File 1987-5.

Nelson, J.L. and Bradford, J.A. (1989): Geology and Mineral Deposits of the Cassiar and McDame Map Areas, British Columbia (104P/3, 5), *in* Geological Fieldwork 1988, *B.C. Ministry of Energy, Mines and Petroleum Resources*, Paper 1989-1, pages 323-338.

Nelson, J.L. and MacIntyre, D.G. (1988): Metallogeny of Northeastern British Columbia; *Geoscience Canada*, Volume 15, Number 2, pages 113-116.

Nelson, J.L., Bradford, J.A., Green, K.C. and Marsden, H. (1988a): Geology and Patterns of Mineralization, Blue Dome Map Area (104P/12); *in* Geological Fieldwork 1987, *B.C. Ministry of Energy, Mines and Petroleum Resources*, Paper 1988-1, pages 233-243.

Nelson, J., Harms, T., Bradford, J., Green, K.C. and Marsden, H. (1988b): Geology of the Blue Dome Map Area, 104P/12; *B.C. Ministry of Energy, Mines and Petroleum Resources*, Open File 1988-10.

Nelson, J.L., Bradford, J.A., MacLean, M. and Maddison, L. (1989): Geology and Metallogeny of the Cassiar and McDame Map Areas (104P/5, 104P/3 NW 1/4); *B.C. Ministry of Energy, Mines and Petroleum Resources*, Open File 1989-9.

Nelson, J.L., Hora, D. and Harvey-Kelley, F. (1990a): A New Rhodonite Occurrence in the Cassiar Area, Northern British Columbia; *in* Geological Fieldwork 1989, Paper 1990-1, *B.C. Ministry of Energy, Mines and Petroleum Resources*, pages 347-351.

Nelson, J.L., Knight, J., McTaggart, K. and Blyth, H. (1990b): Widespread Glacial Dispersal of Placer Gold from Erickson Camp, Cassiar Mountains, British Columbia (104P); *in* Exploration in British Columbia 1989, Part B, *B.C. Ministry of Energy, Mines and Petroleum Resources*, pages 229-236.

Nesbitt, B.E., Murowchick, J.B. and Muehlenbachs, K. (1985): Dual Origins of Lode Gold Deposits in the Canadian Cordillera; *Geology*, Volume 14, pages 506-509.

Nicholas, A., Boudier, F. and Bouchez, J-L. (1980): Interpretation of Peridotite Structures from Ophiolitic and Oceanic Environments; *American Journal of Science*, Volume 280-A, pages 192-210.

O'Hanley, D.S. (1988): The Origin of Alpine-Peridotite Hosted, Chrysotile Asbestos Deposits; *Economic Geology*, Volume 83, pages 256-265.

O'Hanley, D.S. (1990): The Structural Geology of the Mount McDame Area, North-central British Columbia; *in* Geological Fieldwork 1989, *B.C. Ministry of Energy, Mines and Petroleum Resources*, Paper 1990-1, pages 223-228.

O'Hanley, D.S., Kyser, T.K. and Wicks, F.J. (1989): Evidence from Lizardite/Chrysotile Serpentinites for D Exchange Without Recrystallization; *Geological Society of America*, Programs with Abstracts, Volume 21, Number 6, page A12.

O'Hanley, D.S., Schandl, E. and Wicks, F.J. (in preparation): Pressure and Temperature Estimates for Serpentine Recrystallization at Cassiar, British Columbia, Based on $^{18}O/^{16}O$ Serpentine-Magnetite Thermometry and Fluid Inclusions in Rodingite Minerals.

Okulitch, A.V. (1985): Paleozoic Plutonism in Southeastern British Columbia; *Canadian Journal of Earth Sciences*, Volume 22, pages 1409-1424.

Orchard, M.J. and Irwin, S. (1988): Conodont Biostratigraphy, Midway Property, Northern British Columbia; *in* Geological Fieldwork 1987, *B.C. Ministry of Energy, Mines and Petroleum Resources*, Paper 1988-1, pages 249-254.

Pantaleyev, A. (1980): Cassiar Map-area; *in* Geological Fieldwork 1979, *B.C. Ministry of Energy, Mines and Petroleum Resources*, Paper 1980-1, pages 51-60.

Panteleyev, A. and Diakow, L.J. (1982): Cassiar Gold Deposits, McDame Map Area (104P/4, 5); *in* Geological Fieldwork 1981, *B.C. Ministry of Energy, Mines and Petroleum Resources*, Paper 1982-1, pages 156-161.

Patton, W.W. and Box, S.E. (1989): Tectonic Setting of the Yukon-Koyukuk Basin and its Borderlands, Western Alaska; *Journal of Geophysical Research*, Volume 94, B11, pages 15807-15820.

Pearce, J.A. (1982): Trace Element Characteristics of Lavas from Destructive Plate Boundaries; *in* Andesites, Thorpe, R.S., Editor, *John Wiley and Sons*, pages 525-548.

Pearce, J.A. and Cann, J.R. (1973): Tectonic Setting of Basic Volcanic Rocks Determined Using Trace Element Analyses; *Earth and Planetary Science Letters*, Volume 19, pages 290-300.

Pell, J. (1989): The Kechika Yttrium - Rare Earth Prospect, Cassiar Mountains, Northern British Columbia; *Geological Association of Canada*, Program with Abstracts, Volume 14, page A2.

Pinsent, R.H. and Hirst, D.M. (1977): The Metamorphism of the Blue River Ultramafic Body, Cassiar, British Columbia; *Journal of Petrology*, Volume 18, pages 567-594.

Plumb, W.N. (1989): The Making of a Mine: The Early Days of Cassiar; *Mining Review*, September-October 1989, pages 43-49.

Poole, W.H. (1957): Wolf Lake, Yukon Territory; *Geological Survey of Canada*, Map 22-1957.

Pope, M.C. (1989a): Depositional Environment of the Lower Cambrian Rosella Formation, Cassiar Mountains, North-central British Columbia; *Geological Society of America*, Abstracts with Programs, Volume 21, page 129.

Pope, M.C. (1989b): Depositional Environments and Tectonic Setting of the Lower Cambrian Rosella Formation, Cassiar Mountains, North-central British Columbia; unpublished M.Sc. thesis, *University of Montana*, 99 pages.

Potter, R.W., Babcock, R.S. and Brown, D.L. (1977): A New Method for Determining the Solubility of Salts in Aqueous Solutions at Elevated Temperatures; *United States Geological Survey*, Journal of Research, Volume 5, pages 389-395.

Read, P.B. and Okulitch, A.V. (1977): The Triassic Unconformity of South-central British Columbia; *Canadian Journal of Earth Sciences*, Volume 14, pages 606-638.

Rees, C.J. (1987): The Intermontane-Omineca Belt Boundary in the Quesnel Lake Area, East-central British Columbia: Tectonic Implications Based on Geology, Structure and Paleomagnetism; unpublished Ph.D. thesis, *Carleton University*, 409.

Rees, C.J. and Ferri, F. (1983): A Kinematic Study of Mylonitic Rocks in the Omineca-Intermontane Belt Tectonic Boundary in East-central British Columbia; *in* Current Research, Part B, *Geological Survey of Canada*, Paper 83-1B, pages 121-125.

Roback, R. and Walker, N.W. (1989): Stratigraphic Relationships in Late Paleozoic to Middle Mesozoic Rocks of Quesnellia, Northeast Washington and Southeast British Columbia; *Geological Society of America*, Abstracts With Programs, Volume 21, page 134.

Roedder, E. (1985): Fluid Inclusions; *Mineralogical Society of America*, Reviews in Mineralogy, Volume 12.

Roeder, D. and Mull, C.G. (1978): Tectonics of Brooks Range Ophiolites, Alaska; *The American Association of Petroleum Geologists*, Bulletin, Volume 62, pages 1697-1702.

Ross, C. (1969): Upper Paleozoic Fusilinacea: *Eowaeringella* and *Wedekindellina* from Yukon Territory and Giant *Parafusilina* from British Columbia; *in* Contributions to Canadian Paleontology, *Geological Survey of Canada*, Bulletin 182, pages 129-133.

Saleeby, J. (1984): Tectonic Significance of Serpentinite Mobility and Ophiolitic Mélange; *Geological Society of America*, Special Paper 198, pages 153-168.

Saunders, A.D., Tarney, J., March, N.G. and Wood, D.A. (1980): Ophiolites as Ocean Crust or Marginal Basin Crust: A Geochemical Approach; *in* Proceedings of the International Ophiolite Symposium, Cyprus, 1979, *Cyprus Geological Survey Department*, pages 193-204.

Schiarizza, P. and Preto, V.A. (1987): Geology of the Adams Plateau - Clearwater - Vavenby Area; *B.C. Ministry of Energy, Mines and Petroleum Resources*, Paper 1987-2, 88 pages.

Schwartz, M.O. (1989): Determining Phase Volumes of Mixed CO_2-H_2O Inclusions Using Microthermometric Measurements; *Mineralium Deposita*, Volume 24, pages 43-47.

Shervais, J. (1982): Ti-V Plots and the Petrogenesis of Modern and Ophiolitic Lavas; *Earth and Planetary Science Letters*, Volume 59, pages 101-118.

Sibson, R.H., Robert, F., Poulsen, K. and Howard, K.H. (1988): High Angle Reverse Faults, Fluid-Pressure Cycling, and Mesothermal Gold Deposits; *Geology*, Volume 16, pages 551-555.

Sinclair, W.D. (1986): Early Tertiary Topaz Rhyolites and Associated Mineral Deposits in the Northern Canadian Cordillera: Products of Anorogenic Magmatism; *Geological Association of Canada - Mineralogical Association of Canada*, Program with Abstracts, Volume 11, pages 127-128.

Sketchley, D.A. (1986): The Nature of Carbonate Alteration in Basalt at Erickson Gold Mine, Cassiar, North-central British Columbia; unpublished M.Sc. thesis, *The University of British Columbia*, 272 pages.

Sketchley, D.A. and Sinclair, A.J. (1987): Multi-element Lithogeochemistry of Alteration Associated with Qold-Quartz Veins of the Erickson Mine, Cassiar District (104P/4); *in* Geological Fieldwork 1986, *B.C. Ministry of Energy, Mines and Petroleum Resources,* Paper 1987-1, pages 57-64.

Sketchley, D.A., Sinclair, A.J. and Godwin, C.I. (1986): Early Cretaceous Gold-Silver Mineralization in the Sylvester Allochthon, near Cassiar, North Central British Columbia; *Canadian Journal of Earth Sciences*, Volume 23, pages 1455-1458.

Smith, R.B. (1979): Geology of the Harper Ranch Group (Carboniferous-Permian) and Nicola Group (Upper Triassic) Northeast of Kamloops, British Columbia; unpublished M.Sc. thesis, *The University of British Columbia*, 202 pages.

Smitheringale, W.V. (1957): The Mine of Cassiar Asbestos Corporation, Limited, Cassiar, B.C.; *in* The Geology of Canadian Industrial Mineral Deposits, *6th Commonwealth Mining and Metallurgical Congress*, pages 49-53.

Struik, L.C. (1986): Imbricated Terranes of the Cariboo Gold Belt with Correlations and Implications for Tectonics in Southeastern British Columbia; *Canadian Journal of Earth Sciences*, Volume 23, pages 1047-1061.

Struik, L.C. (1988): Structural Geology of the Cariboo Gold Mining District, East-central British Columbia; *Geological Survey of Canada*, Memoir 421, 100 pages.

Struik, L.C. and Orchard, M.J. (1985): Late Paleozoic Conodonts from Ribbon Chert Delineate Imbricare Thrusts Within the Antler Formation of the Slide Mountain Terrane, Central British Columbia; *Geology*, Volume. 13, pages 794-798.

Sun, S.S., Nesbitt, R.W. and Sharaskin, A.Y. (1979): Geochemical Characteristics of Mid-ocean Ridge Basalts; *Earth and Planetary Science Letters*, Volume 44, pages 119-138.

Tempelman-Kluit, D.J. (1972): Geology and Origin of the Faro, Vangorda and Swim Concordant Zinc-Lead Deposits, Central Yukon Territory; *Geological Survey of Canada*, Bulletin 208, 73 pages.

Tempelman-Kluit, D.J. (1979a): Transported Cataclasite, Ophiolite, and Granodiorite in Yukon: Evidence of Arc-Continent Collision; *Geological Survey of Canada*, Paper 79-14.

Tempelman-Kluit, D.J. (1979b): Five Occurrences of Transported Synorogenic Clastic Rocks in Yukon Territory; *in* Current Research, Part A, *Geological Survey of Canada*, Paper 1979-1A, pages 1-12.

Tempelman-Kluit, D.J., Gordey, S.P. and Read, B.C. (1976): Stratigraphic and Structural Studies in the Pelly Mountains, Yukon Territory; *in* Report of Activities, Part A, *Geological Survey of Canada*, Paper 76-1A, pages 97-106.

Turner, R.J.W. and Abbott, G. (1990): Regional Setting, Structure and Zonation of the Marg Volcanogenic Massive Sulphide Deposit, Yukon; *in* Current Research, Part E, *Geological Survey of Canada*, Paper 90-1E, pages 31-41.

Turner, R.J.W., Madrid, R.J. and Miller, E.L. (1989): Roberts Mountains Allochthon: Stratigraphic Comparison with Lower Paleozoic Outer Continental Margin Strata of the Northern Canadian Cordillera; *Geology*, Volume 17, pages 341-344.

Turner, R.J.W. and Rhodes, D. (1990): Boundary Creek Zinc Deposit (NIDD Property), MacMillan Pass, Yukon: Subseafloor Sediment-hosted Mineralization Associated with Volcanism along a Late Devonian Syndepositional Fault; *in* Current Research, Part E, *Geological Survey of Canada*, Paper 1990-1E pages 321-336.

Wei, M. (1982): Geology of the Glen Hope Property, Cassiar, British Columbia; unpublished B.Sc. thesis, *The University of British Columbia*, 35 pages.

Weir, R.H., Jr. and Kerrick, D.M. (1987): Mineralogic, Fluid Inclusion and Stable Isotopic Studies of Several Gold Mines in the Mother Lode, Tuolumne and Mariposa Counties, California; *Economic Geology*, Volume 82, pages 328-344.

Wheeler, J.O., Brookfield, A.J., Gabrielse, H., Monger, J.W.H., Tipper, H.W. and Woodsworth, G.J. (1988): Terrane Map of the Canadian Cordillera; *Geological Survey of Canada*, Open File 1894.

Winchester, J.A. and Floyd, P.A. (1976): Geochemical Magma Type Discrimination: Application to Altered and Metamorphosed Basic Igneous Rocks; *Earth and Planetary Science Letters*, Volume 28, pages 459-469.

Wolfe, W.J. (1965): The Blue River Ultramafic Intrusion, Cassiar District, British Columbia; *Geological Survey of Canada*, Paper 64-48, 15 pages.

APPENDIX 1

DESCRIPTIONS OF CONODONT COLLECTIONS, EXCERPTED FROM THE CORDILLERAN CONODONT DATA FILE

by M.J. Orchard, Geological Survey of Canada

MAP No. (Table 2, Figure 2): 1 **FIELD No.:** 86JB34-01-01
GSC LOC. No.: C-143630 **NTS:** 104O/16
COLLECTOR: J. Nelson/J. Bradford
LOCALITY INFO.: Lat., Long.: 59°57′03″, 130°15′24″
UTM: 429797.2E, 6646410N
MICROFOSSILS: conodonts **CAI:** 5
Conodont taxa:
Gnathodus bilineatus (Roundy) (2)
Gnathodus girtyi Hass (2)
Idioprioniodus sp. (2)
Lochriea commutata (Branson & Mehl) (1)
ramiform elements (3)
AGE: Early Carboniferous (late Mississippian); late Visean - early Namurian

MAP No. (Table 2, Figure 2): 2 **FIELD No.:** 86JB17-18-01
GSC LOC. No.: C-143629 **NTS:** 104O/16
COLLECTOR: J. Nelson/J. Bradford
LOCALITY INFO.: Lat., Long.: 59°55′38″, 130°16′57″
UTM: 428301.3E, 6643798N
MICROFOSSILS: conodonts, ichthyoliths **CAI:** 5
Conodont taxa:
Bispathodus? sp. (2)
cavusgnathoid (1)
ramiform elements (3)
AGE: Early? Carboniferous (Mississippian)

MAP No. (Table 2, Figure 2): 3 **FIELD No.:** 86JB15-01-01
GSC LOC. No.: C-143625 **NTS:** 104O/16
COLLECTOR: J. Nelson/J. Bradford
LOCALITY INFO.: Lat., Long.: 59°57′04″, 130°15′28″
UTM: 429735.4E, 6646439N
MICROFOSSILS: conodonts, ichthyoliths **CAI:** 5-5.5
Conodont taxa:
Bispathodus sp. (15)
Gnathodus? sp. (2)
'Hindeodella' segaformis Bischoff (2)
Polygnathus sp. (1)
Pseudopolygnathus sp. (2)
ramiform elements (70+)
AGE: Early Carboniferous (Mississippian); late Tournaisian

MAP No. (Table 2, Figure 2): 4 **FIELD No.:** 86JB13-07-01
GSC LOC. No.: C-143632 **NTS:** 104O/16
COLLECTOR: J. Nelson/J. Bradford
LOCALITY INFO.: Lat., Long.: 59°59′29″, 130°19′20″
UTM: 426223.8E, 6650982N
MICROFOSSILS: conodonts, ostracodes **CAI:** 5
Conodont taxa:
Bispathodus sp. (1)
'Hindeodella' segaformis Bischoff (2)
Polygnathus sp. (4)
ramiform elements (4)
AGE: Early Carboniferous (Mississippian); late Tournaisian

MAP No. (Table 2, Figure 2): 5 **FIELD No.:** 86TH02-06-01
GSC LOC. No.: C-117623 **NTS:** 104O/16
COLLECTOR: J. Nelson/T.A. Harms
LOCALITY INFO.: Lat., Long.: 59°53′49″, 130°18′30″
UTM: 426791.2E, 6640456N
MICROFOSSILS: conodonts **CAI:** 5
Conodont taxa:
Bispathodus ex gr. stabilis (Branson & Mehl)
ramiform element (1)
AGE: Late Devonian - Early Carboniferous (Mississippian); Famennian-Visean

MAP No. (Table 2, Figure 2): 6 **FIELD No.:** 86KG21-02-01
GSC LOC. No.: C-143637 **NTS:** 104O/16
COLLECTOR: J. Nelson/K. Green
LOCALITY INFO.: Lat., Long.: 59°54′11″, 130°14′41″
UTM: 430370.3E, 6641072N
MICROFOSSILS: conodonts **CAI:** 5
Conodont taxa:
Bispathodus sp. (2)
'Hindeodella' segaformis Bischoff (9)
Polygnathus communis Branson & Mehl (2)
Gnathodus sp. (1)
ramiform elements (10)
AGE: Early Carboniferous (Mississippian); late Tournaisian

MAP No. (Table 2, Figure 2): 7 **FIELD No.:** 86JN22-19-01
GSC LOC. No.: C-117561 **NTS:** 104O/16
COLLECTOR: J. Nelson
LOCALITY INFO.: Lat., Long.: 59°51′32″, 130°15′03″
UTM: 429938.9E, 6636176N
MICROFOSSILS: conodonts, ichthyoliths **CAI:** 5
Conodont taxa:
Bispathodus stabilis (Branson & Mehl) (15)
Gnathodus sp. cf. *G. fexanus* Roundy (2)
Gnathodus pseudosemiglaber Thompson & Fellows (4)
Idioprioniodus sp. (12)
Polygnathus communis Branson & Mehl (1)
Polygnathus sp. (1)
Mestognathus praebeckmanni von Bitter, Sandberg & Orchard (1)
Protognathodus sp. (2)
Eotaphrus sp. (1)
ramiform elements (15)
AGE: Early Carboniferous (Mississippian); late Tournaisian

MAP No. (Table 2, Figure 2): 8 **FIELD No.:** 86JN03-06-01A
GSC LOC. No.: C-143101 **NTS:** 104O/16
COLLECTOR: J. Nelson
LOCALITY INFO.: Lat., Long.: 59°50′04″, 130°19′36″
UTM: 425635.3E, 6633501N
MICROFOSSILS: conodonts **CAI:** 5
Conodont taxa:
Icriodus sp. (3)
Palmatolepis cf. P. transitans Muller (1)
Palmatolepis sp. (2)
Polygnathus sp. (1)
ramiform elements (20)
AGE: Late Devonian; Frasnian

MAP No. (Table 2, Figure 2): 9 **FIELD No.:** 86JN05-08
GSC LOC. No.: C-143102 **NTS:** 104O/16
COLLECTOR: J. Nelson
LOCALITY INFO.: Lat., Long.: 59°59′09″, 130°10′31″
UTM: 434413.1E, 6650210N
MICROFOSSILS: conodonts **CAI:** 5
Conodont taxa:
Gnathodus spp. (15)
Palmatolepis sp. (1)
Polygnathus communis Branson & Mehl (5)
Polygnathus spp. (2)
Pseudopolygnathus sp. (1)
Siphonodella spp. (10)
ramiform elements (18)
AGE: Early Carboniferous (Mississippian); early-middle Tournaisian

MAP No. (Table 2, Figure 2): 10 **FIELD No.:** 86JN22-04-01
GSC LOC. No.: C-143106 **NTS:** 104O/16
COLLECTOR: J. Nelson
LOCALITY INFO.: Lat., Long.: 59°51′28″, 130°17′11″
UTM: 427938.2E, 6636059N
MICROFOSSILS: conodonts **CAI:** 5
Conodont taxa:
Bispathodus stabilis (Branson & Mehl) (30)
Clydagnathus sp. (2)
Geniculatus n. sp. A (4)
Gnathodus spp. (7)
Polygnathus sp. (1)
Siphonodella sp. (1)
ramiform elements (50)
AGE: Early Carboniferous (Mississippian); late? Tournaisian

MAP No. (Table 2, Figure 2): 11 **FIELD No.:** 82MJO-BVH2
GSC LOC. No.: C-087737 **NTS:** 104O/16
COLLECTOR: B. Hall
LOCALITY INFO.: Lat., Long.: 59°59′, 130°14′
UTM: 9
MICROFOSSILS: conodonts **CAI:** 6
Conodont taxa:
Gnathodus punctatus (Cooper) (2)
Polygnathus communis Branson & Mehl (5)
Kladognathus? sp.
ramiform elements
AGE: Early Carboniferous (Mississippian); Tournaisian

MAP No. (Table 2, Figure 2): 12 **FIELD No.:** 82MW-82003I
GSC LOC. No.: C-102871 **NTS:** 104O/16
COLLECTOR: D. MacIntyre
LOCALITY INFO.: Lat., Long.: 59°56′45″, 130°19′55″
UTM: 425380E, 6644290N
MICROFOSSILS: conodonts **CAI:** 5
Conodont taxa:
gnathodid? indet. (1)
ramiform element fragments (13)
AGE: Late Devonian - Early Carboniferous (Mississippian); Famennian-Visean

MAP No. (Table 2, Figure 2): 13 **FIELD No.:** 84GAH-235F
GSC LOC. No.: C-116407 **NTS:** 104O/16
COLLECTOR: T. Harms
LOCALITY INFO.: Lat., Long.: 59°54′, 130°20′
UTM: 9
MICROFOSSILS: Conodonts, ichthyolith, sponge spicules, 'conulariids' **CAI:** 5
Conodont taxa:
Geniculatus n. sp. A (1)
Bispathodus stabilis (Branson & Mehl) (40)
Clydagnathus sp. (3)
Gnathodus sp. indet. (3)
'Hindeodella' segaformis Bischoff (2)
Idioprioniodus sp. (20)
Polygnathus communis Branson & Mehl (3)
P. sp. (2)
Pseudopolygnathus? sp. (1)
ramiform elements (100)
AGE: Early Carboniferous (Mississippian); late Tournaisian

MAP No. (Table 2, Figure 2): 14 **FIELD No.:** 84GAH-238F
GSC LOC. No.: C-116408 **NTS:** 104O/16
COLLECTOR: T.A. Harms
LOCALITY INFO.: Lat., Long.: 59°54′45″, 130°20′00″
UTM: 9
MICROFOSSILS: conodonts **CAI:** 5.5
Conodont taxa:
gnathodids (2)
ramiform elements (12)
AGE: Carboniferous - Early Permian; Visean? - Asselian

MAP No. (Table 2, Figure 2): 15 **FIELD No.:** 84MJO-SV-MTN
GSC LOC. No.: C-118251 **NTS:** 104O/16
COLLECTOR: C.E. Jakobowski
LOCALITY INFO.: Lat., Long.: 59°55′, 130°20′ (approx.)
UTM: 432500E, 6653500N
MICROFOSSILS: conodonts, sphaeromorphs **CAI:** 5-6
Conodont taxa:
Gnathodus? sp.
Hindeodus? sp.
Bispathodus? sp.
ramiform elements
AGE: Late Devonian - Early Carboniferous (Mississippian); late Famennian - early Namurian

MAP No. (Table 2, Figure 2): 16 **FIELD No.:** 84MJO-WJ-84-1
GSC LOC. No.: C-118252 **NTS:** 104O/16
COLLECTOR: C.E. Jakobowski
LOCALITY INFO.: Lat., Long.: 59°55′, 130°20′ (approx.)
UTM: 9
MICROFOSSILS: **CAI:** 5
Conodont taxa:
Idiognathodus sp. (2)
Idiognathoides sp. (30)
Neogondolella sp. cf. *N. Clarki* (Koike) (1)
ramiform elements
AGE: Late Carboniferous (early-middle Pennsylvanian); Bashkirian - Moscovian

MAP No. (Table 2, Figure 2): 17 **FIELD No.:** 84MJO-83-341AC
GSC LOC. No.: C-118253 **NTS:** 104O/16
COLLECTOR: C.E. Jakobowski
LOCALITY INFO.: Lat., Long.: 59°55′, 130°20′ (approx.)
UTM: 425898.15E, 6643965.52N
MICROFOSSILS: conodonts **CAI:** 5
Conodont taxa:
ramiform elements (99)
Palmatolepis sp. cf. *P. regularis* Cooper 1931 (2)
P. glabra acuta Helms 1963
P. glabra glabra Ulrich & Bassler 1926 (1)
P. glabra lepta Ziegler & Huddle 1969 (9)
P. glabra pectinata Ziegler 1962 (16)
P. glabra prima Ziegler & Huddle 1969 (10)
P. klapperi Sandberg & Ziegler 1973 (3)
P. minuta loba Helms 1963 (2)
P. minuta minuta Branson & Mehl 1934 (3)
P. quadrantinodosalobata Sannemann 1955 (1)
P. subperlobata Branson & Mehl 1934 (8)
Polygnathus spp. (2)
AGE: Late Devonian; middle Famennian

MAP No. (Table 2, Figure 2): 18 **FIELD No.:** 84MJO-83-28.2AC
GSC LOC. No.: C-118255 **NTS:** 104O/16
COLLECTOR: C.E. Jakobowski
LOCALITY INFO.: Lat., Long.: 59°55′, 130°20′ (approx.)
UTM: 425740.56E, 6644133.47N
MICROFOSSILS: conodonts, ostracod steinkern, sphaeromorphs **CAI:** 5-6.5
Conodont taxa:
Siphonodella sp. (3)
ramiform elements (5)
AGE: Early Carboniferous (Mississippian); early-middle Tournaisian

MAP No. (Table 2, Figure 2): 19 **FIELD No.:** 84MJO-83-28.1AC
GSC LOC. No.: C-118256 **NTS:** 104O/16
COLLECTOR: C.E. Jakobowski
LOCALITY INFO.: Lat., Long.: 59°55′, 130°20′ (approx.)
UTM: 425740.56E, 6644133.47N
MICROFOSSILS: conodonts **CAI:** 5
Conodont taxa:
Palmatolepis glabra Ulrich & Bassler
P. g. acuta
P. g. lepta Ziegler & Huddle
P. g. pectinata Ziegler
P. sp. cf. *P. regularis* Cooper
P. g. prima Ziegler & Huddle
P. minuta Branson & Mehl
P. quadrantinodosalobata Sannemann
P. aff. rhomboidea Sannemann
P. subperlobata Branson & Mehl
Polygnathus sp.
AGE: Late Devonian; middle Famennian; Upper *crepida* - Lower *rhomboidea* zone

MAP No. (Table 2, Figure 2): 20 **EIELD No.:** 84MJO-82-13
GSC LOC. No.: C-118258 **NTS:** 104O/16
COLLECTOR: C.E. Jakobowski
LOCALITY INFO.: Lat., Long.: 59°55′, 130°20′ (approx.)
UTM: 425707.32E, 6643553.49N
MICROFOSSILS: conodonts **CAI:** 5.5
Conodont taxa:
Siphonodella sp. (1)
ramiform elements (2)
AGE: Early Carboniferous (Mississippian); early-middle Tournaisian

MAP No. (Table 2, Figure 2): 21 **FIELD No.:** 84MJO-EWEN
GSC LOC. No.: C-118275 **NTS:** 104O/16
COLLECTOR: C.E. Jakobowski
LOCALITY INFO.: Lat., Long.: 59°59′, 130°14′
UTM: 433514E 6650875N
MICROFOSSILS: conodonts **CAI:** 6.5
Conodont taxa:
Bispathodus? sp. (1)
Polygnathus communis Branson & Mehl (3)
Siphonodella sp. (2)
ramiform elements (10)
AGE: Early Carboniferous (Mississippian); early-middle Tournaisian

MAP No. (Table 2, Figure 2): 22 **FIELD No.:** 87JN10-1
GSC LOC. No.: C-153811 **NTS:** 104P/12
COLLECTOR: J. Nelson
LOCALITY INFO.: Lat., Long.: 59°41′01.7″, 129°54′52.5″
UTM: 448500E, 6616350N
MICROFOSSILS: conodonts, spicules **CAI:** 5
Conodont taxa:
Bispathodus? sp. (2)
Eotaphrus sp. (1)
Gnathodus cf. G. homopunctatus Ziegler (15)
?'Hindeodella' segaformis Bischoff (2)
Hindeodus sp. (9)
Polygnathus communis Branson & Mehl (2)
ramiform elements (22)
AGE: Early Carboniferous (Mississippian); late Tournaisian

MAP No. (Table 2, Figure 2): 23 **FIELD No.:** 87JN12-1-1
GSC LOC. No.: C-153812 **NTS:** 104P/12
COLLECTOR: J. Nelson
LOCALITY INFO.: Lat., Long.: 59°36′15.7″, 129°54′31.9″
UTM: 448700E, 6607500N
MICROFOSSILS: ?bryozoan, conodonts, corals, gastropod steinkerns **CAI:** 5
Conodont taxa:
Neogondolella cf. *N. inclinata* (Kovacs) (5)
Metapolygnathus sp. (4)
AGE: Middle - Late Triassic; late Ladinian - early Carnian

MAP No. (Table 2, Figure 2): 24 **FIELD No.:** 87JN19-1-1
GSC LOC. No.: C-153815 **NTS:** 104P/12
COLLECTOR: J. Nelson
LOCALITY INFO.: Lat., Long.: 59°35′29.8″, 129°56′06.4″
UTM: 447200E, 6606100N
MICROFOSSILS: conodonts **CAI:** 5-6.5
Conodont taxa:
Hindeodus sp. (2)
Idiognathodus sp. (3)
Neogondolella sp. (90)
Streptognathodus ex gr. *elongatus* Gunnell (5)
ramiform elements (55)
AGE: Pennsylvanian-Permian; Asselian - early Artinskian

MAP No. (Table 2, Figure 2): 25 **FIELD No.:** 87JN39-11
GSC LOC. No.: C-153818 **NTS:** 104P/12
COLLECTOR: J. Nelson
LOCALITY INFO.: Lat., Long.: 59°45′05.8″, 129°58′43.4″
UTM: 445000E, 6623950N
MICROFOSSILS: conodonts, spumellarian radiolarian (1) **CAI:** 5
Conodont taxa:
Rhachistognathus sp. (1)
Gnathodus bilineatus (Roundy) (3)
Gnathodus girtyi Hass (2)
ramiform elements (20)
AGE: Early Carboniferous (late? Mississippian); probably late Visean - early Namurian

MAP No. (Table 2, Figure 2): 26 **FIELD No.:** 87JN26-1
GSC LOC. No.: C-153871 **NTS:** 104P/12
COLLECTOR: J. Nelson
LOCALITY INFO.: Lat., Long.: 59°32′17.0″, 129°49′16.8″
UTM: 453550E, 6600050N
MICROFOSSILS: conodonts **CAI:** 5
Conodont taxa:
?'Hindeodella' segaformis Bischoff (2)
ramiform elements (4)
AGE: Probably Early Carboniferous (Mississippian)

MAP No. (Table 2, Figure 2): 27 **FIELD No.:** 87JB9-8
GSC LOC. No.: C-153834 **NTS:** 104P/12
COLLECTOR: J. Nelson/J. Bradford
LOCALITY INFO.: Lat., Long.: 59°43′24.5″, 129°57′26.8″
UTM: 446150E, 6620800N
MICROFOSSILS: conodonts **CAI:** indet.
Conodont taxa:
Streptognathodus ex gr. *elongatus* Gunnell (2)
ramiform elements (2)
AGE: Pennsylvanian - Early Permian; Gzhelian - early Artinskian

MAP No. (Table 2, Figure 2): 28 **FIELD No.:** 87JB8-9
GSC LOC. No.: C-153869 **NTS:** 104P/12
COLLECTOR: J. Nelson/J. Bradford
LOCALITY INFO.: Lat., Long.: 59°41'47.9", 129°52'39.4"
UTM: 450600E, 6617750N
MICROFOSSILS: conodonts, ostracod **CAI:** 5
Conodont taxa:
Hindeodus sp. (1)
?Bispathodus ex gr. stabilis (Branson & Mehl) (2)
?'Hindeodella' segaformis Bischoff (4)
ramiform elements (21)
AGE: Early Carboniferous (Mississippian); ? late Tournaisian

MAP No. (Table 2, Figure 2): 29 **FIELD No.:** 87KG19-7
GSC LOC. No.: C-153879 **NTS:** 104P/12
COLLECTOR: J. Nelson/K. Green
LOCALITY INFO.: Lat., Long.: 59°33'48.3", 129°55'19.0"
UTM: 447900E, 6602950E
MICROFOSSILS: conodonts, ichthyoliths **CAI:** 5.5-6.5
Conodont taxa:
Adetognathus? sp. (1)
Diplognathodus sp. (1)
Hindeodus sp. (4)
Idiognathodus? sp. (1)
Neogondolella ex gr. *idahoensis* (Youngquist, Hawley & Miller) (34)
Streptognathodus ex gr. *elongatus* Gunnell (1)
Sweetognathus sp. cf. *S. whitei* (Rhodes) (1)
ramiform elements (3)
AGE: Early Permian; early Artinskian

MAP No. (Table 2, Figure 2): 30 **FIELD No.:** 87KG13-5
GSC LOC. No.: C-153821 **NTS:** 104P/12
COLLECTOR: J. Nelson/K. Green
LOCALITY INFO.: Lat., Long.: 59°37'33.6", 129°57'39.2"
UTM: 445800E, 6609950N
MICROFOSSILS: conodonts **CAI:** 4
Conodont taxa:
'Hindeodella' segaformis Bischoff (3)
Polygnathus? sp. (1)
AGE: Early Carboniferous (Mississippian); late Tournaisian

MAP No. (Table 2, Figure 2): 31 **FIELD No.:** 87KG38-7-2
GSC LOC. No.: C-153825 **NTS:** 104P/12
COLLECTOR: J. Nelson/K. Green
LOCALITY INFO.: Lat., Long.: 59°44'22.5", 129°57'50.9"
UTM: 445800E, 6622600N
MICROFOSSILS: conodonts **CAI:** 4.5-5
Conodont taxa:
Gnathodus bilineatus (Roundy) (2)
Idioprioniodus sp. (1)
Vogelgnathus? sp. (1)
ramiform element (1)
AGE: Early Carboniferous (late Mississippian); late Visean - early Namurian

MAP No. (Table 2, Figure 2): 32 **FIELD No.:** 87KG41-10
GSC LOC. No.: C-153829 **NTS:** 104P/12
COLLECTOR: J. Nelson/K. Green
LOCALITY INFO.: Lat., Long.: 59°36'01.9", 129°48'34.5"
UTM: 454300E, 6607000N
MICROFOSSILS: conodonts **CAI:** 5
Conodont taxa:
cavusgnathoid (1)
Bispathodus? ex gr. stabilis (Branson & Mehl) (2)
ramiform elements (10)
AGE: Early Carboniferous (Mississippian)

MAP No. (Table 2, Figure 2): 33 **FIELD No.:** 87HM6-1-2
GSC LOC. No.: C-153861 **NTS:** 104P/13
COLLECTOR: J. Nelson/H. Marsden
LOCALITY INFO.: Lat., Long.: 59°44'57.8", 129°50'42.7"
UTM: 452500E, 6623600N
MICROFOSSILS: conodonts **CAI:** 4-6
Conodont taxa:
Idiognathodus? sp. indet. (4)
Neogondolella sp. indet. (4)
ramiform elements (2)
AGE: Late Carboniferous (Pennsylvanian) - Early Permian

MAP No. (Table 2, Figure 2): 34 **FIELD No.:** 87HM17-4
GSC LOC. No.: C-153881 **NTS:** 104P/12
COLLECTOR: J. Nelson/H. Marsden
LOCALITY INFO.: Lat., Long.: 59°34'31.5", 129°56'23.8"
UTM: 446900E, 6604300N
MICROFOSSILS: conodonts, ichthyoliths **CAI:** 6
Conodont taxa:
Neognathodus? sp. (1)
Streptognathodus? sp. (1)
AGE: Late Carboniferous (Pennsylvanian) - Early Permian

MAP No. (Table 2, Figure 2): 35 **FIELD No.:** 87HM40-4
GSC LOC. No.: C-153889 **NTS:** 104P/12
COLLECTOR: J. Nelson/H. Marsden
LOCALITY INFO.: Lat., Long.: 59°44'34.7", 129°55'43.1"
UTM: 447800E, 6622950N
MICROFOSSILS: conodonts **CAI:** 5
Conodont taxa:
Bispathodus ex gr. stabilis (Branson & Mehl) (5)
Clydagnathus? sp. (1)
Gnathodus sp. (1)
'Hindeodella' segaformis Bischoff (46)
Polygnathus communis Branson & Mehl (5)
ramiform elements (40)
AGE: Early Carboniferous (Mississippian); late Tournaisian

MAP No. (Table 2, Figure 2): 36 **FIELD No.:** 87HM17-1
GSC LOC. No.: C-153880 **NTS:** 104P/12
COLLECTOR: J. Nelson/H. Marsden
LOCALITY INFO.: Lat., Long.: 59°34'21.8", 129°56'17.2"
UTM: 447000E, 6604000N
MICROFOSSILS: conodonts **CAI:** 6-7
Conodont taxa:
Hindeodus sp. (1)
Neogondolella sp. cf. *N. intermedia* Igo (60)
Streptognathodus ex gr. *elongatus* Gunnell (5)
Sweetognathus cf. *S. whitei* Rhodes (1)
ramiform elements (12)
AGE: Early Permian; early Artinskian

MAP No. (Table 2, Figure 2): 37 **FIELD No.:** 87HM6-3
GSC LOC. No.: C-153862 **NTS:** 104P/12
COLLECTOR: J. Nelson/H. Marsden
LOCALITY INFO.: Lat., Long.: 59°44'54.7", 129°50'13.8"
UTM: 452950E, 6623500N
MICROFOSSILS: conodonts **CAI:** 5-7
Conodont taxa:
Gondolella? sp. (1)
Neogondolella sp. (1)
Streptognathodus cf. *S. expansus* (Igo & Koike) (2)
gnathodids indet. (3)
ramiform elements (8)
AGE: Probably Late Carboniferous (Pennsylvanian); ?Bashkirian - Moscovian

MAP No. (Table 2, Figure 2): 38 **FIELD No.:** 87HM20-1
GSC LOC. No.: C-153883 **NTS:** 104P/12
COLLECTOR: J. Nelson/H. Marsden
LOCALITY INFO.: Lat., Long.: 59°32'39.4", 129°53'54.3"
UTM: 449200E, 6600800N
MICROFOSSILS: conodonts **CAI:** 6-7
Conodont taxa:
Neogondolella sp. indet. (5)
AGE: Permian

MAP No. (Table 2, Figure 2): 39 **FIELD No.:** 87HM41-19
GSC LOC. No.: C-153891 **NTS:** 104P/12
COLLECTOR: J. Nelson/H. Marsden
LOCALITY INFO.: Lat., Long.: 59°42'11.6", 129°57'50.3"
UTM: 445750E, 6618550N
MICROFOSSILS: conodonts **CAI:** 5-5.5
Conodont taxa:
Gondolella? sp. (2)
Idiognathodus sp. (3)
Streptognathodus sp. (1)
Neostreptognathodus? sp. (1)
ramiform element (1)
AGE: Late Carboniferous (Pennsylvanian) - Early Permian; Bashkirian - Asselian

MAP No. (Table 2, Figure 2): 40 **FIELD No.:** 87JN4-8
GSC LOC. No.: C-153835 **NTS:** 104P/12
COLLECTOR: J. Nelson
LOCALITY INFO.: Lat., Long.: 59°41'35.5", 129°46'50.6"
UTM: 456050E, 6617300N
MICROFOSSILS: conodonts, spumellarian radiolarians **CAI:** 5
Conodont taxa:
Palmatolepis perlobata aff. *P. p. schindewolfi* Muller (1)
Mehlina? sp. (2)
Polygnathus sp. indet. (1)
ramiform elements (7)
AGE: Late Devonian; middle - late Famennian

MAP No. (Table 2, Figure 2): 41 **FIELD No.:** 87-KG-43-6
GSC LOC. No.: C-153830 **NTS:** 104O/9
COLLECTOR: J. Nelson/K. Green
LOCALITY INFO.: Lat./Long.: 59°41'37.3", 130°05'00"
UTM: Zone 9; 438750E, 6617600N.
MICROFOSSILS: conodonts **CAI:** 6
Conodont taxa:
cavusgnathoid? (1)
ramiform elements (20)
Bispathodus ex. gr. *stabilis* (Branson & Mehl 1934) (12)
Hindeodus? sp. (1)
AGE: Early Carboniferous (Mississippian); Tournaisian - Visean

MAP No. (Table 2, Figure 2): 42 **FIELD No.:** 87JN-KG-43-6
GSC LOC. No.: C-153830 **NTS:** 104O/9
COLLECTOR: J. Nelson/K. Green
LOCALITY INFO.: Lat., Long.: 59°41'37.4", 130°05'17"
UTM: 438750E, 6617600N
MICROFOSSILS: conodonts **CAI:** 6
Conodont taxa:
Bispathodus ex gr. stabilis (Branson & Mehl) (12)
Hindeodus? sp. (1)
cavusgnathoid (1)
ramiform elements (20)
AGE: Early Carboniferous (Mississippian); Tournaisian-Visean

MAP No. (Table 2, Figure 2): 43 **FIELD No.:** 88JN6-4
GSC LOC. No.: C-154420 **NTS:** 104P/5
COLLECTOR: J. Nelson
LOCALITY INFO.: Lat., Long.: 59°23'39.1", 129°50'55.2"
UTM: 451800E, 6584050N
MICROFOSSILS: conodonts **CAI:** 5
Conodont taxa:
Palmatolepis ex. gr. *glabra* Ulrich & Bassler (4)
Palmatolepis minuta Branson & Mehl (2)
Palmatolepis sp. cf. *P. subperlobata* Branson & Mehl (2)
P. sp. cf. *P. delicatula* Branson & Mehl (1)
ramiform element (1)
AGE: Late Devonian; early-middle Famennian

MAP No. (Table 2, Figure 2): 44 **FIELD No.:** 88JN9-12
GSC LOC. No.: C-158760 **NTS:** 104P/5
COLLECTOR: J. Nelson
LOCALITY INFO.: Lat., Long.: 59°18'34.6", 129°38'34.1"
UTM: 463400E, 6574500N
MICROFOSSILS: conodonts **CAI:** 5
Conodont taxa:
Bispathodus? sp. (2)
Hindeodus? sp. (1)
ramiform elements (15)
AGE: Probably Early Carboniferous (Mississippian)

MAP No. (Table 2, Figure 2): 45 **FIELD No.:** 88JN14-8
GSC LOC. No.: C-158752 **NTS:** 104P/5
COLLECTOR: J. Nelson
LOCALITY INFO.: Lat., Long.: 59°15'01.8", 129°46'48.8"
UTM: 455500E, 6568000N
MICROFOSSILS: conodonts, ichthyoliths **CAI:** 5
Conodont taxa:
Bispathodus ex gr. *stabilis* (Branson & Mehl) (4)
Gnathodus sp. (4)
ramiform elements (12)
AGE: Early Carboniferous (Mississippian)

MAP No. (Table 2, Figure 2): 46 **FIELD No.:** 88JN20-6
GSC LOC. No.: C-154447 **NTS:** 104P/5
COLLECTOR: J. Nelson
LOCALITY INFO.: Lat., Long.: 59°22'37.1", 129°38'19.7"
UTM: 463700E, 6582000N
MICROFOSSILS: conodonts **CAI:** 5.5
Conodont taxa:
Polygnathus sp. (2)
ramiform element (1)
AGE: Middle Devonian - Early Carboniferous (Mississippian); Givetian-Tournaisian

MAP No. (Table 2, Figure 2): 47 **FIELD No.:** 88JN44-2
GSC LOC. No.: C-159036 **NTS:** 104P/4
COLLECTOR: J. Nelson
LOCALITY INFO.: Lat., Long.: 59°08'04.8", 129°59'23.0"
UTM: 473360E, 6555260N
MICROFOSSILS: conodonts **CAI:** 5.5-6.5
Conodont taxa:
Idiognathodus sp. (3)
AGE: Late Carboniferous (Pennsylvanian) - Early Permian; Bashkirian - Asselian

MAP No. (Table 2, Figure 2): 48 **FIELD No.:** 88JN44-9
GSC LOC. No.: C-159035 **NTS:** 104P/3
COLLECTOR: J. Nelson
LOCALITY INFO.: Lat., Long.: 59°14'31.5", 129°28'22.2"
UTM: 473025E, 6555900N
MICROFOSSILS: conodonts **CAI:** 5-5.5
Conodont taxa:
Idiognathodus sp. (3)
Streptognathodus? sp. (2)
ramiform elements (10)
AGE: Late Carboniferous (Pennsylvanian)-Early Permian; Bashkirian - Asselian

MAP No. (Table 2, Figure 2): 49 **FIELD No.:** 88MM1-8
GSC LOC. No.: C-154417 **NTS:** 104P/5
COLLECTOR: J. Nelson/ M. McLean
LOCALITY INFO.: Lat., Long.: 59°18'41.1", 129°48'16.0"
UTM: 454200E, 6574800N
MICROFOSSILS: conodonts, ichthyoliths **CAI:** 5
Conodont taxa:
Bispathodus ex gr. *stabilis* (Branson & Mehl) (15)
Clydagnathus? sp. (1)
Gnathodus sp. (1)
Polygnathus sp. (1)
Pseudopolygnathus sp. (1)
ramiform elements (30)
AGE: Early Carboniferous (Mississippian); Tournaisian

MAP No. (Table 2, Figure 2): 50 **FIELD No.:** 88MM7-1A
GSC LOC. No.: C-154406 **NTS:** 104P/5
COLLECTOR: J. Nelson/M. McLean
LOCALITY INFO.: Lat., Long.: 59°18'10.2", 129°33'17.6"
UTM: 468400E, 6573700N
MICROFOSSILS: conodonts **CAI:** 5
Conodont taxa:
Bispathodus stabilis (Branson & Mehl) (14)
Clydagnathus sp. (2)
Dollymae? sp. (1)
Geniculatus? sp. (1)
Gnathodus sp. (2)
Hindeodus? sp. (1)
Polygnathus communis Branson & Mehl (2)
Pseudopolygnathus sp. (1)
ramiform elements (40)
AGE: Early Carboniferous; late? Tournaisian

MAP No. (Table 2, Figure 2): 51 **FIELD No.:** 88MM7-1B
GSC LOC. No.: C-154405 **NTS:** 104P/5
COLLECTOR: J. Nelson/M. McLean
LOCALITY INFO.: Lat., Long.: 59°18'10.2", 129°33'17.6"
UTM: 468400E, 6573700N
MICROFOSSILS: conodonts **CAI:** 5
Conodont taxa:
Bispathodus stabilis (Branson & Mehl) (6)
Clydagnathus? sp. (1)
Gnathodus sp. (2)
Siphonodella sp. (1)
ramiform elements (25)
AGE: Early Carboniferous (Mississippian); early-middle Tournaisian

MAP No. (Table 2, Figure 2): 52 **FIELD No.:** 88MM7-16
GSC LOC. No.: C-154407 **NTS:** 104P/5
COLLECTOR: J. Nelson/M. McLean
LOCALITY INFO.: Lat., Long.: 59°18'13.4", 129°33'24.0"
UTM: 468300E, 6573800N
MICROFOSSILS: conodonts **CAI:** 5
Conodont taxa:
Bispathodus? sp. (2)
Gnathodus sp. (3)
ramiform elements (15)
AGE: Early Carboniferous (Mississippian)

MAP No. (Table 2, Figure 2): 53 **FIELD No.:** 88MM-24-17
GSC LOC. No.: C-154446 **NTS:** 104P
COLLECTOR: J. Nelson/McLean
LOCALITY INFO: Lat./Long.: 59°23'51.4", 129°38'33.7"
UTM: Zone 9; 463500E, 6584300N.
MICROFOSSILS: conodonts, sponge spicules **CAI:** 5
Conodont taxa:
ramiform elements (9)
AGE: Ordovician - Triassic

MAP No. (Table 2, Figure 2): 54 **FIELD No.:** 88MM47-1
GSC LOC. No.: C-159007 **NTS:** 104P/3
COLLECTOR: J. Nelson/M. McLean
LOCALITY INFO.: Lat., Long.: 59°04'18.1", 129°38'05.5"
UTM: 463600E, 6548000N
MICROFOSSILS: conodonts **CAI:** 4.5-6
Conodont taxa:
Hindeodus sp. (2)
Neogondolella sp. (4)
Neostreptognathodus? sp. (2)
ramiform elements (5)
AGE: Early Permian; ?Artinskian

MAP No. (Table 2, Figure 2): 55 **FIELD No.:** 88LM2-1
GSC LOC. No.: C-154416 **NTS:** 104P/5
COLLECTOR: J. Nelson/L. Maddison
LOCALITY INFO.: Lat., Long.: 59°17'13.5", 129°44'34.3"
UTM: 457675E, 6572050N
MICROFOSSILS: conodonts **CAI:** 5
Conodont taxa:
Epigondolella spp. (5)
Neogondolella cf. *N. regale* Mosher (1)
AGE: Late Triassic; middle? Norian

MAP No. (Table 2, Figure 2): 56 **FIELD No.:** 88LM2-2
GSC LOC. No.: C-154415 **NTS:** 104P/5
COLLECTOR: J. Nelson/L. Maddison
LOCALITY INFO.: Lat., Long.: 59°17'19.8", 129°44'58.2"
UTM: 457300E, 6572250N
MICROFOSSILS: conodonts **CAI:** 5
Conodont taxa:
Epigondolella sp. cf. *E. mosheri* Kozur & Mosher (9)
Metapolygnathus sp. (1)
ramiform elements (2)
AGE: Late Triassic; late? Norian

MAP No. (Table 2, Figure 2): 57 **FIELD No.:** 88LM2-7
GSC LOC. No.: C-154411 **NTS:** 104P/5
COLLECTOR: J. Nelson/L. Maddison
LOCALITY INFO.: Lat., Long.: 59°17'30.8", 129°45'58.5"
UTM: 456350E, 6572600N
MICROFOSSILS: conodonts, ichthyoliths, crinoids (in hand specimen) **CAI:** 5
Conodont taxa:
Epigondolella triangularis (Budurov) (120)
Neogondolella sp. (1)
ramiform elements (4)
AGE: Late Triassic; early Norian

MAP No. (Table 2, Figure 2): 58 **FIELD No.:** 88LM2-11
GSC LOC. No.: C-154413 **NTS:** 104P/5
COLLECTOR: J. Nelson/L. Maddison
LOCALITY INFO.: Lat., Long.: 59°17'30.3", 129°47'23.8"
UTM: 455000E, 6572600N
MICROFOSSILS: conodonts **CAI:** 5
Conodont taxa:
Siphonodella sp. (3)
ramiform elements (4)
AGE: Early Carboniferous (Mississippian); early-middle Tournaisian

MAP No. (Table 2, Figure 2): 59 **FIELD No.:** 88LM26-15
GSC LOC. No.: C-158787 **NTS:** 104P/5
COLLECTOR: J. Nelson/L. Maddison
LOCALITY INFO.: Lat., Long.: 59°28'06.0", 129°50'26.3"
UTM: 452360E, 6592300N
MICROFOSSILS: conodonts **CAI:** 6.5-7
Conodont taxa:
'Hindeodella' segaformis? Bischoff (2)
platform indet. (1)
ramiform elements (8)
AGE: Early Carboniferous (Mississippian), ?late Tournaisian

MAP No. (Table 2, Figure 2): 60 **FIELD No.:** 88LM28-13
GSC LOC. No.: C-158785 **NTS:** 104P/5
COLLECTOR: J. Nelson/L. Maddison
LOCALITY INFO.: Lat., Long.: 59°21'59.5", 129°49'19.3"
UTM: 453275E, 6580950N
MICROFOSSILS: conodonts **CAI:** 5
Conodont taxa:
Bispathodus? sp. (2)
ramiform elements (12)
AGE: Probably Early Carboniferous

MAP No. (Table 2, Figure 2): 61 **FIELD No.:** 88LM31-9A
GSC LOC. No.: C-158786 **NTS:** 104P/5
COLLECTOR: J. Nelson/ L. Maddison
LOCALITY INFO.: Lat., Long.: 59°26'59.3", 129°40'03.1"
UTM: 462150E, 6590125N
MICROFOSSILS: conodonts **CAI:** 6
Conodont taxa:
Neogondolella sp. (1)
ramiform elements (3)
AGE: Probably Permian

MAP No. (Table 2, Figure 2): 61 **FIELD No.:** 88LM31-9C
GSC LOC. No.: C-158781 **NTS:** 104P/5
COLLECTOR: J. Nelson/L. Maddison
LOCALITY INFO.: Lat., Long.: 59°27'03.3", 129°40'09.5"
UTM: 462050E, 6590250N
MICROFOSSILS: conodonts **CAI:** 6
Conodont taxa:
Neogondolella sp. (3)
AGE: Probably Permian

MAP No. (Table 2, Figure 2): 61 **FIELD No.:** 88LM31-9F
GSC LOC. No.: C-159211 **NTS:** 104P/5
COLLECTOR: J. Nelson/L. Maddison
LOCALITY INFO.: Lat., Long.: 59°26'48.7", 129°40'13.6"
UTM: 461980E, 6589800N
MICROFOSSILS: conodonts **CAI:** 6-7
Conodont taxa:
Neogondolella sp. (6)
AGE: Permian

MAP No. (Table 2, Figure 2): 61 **FIELD No.:** 88LM31-9G
GSC LOC. No.: C-158779 **NTS:** 104P/5
COLLECTOR: J. Nelson/L. Maddison
LOCALITY INFO.: Lat., Long.: 59°26'50.3", 129°40'14.9"
UTM: 461960E, 6589850N
MICROFOSSILS: conodonts **CAI:** 6.5
Conodont taxa:
Neogondolella sp. (1)
AGE: Probably Permian

MAP No. (Table 2, Figure 2): 62 **FIELD No.:** 88LM43-15
GSC LOC. No.: C-159013 **NTS:** 104P/3
COLLECTOR: J. Nelson/L. Maddison
LOCALITY INFO.: Lat., Long.: 59°14'21.6", 129°29'33.0"
UTM: 471900E, 6566600N
MICROFOSSILS: conodonts **CAI:** 5
Conodont taxa:
'Hindeodella' sp. cf. *H. segaformis* Bischoff (5)
ramiform elements (25)
AGE: Early Carboniferous (Mississippian); probably late Tournaisian

MAP No. (Table 2, Figure 2): 63 **FIELD No.:** 88JB6-7
GSC LOC. No.: C-154403 **NTS:** 104P/5
COLLECTOR: J. Nelson/J. Bradford
LOCALITY INFO.: Lat., Long.: 59°20'46.8", 129°49'11.2"
UTM: 453375E, 6578700N
MICROFOSSILS: conodonts **CAI:** 5
Conodont taxa:
Siphonodella sp. (1)
ramiform element (1)
AGE: Early Carboniferous (Mississippian); early-middle Tournaisian

MAP No. (Table 2, Figure 2): 64 **FIELD No.:** 88JB9-12
GSC LOC. No.: C-158753 **NTS:** 104P/5
COLLECTOR: J. Nelson/J. Bradford
LOCALITY INFO.: Lat., Long.: 59°20'46.7", 129°34'17.1"
UTM: 467500E, 6578550N
MICROFOSSILS: conodonts, ostracodes, sponge spicules **CAI:** 5
Conodont taxa:
Eotaphrus? sp. (1)
gnathodid (1)
ramiform elements (20)
AGE: Early Carboniferous (Mississippian), ?Tournaisian

MAP No. (Table 2, Figure 2): 65 **FIELD No.:** 88JB34-14
GSC LOC. No.: C-158770 **NTS:** 104P/5
COLLECTOR: J. Nelson/J. Bradford
LOCALITY INFO.: Lat., Long.: 59°25'57.3", 129°39'20.0"
UTM: 462810E, 6588200N
MICROFOSSILS: conodonts **CAI:** 6.5-7
Conodont taxa:
Neogondolella sp. (1)
ramiform elements (2)
AGE: Probably Permian

MAP No. (Table 2, Figure 2): 66 **FIELD No.:** 88JB41-17
GSC LOC. No.: C-159017 **NTS:** 104P/3
COLLECTOR: J. Nelson/J. Bradford
LOCALITY INFO.: Lat., Long.: 59°11'41.7", 129°20'25.6"
UTM: 480550E, 6561600N
MICROFOSSILS: conodonts **CAI:** 5.5-7
Conodont taxa:
Diplognathodus sp. (2)
Idiognathodus sp. (4)
Neognathodus? sp. (2)
ramiform elements (8)
AGE: Late Carboniferous (Pennsylvanian); probably Bashkirian - Moscovian

MAP No. (Table 2, Figure 2): 67 **FIELD No.:** 88JB42-9
GSC LOC. No.: C-159015 **NTS:** 104P/3
COLLECTOR: J. Nelson/J. Bradford
LOCALITY INFO.: Lat., Long.: 59°12'15.4", 129°17'23.2"
UTM: 483450E, 6562630N
MICROFOSSILS: conodonts **CAI:** 5
Conodont taxa:
?Bispathodus ex. gr. *stabilis* Branson & Mehl (2)
ramiform elements (12)
AGE: Devonian - Early Carboniferous (Mississippian)

MAP No. (Table 2, Figure 2): 68 **FIELD No.:** 88JB58-10
GSC LOC. No.: C-159047 **NTS:** 104P/5
COLLECTOR: J. Nelson/J. Bradford
LOCALITY INFO.: Lat., Long.: 59°20′19.4″, 129°48′53.7″
UTM: 453640E, 6577850N
MICROFOSSILS: conodonts, ichthyoliths **CAI:** 5
Conodont taxa:
Bispathodus ex gr. *stabilis* (Branson & Mehl) (20)
Gnathodus sp. (2)
ramiform elements (50)
AGE: Early Carboniferous (Mississippian)

MAP No. (Table 2, Figure 2): 69 **FIELD No.:** 88TH01-08
GSC LOC. No.: C-154422 **NTS:** 104P/4
COLLECTOR: J. Nelson/T. Harms
LOCALITY INFO.: Lat., Long.: 59°08′21.8″, 129°33′23.8″
UTM: 468150E, 6555500N
MICROFOSSILS: conodonts **CAI:** 7-8
Conodont taxa:
Idiognathoides? sp. (1)
AGE: Probably Late Carboniferous (Pennsylvanian)

MAP No. (Table 2, Figure 2): 70 **FIELD No.:** 88TH01-09
GSC LOC. No.: C-154423 **NTS:** 104P/4
COLLECTOR: J. Nelson/T. Harms
LOCALITY INFO.: Lat., Long.: 59°08′39.3″, 129°34′33.3″
UTM: 467050E, 6556050N
MICROFOSSILS: conodonts, ichthyoliths **CAI:** 6.5
Conodont taxa:
Declinognathodus sp. (2)
AGE: Late Carboniferous (Pennsylvanian); Bashkirian

MAP No. (Table 2, Figure 2): 71 **FIELD No.:** 88TH2-4-1
GSC LOC. No.: C-154424 **NTS:** 104P/4
COLLECTOR: J. Nelson/T. Harms
LOCALITY INFO.: Lat., Long.: 59°10′06.9″, 129°33′19.2″
UTM: 468250E, 6558750N
MICROFOSSILS: conodonts **CAI:** 6-6.5
Conodont taxa:
Declinognathodus sp. (2)
AGE: Late Carboniferous (Pennsylvanian); Bashkirian

MAP No. (Table 2, Figure 2): 72 **FIELD No.:** 88TH3-4-2
GSC LOC. No.: C-154426 **NTS:** 104P/4
COLLECTOR: J. Nelson/T. Harms
LOCALITY INFO.: Lat., Long.: 59°09′13.1″, 129°35′11.6″
UTM: 466450E, 6557100N
MICROFOSSILS: conodonts, ichthyoliths **CAI:** 5
Conodont taxa:
Hindeodus sp. (1)
Neogondolella sp. cf. *N. serrata* Clark & Ethington (2)
AGE: Late? Permian; ?Wordian

MAP No. (Table 2, Figure 2): 73 **FIELD No.:** 88TH09-08
GSC LOC. No.: C-154427 **NTS:** 104P/4
COLLECTOR: J. Nelson/T. Harms
LOCALITY INFO.: Lat., Long.: 59°08′27.7″, 129°43′24.7″
UTM: 458600E, 6555775N
MICROFOSSILS: conodonts **CAI:** 5
Conodont taxa:
Palmatolepis gracilis sigmoidalis Ziegler (1)
Pseudopolygnathus sp. (2)
ramiform elements (6)
AGE: Late Devonian; late Famennian

MAP No. (Table 2, Figure 2): 74 **FIELD No.:** 88TH11-01
GSC LOC. No.: C-154429 **NTS:** 104P/4
COLLECTOR: J. Nelson/T. Harms
LOCALITY INFO.: Lat., Long.: 59°12′47.2″, 129°34′40.6″
UTM: 467000E, 6563720N
MICROFOSSILS: conodonts **CAI:** 5
Conodont taxa:
Epigondolella quadrata Orchard (2)
E. triangularis (Budurov) (3)
E. sp. indet. (5)
ramiform element (1)
AGE: Late Triassic; early Norian

MAP No. (Table 2, Figure 2): 75 **FIELD No.:** 81GGAS-2A1
GSC LOC. No.: C-087675 **NTS:** 104P/3
COLLECTOR: S.P. Gordey
LOCALITY INFO.: Lat., Long.: 59°12′18″, 129°18′12″
MICROFOSSILS: conodonts **CAI:** 5
Conodont taxa:
Bispathodus ex. gr. *stabilis* Branson & Mehl (3)
Idioprianriodus sp. (1)
AGE: Early Carboniferous (Mississippian); Tournaisian-Visean

MAP No. (Table 2, Figure 2): 76 **FIELD No.:** 81GGAS-5B1
GSC LOC. No.: C-087682 **NTS:** 104P/3
COLLECTOR: S.P. Gordey
LOCALITY INFO.: Lat., Long.: 59°12′12″, 129°24′12″
MICROFOSSILS: conodonts **CAI:** 5
Conodont taxa:
Neogondolella sp. cf. *N. intermedia* Igo (10)
ramiform elements (10)
AGE: Early Permian; Artinskian

MAP No. (Table 2, Figure 2): 77 **FIELD No.:** 81GGAS-8B2
GSC LOC. No.: C-087678 **NTS:** 104P/3
COLLECTOR: S.P. Gordey
LOCALITY INFO.: Lat., Long.: 59°09′, 129°25′48″
MICROFOSSILS: conodonts, foraminifera, fusulinids **CAI:** 4?-5
Conodont taxa:
Neogondolella sp. (9)
ramiform elements (2)
AGE: Late? Permian

MAP No. (Table 2, Figure 2): 78 **FIELD No.:** 81GGAS-13A1
GSC LOC. No.: C-087679 **NTS:** 104P/3
COLLECTOR: S.P. Gordey
LOCALITY INFO.: Lat., Long.: 59°08′06″, 129°28′12″
MICROFOSSILS: conodonts **CAI:** 6-7
Conodont taxa:
Neogondolella sp. (8)
ramiform element (1)
AGE: Permian; Artinskian - Guadalupian

MAP No. (Table 2, Figure 2): 79 **FIELD No.:** 81GGAS-13A2
GSC LOC. No.: C-087680 **NTS:** 104P/3
COLLECTOR: S.P. Gordey
LOCALITY INFO.: Lat., Long.: 59°08′06″, 129°27′42″
MICROFOSSILS: conodonts **CAI:** 6-7
Conodont taxa:
Neogondolella sp. (6)
ramiform element (1)
AGE: Permian; late Artinskian - Guadalupian

MAP No. (Table 2, Figure 2): 80 **FIELD No.:** 81GGAS-13A3
GSC LOC. No.: C-101995 **NTS:** 104P/3
COLLECTOR: S.P. Gordey
LOCALITY INFO.: Lat., Long.: 59°08′06″, 129°27′42″
MICROFOSSILS: conodonts **CAI:** 6
Conodont taxa:
Neogondolella sp. indet. (1)
AGE: Permian

MAP No. (Table 2, Figure 2): 81 **FIELD No.:** 81GGAS-15E1
GSC LOC. No.: C-087676 **NTS:** 104P/4
COLLECTOR: S.P. Gordey
LOCALITY INFO.: Lat., Long.: 59°10′30″, 129°36′12″
MICROFOSSILS: conodonts **CAI:** 5-6
Conodont taxa:
ramiform elements (8)
Idiognathoides sp. (2)
Neognathodus sp. cf. *N. symmetricus* (Lane) (13)
AGE: Late Carboniferous (Pennsylvanian); late Namurian - Bashkirian

MAP No. (Table 2, Figure 2): 82 **FIELD No.:** 81GGAS-18D1
GSC LOC. No.: C-087677 **NTS:** 104P/3
COLLECTOR: S.P. Gordey
LOCALITY INFO.: Lat., Long.: 59°08′12″, 129°29′00″
MICROFOSSILS: conodonts **CAI:** 5.5-7
Conodont taxa:
ramiform elements (20)
Idiognathodus delicatus Gunnell (30)
Neogandolella clarki (Keike) (6)
Idiognathoides sp. (6)
Diplognathodus? sp. (1)
Neognathodus sp. cf. *N. medadultimus* Merrill (9)
Gondolalla laevis (Kosenko & Kozitskaya) (2)
Streptognathodus? sp. (4)
AGE: Late Carboniferous (Pennsylvanian); late Namurian - Moscovian

MAP No. (Table 2, Figure 2): 83 **FIELD No.:** 82DY-2248
GSC LOC. No.: C-081700 **NTS:** 104P/4
COLLECTOR: K.M. Dawson
LOCALITY INFO.: Lat., Long.: 59°14′, 129°47′
MICROFOSSILS: conodonts **CAI:** 5
Conodont taxa:
ramiforms (60)
'Bispathodus' ex. gr. *stabilis* (Branson & Mehl) (10)
Hindeodus sp. (1)
AGE: Early Carboniferous (Mississippian)

MAP No. (Table 2, Figure 2): 84 **FIELD No.:** 82DY-2249
GSC LOC. No.: C-102619 **NTS:** 104P/4
COLLECTOR: K.M. Dawson
LOCALITY INFO.: Lat., Long.: 59°14′, 129°47′
MICROFOSSILS: conodonts **CAI:** 5
Conodont taxa:
'Bispathodus' ex. gr. *stabilis* (Branson & Mehl) (5)
ramiform elements (70)
AGE: Early Carboniferous (Mississippian)

MAP No. (Table 2, Figure 2): 85 **FIELD No.:** CDY2819
GSC LOC. No.: C-103507 **NTS:** 104P/4
COLLECTOR: K.M. Dawson
LOCALITY INFO.: Lat., Long.: 59°14′, 129°47′
MICROFOSSILS: conodonts **CAI:** 5
Conodont taxa:
Polygnathus communis Branson & Mehl (1)
'Bispathodus' ex. gr. *stabilis* (Branson and Mehl) (15)
Doliognathus sp. (1)
ramiform elements (40)
AGE: Early Carboniferous (Mississippian); Tournaisian

MAP No. (Table 2, Figure 2): 86 **FIELD No.:** CDY2820
GSC LOC. No.: C-103508 **NTS:** 104P/4
COLLECTOR: K.M. Dawson
LOCALITY INFO.: Lat., Long.: 59°14′, 129°37′
MICROFOSSILS: conodonts **CAI:** 5
Conodont taxa:
Polygnathus sp. (1)
'Bispathodus' ex. gr. *stabilis* (Branson & Mehl) (8)
?'Hindeodella' segaformis Bischoff
ramiform elements (40)
AGE: Early Carboniferous (Mississippian); late? Tournaisian

MAP No. (Table 2, Figure 2): 87 **FIELD No.:** CDY2821
GSC LOC. No.: C-103509 **NTS:** 104P/4
COLLECTOR: K.M. Dawson
LOCALITY INFO.: Lat., Long.: 59°14′, 129°47′
MICROFOSSILS: conodonts **CAI:** 5
Conodont taxa:
Grathodus sp. cf. *G. homopunctatus* Ziegler (1)
'Bispathodus' ex. gr. *stabilis* (Branson & Mehl) (13)
Polygnathus communis Branson & Mehl (3)
P. sp. indet. (2)
ramiform elements (40)
AGE: Early Carboniferous (Mississippian); Tournaisian

MAP No. (Table 2, Figure 2): 88 **FIELD No.:** CDY2581
GSC LOC. No.: C-103518 **NTS:** 104P/4
COLLECTOR: K.M. Dawson
LOCALITY INFO.: Lat., Long.: 59°12′57″, 129°38′
MICROFOSSILS: conodonts **CAI:** 5
Conodont taxa:
Epigondolella serrulata Orchard (20)
Neogondolella sp. (4)
ramiform elements (35)
AGE: Late Triassic; late middle Norian

MAP No. (Table 2, Figure 2): 89 **FIELD No.:** 83MJO-P83-62F
GSC LOC. No.: C-103665 **NTS:** 104P/5
COLLECTOR: J.F. Psutka
LOCALITY INFO.: Lat., Long.: 59°16′03″, 129°40′20″
MICROFOSSILS: conodonts **CAI:** 5-6
Conodont taxa:
Idiognathoides? sp. (2)
ramiform elements (2)
AGE: Late? Carboniferous (Pennsylvanian)

MAP No. (Table 2, Figure 2): 90 **FIELD No.:** 83MJO-P83-63F
GSC LOC. No.: C-103666 **NTS:** 104P/5
COLLECTOR: J.F. Psutka
LOCALITY INFO.: Lat., Long.: 59°15′55″, 129°39′55″
MICROFOSSILS: conodonts **CAI:** 6-7
Conodont taxa:
Idiognathoides sp. (1)
ramiform elements (5)
AGE: Late Carboniferous (Pennsylvanian)

MAP No. (Table 2, Figure 2): 91 **FIELD No.:** 84GA-SYL1
GSC LOC. No.: C-116151 **NTS:** 104P/12
COLLECTOR: Brinco Mines
LOCALITY INFO.: Lat., Long.: 59°31′, 129°48′
MICROFOSSILS: conodonts, ichthyoliths, organic fragments **CAI:** 4.5
Conodont taxa:
Metapolygnathus ex. gr. *polygnathiformis* (Budurov & Stefanov) (1)
AGE: Late Triassic; early? Carnian

MAP No. (Table 2, Figure 2): 92 **FIELD No.:** 84GAH-213F
GSC LOC. No.: C-116401 **NTS:** 104P/5
COLLECTOR: T. Harms
LOCALITY INFO.: Lat., Long.: 59°19′15″, 129°48′15″
MICROFOSSILS: conodonts **CAI:** 5
Conodont taxa:
'Hindeodella' segaformis Bischoff (1)
Gnathodus sp. indet. (2)
Bispathodus ex. gr. *stabilis* (Branson & Mehl) (35)
Polygnathus sp. indet. (3)
Siphonodella? sp. indet. (1)
ramiform elements (100)
AGE: Early Carboniferous (Mississippian); late Tournaisian

MAP No. (Table 2, Figure 2): 93 **FIELD No.:** 84GAH-229F
GSC LOC. No.: C-116406 **NTS:** 104P/5
COLLECTOR: T. Harms
LOCALITY INFO.: Lat., Long.: 59°19′30″, 129°48′45″
MICROFOSSILS: conodonts **CAI:** 5
Conodont taxa:
'Hindeodella' segaformis Bischoff (1)
Bispathodus ex. gr. *stabilis* (Branson & Mehl) (5)
Polygnathus communis Branson & Mehl (2)
ramiform elements (50)
AGE: Early Carboniferous (Mississippian); late Tournaisian

MAP No. (Table 2, Figure 2): 94 **FIELD No.:** 85GAH-215R
GSC LOC. No.: C-149998 **NTS:** 104P/5
COLLECTOR: T. Harms
LOCALITY INFO.: Lat., Long.: 59°19′15″, 129°48′15″
MICROFOSSILS: conodonts **CAI:** 5-6
Conodont taxa:
Gondolella sp. cf. *G. laevis* Kosenko & Kozitskaya (1)
ramiform elements (5)
AGE: Late Carboniferous (Pennsylvanian); ?Bashkirian - Moscovian

MAP No. (Table 2, Figure 2): 103 **FIELD No.:** 88JB12-3
GSC LOC. No.: C-158754 **NTS:** 104P/5
COLLECTOR: J. Nelson/J. Bradford
LOCALITY INFO.: Lat., Long.: 59°20′51.2″, 129°35′49.0″
UTM: 466050E, 6578700N
MICROFOSSILS: conodonts **CAI:** 5.5
Conodont taxa:
platform element (1)
ramiform elements (6)
AGE: Probably Devonian - Permian

MAP No. (Table 2, Figure 2): 104 **FIELD No.:** 88JB40-8
GSC LOC. No.: C-158796 **NTS:** 104P/3
COLLECTOR: J. Nelson/J. Bradford
LOCALITY INFO.: Lat., Long.: 59°11′57.1″, 129°20′17.6″
UTM: 480680E, 6562075N
MICROFOSSILS: conodonts **CAI:** 5.5
Conodont taxa:
Neogondolella sp. (10)
ramiform elements (4)
AGE: Permian

MAP No. (Table 2, Figure 2): 105 **FIELD No.:** 88JB41-19
GSC LOC. No.: C-159018 **NTS:** 104P/3
COLLECTOR: J. Nelson/J. Bradford
LOCALITY INFO.: Lat., Long.: 59°11′37.7″, 129°20′17.7″
UTM: 480675E, 6561475N
MICROFOSSILS: conodonts, sponge spicules **CAI:** 5.5
Conodont taxa:
Neogondolella sp. (6)
ramiform element (1)
AGE: Permian

MAP No. (Table 2, Figure 2): 106 **FIELD No.:** 88JB42-10
GSC LOC. No.: C-159016 **NTS:** 104P/3
COLLECTOR: J. Nelson/J. Bradford
LOCALITY INFO.: Lat., Long.: 59°12′20.6″, 129°17′21.7″
UTM: 483475E, 6562790N
MICROFOSSILS: conodonts **CAI:** 6
Conodont taxa:
Gondolella ex gr. *laevis* Kosenkof & Kozitskaya (3)
Idiognathodus? sp. (1)
ramiform elements (2)
AGE: Late Carboniferous (Pennsylvanian); Bashkirian - Moscovian

MAP No. (Table 2, Figure 2): 107 **FIELD No.:** 88JB48-4
GSC LOC. No.: C-159029 **NTS:** 104P/3
COLLECTOR: J. Nelson/J. Bradford
LOCALITY INFO.: Lat., Long.: 59°13′56.0″, 129°28′03.7″
UTM: 473310E, 6565800N
MICROFOSSILS: conodonts **CAI:** 6-7
Conodont taxa:
Neogondolella sp. (3)
ramiform elements (4)
AGE: Permian

MAP No. (Table 2, Figure 2): 108 **FIELD No.:** 88JB50-11
GSC LOC. No.: C-159028 **NTS:** 104P/3
COLLECTOR: J. Nelson/J. Bradford
LOCALITY INFO.: Lat., Long.: 59°12′51.0″, 129°28′31.8″
UTM: 472850E, 6563790N
MICROFOSSILS: conodonts **CAI:** 6-7
Conodont taxa:
Neogondolella intermedia Igo (15)
ramiform elements (8)
AGE: Early Permian; probably Artinskian

MAP No. (Table 2, Figure 2): 109 **FIELD No.:** 88JN4-10
GSC LOC. No.: C-154408 **NTS:** 104P/5
COLLECTOR: J. Nelson
LOCALITY INFO.: Lat., Long.: 59°17′53.0″, 129°39′11.3″
UTM: 462800E, 6573220N
MICROFOSSILS: conodonts **CAI:** 7
Conodont taxa:
Neogondolella sp. (1)
ramiform element (1)
AGE: Probably Permian

MAP No. (Table 2, Figure 2): 110 **FIELD No.:** 88LM1-9
GSC LOC. No.: C-154414 **NTS:** 104P/5
COLLECTOR: J. Nelson/L. Maddison
LOCALITY INFO.: Lat., Long.: 59°17′57.6″, 129°47′49.7″
UTM: 454600E, 6573450N
MICROFOSSILS: conodonts **CAI:** 5
Conodont taxa:
Bispathodus? sp. (2)
'Hindeodella' cf. *H. segaformis* Bischoff (1)
ramiform elements (12)
AGE: Early Carboniferous (Mississippian)

MAP No. (Table 2, Figure 2): 111 **FIELD No.:** 88LM28-4
GSC LOC. No.: C-159048 **NTS:** 104P/5
COLLECTOR: J. Nelson/L. Maddison
LOCALITY INFO.: Lat., Long.: 59°22′20.2″, 129°48′05.3″
UTM: 454450E, 6581580N
MICROFOSSILS: conodonts **CAI:** 5
Conodont taxa:
Gnathodus bilineatus (Roundy) (2)
Gnathodus girtyi Hass (6)
Idioprioniodus sp. (15)
Lochriea commutata (Branson & Mehl) (1)
ramiform elements (15)
AGE: Early Carboniferous (Mississippian); late Visean - early Namurian

MAP No. (Table 2, Figure 2): 112 **FIELD No.:** 88LM35-7
GSC LOC. No.: C-158797 **NTS:** 104A/11
COLLECTOR: J. Nelson/L. Maddison
LOCALITY INFO.: Lat., Long.: 59°30'19.1", 129°17'26.9"
UTM: 482100E, 6262150N
MICROFOSSILS: conodonts **CAI:** 6
Conodont taxa:
Streptognathodus ex. gr. *elongatus* Gunnell (2)
ramiform elements (2)
AGE: Late Carboniferous (Pennsylvanian) - Early Permian; probably Gzhelian - Artinskian

MAP No. (Table 2, Figure 2): 113 **FIELD No.:** 88LM42-12
GSC LOC. No.: C-159011 **NTS:** 104P/3
COLLECTOR: J. Nelson/L. Maddison
LOCALITY INFO.: Lat., Long.: 59°13'57.5", 129°28'54.8"
UTM: 472500E, 6565850N
MICROFOSSILS: conodonts **CAI:** 6-7
Conodont taxa:
Neogondolella sp. (4)
ramiform elements (3)
AGE: Permian

MAP No. (Table 2, Figure 2): 114 **FIELD No.:** 88LM45-2
GSC LOC. No.: C-159014 **NTS:** 104P/3
COLLECTOR: J. Nelson/L. Maddison
LOCALITY INFO.: Lat., Long.: 59°14'30.0", 129°28'01.7"
UTM: 473350E, 6566850N
MICROFOSSILS: conodonts **CAI:** 5
Conodont taxa:
Geniculatus n. sp. A. (1)
Bispathodus? sp. (2)
'Hindeodella' segaformis Bischoff (40)
Polygnathus sp. (1)
ramiform elements (10)
AGE: Early Carboniferous (Mississippian); late Tournaisian

MAP No. (Table 2, Figure 2): 115 **FIELD No.:** 88MM12-6
GSC LOC. No.: C-158759 **NTS:** 104P/5
COLLECTOR: J. Nelson/M. McLean
LOCALITY INFO.: Lat., Long.: 59°21'46.4", 129°34'37.1"
UTM: 467200E, 6580400N
MICROFOSSILS: conodonts **CAI:** 4.5
Conodont taxa:
'Hindeodella' cf. *H. segaformis* Bischoff (2)
ramiform elements (4)
AGE: Early Carboniferous (Mississippian); ?late Tournaisian

MAP No. (Table 2, Figure 2): 116 **FIELD No.:** 88MM24-12
GSC LOC. No.: C-159210 **NTS:** 104P/5
COLLECTOR: J. Nelson/M. McLean
LOCALITY INFO.: Lat., Long.: 59°24'28.7", 129°38'06.0"
UTM: 463950E, 6585450N
MICROFOSSILS: conodonts **CAI:** 5.5-6.5
Conodont taxa:
Idiognathodus sp. (3)
Streptognathodus ex. gr. *elongatus* Gunnell (3)
ramiform elements (4)
AGE: Late Carboniferous (Pennsylvanian) - Early Permian; Gzhelian - Asselian

MAP No. (Table 2, Figure 2): 117 **FIELD No.:** 88MM36-5
GSC LOC. No.: C-158795 **NTS:** 104P/5
COLLECTOR: J. Nelson/McLean
LOCALITY INFO.: Lat., Long.: 59°25'37.1", 129°41'39.8"
UTM: 460600E, 6587600N
MICROFOSSILS: conodonts **CAI:** 6
Conodont taxa:
Streptognathodus ex. gr. *elongatus* Gunnell (1)
AGE: Late Carboniferous (Pennsylvanian)-Early Permian; probably Gzhelian - early Artinskian

MAP No. (Table 2, Figure 2): 118 **FIELD No.:** 88MM36-7
GSC LOC. No.: C-158765 **NTS:** 104P/4
COLLECTOR: J. Nelson/M. McLean
LOCALITY INFO.: Lat., Long.: 59°25'33.9", 129°41'33.4"
UTM: 460700E, 6587500N
MICROFOSSILS: conodonts **CAI:** 5
Conodont taxa:
Neogondolella sp. (1)
AGE: Probably Permian, possibly Triassic

MAP No. (Table 2, Figure 2): 119 **FIELD No.:** 88JN53-01
GSC LOC. No.: C-159203 **NTS:** 104O/16
COLLECTOR: J. Nelson/L. Maddison
LOCALITY INFO.: UTM: 429500E, 6640400N
MICROFOSSILS: conodonts **CAI:** 5-5.5
Conodont taxa:
Neogondolella sp. (15)
ramiform elements (3)
AGE: Late? Permian

MAP No. (Table 2, Figure 2): 121 **FIELD No.:** 89JN-87KG-38-8
GSC LOC. No.: C-159220 **NTS:** 104P/12
COLLECTOR: J. Nelson/K. Green
LOCALITY INFO.: UTM: 445910E, 6622680N
MICROFOSSILS: conodonts **CAI:** 6.5-7
Conodont taxa:
Neogondolella sp. (3)
Streptognathodus ex. gr. *elongatus* Gunnell (1)
ramiform elements (2)
AGE: Early Permian; Asselian - early Artinskian

MAP No. (Table 2, Figure 2): 126 **FIELD No.:** 89JN-87JB-10-3
GSC LOC. No.: C-159217 **NTS:** 104P/12
COLLECTOR: J. Nelson/J. Bradford
LOCALITY INFO.: UTM: 447770E, 6622840N
MICROFOSSILS: conodonts **CAI:** 5
Conodont taxa:
Neogondolella sp. (10)
Streptognathodus sp. (1)
AGE: Late Carboniferous - Early Permian; probably Asselian - Sakmarian

MAP No. (Table 2, Figure 2): 127 **FIELD No.:** 89JN-87JB-10-4
GSC LOC. No.: C-159218 **NTS:** 104P/12
COLLECTOR: J. Nelson/J. Bradford
LOCALITY INFO.: UTM: 448460E, 6622900N
MICROFOSSILS: conodonts **CAI:** 5
Conodont taxa:
Gnathodus cf. *bilineatus* (Roundy) (1)
Gnathodus cf. *girtyi* Hass (6)
ramiform elements (50)
AGE: Early Carboniferous; late Visean - early Namurian

MAP No. (Table 2, Figure 2): 128 **FIELD No.:** 89JN-87KG-38-10
GSC LOC. No.: C-159221 **NTS:** 104P/12
COLLECTOR: J. Nelson/K. Green
LOCALITY INFO.: UTM: 446080E, 6623090N
MICROFOSSILS: conodonts, spumellarian radiolarians (1) **CAI:** 5
Conodont taxa:
Gnathodus bilineatus (Roundy) (3)
Gnathodus girtyi Hass (22)
Vogelgnathus campbelli Rexroad (3)
Rhachistognathus prolixus Baesemann & Lane (4)
Lochriea commutata (Branson & Mehl) (5)
Lochriea homopunctatus (4)
Polygnathus sp. (1)
ramiform elements (75)
AGE: Early Carboniferous; late Visean - early Namurian

MAP No. (Table 2, Figure 2): 129 **FIELD No.:** 89JN-87KG-7-1
GSC LOC. No.: C-159223 **NTS:** 104P/12
COLLECTOR: J. Nelson/K. Green
LOCALITY INFO.: UTM: 449170E, 6623340N
MICROFOSSILS: conodonts **CAI:** 5
Conodont taxa:
Idioprioniodus? sp. (3)
AGE: Carboniferous?

MAP No. (Table 2, Figure 2): 130 **FIELD No.:** 89JN-DS089-004
GSC LOC. No.: C-153839 **NTS:** 104O
COLLECTOR: J. Nelson/J. Nelson
LOCALITY INFO.: UTM: 453345E, 6576712N
MICROFOSSILS: conodonts **CAI:** 5
Conodont taxa:
Neogondolella sp. (3)
ramiform elements (8)
AGE: Probably Permian

MAP No. (Table 2, Figure 2): 131 **FIELD No.:** 89JN-87HM-40-10
GSC LOC. No.: C-159219 **NTS:** 104P/12
COLLECTOR: J. Nelson/H. Marsden
LOCALITY INFO.: UTM: 446140E, 6622300N
MICROFOSSILS: conodonts **CAI:** 6-7
Conodont taxa:
Streptognathodus sp.
Neogondolella sp. (1)
ramiform elements (2)
AGE: Late Carboniferous - Early Permian; Bashkirian - early Artinskian

MAP No. (Table 2, Figure 2): 132 **FIELD No.:** 89JN8-5
GSC LOC. No.: C-159227 **NTS:** 104P/13
COLLECTOR: J. Nelson/J. Nelson
LOCALITY INFO.:
MICROFOSSILS: conodonts **CAI:** 6
Conodont taxa:
Idiognathoides sp. (1)
Gondolella? sp. (1)
ramiform elements (5)
AGE: Late Carboniferous; probably Bashkirian - Moscovian

MAP No. (Table 2, Figure 2): 133 **FIELD No.:** 89JN9-7
GSC LOC. No.: C-159231 **NTS:** 104P/12
COLLECTOR: J. Nelson/J. Nelson
LOCALITY INFO.: UTM: 462200E, 6574780N
MICROFOSSILS: conodonts **CAI:** 6
Conodont taxa:
ramiform elements (5)
AGE: Ordovician-Triassic

MAP No. (Table 2, Figure 2): 135 **FIELD No.:** 89JN-13-4
GSC LOC. No.: C-159236 **NTS:** 104P/5
COLLECTOR: J. Nelson/J. Nelson
LOCALITY INFO: UTM: Zone 9; 464350E, 6572130N.
MICROFOSSILS: conodonts **CAI:** 5
Conodont taxa:
ramiform elements (8)
AGE: Ordovician - Triassic

MAP No. (Table 2, Figure 2): 136 **FIELD No.:** 89JN-KG-9-2
GSC LOC. No.: C-159229 **NTS:** 104P/12
COLLECTOR: J. Nelson/K. Green
LOCALITY INFO: UTM: Zone 9; 446700E, 6625100N.
MICROFOSSILS: conodonts **CAI:** 5-6
Conodont taxa:
gnathodids (2)
ramiform elements (5)
AGE: Carboniferous - Permian

MAP No. (Table 2, Figure 2): 137 **FIELD No.:** 89JN-DSO-006
GSC LOC. No.: C-153841 **NTS:** 104P
COLLECTOR: J. Nelson/J. Nelson
LOCALITY INFO.: UTM: 453804E, 6577119N
MICROFOSSILS: conodonts **CAI:** 5
Conodont taxa:
Pseudopolygnathus sp. (1)
ramiform elements (9)
AGE: Late Devonian - Early Carboniferous; Famennian-Tournaisian

MAP No. (Table 2, Figure 2): 138 **FIELD No.:** 89JN-DSO-007
GSC LOC. No.: C-153842 **NTS:** 104P
COLLECTOR: J. Nelson/J. Nelson
LOCALITY INFO.: UTM: 453302E, 6576673N
MICROFOSSILS: conodonts **CAI:** 5
Conodont taxa:
Bispathodus? sp. (1)
ramiform elements (20)
AGE: ?Early Carboniferous

APPENDIX 2
WHOLE-ROCK AND TRACE-ELEMENT DATA — SECTION A

SAMPLE	88jb37-11	87-thx-1	88mm25-5b	86kg20-1	88jb9-1	87jn24-1-2	87jn24-2	87kg24-1	87jn24-8	87jb14-4	88th06-05	88th17-08	88jn39-5
LAB NUMBER	37635	34745	37628	33194	37632	34741	34742	34743	34744	34747	37647	37649	37627
EASTING	460468		457182	434766	465866	444612	444582	444550	444071	444242	458750	462525	452035
NORTHING	6595771		6580168	6641605	6578816	6599541	6599249	6598962	6599782	6609844	6557025	6563275	6586687
UNIT	IPPs	Cry Lk.	IICgb	IIFMgb	IIMPvsu	IIMvs	IIMvs	IIMvs	IIMvs	IIMvs	IIMvs	IIMvs	IIPPsi
LITHOLOGY	basalt	diabase	plagiogranite	gabbro	basalt	basalt	basalt	basalt	basalt	basalt	basalt	basalt	gabbro
SiO_2	48.05	48.73	69.19	52.24	55.97	50.96	48.14	51.30	48.30	44.92	50.63	49.11	46.17
TiO_2	1.97	1.46	0.29	0.54	1.00	1.56	0.97	1.99	2.14	1.81	1.87	1.35	0.86
Al_2O_3	16.34	13.83	14.58	16.15	15.54	13.81	14.86	12.86	12.67	13.81	14.92	13.50	18.12
Fe_2O_3	10.93	11.23	4.44	7.94	9.72	11.47	10.79	11.05	13.64	12.53	13.93	10.85	8.34
FeO	7.63	7.68	1.14	5.96	7.13	9.15	8.30	8.24	9.42	9.85	7.49	0.14	4.85
MnO	0.45	0.20	0.04	0.14	0.21	0.18	0.20	0.18	0.18	0.15	0.39	0.22	0.14
MgO	5.71	6.80	0.55	6.97	3.60	6.40	8.64	5.14	5.10	8.42	4.57	7.52	7.33
CaO	4.29	8.66	4.71	10.86	5.86	7.30	8.97	8.19	11.07	8.63	5.39	11.26	12.07
Na_2O	3.86	3.43	4.90	3.18	3.79	3.78	2.30	4.61	2.15	1.45	3.84	2.76	2.48
K_2O	1.65	0.11	0.02	0.08	0.30	0.85	0.92	0.25	0.15	0.03	0.42	0.46	0.43
P_2O_5	0.51	0.13	0.03	0.03	0.17	0.13	0.06	0.15	0.17	0.15	0.16	0.10	0.06
LOI	6.07	3.32	1.36	2.26	4.18	2.55	2.94	3.34	2.20	7.60	3.40	2.79	3.84
SUM	99.83	97.90	100.11	100.39	100.34	98.99	98.79	99.06	97.77	99.50	99.52	99.92	99.84
Rb	26	7	<10	33	<10	20	34	<7	1	7	<10	<10	<10
Sr	356	194	200	105	547	150	38	126	400	80	128	166	426
Ba	638	n.a.	69	n.a.	819	n.a.	n.a.	n.a.	n.a.	n.a.	2292	190	848
U	45	19	32	n.a.	35	11	20	5	6	14	36	42	34
Ta	8	2	11	n.a.	11	<1	n.a.	n.a.	n.a.	n.a.	8	6	8
Nb	87	8	6	44	9	8	9	3	n.a.	7	6	9	7
Zr	149	114	<20	397	119	96	58	125	133	117	124	84	66
Ti	11248	n.a.	1682	n.a.	5841	n.a.	n.a.	n.a.	n.a.	n.a.	10866	8210	5288
Y	35	39	<10	66	27	36	28	40	50	39	34	33	23
V	238	323	61	184	250	467	284	472	488	403	443	339	235
Sc	24.0	n.a.	5.0	33.0	27.0	n.a.	n.a.	n.a.	n.a.	n.a.	32.0	45.0	37.0
Cr	245	211	19	75	60	256	364	54	31	207	67	342	85
Ni	121	86	4	58	19	90	127	32	29	67	17	86	100

APPENDIX 2
WHOLE ROCK AND TRACE ELEMENT DATA — SECTION B

SAMPLE	86jn26-11	86kg13-1	86jn34-6	86jn34-8	87jn6-6	87jn6-8	87kg8-6	87kg14-11	87jn17-1	87jn15-9	87kg16-2	87jb7-5a	87jb7-5b
LAB NUMBER	32215	32497	32501	32502	33404	33405	33637	33653	33654	33655	33656	34746	34753
EASTING	436425	429930	434802	435244	452555	452364	451308	453033	451104	451041	450438	450008	450008
NORTHING	6640101	6633111	6628041	6628304	6615449	6615311	6615134	6610378	6609600	6611589	6610460	6620614	6620614
UNIT	IIPPvs	IIPPvs	IIPPvs	IIPPvs	IIPPvs	IIPPvs	IIPPvs	IIPPvs	IIPPvs	IIPPvs	IIPPvs	IIPPvs	IIPPvs
LITHOLOGY	basalt	basalt	basalt	diabase	gabbro	gabbro	gabbro	basalt	basalt	basalt	basalt	diabase	basalt
SiO_2	50.03	49.05	47.40	47.01	51.14	49.92	51.79	49.41	48.75	49.53	48.85	48.85	48.59
TiO_2	1.53	1.70	1.70	1.42	1.44	1.78	2.05	1.29	1.03	1.30	1.16	1.31	1.33
Al_2O_3	15.25	14.74	14.59	15.91	14.10	16.49	14.02	14.19	14.02	14.15	14.63	14.49	14.73
Fe_2O_3	10.77	11.43	12.32	11.03	11.23	10.76	13.12	11.42	8.33	10.16	10.09	10.20	10.60
FeO	7.09	8.81	9.88	7.16	0.00	0.00	8.49	0.00	0.00	0.00	0.00	6.70	7.04
MnO	0.16	0.17	0.19	0.21	0.43	0.35	0.22	0.22	0.16	0.16	0.18	0.17	0.19
MgO	5.24	6.52	7.20	7.80	6.77	5.78	3.46	7.22	5.18	5.79	6.43	6.11	6.47
CaO	8.13	8.52	9.78	7.05	7.07	4.83	5.80	8.08	9.80	9.60	8.70	10.28	10.47
Na_2O	4.47	3.88	2.90	4.18	4.26	4.89	5.37	3.53	5.16	3.62	3.82	3.68	2.98
K_2O	0.18	0.06	0.23	0.42	0.23	0.33	0.12	0.37	0.08	0.03	0.65	0.18	0.14
P_2O_5	0.14	0.14	0.13	0.10	0.12	0.14	0.22	0.11	0.09	0.13	0.09	0.10	0.11
LOI	3.08	3.21	3.13	4.55	2.89	3.46	2.51	2.82	4.95	3.07	2.87	3.53	3.86
SUM	98.98	99.42	99.57	99.68	99.68	98.73	98.68	98.66	97.55	97.54	97.47	98.90	99.47
Rb	1	2	4	9	4	4	<10	n.a.	n.a.	n.a.	n.a.	6	14
Sr	158	133	177	74	162	267	135	265	275	88	205	274	134
Ba	73	208	984	56	<100	6000	140	970	120	<100	<100	n.a.	n.a.
U	<5	<5	<5	<5	n.a.	n.a.	n.a.	n.a.	n.a.	n.a.	n.a.	10	15
Ta	<2	n.a.	<2	n.a.	<1	<1	n.a.	0	n.a.	n.a.	n.a.	n.a.	n.a.
Nb	2	4	<5	1	1	1	12	16	13	14	11	3	8
Zr	111	119	118	73	99	113	165	120	100	125	120	85	92
Ti	9757	10657	10629	8797	n.a.	n.a.	n.a.	n.a.	n.a.	n.a.	n.a.	n.a.	n.a.
Y	35	36	36	30	27	33	35	35	27	26	30	31	36
V	333	326	334	262	313	378	123	296	221	306	290	309	320
Sc	33.0	39.0	39.0	35.0	36.0	29.0	38.0	n.a.	n.a.	n.a.	n.a.	n.a.	n.a.
Cr	113	176	201	375	222	23	<50	170	200	160	230	212	225
Ni	39	61	76	139	88	24	0	56	130	100	81	77	71

APPENDIX 2
WHOLE ROCK AND TRACE ELEMENT DATA — SECTION C

SAMPLE	88jb48-2	88th05-07	88th14-14	86jb49-7	88lm38-4	87jn14-4	87jn14-5	87jn14-6	87jn13-4	87kg19-3	87jn19-14	87jn19-18	87jb20-10b
LAB NUMBER	37640	37646	37648	38181	37625	33633	33634	33635	33636	34568	34569	34570	34749
EASTING	473470	469950	467840	428024	478177	448267	448100	447974	447390	446444	446453	446766	448663
NORTHING	6565930	6564225	6567225	6649486	6557689	6606507	6606477	6606482	6607494	6605249	6604403	6605610	6604196
UNIT	IIPPvs	IIPPvs	IIPPvs	IIPPvs	IIIMt	IIIPPHv	IIIPPHv	IIIPPHv	IIIPPHv	IIIPPHv	IIIPPHv	IIIPPHv	IIIPPHv
LITHOLOGY	basalt	basalt	basalt	basalt	tonalite	basalt	andesite	andesite	andesite	andesite	dacite	basalt	basalt
SiO_2	48.34	60.09	48.81	50.50	49.17	49.36	54.07	59.41	55.53	54.46	64.17	51.57	50.20
TiO_2	1.58	1.39	1.50	1.34	1.39	0.84	0.99	0.58	0.61	0.83	0.35	0.79	0.70
Al_2O_3	14.12	12.16	14.20	15.96	12.42	18.95	17.80	16.25	17.34	18.16	16.77	15.22	19.43
Fe_2O_3	12.21	10.09	10.62	9.96	10.47	9.88	8.40	6.58	7.42	7.96	3.63	8.27	8.56
FeO	7.34	7.27	8.06	6.75	8.02	6.82	6.35	4.03	3.82	2.33	2.12	4.09	4.37
MnO	0.20	0.20	0.18	0.18	0.18	0.17	0.16	0.13	0.15	0.15	0.09	0.13	0.30
MgO	8.49	4.37	7.07	3.70	6.60	3.81	2.77	2.51	3.06	6.14	2.08	7.64	3.45
CaO	5.91	5.41	8.55	10.97	8.15	5.17	6.89	5.62	7.55	7.06	4.17	9.24	7.81
Na_2O	2.33	3.08	2.35	2.34	2.85	5.57	2.93	4.48	4.19	4.55	5.29	1.93	4.15
K_2O	2.37	0.38	1.92	0.17	0.12	0.85	2.04	0.46	0.11	0.17	0.75	0.05	0.56
P_2O_5	0.15	0.14	0.13	0.14	0.25	0.24	0.37	0.12	0.17	0.16	0.12	0.10	0.14
LOI	4.08	2.96	3.18	4.74	8.40	4.16	3.22	3.26	2.86	2.93	1.85	4.01	3.27
SUM	99.78	100.27	98.41	100.00	100.00	99.00	99.64	99.40	98.99	99.57	99.27	98.95	98.57
Rb	35	<10	33	n.a.	<10	18	36	<7	<7	2	14	<7	11
Sr	84	115	77	n.a.	352	390	310	343	380	812	718	507	463
Ba	507	411	1294	n.a.	96	n.a.	n.a.	n.a.	<100	n.a.	n.a.	n.a.	n.a.
U	43	42	43	n.a.	37	n.a.	11	n.a.	10	14	15	7	9
Ta	6	6	5	n.a.	8	2	3	n.a.	<2	1	2	<2	1
Nb	15	12	12	<5	16	1	10	n.a.	4	7	7	6	2
Zr	91	133	104	110	115	103	133	90	85	91	63	62	57
Ti	9207	7951	9052	n.a.	8218	n.a.	n.a.	n.a.	n.a.	n.a.	n.a.	n.a.	n.a.
Y	39	33	33	34	30	20	31	9	19	26	10	19	22
V	422	285	336	0	279	245	172	114	293	216	97	334	272
Sc	41.0	25.0	44.0	n.a.	33.0	35.0	31.0	33.0	n.a.	n.a.	n.a.	n.a.	n.a.
Cr	260	122	338	260	302	3	14	0	11	17	55	213	4
Ni	93	55	76	0	65	6	10	4	13	11	52	69	8

APPENDIX 2

WHOLE ROCK AND TRACE ELEMENT DATA — SECTION D

SAMPLE	87hm12-11	87hm18-13	88mm49-1	88mm50-7	88TH02-03	86jn29-1	86jn29-2	86jn29-6	86jn8-6	86jn29-5	86jn8-4	86jn8-7	88jb47-9
LAB NUMBER	34751	34752	37630	37631	37645	32216	32217	32219	32020	32218	32499	32500	37639
EASTING	444640	447497	474743	473237	466450	433206	433452	433563	437494	433657	437963	436951	479639
NORTHING	6608268	6604562	6559165	6559595	6558500	6637239	6636801	6636086	6630264	6636389	6630502	6629857	6556414
UNIT	IIIPPHv	IIIPPHv	IIIPPHv	IIIPPHv	IIIPPHv	IIIPi	IIIPi	IIIPi	IIISPv	IIISPv	IIISPv	IIISPv	IIIvs
LITHOLOGY	basalt	basalt	andesite	basalt	basalt	granodiorite	tonalite	gabbro	latite	monzonite	latite	andesite	andesite
SiO_2	50.28	49.25	56.15	49.73	49.94	66.23	57.70	46.86	53.27	51.58	51.66	53.53	68.20
TiO_2	0.80	0.70	0.97	1.54	0.97	0.39	0.84	0.79	0.95	0.71	0.91	0.79	0.72
Al_2O_3	16.81	17.89	16.55	14.76	15.75	14.42	15.75	16.15	18.22	15.85	19.49	18.24	13.04
Fe_2O_3	10.08	9.10	7.93	11.09	10.13	2.61	6.36	10.12	8.48	10.01	7.84	7.06	5.10
FeO	7.81	7.04	4.84	7.56	5.56	2.56	4.06	7.06	0.00	7.56	3.72	4.01	3.42
MnO	0.19	0.23	0.10	0.21	0.19	0.03	0.13	0.16	0.19	0.10	0.23	0.29	0.08
MgO	8.24	5.03	4.76	5.43	6.65	1.48	4.32	7.75	2.98	5.96	2.18	2.40	3.26
CaO	8.27	6.11	3.77	8.52	9.02	3.05	6.07	11.98	5.64	4.28	7.84	7.11	1.87
Na_2O	2.77	4.67	3.02	2.69	3.06	2.83	2.80	0.84	3.29	3.90	3.70	5.10	3.46
K_2O	0.19	0.51	2.62	1.91	0.47	3.75	2.04	0.72	2.62	2.97	2.70	1.37	1.58
P_2O_5	0.15	0.12	0.27	0.35	0.13	0.08	0.14	0.07	0.26	0.12	0.21	0.11	0.09
LOI	2.31	5.79	3.85	3.42	3.85	2.04	2.68	2.76	2.94	3.33	2.52	3.79	2.64
SUM	100.09	99.40	99.99	99.65	100.16	96.91	98.83	98.20	98.84	98.81	99.28	99.79	100.04
Rb	7	16	53	24	<10	131	72	24	72	98	75	28	36
Sr	370	459	436	268	164	201	243	340	322	165	618	438	180
Ba	n.a.	n.a.	838	1253	218	1181	1058	269	988	923	1188	803	806
U	16	11	34	37	45	<5	<5	1	2	<5	5	2	38
Ta	n.a.	n.a.	11	10	9	<2	<2	<2	<2	<2	<2	1	8
Nb	12	5	13	26	14	5	6	<5	1	1	2	2	17
Zr	59	52	156	199	73	149	90	40	117	85	131	99	128
Ti	n.a.	n.a.	5651	9331	5712	2409	5249	4929	5827	4435	5630	4866	3983
Y	19	23	26	33	21	11	16	9	21	16	21	18	17
V	295	266	198	368	293	34	143	377	214	193	226	171	101
Sc	n.a.	n.a.	15.0	34.0	38.0	6.9	21.0	38.0	22.0	21.0	21.0	23.0	10.0
Cr	193	52	65	222	214	54	109	241	18	143	25	21	205
Ni	75	28	21	80	56	18	27	74	20	43	22	16	56

NOTES: All trace-element data in parts per million.
n.a.=not analysed.

APPENDIX 2

RARE-EARTH DATA FOR SELECTED DIVISION I AND II SAMPLES														
SAMPLE	**LAB No.**	**EAST**	**NORTH**	**DIV.**	**UNIT**	**LITHOLOGY**	**La**	**Ce**	**Nd**	**Sm**	**Eu**	**Ho**	**Yb**	**Lu**
88TH6-5	37647	458750	6557050	II	IIMvs	basalt	6.3	21	16	10.20	1.7	1.2	3.3	0.50
88JN39-5	37627	477424	6563740	II	IIPPsi	gabbro	2.5	8	<10	2.30	0.9	<1.0	1.7	0.30
87KG16-2	33656	450529	6610306	II	IIPPvs	basalt	2.8	11	14	3.00	1.0	1.1	2.4	0.40
88JB49-7	37640	473713	6564788	II	IIPPvs	basalt	7.5	20	18	3.90	1.1	<1.0	3.4	0.50
87JN14-4	33633	448267	6606507	III	IIIPPHv	basalt	12.5	31	22	4.00	1.3	<1.0	1.7	0.30
87JN14-5	33634	448100	6606477	III	IIIPPHv	andesite	16.9	40	27	5.50	1.4	<1.0	2.4	0.30
87JN14-6	33635	447974	6606482	III	IIIPPHv	andesite	12.9	29	17	2.70	0.9	<1.0	1.3	0.20
88MM50-7	37631	473237	6559595	III	IIIPPHv	basalt	21.9	52	29	5.50	1.6	1.7	2.4	0.40

APPENDIX 3
FLUID INCLUSION DATA, ERICKSON GOLD CAMP

Number	%vap	T_{m*}	T_e	T_{mi}	T_{mc}	T_{hc}	T_h	T_{dec}
Taurus								
AP-21	5	–57.7	–30	—	7.6	—	272	340
	10	–58.4	–33	—	8.5	13.7	295	340
	5	–58.1	—	—	7.9	18.8	268	340
	5	—	—	—	—	—	270	340
	5	—	—	—	—	—	269	340
	5	—	—	—	—	—	267	340
	5	—	—	—	—	—	259	340
	5	—	—	—	—	—	282	340
	5	—	—	—	—	—	284	340
AP-21	20	–57.5	–38?	—	7.4	27.0	290	350
	40	–57.5	—	—	8.3	24.4	281	350
	20	–57.6	–31	—	7.9	22.2	—	350
	20	—	—	—	8.0	25.7	—	325
	30	–57.5	—	—	7.2	25.9	—	360
	15	–57.5		—	8.8	—	243	360
	—	—	—	—	—	25.1	—	360
	—	—	—	—	—	22.3	—	360
AP-21	5	—	—	—	8.4	—	—	275
	5	—	—	—	7.7	—	—	275
	5	—	—	—	8.0	—	—	275
AP-21	10	–57.6	—	—	8.9	—	—	250
	10	—	–24	—	9.0	8.4	—	250
	10	—	—	—	8.8	—	—	246
	15	–57.1	—	—	—	—	270	290
	10	—	—	—	9.3	–2.5	—	290
	10	—	—	—	10.0	—	263	290
	15	—	—	—	—	26.4	—	290
	15	—	—	—	—	13.0	—	290
	15	—	—	—	—	14.5	—	290
	15	—	—	—	—	23.2	—	290
	15	—	—	—	—	24.4	—	290
	15	—	—	—	—	27.5	—	290
	15	—	—	—	—	—	260	290
	15	—	—	—	—	—	248	290
	15	—	—	—	—	—	264	290
	15	—	—	—	—	—	266	290
AP-21	15	—	—	—	8.1	—	—	—
	—	—	—	—	10.3	—	—	—
	3	—	—	—	8.9	—	—	—
AP-21	6	—	—	—	—	—	255	—
	4	—	—	—	—	—	210	—
	9	—	—	—	—	—	220	—
	4	—	—	—	—	—	227	—
	4	—	—	—	—	—	215	—
	4	—	—	—	—	—	203	—
	5	—	—	—	—	—	250	—
	5	—	—	—	—	—	212	—
AP-21	7	—	—	—	—	—	221	—
	7	—	—	—	—	—	215	—
	5	—	—	—	—	—	220	—
	8	—	—	—	—	—	—	279
	3	—	—	—	—	—	220	—
	2	—	—	—	—	—	209	—
AP-21	5	—	—	—	—	—	235	—
	10	—	—	—	—	—	186	—
	10	—	—	—	—	—	220	—
	5	—	—	—	—	—	209	—
	6	—	—	—	—	—	201	—
	5	—	—	—	—	—	165	—
	6	—	—	—	—	—	165	—
	3	—	—	—	—	—	150	—
	8	—	—	—	—	—	225	—

Number	%vap	T_{m*}	T_e	T_{mi}	T_{mc}	T_{hc}	T_h	T_{dec}
Lyla-Boomerang								
LM2-7	15	—	—	—	8.6	—	—	—
	5	—	—	—	8.6	—	—	—
	60	—	—	—	9.4	—	—	—
	5	—	—	–2.8	—	—	248	360
	5	—	—	–2.7	—	—	235	360
	5	—	—	–2.6	—	—	234	360
	5	—	—	–2.7	—	—	249	360
	5	—	—	—	—	—	247	360
	7	—	—	–2.8	—	—	233	360
Elan								
JN1-5s	15	–57.0	—	—	8.9	26.0	—	260
	30	–56.9	—	—	8.5	16.6	240	260
	50	—	—	—	8.5	14.6	—	—
	—	—	—	—	8.5	16.0	—	—
	—	—	—	—	8.5	16.1	—	—
	30	–57.2	—	—	8.7	22.4	—	265
	50	—	—	—	8.5	25.0	—	—
	60	—	—	—	8.5	29.5	—	—
	—	–57.3	—	—	8.6	17.9	—	200
JN1-5	20	–57.1	–24	—	7.6	26.3	—	260
	15	—	—	—	10.1	17.7	—	262
	15	–57.3	—	—	7.4	25.5	—	270
AP-45	20	–57.2	—	—	8.4	13.3	263	—
	15	—	—	—	9.4	—	252	—
	20	—	—	–4.8	9.4	—	266	—
	20	—	—	—	9.0	—	246	—
	15	—	—	–4.5	8.4	20.9	dec	—
	7	—	—	—	9.0	—	256	—
	7	—	—	—	8.8	—	241	—
	7	—	—	–4.0	9.1	—	255	—
Berubé's								
AP-124	15	–57.3	–39?	—	8.5	24.2	—	270
	20	–57.1	–30	—	8.4	23.9	—	270
	15	–57.4	–43?	—	8.3	24.3	257	270
	15	–57.4	–43	—	8.3	24.2		270
	15	—	—	—	8.3	24.0	261	270
	—	—	—	—	—	23.5	—	270
	—	—	—	—	—	23.6	—	270
AP-124	3	—	–28?	–3.5	—	—	187	—
	3	—	–28?	–3.6	—	—	176	—
	3	—	—	–3.5	—	—	181	—
	3	—	—	–3.5	—	—	185	—
	3	—	–28	–3.6	—	—	178	—
	3	—	–28	–3.6	—	—	180	—
	3	—	—	–3.6	—	—	179	—
	3	—	—	—	—	—	188	—
	3	—	—	—	—	—	189	—
AP-124	3	—	—	–3.3	—	—	191	—
	3	—	–29	–3.1	—	—	189	—
	3	—	—	–3.0	—	—	188	—
	3	—	—	–2.8	—	—	189	—
Unnamed veins north of Berubé's								
JN4-1	3	—	—	–2.5	—	—	194	—
	3	—	—	–3.1	—	—	193	—
	3	—	—	–2.4	—	—	191	—
	3	—	—	–2.7	—	—	194	—
AP-36	4	—	–20.8	—	—	—	198	—
	2	—	–22.0	–4.3	—	—	188	—
	4	—	—	–4.3	—	—	180	—
	4	—	–20.2	—	—	—	191	—
	2	—	–20.1	–4.1	—	—	185	—

APPENDIX 3
FLUID INCLUSION DATA, ERICKSON GOLD CAMP — *Continued*

Number	%vap	T_{m*}	T_e	T_{mi}	T_{mc}	T_{hc}	T_h	T_{dec}
Unnamed veins north of Berubé's — *Continued*								
AP-36	4	—	–24.0	–5.1	—	—	188	—
	2	—	–20.2	–4.8	—	—	181	—
	3	—	–22.2	–4.9	—	—	193	—
	4	—	–24.0	–5.0	—	—	187	—
	5	—	—	—	—	—	187	—
	4	—	–23.5	–5.0	—	—	182	—
	4	—	–24.0	–5.6	—	—	192	—
	3	—	—	—	—	—	178	—
	3	—	—	–5.0	—	—	182	—
	—	—	—	–5.1	—	—	—	—
AP-13	4	—	—	–3.3	—	—	—	—
	4	—	—	–3.1	—	—	—	—
	4	—	—	–3.1	—	—	—	—
	4	—	—	–3.2	—	—	—	—
	4	—	—	—	—	—	142	—
	3	—	—	—	—	—	140	—
	3	—	—	—	—	—	153	—
	4	—	—	—	—	—	141	—
	4	—	—	—	—	—	142	—
	4	—	—	—	—	—	141	—
	3	—	—	—	—	—	165	—
	5	—	—	—	—	—	172	—
	3	—	—	—	—	—	174	—
Zus Mountain gabbro								
JN23-2	5	—	—	—	8.7	—	240	240
	3	—	—	–2.6	—	—	206	—
	3	—	—	—	—	—	212	—
	3	—	—	—	—	—	216	—
	3	—	—	—	—	—	208	—
Juniper Mountain alteration zone								
JN49-5	4	—	–21	–2.5	—	—	172	330
	4	—	—	–2.5	—	—	178	320
	3	—	—	–2.6	—	—	171	340
	3	—	—	–2.5	—	—	165	335
	3	—	—	–2.5	—	—	169	325
Hopefull								
JN1-6B	15	–57.3	–37	—	8.7	26.4	—	250
	15	—	—	—	8.2	21.0	—	260
	15	—	—	—	—	26.0	—	260
	20	—	—	—	—	26.0	268	330
	15	–57.4	—	—	8.5	26.3	236	260
	15	—	—	—	8.5	23.6	—	260
	15	—	—	—	8.7	26.8	237	260
JN1-6B	10	–57.3	—	—	8.2	25.6	—	240
	15	–57.3	—	—	8.2	25.4	—	315
	15	–57.3	—	—	8.2	25.1	—	280
	15	—	—	—	—	23.7	—	315
	15	—	—	—	8.1	25.6	—	260
	15	—	—	—	8.2	25.7	262	280
	10	—	—	—	8.0	—	194	260
	10	—	—	—	—	—	268	—
	10	—	—	—	—	—	265	—
	10	—	—	—	—	—	270	—
Rich								
JN1-1	5	—	–24	–3.3	—	—	184	317
	5	—	—	–4.1	—	—	183	300
	5	—	—	–3.2	—	—	198	300
	5	—	—	–3.0	—	—	194	300
	5	—	—	–4.0	—	—	—	350
	5	—	—	—	—	—	197	350
	5	—	—	—	—	—	203	350
	5	—	—	—	—	—	206	350

Number	%vap	T_{m*}	T_e	T_{mi}	T_{mc}	T_{hc}	T_h	T_{dec}
Troutline								
AP-41	5	—	—	—	—	—	210	—
	5	—	—	—	—	—	206	—
	5	—	—	—	—	—	205	—
	6	—	—	—	—	—	249	—
	4	—	—	—	—	—	240	—
	4	—	—	—	—	—	211	—
	5	—	—	—	—	—	236	—
	7	—	—	—	—	—	218	—
	8	—	—	—	—	—	239	—
	4	—	—	—	—	—	234	—
	5	—	—	—	—	—	244	—
	5	—	—	—	—	—	224	—
	5	—	—	—	—	—	210	—
	5	—	—	—	—	—	221	—
	7	—	—	—	—	—	214	—
	5	—	—	—	—	—	205	—
	5	—	—	—	—	—	204	—
	5	—	—	—	—	—	203	—
	5	—	—	—	—	—	221	—
	5	—	—	—	—	—	218	—
	10	–57.4	—	—	8.5	25.8	—	285
	15	—	—	—	8.1	—	283	—
	15	—	—	—	8.6	—	272	280
Snowy Creek (Hoag)								
AP30-A	—	—	—	—	—	325	—	
	10	—	—	—	—	—	280	—
	8	—	—	—	—	—	287	—
	10	—	—	—	—	—	dec	—
	10	—	—	—	—	—	dec	—
AP-30A	15	—	—	—	—	—	305	—
	15	—	—	—	—	—	298	—
	15	—	—	—	—	—	353	—
AP-30A	10	—	—	–4.6	8.0	—	274	—
	12	—	—	–4.5	—	—	322	—
	10	—	—	–4.5	—	—	257	—
	20	—	—	—	—	—	283	—
	—	—	—	—	—	—	275	—
	—	—	—	—	—	—	341	—
	—	—	—	—	8.0	—	280	—
	—	—	—	–4.2	—	—	300	—
	15	—	—	–5.0	8.5	—	320	—
	—	–58.4	—	—	—	—	—	—
AP-30A	—	—	—	–4.1	7.0	—	—	—
AP-30A	—	—	—	–3.5	—	—	—	—
AP-30A	—	–58.1	—	—	8.8	—	—	—
AP-30A	—	—	—	–3.1	—	—	297	—
	—	–58.4	—	–3.0	—	—	306	—
AP-30A	10	—	—	—	—	—	294	—
	30	—	—	—	—	—	268	—
	25	—	—	—	—	—	259	—
	20	—	—	—	—	—	—	333
	10	—	—	—	—	—	268	—
AP-30A	15	—	—	—	—	—	312	—
	17	—	—	—	—	—	313	—
	18	—	—	—	—	—	285	—
	15	—	—	—	—	—	255	—
	—	—	—	—	—	—	325	—
	10	—	—	—	—	—	278	—
AP-30A	30	—	—	—	—	—	335	—
	20	—	—	—	—	—	330	—

APPENDIX 3
FLUID INCLUSION DATA, ERICKSON GOLD CAMP — *Continued*

Number	%vap	T_{m*}	T_e	T_{mi}	T_{mc}	T_{hc}	T_h	T_{dec}
Snowy Creek (Hoag) — *Continued*								
AP-30A	40	—	—	—	—	—	310	—
	20	—	—	—	—	—	307	—
	15	—	—	—	—	—	230	—
	15	—	—	—	—	—	306	—
	15	—	—	—	—	—	285	—
AP-30A	—	—	-22.9	-3.9	8.0	—	—	—
	—	—	—	-4.5	10	—	—	—
AP-30A	10	—	—	—	—	—	289	—
	15	—	—	—	—	—	287	—
	20	—	—	—	—	—	306	—
AP-30A	25	—	—	—	—	—	349	—
	10	—	—	—	—	—	271	—
	10	—	—	—	—	—	306	—
	20	—	—	—	—	—	269	—
AP-30A	—	—	-24.0	-4.5	—	—	—	—
Cusac								
Eil-3	10	-57.2	—	—	—	—	261	340
	40	-57.5	—	—	—	—	—	340
	15	-57.3	—	—	9.3	—	285	340
	20	—	—	—	9.2	—	—	370
Eil-3	30	-57.6	—	—	6.0	25v	—	360
	40	-57.6	—	—	6.2	—		370
Eil-3	—	—	—	—	—	—	270	350
	—	—	—	—	—	—	276	350
	—	—	—	—	—	—	279	350
	—	—	—	—	—	—	280	350
	—	—	—	—	—	—	280	350
	—	—	—	—	—	—	279	350
	—	—	—	—	—	—	276	350
	—	—	—	—	—	—	281	350
	—	—	—	—	—	—	282	350
	—	—	—	—	—	—	283	350
Eil-3	10	—	-32	—	—	—	238	300
	15	-57.4	—	—	10.3	11.3	—	280
	10	-57.2			9.4	—	305	>410
	5	—	—	—	—	—	304	>410
	25	-57.3	—	—	9.1	—	292	320
	10	—	—	2.40	—	—	—	280
Eil-3	5	-57.8	-32	—	9.8	—	300	336
	5	-57.7	—	—	9.8	—	302	336
	5	-57.5	—	—	9.5	—	304	336
	5	-57.6	—	—	9.7	—	272	336
	5	-57.6	—	—	9.8	—	274	336

Number	%vap	T_{m*}	T_e	T_{mi}	T_{mc}	T_{hc}	T_h	T_{dec}
Eil-3	5	—	—	—	10.0	—	271	336
	5	—	—	—	—	—	277	336
Eil-3	10	—	—	—	9.3	—	250	290
	50	—	—	—	10.2	—	270v	315
	50	-57.5	—	—	9.4	—	265v	275
	10				—		256	300
	15	—	—	—	—	—	245	285
Eil-3s	5	-58.5	—	-3.0?	8.8	—	—	—
AP-Cus	10	-57.2	—	—	9.1	—	—	—
	10	-57.4	—	—	9.1	—	—	—
	10	—	—	—	9.1	—	—	—
	10	—	—	—	9.0	—	—	—
AP-Cus	—	—	—	-2.8	9.5	—	228	—
	—	—	—	-2.9	—	—	222	—
	—	—	—	—	9.3	—	228	—
	—	—	—	-3.4	—	—	249	—
	—	—	—	-4.1	8.8	—	226	—
	—	—	—	—	9.4	—	248	—
	—	—	—	—	—	—	228	—
	—	—	—	—	—	—	230	—
	—	—	—	—	—	—	232	—
	—	—	—	—	—	—	235	—
AP-Cus	—	—	—	-2.2	—	—	207	—
	—	—	—	-1.9	—	—	209	—
AP-Cus	—	—	-22.9	-3.0	8.6	—	221	—
	—	—	—	-2.7	9.0	—	245	—
	—	—	—	-3.2	—	—	246	—
	—	—	—	-3.4	8.7	—	231	—
	—	—	—	-1.9	—	—	205	—
	—	—	—	-3.3	8.5	—	221	—
	—	—	—	-4.0	8.8	—	235	

%vap=per cent vapour
T_{m*}=final melting temperature of carbonic phase
T_e=first melting (eutectic) of the aqueous phase
T_{mi}=final melting of ice
T_{mc}=final melting of clathrate
T_{hc}=homogenization of carbonic phase
T_h=total homogenization
T_{dec}=temperature of decrepitation

NOTES:
1. Different inclusion groups within the same sample are separated by a blank line.
2. All melting temperatures other than eutectic melting refer to last melt.
3. "%vap" for three phase inclusions refers to per cent CO_2, including liquid and vapour phases.
4. All T_h and T_{hc} are to liquid phase, unless followed by "v".
5. Sample numbers followed by "s" indicate inclusions in sphalerite; all others were in quartz.

APPENDIX 4
METAMORPHIC ASSEMBLAGES IN BASIC ROCKS OF THE SYLVESTER ALLOCHTHON

Sample No.	UTM Coordinates Easting	Northing	Assemblages
GROUP 1 (transitional)			
86JB49-7	428024	6649486	pp-cz-ca(m)
Sentinel	428141	6649082	pr-ep-chl(m)
Sentinel basalt	428259	6650050	act-ep-ca(m);pr-ep-chl ca(v)
GROUP 2 (prehnite-pumpellyite; transitional)			
86JB17-13	429413	6644172	pp-pr-chl(m);chl-ca(v)
88JN53-1	412952	6640293	chl-pp-ca(m)
86JN26-1	434801	6641485	pr-ca(v)
86JN26-11	436425	6640101	pp-chl(a)
86JN25-9	429698	6639413	chl-cz-pp(m);pp-chl-pr(v);pr-ca-cz(v);pp-cz(a)
86KG20-1	434766	6641605	pr-ep(m);ep,cz,chl,ca(v)
86KG23-5	433162	6637103	chl-pp-ep-pr(m);pp-ct-chl(m);pp-ep-chl(m);pr(v)
86JN29-1	433206	6637239	pp-chl-ep-ca(m);cz(v)
86JN29-2	433452	6636801	ep-chl-ca(m);pr-ca(v,a)
86JN29-6	433563	6636086	pr-ca(v)
GROUP 3 (prehnite-pumpellyite; transitional)			
86KG13-1	429930	6633111	pp-chl(m);chl-pr(v),pr-pp-chl-cz(v)
86KG13-3	429911	6633220	pp-chl(v)
86JN34-8	435244	6628304	chl-ca(m);chl-ca-pr(v); chl-ep-ca(v)
86JN17-4	441341	6625718	pr-chl(m)
89JN10-8	438675	6623925	chl-cz(m)
89JN10-9	437550	6625425	chl-cz(m)
GROUP 4 (prehnite-pumpellyite)			
87JB7-5	450008	6620614	pp-chl-ep(m);pp-pr-chl(m)
87JB8-8	450507	6619090	pp-pr-chl(m)
87KG36-1	446222	6619393	pr-pp-chl(m);pr-ca(v)
87HM8-12	446414	6619435	pp-chl(m);ca(m)
87HM7-16-2	447809	6609979	pr-ca-cz(m);pr-ca(v)
87JN6-6	452555	6615449	chl-pp(m);chl-pp(v)
87JN6-8	452364	6615311	chl-pp(m)
87JN6-9-1	452292	6615957	pp-chl(m)
GROUP 5 (prehnite-pumpellyite)			
87JB17-6	448813	6611910	pp-chl-ca(a)
87JB17-10	448523	6611441	pp(a);cz(v)
87JB17-10	448523	6611441	pp-cz(v)
87JN17-1	451104	6609600	pp-ca(m);pp-chl-ca(a)
87JN14-6	447974	6606482	pr-ca(m);pp-ep-chl(m) pr-ca(v);ca-ep-chl(v)
87JN12-1-2	448783	6607494	pp-chl(m)
87JN14-1	448089	6607125	pp-chl(m)
87JN14-4	448267	6606507	pr-ep-chl-ca(m);pp-ep(m)
87JN14-6	447974	6606482	pp-ep(m),ep-chl-ca(m); pr-ca(v)
87JN23-8	447336	6598402	pp-cz-ca-chl(m);pp-ca(v)
GROUP 6 (transitional)			
87JB14-5	444320	6609635	pp-chl-ca(m)
87HM10-6	444775	6608635	chl-ep-pr(m);pr-pp-ca(m);pp-chl(m)
87HM11-8	446578	6607747	chl-pr-ca(m);pr-ca(a)
87JN13-4	447390	6607494	pr-chl-ep(m);pp-ep(m)
87JN19-10	446699	6604806	chl-ca(m)
87JB20-10A,B	448663	6604196	pr-ep-chl-pp(m);ca-chl-cz(v)
87JN19-14	446453	6604403	pr-ep(m)
GROUP 7 (greenschist)			
87HM45-15	441800	6611800	act-chl(m)
87JB13-6	444378	6610990	act-ca-chl(m)
87JB14-4	444242	6609844	act-chl-ca(m);chl-cz(v)
87JB12-10a	446103	6607472	cat-ca-chl(m);ca-chl-ep(v)
87KG20-8	445628	6605624	act-cz(m) Retrograde:pr(v)
87KG19-3	446444	6605249	ep-ca-chl(m)
87HM17-5	446767	6604172	chl-ca(m)
87HM17-6	446970	6604395	act-chl-ep(m)
87JN24-1-2	444612	6599541	act-cz(m);ca-chl-cz(v); ca-act(v)
87JN24-2	444582	6599249	act-cz(m);act-chl-cz(v)
87KG24-1	444550	6598962	act-chl(m);ca-chl(m); chl-ca-ep(v)
87JN24-8	444071	6599737	act-chl-ep(m);act, chl(v)
GROUP 8 (prehnite-pumpellyite; transitional)			
88LM21-5	456759	6581946	pp-chl-cz(m)
88MM30-5	453800	6592130	pp-chl-stilp.(m)
88JN26-7	458180	6593357	pr-chl(m);ep-chl(m)
88LM31-9	462150	659150	pp-pr-ca(a)
88MM34-15	461259	6588210	chl-ep(m)
88JB21-10	447370	6602493	pr-chl(m);ca-chl(m)
88JN20-3	462858	5682450	pr-ca-chl(m)
88JB11-7	463580	6580316	pr-chl-cz(v)
88MM11-14	467117	6577710	pp-chl(m);pr(v)
88MM14-3	466631	6577224	pp-chl-cz(m)
GROUP 9 (greenschist)			
88LM1-6	454818	6572837	act-chl-ep(m)
88MM2-3	456885	6572200	act-chl(m)
88MM31-3	454691	6585928	act-ep-chl-ca(m)
88MM32-4	455325	6583653	act-chl-ca(m)
88JN19-8	458904	6580953	pp-ep(m);act-chl(m); chl-cz(v)
89JN6-4	453600	6577500	act-chl-ep-ca(m)
88JB38-4	461349	6575342	act-chl(m)
88JN9-9	462139	6574995	act-chl-ep-ca(m)
89JN13-1	463025	6573150	act-chl(m) Retrograde:pp-pr-chl-ep(v) act-pp-pr-chl;pr-ca(v);pp
89JN13-4	464325	6572100	act-chl(m) Retrograde:pp-chl-cz(v); ca-gypsum-barite-qz vein
89JN13-6	462300	6573700	pp-chl(m);pr-ca(v); pp-cz-ca(v)
88JN5-9A	466019	6573095	act-chl-ca(m)
88JN5-2	464861	6572129	act-ep(m);act-chl-ep(v)
81AP27	464000	6571100	act-ep(m) Retrograde:pp-ep-chl(v); pr-ca(v)
81AP9	466350	6570250	act-chl-ep(m);pp(in plag)
81AP12	464940	6571550	act-chl-ep(v); chl-ca(v) Retrograde:pp,pr,ca,ep
81AP3 (Lamprophyre)	462560	6570100	pr-ep-ca-chl(m); pp-chl-ca(m); pr-pp-chl(m)
80AP125	463520	6570400	ca-chl-ep+ sulfide,gypsum(m,v)
80AP69	462400	6570125	chl-ep-ca+sulphide(m)
80AP20	460750	6569525	act-ep-chl(m,v)
81AP41	464150	6568475	act-chl(m,a) Retrograde:pr-chl-pp-ca(v) pr-pp-chl-ep-ca(v)
88TH14-4	468400	6567600	act-chl(m)
88JB48-2	473470	6565930	act-ep-chl(m);act-ca-chl-ep(m)
88JB48-3	473381	6565848	act-chl-ca(m);act-chl-ep(m)
88JB48-4	473346	6565784	chl-ca(m)
88TH5-7	469920	6564200	act-chl-ep(m);ca-chl(m)
88LM44-7	471301	6563892	act-ep-ca(m)
88TH17-8	462525	6563275	act-chl-ca(m)
TM-1	465600	6562025	act-ep-chl(m)

APPENDIX 4

METAMORPHIC ASSEMBLAGES IN BASIC ROCKS OF THE SYLVESTER ALLOCHTHON — *Continued*

Sample No.	UTM Coordinates		Assemblages
	Easting	Northing	
GROUP 9 (greenschist) — *Continued*			
88TH2-3	466450	6558520	chl-ep(v)
88TH6-5	458770	6557025	act-chl(m)
GROUP 10 (prehnite-pumpellyite; transitional)			
88MM42-11	480102	6562278	pp-ep-chl(m);pp-ep-ca(v) pr-ca-ep(v)
88MM42-15	476927	6565922	chl-ep-ca(m);pr-chl(v) pr-ep(v)
Notes: (m)=matrix, (v)=vein, (a)=amygdule			
GROUP 10 (prehnite-pumpellyite; transitional)			
Jpp	474150	6560425	pp-ep-chl(v);pp-ca-ep(a)
88MM49-11	473502	6558192	pp-chl-ca(m);pp-chl-ca(v)
88MM49-12	473548	6558002	pp-ep(m)
88MM49-15	473684	6557718	act-ep-chl-ca(m)
88MM49-17	473829	6557532	chl-ep-ca(v);ep-ca(m)
88JN44-10	472814	6556114	chl-ca(m)
88JN43-13	475072	6554984	pp-chl(m)
88JN46-3	476279	6556525	pr-ca(m)
88JN46-10	476898	6556707	pu-chl-ca(v)
88JB45-12	478328	6557668	pp-chl(m)
88JB45-11	478022	6556728	pr-ca(v);pr-chl(v)
88JB44-1	478661	6558034	pp(m)
88JN43-1	476817	6555844	act-chl(m)
88JN43-13	475072	6554984	pp-chl(m)
88MM44-9	476397	6556445	chl-ca(m)
88MM44-5	476875	6556300	pr-chl(m);chl-ep-ca(m)
88JB47-1	479333	6557089	pr-pp-chl(m);ep-chl(m)
88JB47-3	479719	6556830	pp-chl(m);chl-ca(m); pr-ca(v)
88JN47-7	478136	6557972	chl(m);pr-ca(v)
88JN47-6	478055	6557885	pr-pu-chl(v)
88MM50-7	473237	6559595	pp-pr-chl(m);pp-pr-chl(v)

NOTES: act: actinolite
ca: calcite
chl: chlorite
cz: clinozorsite
ep: epidote
pp: pumpellyite
pr: prennite
stilp.: stilpnomelane
(a): amygdule assemblage
(v): veinlet assemblage
(m): matrix assemblage

Queen's Printer for British Columbia©
Victoria, 1992

QPJ — 185025 — 03/92

Energy, Mines and Resources Canada

BC Province of British Columbia

This project is a contribution to the Canada/British Columbia Mineral Development Agreement, 1985–1990.

BC Ministry of Energy, Mines and Petroleum Resources

Geological Survey Branch

BRITISH COLUMBIA GEOLOGICAL SURVEY

This map is to accompany

BULLETIN 83

GEOLOGY OF THE MIDWAY-CASSIAR AREA NORTHERN BRITISH COLUMBIA

NTS 104O; 104P

Compiled by J.L.Nelson 1989, 1990

Geology by J.L.Nelson and J.A.Bradford, 1986, 1987, 1988, 1989, T.Harms 1988, H.Gabrielse 1950-1954, A.Panteleyev and L.J.Diakow 1978-1980, C.Bloomer 1981, I.Lyn 1983

Scale 1:100 000

0 1 2 3 4 5 Kilometres

N

LEGEND

INTRUSIVE ROCKS

EOCENE

Egr — Granite, medium to fine grained

CRETACEOUS

Kgr — Granite, coarse grained, commonly K-feldspar megacrystic

Kgd — Granodiorite, coarse grained equigranular

POST–ACCRETIONARY STRATA

PLEISTOCENE–RECENT
TUYA VOLCANICS

Qtv — Olivine basalt flows

SYLVESTER ALLOCHTHON (DEVONIAN TO TRIASSIC)

DIVISION III (MISSISSIPPIAN TO PERMIAN)

LATE PERMIAN

IIPls — *Parafusulina*–rich limestone

PENNSYLVANIAN TO PERMIAN

IIPPs — Limestone, limestone with volcanic clasts, tuffaceous sandstone, red and green chert, volcanic breccia

PENNSYLVANIAN TO PERMIAN
HUNTERGROUP VOLCANICS

IIPPHv — Augite (hornblende, plagioclase) porphyry, lapilli tuff, tuffaceous sandstone, limestone, minor chert and argillite

AGE UNKNOWN
SOUTH POST RIDGE VOLCANICS

IISPv — Trachyandesite, latite flows, subvolcanic intrusions, pyroclastic and epiclastic equivalents

PERMIAN

IIPi — Zoned hornblende gabbro–tonalite–granodiorite complex

AGE UNKNOWN; PRE–MISSISSIPPIAN

IIvs — Tuff, limestone, quartz arenite, slate, variolitic basalt, green chert

EARLY MISSISSIPPIAN

IIMt — Tonalite, medium to coarse grained, equigranular

DIVISION II (MISSISSIPPIAN TO TRIASSIC)

TRIASSIC
TABLE MOUNTAIN SEDIMENTS

IITrMs — Slate, calcareous siltstone, *halobia*–bearing limestone

BLUE DOME FAULT ZONE
PERMIAN AND OLDER?
BLUE DOME MELANGE

IIBDm — Serpentinite–matrix melange: serpentinite, blocks and slice of gabbro, basalt, ultramafite; tectonic, debris–flow and talus breccia

PERMIAN AND OLDER?
FOGGY MOUNTAIN MELANGE

IIFMm — Serpentinite–matrix melange: serpentinite, blocks and slices of gabbro, basalt, ultramafite; tectonic, debris–flow and talus breccia

PERMIAN OR OLDER
FOGGY MOUNTAIN GABBRO

IIFMgb — Coarse grained gabbro, tectonic gabbro breccia, amphibolite, diabase dikes

MISSISSIPPIAN TO PERMIAN

IIMPvsu — Basalt, diabase, chert, argillite, slivers of serpentinite

ULTRAMAFIC AND GABBROIC THRUST SHEETS
PERMIAN
ZUS MOUNTAIN GABBRO

IIPZMgb — Gabbro, in part layered, foliated

PERMIAN?
ZUS MOUNTAIN–BLUE RIVER ULTRAMAFITE

IIZMum — Dunite, harzburgite tectonite, serpentinite, pyroxenite

PERMIAN (?)
CASSIAR–QUARTZROCK CREEK GABBRO

IIPCgb — Gabbro

AGE UNKNOWN
CASSIAR–QUARTZROCK CREEK ULTRAMAFITE

IICum — Serpentinite, harzburgite tectonite, pyroxenite, gabbro

AGE UNKNOWN

Sp — Serpentinite

SUPRACRUSTAL UNITS
PENNSYLVANIAN–PERMIAN

IIPPsi — Black and grey well–bedded chert, argillite, diabase, basalt

AGE UNKNOWN

IIb — Massive and pillowed basalt flows, lesser tuff

PENNSYLVANIAN–PERMIAN

IIPPvs — Basalt flows and tuffs (including maroon, red and green), volcaniclastics, variegated chert, polymictic breccia, phyllite, argillite, quartz–chert sandstone, rhodonite, diabase

MISSISSIPPIAN TO PERMIAN

IIMPsi — Argillite, chert, chert–quartz sandstone of units IMs and IPPs, undivided, with abundant sills of basalt and diabase

MISSISSIPPIAN

IIMvs — Basalt, diabase, grey and green chert, black, grey and green argillite, calcarenite, quartz–chert sandstone, chert pebble conglomerate

IIMsi — Black, grey and green argillite, grey and green chert, calcarenite, quartz–chert sandstone, diabase

IIMs — Black argillite, quartz–chert sandstone, grey chert, calcarenite

DIVISION I (MISSISSIPPIAN TO PERMIAN)

PENNSYLVANIAN–PERMIAN

IPPs — Green, red and grey chert, argillite, phyllite

MISSISSIPPIAN

IMs,IMsi — Black, grey and green argillite, quartz–chert sandstone, grey, green and black chert, calcarenite, minor tuff, siliceous exhalite, diabase

CASSIAR TERRANE (AUTOCHTHONOUS STRATA)

PENNSYLVANIAN–PERMIAN

MPs — Red, green, pink, grey, black chert and argillite, minor calcarenite lenses, rare amygdaloidal basalt

DEVONIAN TO MISSISSIPPIAN
EARN GROUP

DMe — Slate (variably graphitic, calcareous, pyritic), siltstone, sandstone, conglomerate, porcellanite, dark grey limestone, siliceous and baritic exhalite

MIDDLE DEVONIAN
MCDAME GROUP

mDM — Limestone, dolostone, limestone–dolostone breccia

SILURIAN TO LOWER DEVONIAN
TAPIOCA SANDSTONE

SDTs — Dolomitic quartz arenite, quartzite, dolostone, limestone

ORDOVICIAN TO LOWER DEVONIAN
SANDPILE GROUP

OSDsa — Dolostone, limestone, dolomitic quartz arenite, siltstone, quartzite

ORDOVICIAN TO SILURIAN
ROAD RIVER GROUP

OSRR — Black, commonly limy slate, locally graptolitic, argillaceous limestone

CAMBRIAN TO ORDOVICIAN
KECHIKA GROUP

€Ok — Pale–coloured calcareous slate, siltstone, limestone, calcsilicate and biotite hornfels (may include some OSRR)

LOWER CAMBRIAN
ATAN GROUP
ROSELLA FORMATION

1€R — Limestone, dolostone, calcareous slate, red and green slate

BOYA FORMATION

1€B — Quartzite, siltstone, slate, phyllite

HADRYNIAN
INGENIKA GROUP
STELKUZ FORMATION

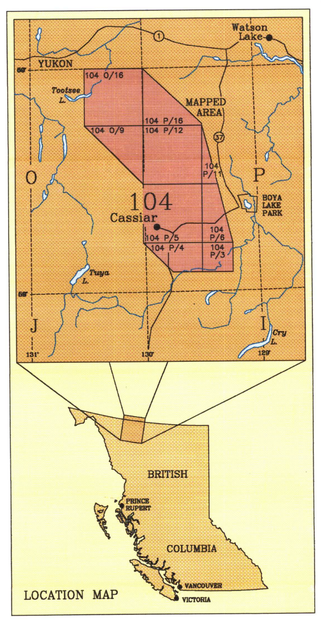
HSt — Eastern facies: grey, red and green slate, limestone. Western facies: grey, green–grey phyllite, siltstone, quartzite, limestone

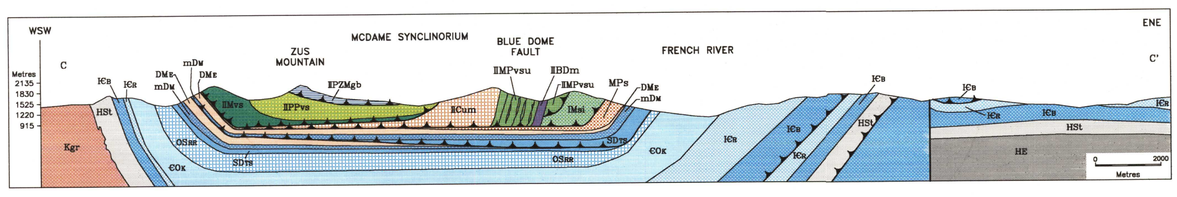
ESPEE FORMATION

HE — Limestone, grey slate

SYMBOLS

- Thrust fault (defined, approx. assumed)
- Fault (defined, approx. assumed)
- Contact (defined, approx. assumed)
- Bedding (horizontal, inclined, vertical)
- Bedding with tops observed (inclined, vertical, overturned)
- Schistosity, gneissosity, foliation (inclined, vertical; phases indicated by numbers of ticks)
- Anticline (defined, approximate, assumed)
- Syncline (defined, approximate, assumed)
- Axial plane of minor fold (inclined, vertical)
- Fold axis of minor fold
- Lineations
- Cross section line (A,B,D,E on Figure 6)
- Macrofossil locality
- Microfossil locality
- Mine
- Mineral Occurrence/Showing
- Potassium–argon isotopic age locality





420 000m N
430 000m N
440 000m N
450 000m N
460 000m N
470 000m N
480 000m N
130°15'
130°00'
129°45'
129°30'
129°15'
60°00'
59°45'
59°30'
59°15'
6 650 000m N
6 640 000m N
6 630 000m N
6 620 000m N
6 610 000m N
6 600 000m N
6 590 000m N
6 580 000m N
6 570 000m N
6 560 000m N
6 630 000m N
6 620 000m N
6 610 000m N
6 600 000m N
6 590 000m N
6 580 000m N
6 570 000m N
6 560 000m N
104 O/104 P
YUKON
BRITISH COLUMBIA
Midway
Cassiar
McDame
Erickson
Toozzes
Lake
Creek
River
Mountain
Ridge
Plateau
Hill
Lake
Creek
Mountain
Ridge
Creek
Creek
Creek